Numerical analysis of the reinforcement of existing foundations by the Soil Mixing technique

Anna Marta Grzyb-Faddoul

Le N° d'ordre: 2014ISAL0141 Année 2014

Thèse

Numerical analysis of the reinforcement of existing foundations by the Soil Mixing technique

Renforcement de fondations existantes par Soil – Mixing - analyse par modélisation numérique

Présentée devant
L'Institut National des Sciences Appliquées de Lyon

Pour obtenir
Le grade de docteur

Formation doctorale : Geotechnique - Génie Civil

École doctorale : Mécanique - Energétique - Génie Civil – Acoustique (MEGA)

Par
Anna Marta GRZYB-FADDOUL
(Ingénieur)

Soutenue le 22 décembre 2014 devant la Commission d'examen

Jury

Président	M. Emmanuel FERRIER	Professeur (UCBL)
Rapporteur	M. Yu-Jun CUI	Professeur (Ecole des Ponts ParisTech)
Rapporteur	M. Daniel DIAS	Professeur (Polytech Grenoble)
Examinateur	M. Henry WONG	Directeur de Recherche CNRS (ENTPE, Lyon)
Examinateur	M. Philippe GOTTELAND	Chercheur FNTP
Examinateur	M. Richard KASTNER	Professeur Emérite (INSA Lyon)
Invité	M. Alain GUILLOUX	Président enterprise TERRASOL Paris
Directeur de thèse	M. Ali LIMAM	Professeur (INSA Lyon)
Co-directeur de thèse	M. Frederic PELLET	Professeur (MINES ParisTech)

Laboratoire de Génie Civil et d'Ingénierie Environnementale (LGCIE)

To my beloved family

Abstract

The increasing densification of constructions in urban areas creates new challenges for civil engineers. Soils, which used to be classified as inappropriate for construction purposes need to be redefined. Moreover, renovations of existing buildings, which usually lead to an additional load transferred to the foundations, require foundations' support. In order to provide required capacity of soil, the ground improvement is needed. The method of reinforcement is expected to be efficient and with the minimal environmental impact. Furthermore, it should be possible to apply it in almost all ground conditions. In this context the Soil Mixing (SM) technique, which consists in the creation of elements of mixed-in-place soil with a cementitious material in order to create composite stiff elements, seems to fulfil all expectations.

The aim of this work is to analyse the influence of soil reinforcement executed by the Soil Mixing method on the behaviour of shallow and deep foundations. Numerical investigation has been carried out - with the use of Finite Element (FE) analyses in ABAQUS - in an attempt to identify the mechanisms guiding the performance of supported foundations.

To be able to use SM columns as the foundation's improvement, it is necessary to fully understand their performance under applied static, axial load. Therefore, a set of simulations reproducing loading tests of single and group of columns have been carried out. Full and small scale tests have been modelled and their results compared with experimental observations. Good agreement between numerical predictions and measurements, confirms proper calibration of the chosen constitutive laws of soils, columns and interactions between them. Moreover, this study has revealed that the SM column acts in a similar way to concrete pile, hence its behaviour is governed mainly by the interface.

Afterwards, numerical modelling of small scale shallow foundation has been accomplished. Two kinds of reinforcement have been investigated. The first one consists of a single column situated centrally under the analysed footing. The second kind of improvement involves group of four SM columns. Two densities of soil have been analysed. The goal of the modelling is to identify the efficiency of the reinforcement in terms of bearing capacity of the foundation and reduction of its vertical displacement. Despite significant difference between total forces borne by the foundation tested on soil with different densities, it has been found that the percentage of the total force that was taken by the soil is density independent.

The influence of reinforcement executed by group of SM columns on a deep foundation has been studied. Numerical modelling of a theoretical, single pile, installed in homogeneous soil, has been carried out. The aim of the investigation is to detect the impact of parameters such as: pattern of reinforcing elements, horizontal distance between SM columns, vertical distance between columns' heads and tip of the pile, diameter and length of SM elements, on the bearing capacity of the foundation. It has been found that the distance between columns and their diameter has the biggest influence on the borne force. However, the length of the reinforcement has shown the least significant influence.

A numerical study of two existing deep foundations, qualified for improvement has been accomplished. In both cases, reinforcement is assumed in layers of soft soil. The first foundation is studied in order to recognize the influence of spacing of reinforcing columns on the reduction of pile's vertical displacement. A linear relation between those two parameters has been found. For the second existing foundation, the spacing between reinforcing elements was kept constant. Two methods of analyzing improved soft soil are tested. The direct method consists in modelling soil and installed SM elements. The simplified method assumes that the whole reinforced area is replaced by new material with equivalent properties. The results of the modelling reveal a coherent reduction of the foundation’s vertical displacement among both methods. Hence, it can be concluded that the simplified method could be used to preliminary estimate the behaviour of the deep foundation.

Keywords: Soil Mixing, shallow foundation, deep foundation, numerical modelling, constitutive law, reinforced foundation

Résumé

La densification croissante des constructions dans les zones urbaines crée des nouveaux défis pour les ingénieurs de génie civil. Les sols qui étaient classés comme non convenables pour l'utilisation dans la construction doivent être reclassés. En outre, la rénovation des bâtiments existants conduit généralement à une augmentation de la charge transférée à la fondation, d'où son nécessaire renforcement. La méthode de renforcement doit non seulement être efficace mais devra induire un impact minimal sur l'environnement. En outre, il devrait être possible de l'appliquer à pratiquement toutes les conditions de sols. Dans ce contexte, la technique de Soil Mixing (SM) semble satisfaire toutes les attentes. Cette méthode consiste à la création d'éléments de sol mélangés sur place avec un matériau cimentaire afin de créer des éléments de structures composites rigides.

L'objectif de ce travail est d'analyser l'influence du renforcement du sol par la method Soil Mixing sur le comportement des fondations superficielles et profondes. Une étude numérique a été effectuée – avec des analyses éléments finis dans ABAQUS - dans le but d'acquérir une compréhension du fonctionnement et une estimation de la performance des fondations améliorées.

Pour être en mesure d'utiliser des colonnes SM pour l'amélioration de la fondation, il est nécessaire de bien comprendre leur performance sous charge axiale statique. Par conséquent, une série de simulations reproduisant des essais de chargement d'une seule colonne, et d'un groupe de colonnes ont été réalisées. Les essais à pleine et petite échelle ont été modélisés et leurs résultats comparés avec les observations expérimentales. Un bon accord entre les prédictions numériques et les mesures confirme une bonne calibration des lois constitutives des sols, des colonnes et de l'interface sol/colonne en SM. En outre, cette étude a révélé que la colonne SM agit d'une manière similaire à un pieu en béton, son comportement est régi principalement par l'interface.

Ensuite, la modélisation numérique d'une fondation superficielle à petite échelle a été menée. Deux types de renforcement ont été étudiés. Le premier consiste en une seule colonne, située au centre sous la semelle analysée. Le second cas correspond à un groupe de quatre colonnes SM. Deux densités de sol ont été analysés. L'objectif de la modélisation est d'identifier l'efficacité du renforcement en termes de capacité portante de la fondation et de la réduction de son déplacement vertical. Il a été trouvé que la densité du sable a un impact significatif sur le comportement de la semelle. La variation de densité a entraîné une différence significative entre les forces totales portées par les fondations. Mais, il a été constaté que le pourcentage de la force reprise par le sol par rapport à la force total, est indépendant de la densité.

L'influence du renforcement obtenu par un groupe de colonnes SM sur une fondation profonde, a été étudiée. La modélisation numérique d'un seul pieu théorique installé dans le sol homogène, a été réalisée. L'objectif de l'étude est de détecter l'impact de divers paramètres, tels que la distance horizontale entre les colonnes de SM, la distance verticale entre les têtes de colonnes et la pointe de pieu, le diamètre et la longueur des éléments SM, sur la capacité portante de la fondation. On a montré que la distance entre les colonnes et leur diamètre ont la plus grande influence sur la force de charge, la longueur de renforcement conduit à une moindre influence.

L'étude numérique de deux fondations profondes a été menée. Dans les deux cas, on suppose que le renforcement est dans les couches de sol faible. La première fondation est étudiée afin de qualifier l'influence de l'espacement des colonnes de renfort sur la réduction du déplacement vertical du pieu. Une relation linéaire entre ces deux paramètres a été trouvée. Cependant, pour la deuxième fondation, l'espacement entre les éléments du renforcement a été fixé comme une constante. Deux méthodes d'analyse de l'amélioration des sols faibles sont testées. La méthode directe qui consiste à modéliser le sol et les éléments de SM. La méthode simplifiée qui suppose que la totalité de la zone renforcée est remplacée par un matériau ayant des propriétés équivalentes. Les résultats de la modélisation montrent une amélioration de la fondation qui est cohérente entre les deux méthodes. Par conséquent, on peut conclure que la méthode simplifiée peut être utilisée pour l'estimation préliminaire du comportement de la fondation profonde.

Mots-clés: Soil Mixing, fondations superficielles, fondations profondes, modélisation numérique, loi constitutif, fondation renforcée

Acknowledgements

This thesis was funded by French National Project RUFEX (Renforcement et Reutilisation des plateformes Ferroviaires et des Fondations Existantes). I would like to thank for the financial support of my research work.

I would like to express my gratitude to my PhD advisors, Professor Ali Limam and Professor Frederic Pellet for encouraging my studies and for allowing me to grow as a research scientist.

Besides my advisors, I would like to thank my Committee members: Professor Yu-Jun Cui and Professor Daniel Dias who kindly accepted being reviewers of my manuscript, Professor Emmanuel Ferrier, Professor Henry Wong, Professor Richard Kastner, Doctor Philippe Gotteland and Doctor Alain Guilloux for accepting to be part of my thesis defence, insightful feedback and interesting questions.

My sincere thanks also goes to all members of the RUFEX project for many valuable comments, interesting scientific discussions and exchange of ideas. I would especially like to thank my closest project partner, office mate and friend – Mahmoud Dhaybi, for four years of teamwork.

I would like to thank my dear friend Fidaa Kassem for being my guardian angel.

These acknowledgements would not be complete if I did not mention my friends Itziar Serrano-Munoz, Fatima Anis, Wahib Arairo, Roman Anufriev, Mohammad Abdur Razzak, Hadi Chahal, Amin Louhi and Tan Trung Bui for providing support that I needed, new ideas, friendship and all great moments we shared together. You made my PhD time unforgettable!

Last, but certainly not least, I must acknowledge with tremendous and deep thanks my beloved family; my parents, my sister and husband – people who have never doubted that I will succeed.

Table of content

1. Introduction

1.1. Background

During the past few decades, construction activities have considerably increased. Densification of buildings and development of transport network create new challenges for civil engineers. Soft soils, which used to be classified as inappropriate for construction purposes, need to be reassigned due to growth of the cities and their infrastructure.

Figure 1.1 French railway network, after Réseau Ferré de France (RFF, 2013)

French railway network, presented in Figure 1.1, consists of about 30000 km long 'classic lines' (black) and 2000 km long 'high-speed lines' (blue). By the 'classic lines' are understood all lines where allowed speed is about 220 km / h. They are built before 1980 and represent about 94% of the whole network. The 'high-speed lines' (**T**rain à **G**rande **V**itesse) represent only 6% of the network and permitted speed at this part of the tracks is higher than 220 km / h.

Progressive development of network as well as need to ensure an effective and safe service forced SNCF (**S**ociété **N**ationale des **C**hemins de fer **Fr**ançais - French National Railway Company) and RFF (**R**éseau **F**erré de **F**rance - French Rail Network) to accelerate and double renewal of pathways from annual rate of 400 km / year to 800 km / year. However it requests to be accomplished while facing: on the one hand a growing demand for capacity and on the other hand requirement for control operating costs. To help to come up against obstacles French national project RUFEX (**R**enforcement et **R**e**U**tilisation des plateformes **F**erroviaires et des **F**ondations **EX**istantes) was established. It covers the reuse of rail platforms, existing foundations of buildings and engineering structures.

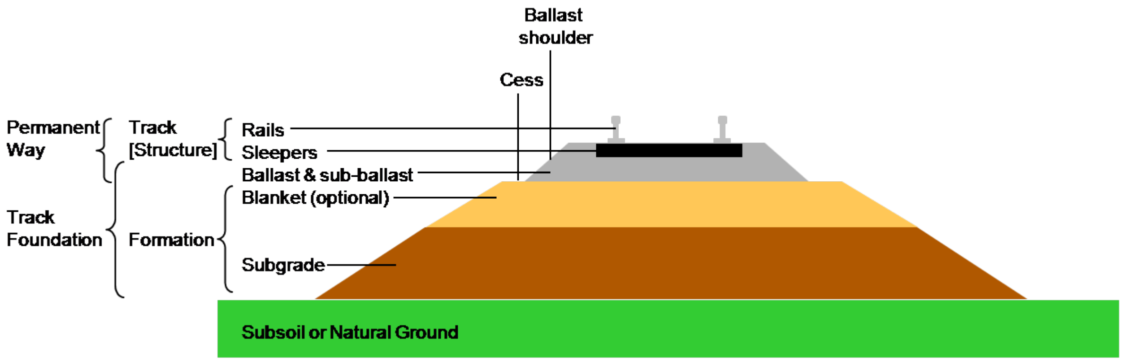

Figure 1.2 Section through railway track and foundation showing the ballast and formation layers (Wikipedia, 2013)

The main objective of the project is to develop an innovative method of platform reinforcement, as well as the tools needed to carry out the process, without long term disruption of the traffic. The maintenance of the railway foundations is one of the key aspects in rail maintenance process. Their mechanical properties play a fundamental role in the quality of the tracks. If deformations of the railway foundations are insufficiently reduced, they influence the track geometry, which leads to significant reduction of the life of the track and ballast in particular. Figure 1.2 illustrates section of a railway track and an embankment.

Conventional repair techniques are very restrictive and they require temporarily removing parts of the embankment. It has a significant impact on the operation of the line, namely circulation needs to be suspended. That is why, SNCF is looking for a method to improve the quality of subgrade (Figure 1.2) while keeping constant traffic capacity of the line.

The second objective of the project is to find a method of reinforcement of existing foundations (shallow and deep). Chosen reinforcing technique needs to ensure safety of the foundation and whole supported structure, while being efficient and environmental friendly.

As the most appropriate method the Soil Mixing (SM) has been chosen. This technique allows strengthening of rail platforms as well as foundations by creation of columns, which are mixed in place from existing soil with cemetitious material.

The RUFEX research project is a cooperation between three industrial partners SNCF, Soletanche Bachy and Terrasol, and three universities IFSTTAR Paris, Ecole de Ponts ParisTech and INSA Lyon. It consists of technological research on tools and compositions of binders. Moreover, behaviour of structures, where the existing foundation continues working in association with the implemented reinforcement, is studied.

1.2. Objectives and scope of the study

Originally, the Soil Mixing technique was dedicated to ground improvement but currently, it offers solutions in a wide range of applications, such as foundation engineering, excavation control, hydraulic cut-off walls, liquefaction mitigation, environmental remediation and reinforcement of foundations. However, to be able to use SM elements in any of presented cases, it is necessary to perform detailed investigation and fully understand their behaviour. Knowledge of properties of the material is crucial, nevertheless it is not sufficient. Without complete analysis of the behaviour under loading, it is not possible to capture all characteristics of the Soil Mixing element.

The present research is a numerical study. Its main four objectives are:

- First, to understand behaviour of the SM column working as a single element or in a group. The analysed columns are subjected to static axial load. The loading test is modelled by finite element method (FEM) model in ABAQUS. Proper modelling is possible only by correctly chosen and calibrated constitutive laws obeyed by soil/soils, column and interaction between them;
- Second, to analyse behaviour of the small scale shallow foundation. Knowledge of the SM column characteristics is combined with behaviour of the shallow foundation. It allows to analyze reinforced foundation. Two densities of soil, two ages of the SM elements, sizes of the shallow foundation are tested in order to find parameter which has the biggest influence on the behaviour of the reinforced foundation;
- Third, to understand mechanism guiding efficiency of the reinforcement of the deep foundation, executed by group of SM columns. It is investigated by numerical study of a single pile in homogenous soil. Various parameters, such as: column pattern, horizontal distance between reinforcing elements, vertical distance between columns' heads and tip of the foundation, SM elements diameter and length, are tested to recognize their influence on the efficiency of the reinforcement;
- Fourth, to investigate the improvement brought by the group of SM columns installed under the foundation, inside weak soil layer. By two reference RUFEX projects, the influence of columns' spacing and two methods of analysing reinforced volume of soil, is studied.

1.3. Outline of the thesis

In addition to the introduction, this thesis contains of seven chapters. The content of each of them is summarized as follows:

Chapter 2 presents state of the art review. Firstly, concept of the Soil Mixing technique is described and ways of its classification are presented. Secondly, the main advantages and fields of applications are reported. Afterwards, the unconfined compressive strength and modulus of elasticity of the Soil Mixing material as a function of soil type, age of the mixture and type of the binder are discussed by a summary of results available in literature. Then, the types of failure of the Soil Mixing elements are presented and some guides considering design are given. Lastly, synthesis of the published numerical analysis of soils treated by the Soil Mixing method is presented.

Chapter 3 reviews briefly constitutive models of soil. Their importance and influence on the results of the modelling of soil is pointed out. Then, the elastoplastic model with four failure criteria are discussed. Firstly, the most commonly used in numerical approach, the Mohr-Coulomb criterion is presented. Secondly, two definitions of the Drucker-Prager criterion (classical and modified) are described. Limitations of the classical definition, regarding granular materials are presented. Afterwards, the modified version of the criterion is introduced and differences between definitions are discussed. The last presented criterion is the modified Drucker-Prager with cap. Formulation of the model is given. The influence of each parameter of the criterion is visualised by an example. Lastly, all presented criteria are compared by analysing behaviour of small scale shallow foundation placed on a homogeneous layer of the Hostun sand.

Chapter 4 presents analyses of behaviour of a Soil Mixing column. The first numerically studied case is static loading test of Soil Mixing column installed in the experimental site in Vernouillet, France. Two steps, preliminary and advanced, of calculations are presented. The second part of the chapter consists of numerical analyses of small scale columns. The characteristics of Hostun sand, Soil Mixing columns and contact between soil and column, obtained from laboratory tests are described. Moreover, parameters used in numerical approach are presented. Then, experimental setup is introduced, followed by numerical analyses of single column and 'group of columns' in 'dense' and 'loose' sand. Influence of soil density, column age and spacing between columns in a group are studied.

Chapter 5 consists of study of a shallow foundation reinforced by a Soil Mixing column. Firstly, the shallow type of foundation, its modes of failure and ways of estimating bearing capacity, are presented. Secondly, the experimental setup of the 1g, small scale laboratory test, is introduced. In the main part of the chapter, results of experiments of the shallow foundation with and without reinforcement (single and four columns) are numerically reproduced. Results are compared in terms of total bearing capacity and distributions of force and stress. Two sizes of foundations, two densities and two ages of columns are tested and their influence on the behaviour of the mixed foundation is pointed out.

Chapter 6 presents deep foundation reinforced by the Soil Mixing technique. At the beginning, the deep type of foundation is described. Two ways of estimating bearing capacity are presented and specificity of the group behaviour is discussed. The main part of the chapter concentrates on theoretical investigation of the behaviour of pile foundation supported by the Soil Mixing columns. Analyses are accomplished by parametric study, where varied parameters are: columns' pattern, horizontal distance between reinforcing elements, vertical distance between columns' heads and pile's tip, and length and diameter of the Soil Mixing columns.

Chapter 7 concentrates on analysis of two, defined in RUFEX specification (RUFEX, 2010), cases of deep foundations, which has been classified for reinforcement. In both cases reinforcement, by the Soil Mixing columns, is situated under the foundation, inside weak soil layer. The aim of the first investigated project, is to detect influence of the spacing of columns on the reduction of the vertical displacement of the foundation. In the second project, impact of the way of analysing column passing through more than one layer, is examined. Two methods of considering treated by columns volume of soil are presented. The direct one consists in analysing reinforced soil and reinforcing elements as they are. The simplified method assumes that the whole improved volume is replaced by new material with equivalent properties.

Chapter 8 summarizes the main findings of this study and suggests some area requiring further investigation.

2. State of the art review

2.1. Introduction

Up to now, many soil reinforcement methods have been developed. Some of the most commonly used techniques are: pre-fabricated vertical drains, preloading, jet-grouting columns, geosynthetics, light-weight fill, vertical rigid inclusions (concrete piles, stone columns), the Soil Mixing method, etc.

The Soil Mixing (SM), known also as Deep Mixing and Deep Cement Mixing, is the whole family of techniques treating soils by mixing *in situ* existing soil with a binder, in order to create composite stiff element. The method was initiated in Japan about five decades ago. Since then, it became widely used and until now it has been evolving, especially in Scandinavian countries and USA (Archeewa, et al., 2011).

This chapter describes concept of the technique, its classification and main characteristics. Furthermore, different ways of application of the SM elements are presented. Afterwards, properties of material obtained from relevant *in situ* and laboratory studies, as well as theoretical works and reported. The last paragraph of the chapter concerns estimation of the bearing capacity of the SM elements and their modes of failure.

Although, there are many stabilizing agents used in SM method, in this work a strong emphasise is laid on cement-type ones.

2.2. Soil Mixing method

2.2.1. Concept and classification

The SM method is frequently applied as a soil improvement, since 1960s, when it was created in Japan, USA and Scandinavian countries (Porbaha, 1998). Originally the technique was dedicated to improve engineering and environmental properties of soft or contaminated ground. Use of the method has increased lately, especially in countries of its origin, but also in Southeast Asia, China, Poland, France, Germany and UK, and to some extent in other countries. This indicates growing international interest and acceptance of this relatively new and quickly developing technology (Topolnicki, 2004). The technique is able to fulfil cost-efficiency criteria while being environmental friendly. The SM method consists in the creation of elements of mixed-in-place soil with a cementitious material (such as cement, lime, gypsum, fly ash, etc.) in order to create composite stiff elements. Specially designed machines equipped with shafts with mixing blades and stabilizer injection nozzles are used to produce *in situ* treated soil columns. The binder can be introduced as powder – dry method or slurry – wet method. The dry method is more suitable for soft soils with very high moisture content, and hence appropriate for mixing with dry binders. Whereas, the wet method is more appropriate in soft clays, silts and fine-grained sands with lower water content and in stratified ground conditions including interbedded soft and stiff or dense soil layers (KELLER, 2013). The *in situ* remoulding and mixing of the soil is achieved with rotary tools. Various tools have been developed. Their type depends on the expected shape of the SM element. Hence, to create single columns, simple rotary tools are used. Some examples of this type of augers can be found in Figure 2.1 and Figure 2.2, for dry and wet methods respectively. In order to create panels or blocks, multiple augers should be used (Figure 2.3).

Regardless type of the method, installation of the SM element consists of five steps (Figure 2.4). Firstly, equipped shaft is positioned over the designed location. Secondly, the rotary tool is inserted into the soil and continues mixing till expected depth. Afterwards, cementitious agent is introduced, through auger or along the shaft, which is constantly rotating. However in case of some techniques, slurry can be injected also during the penetration. It usually depends on soil conditions. The next step is a withdraw phase, when injection and rotation are continued till ground surface or designed depth. Finally, the reactions taking place between the soil and stabilizing agent increase the strength of the ground.

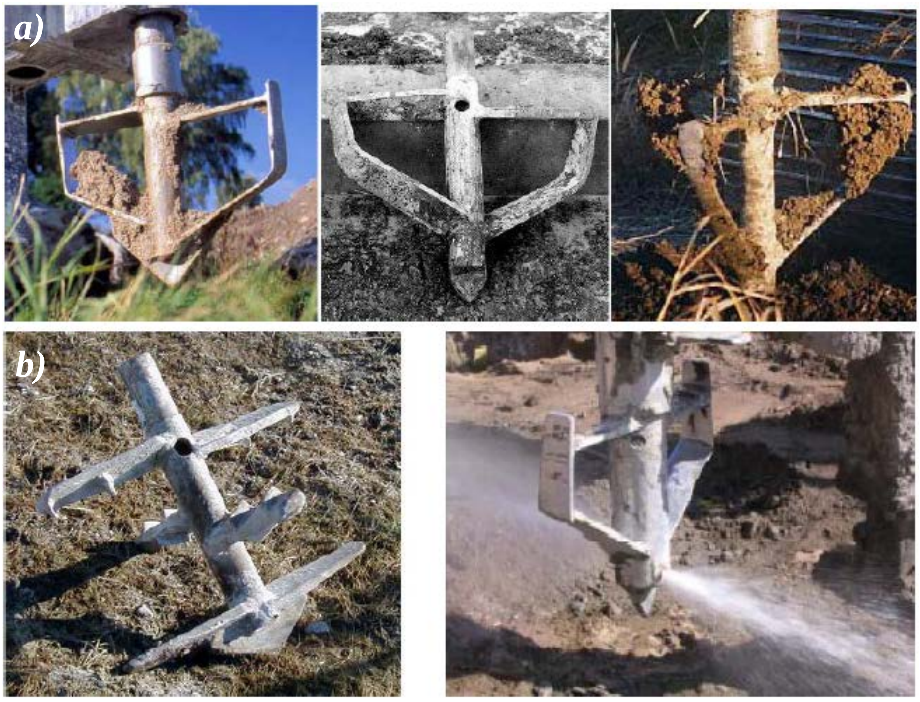

Figure 2.1 Example of simple rotary tools. Nordic dry mixing tools: a) standard, b) modified (Larsson, 2005)

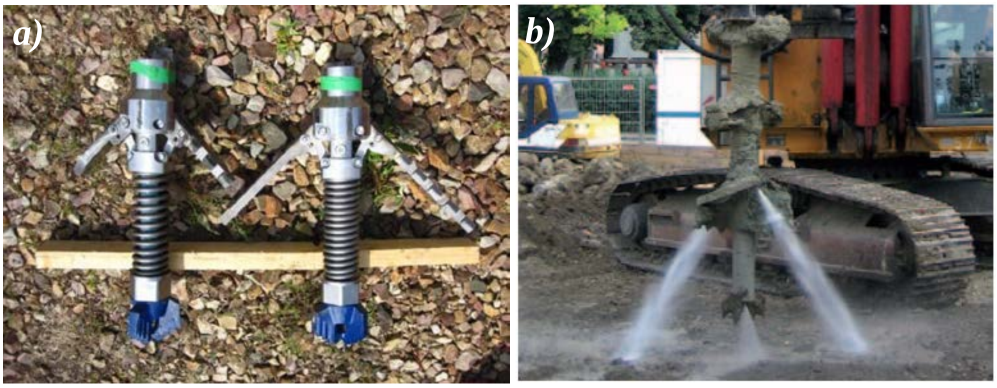

Figure 2.2 Examples of simple rotary tools. Augers used to wet mixing: a) Springsol® by Soletanche Bachy (Guimond-Barrett, et al., 2012), b) DSM rotary tool by Keller (KELLER, 2013)

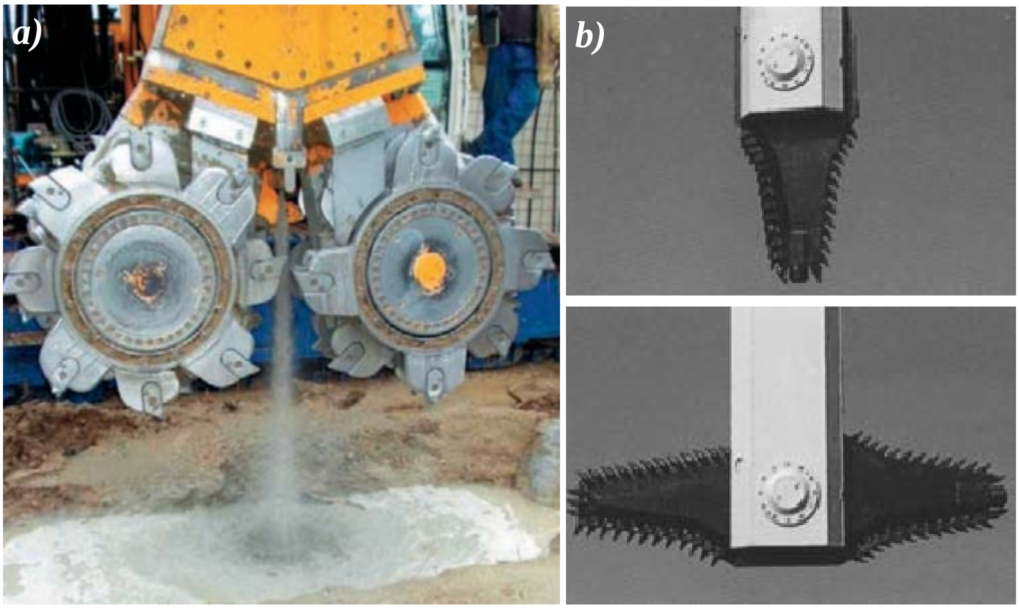

Figure 2.3 Examples of multi augers tools: a) cutter Soil Mixing by Bauer (Caltrans, 2010), b) blade used in Spreadable Wing method by SWING (Topolnicki, 2004)

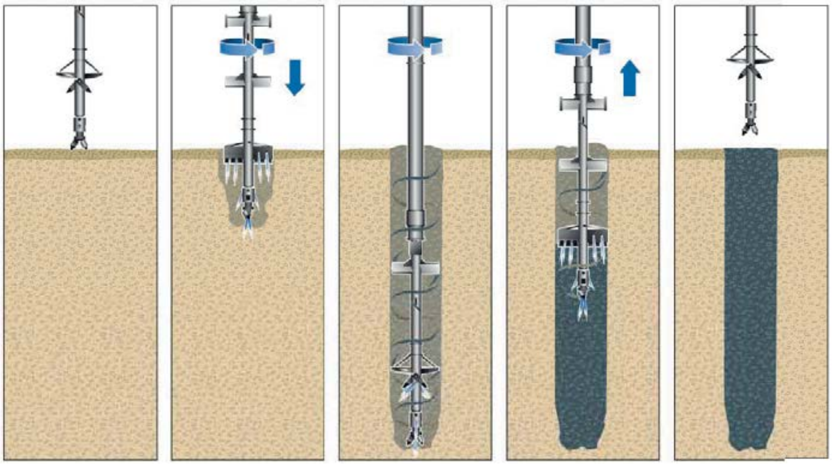

Figure 2.4 The Soil Mixing column production process (LIEBHERR, 2012)

SM method can be classified in different ways. According to FHWA report (Bruce, 2001) all methods can be classified based on three fundamental operational characteristics (Figure 2.5). The distinction between wet and dry technologies with respect to the form of binder introduced into the soil is the most straightforward, and hence the most widely used. In the dry methods, the medium for binder transportation is typically compressed air. Whereas, in case of the wet methods the transportation is executed typically by water.

The second characteristic is related to the mixing method. Three ways of providing agent can be distinguished: mechanical mixing, where the binder is injected at relatively low velocity, jet mixing, where the fluid grout is injected at high velocity (jet grouting), or hybrid mixing, which is combination of both previous techniques.

The third characteristic reflects the location, or vertical distance of the drilling shaft over which mixing occurs in the soil (Topolnicki, 2004). At the bottom of the classification chart, allocation of selected methods developed in various countries is presented.

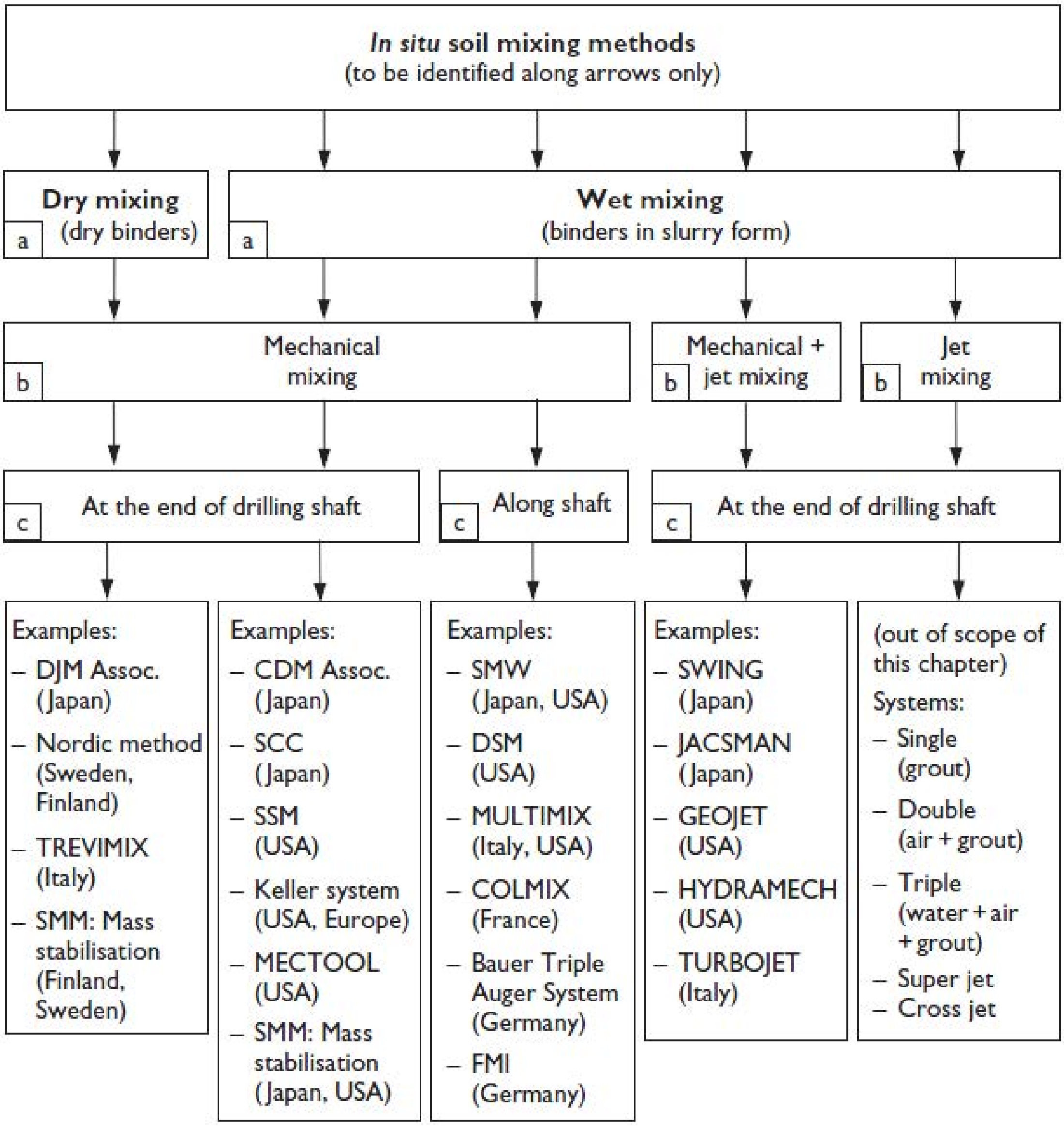

Figure 2.5 General classification of in situ soil mixing based on: a) binder form, b) mixing principle and c) location of mixing action, with allocation of selected fully operational methods developed in various countries (Topolnicki, 2004)

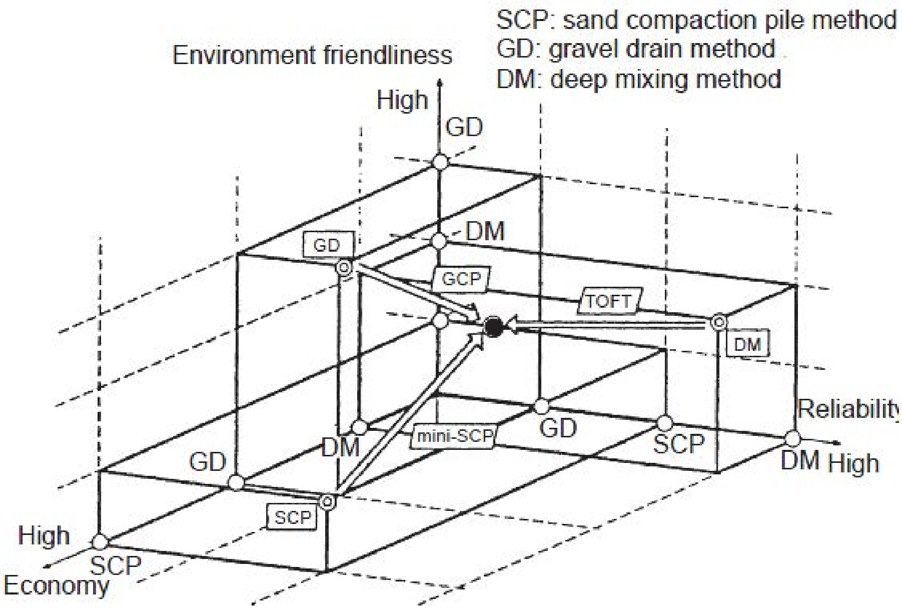

Figure 2.6 Performance of different soil improvement techniques (Ando, et al., 1995)

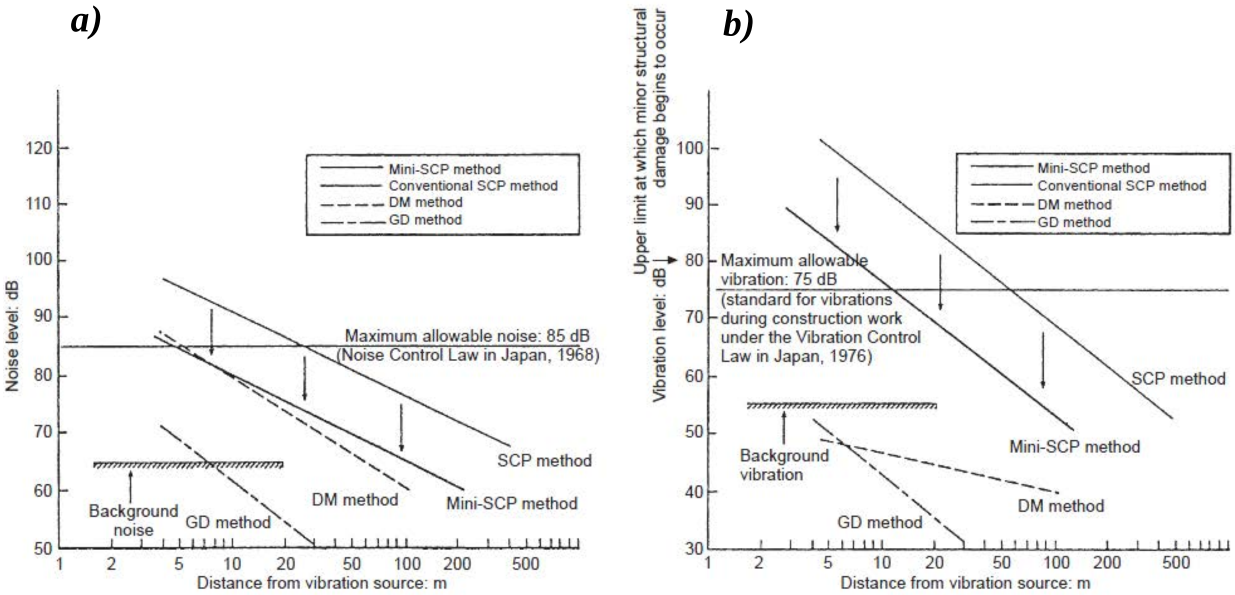

Figure 2.7 Environmental impact of various ground improvement techniques: a) noise effect, b) effect of vibration during construction (Ando, et al., 1995)

2.2.2. Characteristics

Porbaha (Porbaha, 1998) gathers several advantages of SM method and compares them to conventional soil improvement techniques:

- Speed of construction. Rapid solidification that speeds up the construction process is the distinctive feature of SM method. In some cases, for instance: urban areas, existing railway tracks or existing foundations, the construction time is the main factor deciding about the chosen method. The time constraint might be caused by need of maintains traffic service during construction or deadline imposed by the contract.
- Strength calibration. The requisite strength of SM is achieved by varying the ratio of the binder, commonly cement, to suit the project requirements with consideration of loading, soil type, and desired serviceability.
- Reliability. The advancements in terms of mixing equipment, coordination of control devices, and integrated systems for real-time monitoring provide effective quality control of SM elements, and thus enhance the reliability of the technique. In Figure 2.6, comparison of the performance of SM method with other different soil improvement techniques in terms of reliability, cost-effectiveness and environmental friendliness (Ando, et al., 1995) is presented.
- Variety of application. A large number of reported cases in the literature show the broad spectrum of the application areas of SM method. It is discussed in the following paragraph.
- Effective use of resources. Due to solidification the soil *in situ*, the SM method does not require huge quantity of additional material, which needs to be transported and then stored in site. It is extremely beneficial in the case of limited surface. For example granular fill is needed in large volume for stone column or sand compaction method.
- Small environmental impact. Unlike conventional methods of granular soil improvement, such as stone column or sand compaction piles, installation of SM columns generates much lower noise and vibration during construction. The relationships between noise level and the distance from the source of noise for several soil improvement methods are compared in Figure 2.7 (Ando, et al., 1995).

2.2.3. Applications

Soil Mixing technology modifies the engineering properties of existing soil in well defined zones such as columns, panels, or blocks. Through the design of the engineering properties and treatment patterns, SM constructs subsurface soil-cement structures for a wide variety of applications in the areas of civil engineering construction and environmental remediation.

2.2.3.1. Purposes

In general, the main objectives of improvement by SM method are to increase strength, to control deformation, to reduce the permeability of loose or compressible soils, or to clean contaminated sites (Porbaha, et al., 1998). Nevertheless, SM technology has been employed for specific purposes:

- increasing bearing capacity,
- reduction of settlement,
- prevention of sliding failure,
- protecting structures surrounding the excavation site,
- controlling seepage and as a cut-off barrier,
- preventing shear deformation (liquefaction mitigation),
- remediation of contaminated ground,
- increasing drivability for tunnelling in soft ground,
- ground anchorage,
- vibration impediment.

The undisputable advantage of the SM techniques is fact that they can be used for almost all kinds of soil, including soft rocks. Stabilisation of organic soils and sludge is also possible, but is more difficult because requires carefully tailored binders and execution procedures.

2.2.3.2. Patterns

The mixing can be done to a replacement ratio of 100%, which means that the whole soil is treated by the cemetitious agent and is inside a particular block. In case of lower replacement ratio, known also as ratio of area improvement, other kinds of patterns of SM elements such as columns, walls, grids, are used. The chosen ratio reflects, the mechanical capabilities and characteristics of the applied method. Depending on the purpose of SM elements, specific conditions of the site and costs of treatment, different patterns of column installations are used to achieve the desired result by utilising spaced or overlapping and single or combined columns. In order to compare various column patterns in terms of the treatment area, ratio of area improvement, a_p, is defined as in Equation 2.1 where all constants are explained in Figure 2.8 (Topolnicki, 2004). Typical patterns are presented in Figure 2.9.

$$a_p = \frac{A_t}{A} = \frac{net\ area\ of\ SM}{respective\ total\ area} \qquad 2.1$$

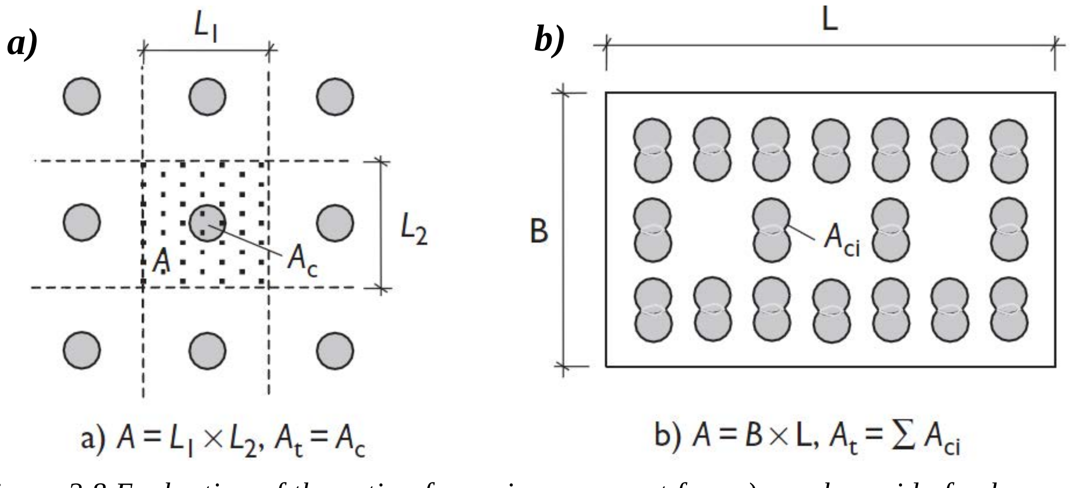

Figure 2.8 Evaluation of the ratio of area improvement for: a) regular grid of columns, b) foundation slab (Topolnicki, 2004)

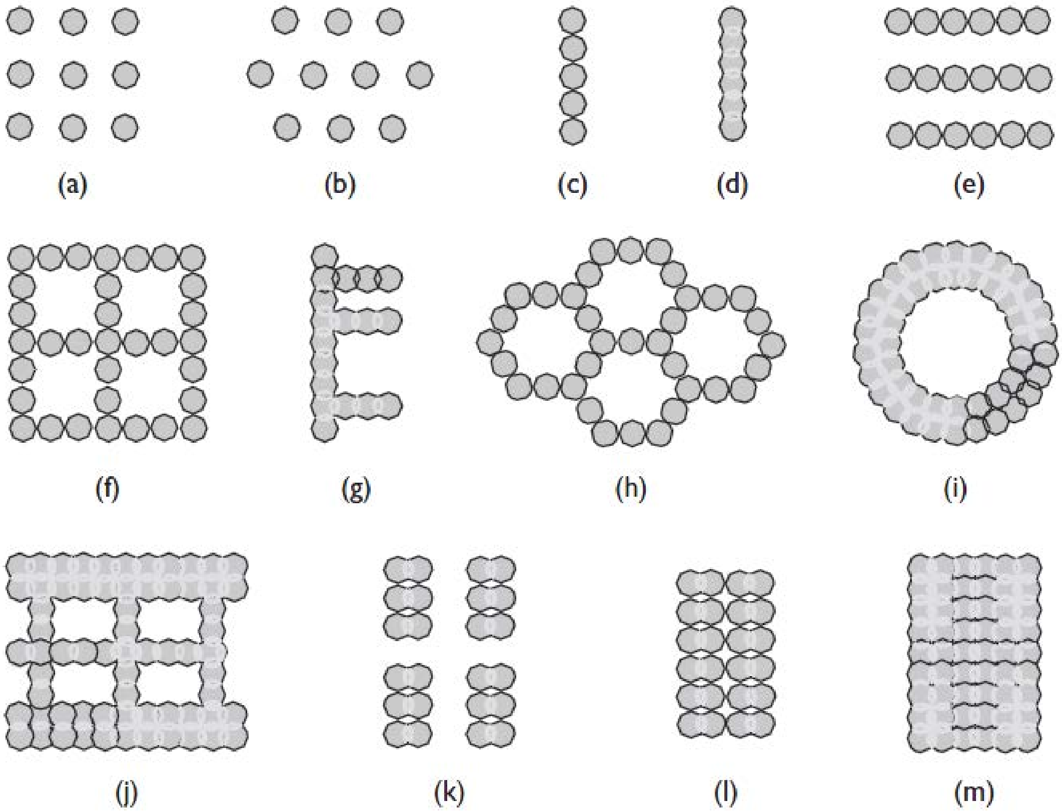

Figure 2.9 Examples of deep soil mixing patterns: a),(b) column-type (square and triangular arrangement), c) tangent wall, d) overlapped wall, e) tangent walls, f) tangent grid, g) overlapped wall with buttresses, h) tangent cells, i) ring; j) lattice, k) group columns, l) group columns in-contact, m) block (Topolnicki, 2004)

2.2.3.3. Fields of application

The technique is able to fulfil cost-efficiency criteria while being environmental friendly, therefore the field of application is significant. It should be noted that SM method is widely employed both in the sea and on land. The major areas of usage for geotechnical and environmental purposes, can be grouped into two main categories: non-structural and structural.

Porbaha et al (Porbaha, et al., 2005) categorized SM application into six main applications:

- hydraulic barrier systems,
- retaining wall systems,
- foundation support systems,
- excavation support systems,
- liquefaction/seismic mitigation systems,
- environmental remediation systems.

Various applications of SM methods are presented also in Figure 2.10. Figure 2.11 and Figure 2.12 illustrate some typical executions of the SM method in projects.

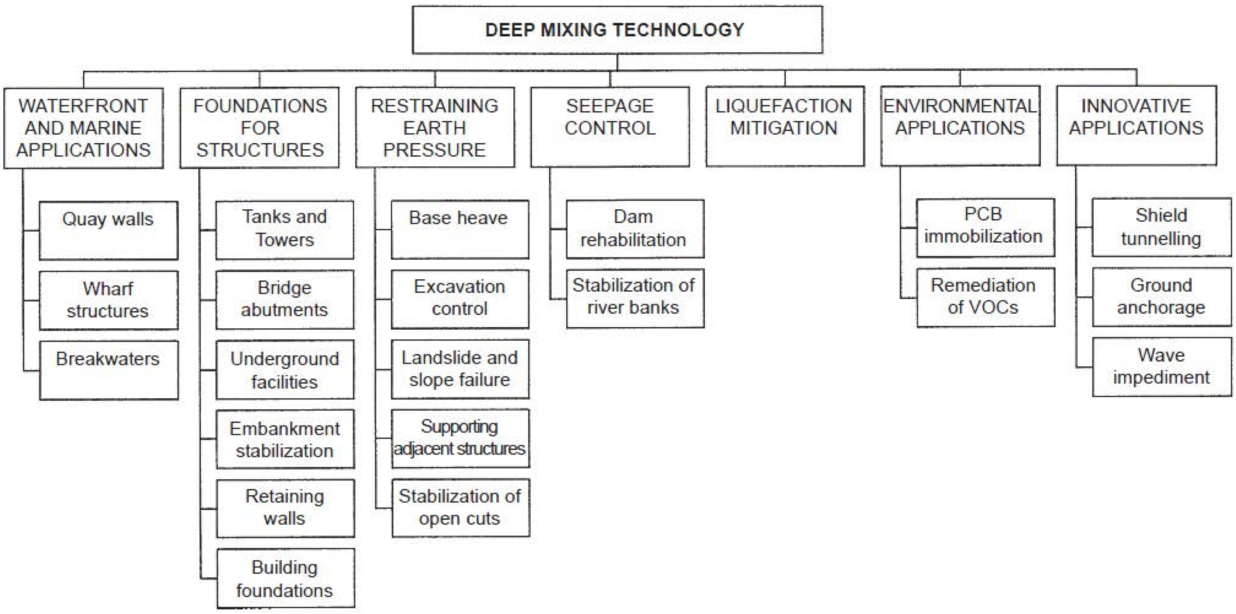

Figure 2.10 Chart of various applications of SM (Deep Mixing) technology (Porbaha, et al., 1998)

Figure 2.11 Foundation support executed by SM method. a) Railroad Bridge supported by deep mixing column at San Francisco International Airport (Porbaha, et al., 2005), b) columns under the foundation for A2 Motorway near Katowice, Poland (Massarsch & Topolnicki, 2005)

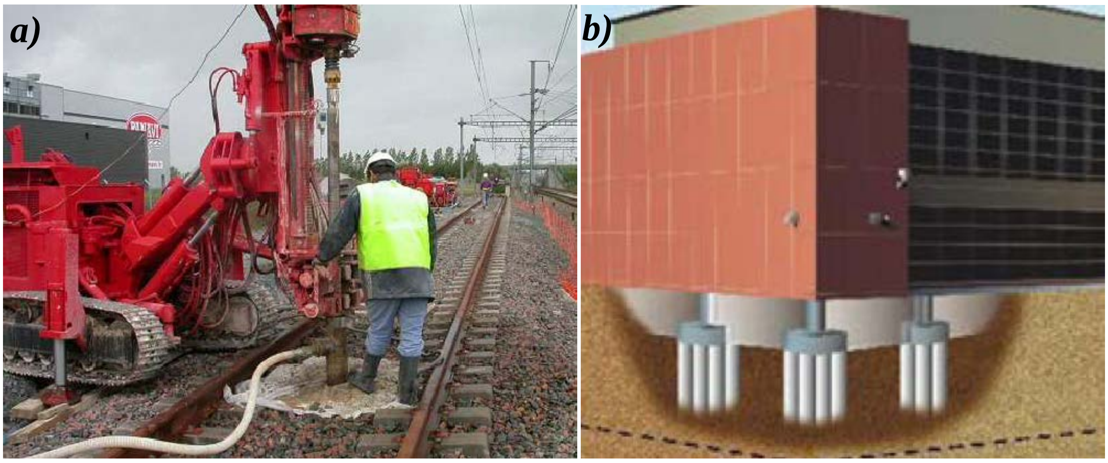

Figure 2.12 Application of SM: a) under the railway track (INNOTRACK, 2009), b) under building foundation (Nozu, 2005)

2.2.4. Properties of the material

The choice of the SM method's type depends on the characteristics of the application site and the desired performance of the treated soil. The physical and chemical properties of soil, such as grain size distribution, water content, type of minerals, organic matter content, cation exchange capacity, highly affect the property of the treated soil. However to be able to understand influence of all of mentioned factors, the process which takes place in the SM material needs to be understood. It has been found that three major categories of reactions have place in case of treated soil: dehydration process, ion exchange and pozzolanic reaction (Porbaha, et al., 2000).

The dehydration process, bases on the consumption of water in the mixture by the introduced agent. It results with appearance of calcium hydroxide, $Ca(OH)_2$. Dissociation of calcium hydroxide in water increases the electrolytic concentration and pH of the pore water, which results in calcium cations, Ca^{2+}, being attracted to the negatively charged (anions) clay particles – ions exchange (Assarson, et al., 1974).

The most significant for increase with time of the shear strength of the treated soil are pozzolanic reactions. Calcium hydroxide in the soil water reacts with the pozzolans (silicates and aluminates) in the clay to form binders or cementing materials. The strength of the SM material depends on the type of binder (cement, lime, fly ash and so on).

The main parameters, which are commonly used to estimate properties of treated by SM method soil is the unconfined compressive strength (UCS) and the modulus of elasticity. As it is mentioned above, many factor have impact on these properties. The most important ones are presented in sections below.

2.2.4.1. Unconfined compressive strength

Stress-strain curve of treated soil (Figure 2.13) has been found to increase abruptly until the peak compressive strength q_u. Then, it suddenly decreases to very low residual value. Due to brittle or quasi-brittle mode of failure, SM material and pure concrete can be considered alike. Even though, this kind of reply to unconfined load has been found for all reported cases, also the huge effect of factors such as: soil type, age, binder, cement and water contents, and strain at failure on the results of the unconfined compressive strength test have been observed.

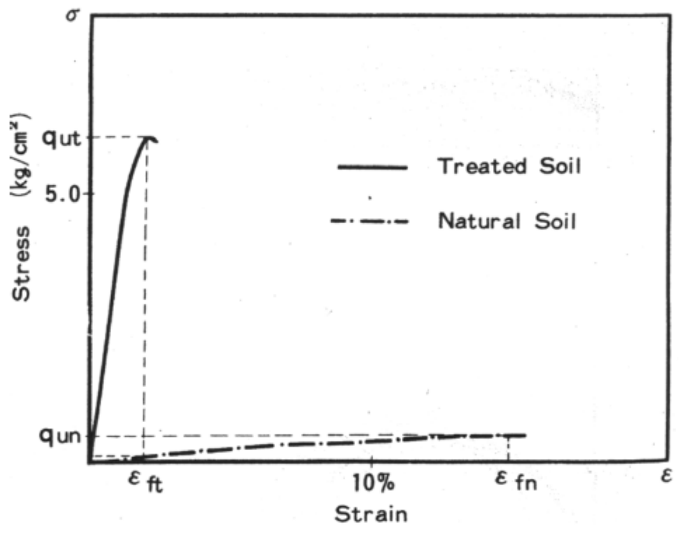

Figure 2.13 Typical stress-strain curve of cemented soil (Endo, 1976)

2.2.4.1.1. *Soil type*

The physical and chemical properties of soil are significant to the final strength of the SM material. It was reported by Hilt and Davidson (Hilt & Davidson, 1960) and Wissa, et al. (Wissa, et al., 1965) that clays containing montmorillonite and kaolinite minerals react more easily than illite owing to poorly defined crystallinity. Moreover, they were found to be effective pozzolanic agents, compared with clays which contained illite. It was proved that the increase of clay content in soil leads to increase in the quantity of the required stabilizing reagent. Bell (Bell, 1993) explained this by the increase in the surface area and the contact between the particles. Kawasaki, et al. (Kawasaki, et al., 1981) studied the influence of different Japanese clays on the unconfined compressive strength of cement-soil mixture, as a function of cement content (Figure 2.14). Figure 2.15 illustrates influence of the grain size of soil on the unconfined compressive strength of SM material, tested for high cement content, reported by Taki and Yang (Taki & Yang, 1991). In case of soils with a high content of organic matter and soils with an excessive salt content, which may retard the hydration of the cement, some difficulties have been reported. Proposed solution was increase of the cement content (Porbaha, et al., 2000).

It has been observed that SM material, prepared in laboratory with the same soil, water and cement contents, does not behave in exact way as the one obtained from field. In comparison with laboratory mixing conditions, material mixed *in situ* manifests lower unconfined compressive strength. Results of carried out investigations for land and marine constructions are presented in Figure 2.16. It has been found that the laboratory strength appears to be 50% to 20% of field strength. It can be explained by the maximum aggregates' size effect discussed by Tang, et al. (Tang, et al., 2011). Typical field strength for ranges of cement contents and soil types are presented in Table 2.1, after Topolnicki (Topolnicki, 2004).

Table 2.1 Typical field strength for ranges of cement contents and soil types (Topolnicki, 2004)

Soil type	Cement ratio [kg/m^3]	q_u after 28 days [MPa]
Sludge	200 – 400	0.1 – 0.4
Peat, organic silts/clays	150 – 350	0.2 – 1.2
Soft clays	150 – 300	0.5 – 1.7
Medium/hard clays	120 – 300	0.7 – 2.5
Silts and silty sands	120 – 300	1.0 – 3.0
Fine-medium sands	120 – 300	1.5 – 5.0
Coarse sands and gravels	120 – 250	3.0 – 7.0

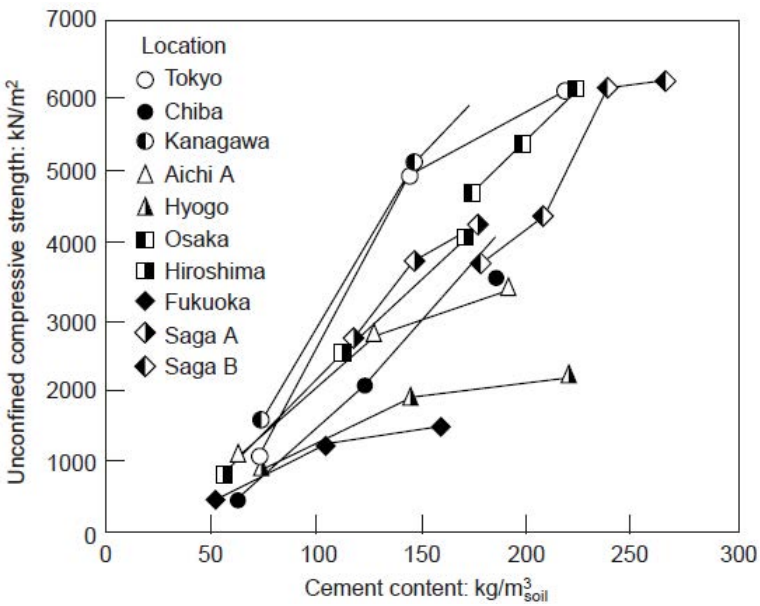

Figure 2.14 Stabilization of different soils in Japan (Kawasaki, et al., 1981)

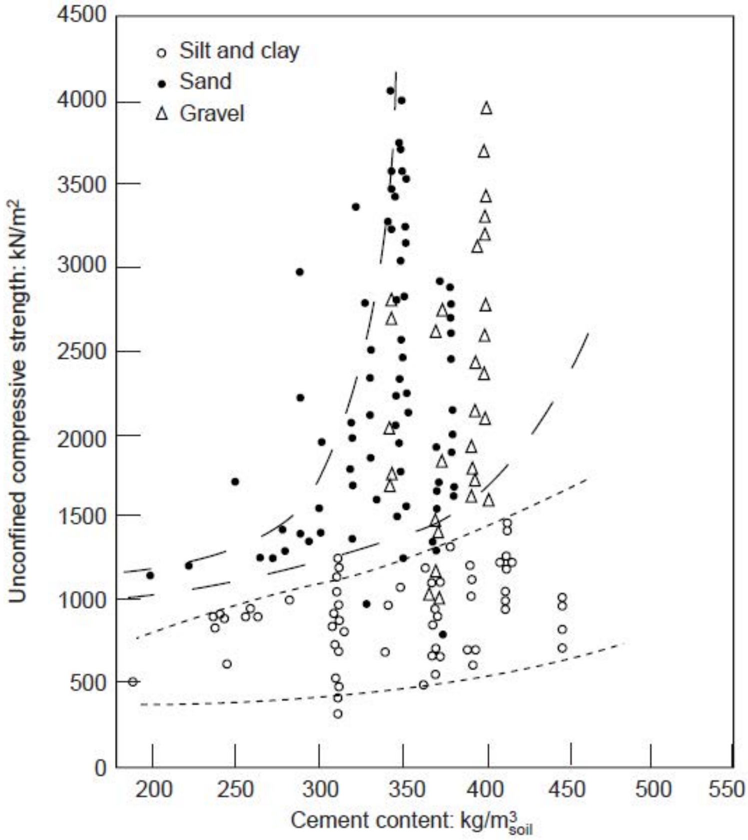

Figure 2.15 Effect of soil type on compressive strength of cement-soil mixture (Taki & Yang, 1991)

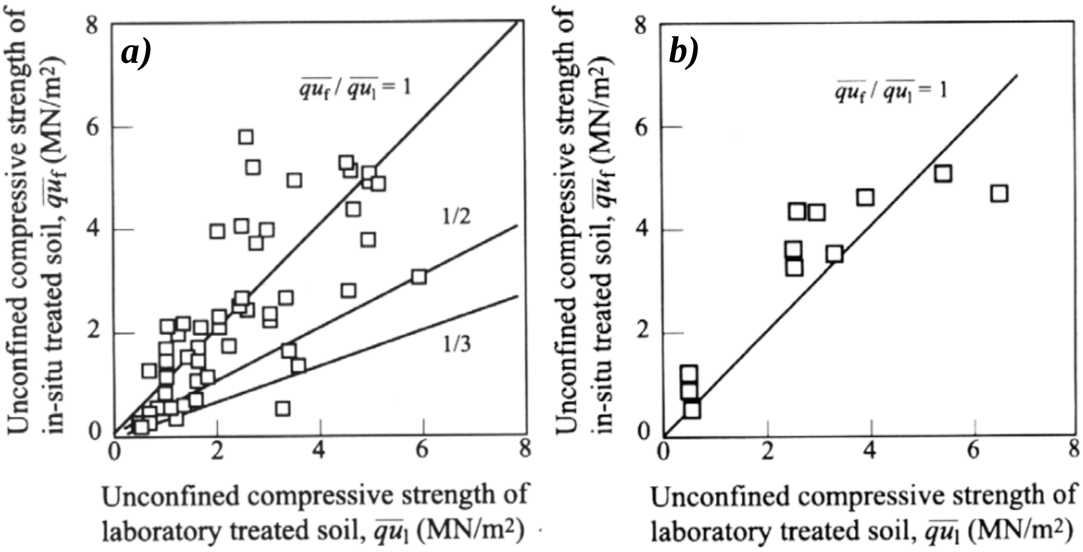

Figure 2.16 Relation between unconfined compressive strength of laboratory and in situ treated soil. a) land construction, b) marine construction, after (Noto, et al., 1983)

2.2.4.1.1. *Binder*

The significance of the binder and its content has been widely studied in the last years. Except different kind of cement, also other substances can be use to stabilize soils. As substitutes for cement (used alone or with cement), with significant influence on all properties of the SM material, can be used (Topolnicki, 2004):

- Bentonite. It improves stability of slurries with high water – cement ratios, furthermore, reduces material permeability,
- Slag. It improves chemical stability and durability, however retards strength gain,
- Kiln dust. This kind of binder is used mainly in environmental applications,

- Fly ash. It increases chemical durability and reduces heat being result of hydration,
- Lime and gypsum. They are used when relatively low strength of the material is needed,
- Silicates, polymers, etc. They are used in special environmental applications.

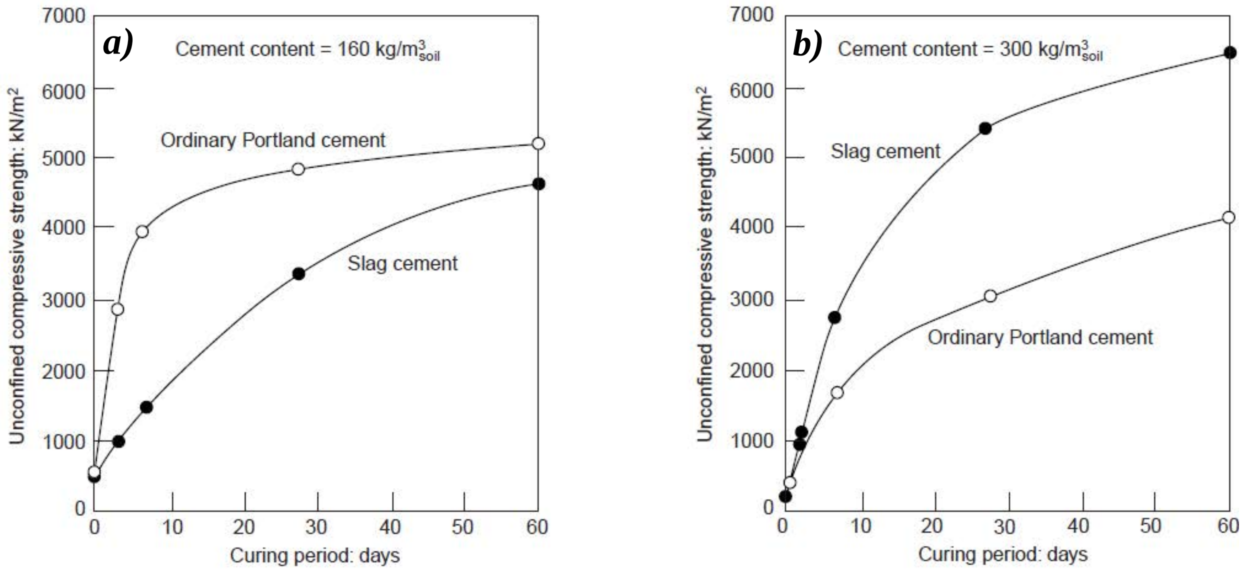

Figure 2.17 Effect of cement type on UCS of SM: a) Kanagawa in the Tokyo Bay area soil mixed with two kinds of cement - cement content 160 kg/m^3, b) Saga in Kyushu Island soil mixed with two kinds of cement - cement content 300 kg/m^3 (Kawasaki, et al., 1981)

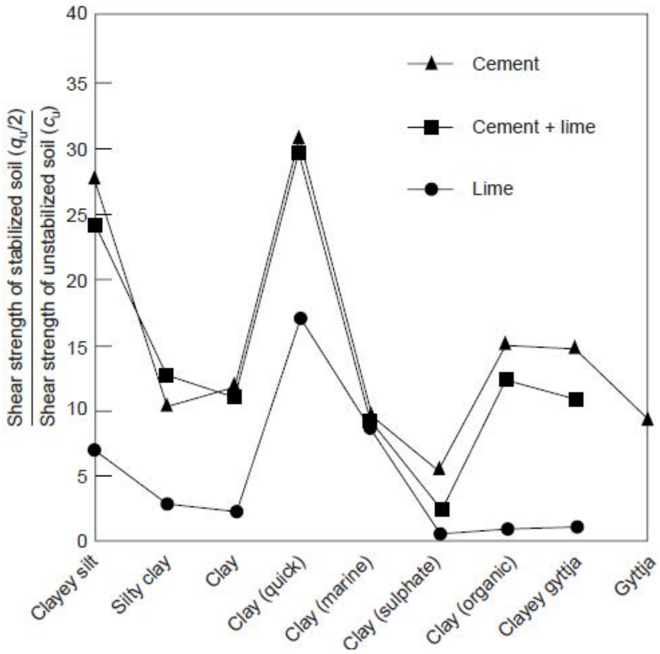

Figure 2.18 Effect of different stabilizers on compressive strength of soil in Sweden (Ahnberg, et al., 1995)

Kawasaki, et al. (Kawasaki, et al., 1981) analysed the difference between slag and Portland cements for two different clays in Japan (Figure 2.17). Obtained by them figures show that the improvement effect of slag cement is different for various soil types. The reason is that many chemical reactions are involved during the hardening process of the stabilized soil, as explained before. Hence, the response to stabilization using slag cement is not unique, meaning that there is not a general trend in the improvement effect. Basically, the effect depends on the chemical components of the slag cement and the properties of the local soil (Porbaha, et al., 2000). It can be concluded, that, improvement effect needs to be verified by laboratory tests in each case. The influence of different stabilizing agents, such as cement, lime and fly ash, was a field of interests of Ahnberg, et al. (Ahnberg, et al., 1995). In Figure 2.18 comparison of the effect of cement, lime and a mixture of cement and lime on SM material based on different soils in Sweden.

Table 2.2 Summary of sites analysed in the USA by British Cement Association (British Cement Association, 2001).

Site	Contaminants	Binder and process
Former power station, Boston, MA	Pb and oil	Asphalt emulsion pre-treatment, cement-based binder
Former gasworks, Cambridge, Boston, MA	Coal tars and diesel	Cement-bentonite binder; in-situ augering
Former wood processing site, Port Newark, NJ	AS, Cr and creosote	Cement-based; in-situ mixing of redeposited soil using rotary mixing head
Jersey Garden Mall, Port Elizabeth, NJ	Mixed contaminants (PCBs, metals)	Cement-based; in-barge mixing using rotary mixing head. Treated product used as engineering fill
Closed landfill site, Salem, NJ	Petroleum fuels from filling stations and road spillage clean-up	Cement-based binder; ex-situ pugmill. Treated product used in capping system
Peak Oil Superfund site, Tampa, FL	Pb, PCBs and trichloroethene	Pre-treatment with phosphate, cement-based binder; ex-situ pugmill

As it was mentioned in case of influence of soil type, the increase of the quantity of the stabilizing agent, rise of the compressive strength can be expected. Figure 2.19 depicts results obtained by Uddin, et al. (Uddin, et al., 1997) from investigations concerning Bangkok clay. They analysed influence of the Cement content on the strength development index (SDI), which is defined as the strength ratio of treated to untreated samples obtained by the unconfined compression test.

In case of treatment of contaminated sites, usually more than one kind of agent is used. Findings provided by British Cement Association (British Cement Association, 2001), concerning results of studied carried out in 6 different, contaminated sites in the USA, are presented in Table 2.2. Table 2.3 summarizes some studies available in the literature. It presents influence of binder type and ratio, and soil on UCS of the SM material.

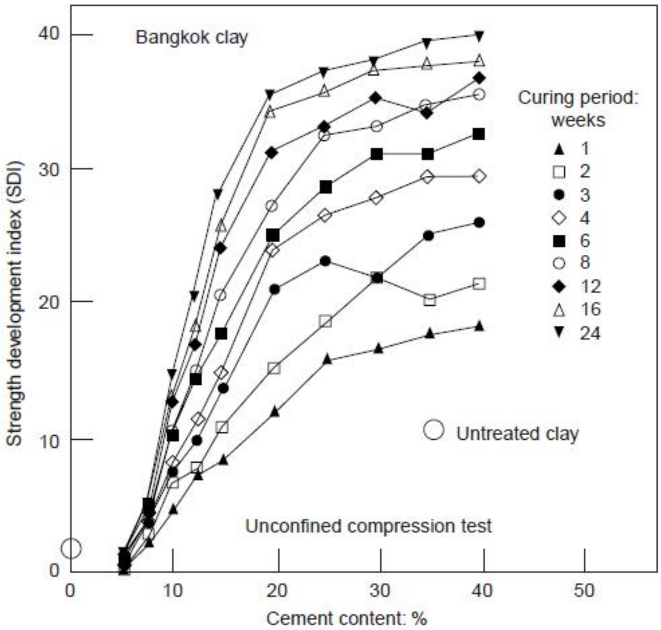

Figure 2.19 Effect of cement content on compressive strength of SM material (Uddin, et al., 1997)

Table 2.3 Relation between binder ratio, unconfined compressive strength and type of binder reported by different authors.

Reference	Binder ratio [kg/m^3]	q_u [MPa]	Binder
Reavis and Freyaldenhoven (Reavis & Freyaldenhoven, 1989)	570	4.8 – 10.3 (clay)	cement + additives
Pagliacci and Pagotto (Pagliacci & Pagotto, 1994)	200 – 250	0.5 – 5.0 (granular) 0.2 – 1.0 (cohesive)	cement, bentonite, additives
Okumura (Okumara, 1996)	100 – 200	0.5 – 4	cement, bentonite, gypsum, fly ash
Burke, et al. (Burke, et al., 1996)	150	0.2 – 1.4 (clays) 3.5 – 10.0 (sands)	varied in response to soil type
Miyoshi and Hirayama (Miyoshi & Hirayama, 1996)	200 and 320	1.0 – 6.0 (silty sand)	cement
Rathmeyer (Rathmeyer, 1996)	80 – 150	0.2 – 2.0	cement and lime
Yang (Yang, 1997)	250 – 750	0.3 – 1.3 (clays) 1.4 – 4.2 (sands)	cement, bentonite, additives
Axtell and Stark (Axtell & Stark, 2008)	no information	1.2 (silt) 3.0 – 3.1 (fine sand) 7.0 – 13.0 (coarse sand)	cement
Guimond-Barrett, et al (Guimond-Barrett, et al., 2011)	210 - 320	0.1 – 10.0 (sand) 0.1 – 1.5 (silt)	cement and cement with bentonite
Melentijevic, et al. (Melentijevic, et al., 2013)	*C/S = 0.6 – 1.2	0.5 – 0.6	cement

**C/S – cement – soil ratio*

2.2.4.1.2. *Age of the mixture*

It is commonly accepted that the strength of cement treated soil increases with time. This behaviour makes it similar to pure concrete. Effect of age, ranging between 2 and 200 days, on the unconfined compressive strength observed by Endo (Endo, 1976) is shown in Figure 2.20.

Correlations between UCS of mixtures after 3, 7, 28 and 60 days of curing, have been proposed by Kawasaki, et al. (Kawasaki, et al., 1981) in accordance with their studies of the Tokyo bay clay mixed with Portland cement (Equations 2.2, 2.3 and 2.4). Where q_{u3}, q_{u7}, q_{u28}, q_{u60} are UCS after 3, 7, 28 and 60 days of curing respectively.

$$0.26q_{u28} < q_{u3} < 0.63q_{u28} \tag{2.2}$$

$$0.49q_{u28} - 64 < q_{u7} < 0.71q_{u28} + 57 \tag{2.3}$$

$$q_{u60} = 1.17q_{u28} \tag{2.4}$$

The Cement Deep Mixing Association of Japan (Cement Deep Mixing Association of Japan, 1994) recommends correlations between UCS of the treated soil, q_{u7}, q_{u28}, q_{u91}, after 7, 28 and 91 days (Equations 2.5, 2.6 and 2.7).

$$q_{u28} = (1.49\ to\ 1.56)q_{u7} \tag{2.5}$$

$$q_{u91} = (1.85\ to\ 1.97)q_{u7} \tag{2.6}$$

$$q_{u91} = (1.20\ to\ 1.33)q_{u28} \tag{2.7}$$

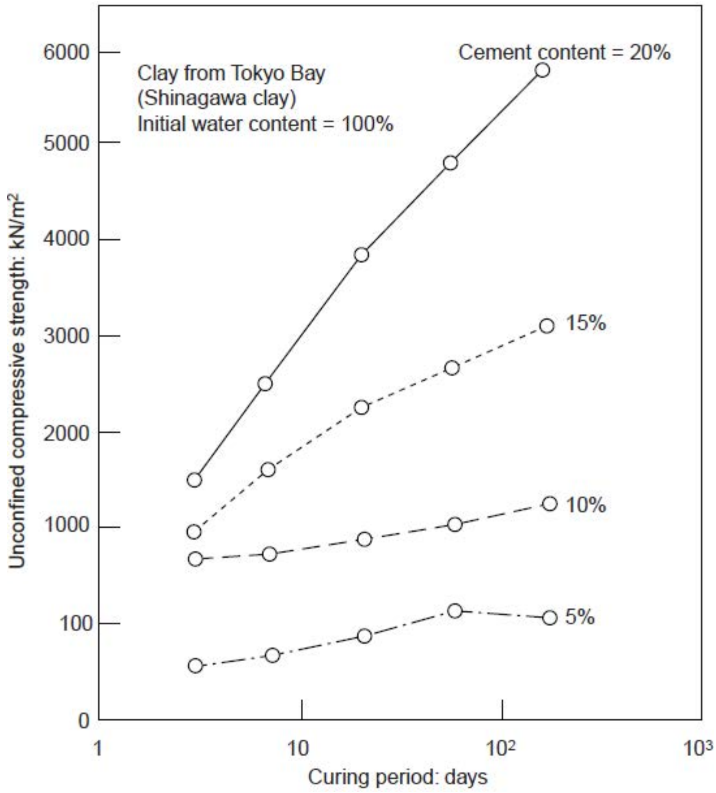

Figure 2.20 Effect of age on compressive strength of SM material (Endo, 1976)

Figure 2.21 depicts relation provided by Guimond-Barrett et al (Guimond-Barrett, et al., 2012) according to their laboratory investigation of Fontainebleau sand stabilized by Portland cement. It was found that ratios representing relation between q_{u28} and q_{u7}, and q_{u90} and q_{u7} decrease with the increase of the cement content. However, in case q_{u90} and q_{u28}, ratio stays constant, regardless quantity of used cement.

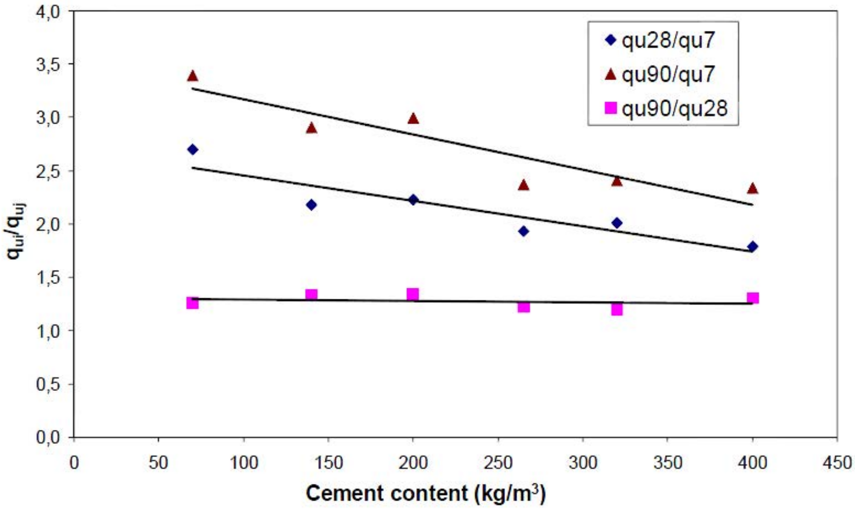

Figure 2.21 Effect of the cement content on the unconfined compressive strength of stabilized Fontainebleau sand after various curing time (Guimond-Barrett, et al., 2012)

Presented above relations and equations are obtained for SM material based only on laboratory tests. Topolnicki (Topolnicki, 2004) in his review of SM methods proposed more general correlations between UCS of mixtures after 4, 7, 28 and 56 days according to type of soil. Relations are presented by general Equations 2.8, 2.9 and 2.10 for clays and silts and Equation 2.11 for sands.

$$q_{u28} = 2q_{u4} \tag{2.8}$$

$$q_{u28} = (1.4\ to\ 1.5)q_{u7} \tag{2.9}$$

$$q_{u56} = (1.4\ to\ 1.5)q_{u28} \tag{2.10}$$

$$q_{u28} = (1.5\ to\ 2.0)q_{u7} \tag{2.11}$$

2.2.4.2. Modulus of elasticity

The Young's modulus of elasticity of the cement treated soil is often determined according to the unconfined compression strength. Relationship between modulus (E50, secant at 50%) of SM material and the UCS have been studied by numerous researchers. Saitoh, et al. (Saitoh, et al., 1980) proposed correlations presented in Equation 2.12, based on results of his extensive studies of soft soils obtained from port areas in Japan (Figure 2.22), treated with 5-15% of Portland cement. Figure 2.23 and Figure 2.24 illustrate correlations between the secant modulus and the unconfined compressive strength for Boston blue clay mixed with type cement CEM II (GeoTesting Express, 1996) and Fontainebleau sand with cement CEM III (Guimond-Barrett, et al., 2011), respectively.

$$350q_u < E_{50} < 1000q_u \tag{2.12}$$

Table 2.4 summarizes relationships between the modulus and the unconfined compressive strength reported by several researchers for different soils.

Table 2.4 Relationships between modulus and unconfined compressive strength

Reference	Relationship
Saitoh et al. (Saitoh, et al., 1980)	$350\ q_u < E_{50} < 1000\ q_u$
Kawasaki et al. (Kawasaki, et al., 1984)	$350\ q_u < E_{50} < 1000\ q_u$
Tatsuoka and Shibuya (Tatsuoka & Shibuya, 1991)	$750\ q_u < E_{50} < 1000\ q_u$
Futaki, et al. (Futaki, et al., 1996)	$100\ q_u < E_{50} < 250\ q_u$
Asano et al. (Asano, et al., 1996)	$140\ q_u < E_{50} < 500\ q_u$
GeoTesting Express (GeoTesting Express, 1996)	$50\ q_u < E_{50} < 150\ q_u$
Yin and Lai (Yin & Lai, 1998)	$35\ q_u < E_{50} < 180\ q_u$
Goh et al. (Goh, et al., 1999)	$150\ q_u < E_{50} < 400\ q_u$
Fang et al. (Fang, et al., 2001)	$30\ q_u < E_{50} < 300\ q_u$
Tan, et al. (Tan, et al., 2002)	$350\ q_u < E_{50} < 800\ q_u$
Topolnicki (Topolnicki, 2004)	$50\ q_u < E_{50} < 300\ q_u$ for $q_u < 2$ MPa $300\ q_u < E_{50} < 1000\ q_u$ for $q_u > 2$ MPa
Lorenzo (Lorenzo, 2005)	$114\ q_u < E_{50} < 170\ q_u$
Axtell and Stark (Axtell & Stark, 2008)	$120\ q_u < E_{50} < 230\ q_u$
Guimond-Barrett et al. (Guimond-Barrett, et al., 2011)	$55\ q_u < E_{50} < 160\ q_u$
Melentijevic, et al. (Melentijevic, et al., 2013)	$50\ q_u < E_{50} < 500\ q_u$
Cuira et al. (Cuira, et al., 2013)	$E_{50} = 1280\ q_u$

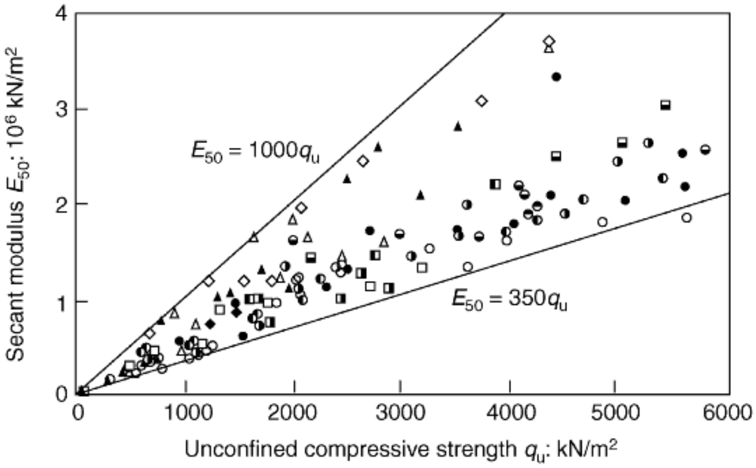

Figure 2.22 Relation between secant modulus and UCS of treated Japanese soils (Saitoh, et al., 1980)

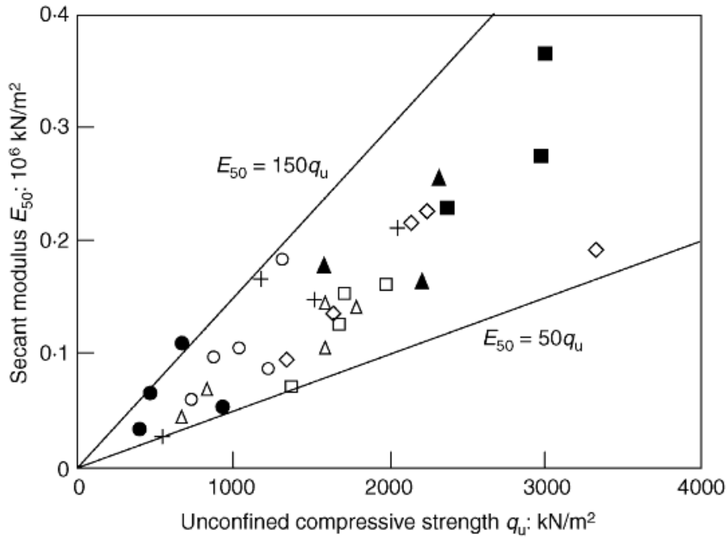

Figure 2.23 Relation between secant modulus and UCS of treated Boston blue clay (GeoTesting Express, 1996)

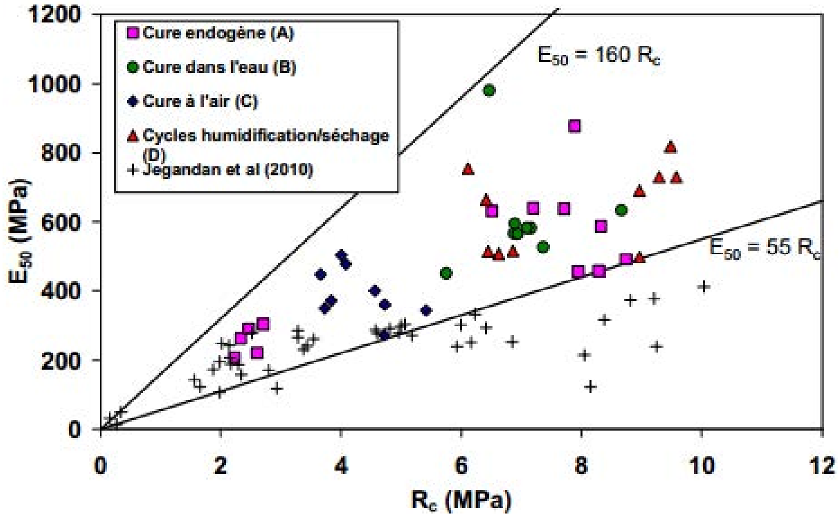

Figure 2.24 Relation between secant modulus and UCS of treated Fontainebleau sand, cement ratio 265 kg/m³(Guimond-Barrett, et al., 2011)

2.2.5. Failure modes and design of the Soil Mixing

2.2.5.1. Mode of failure

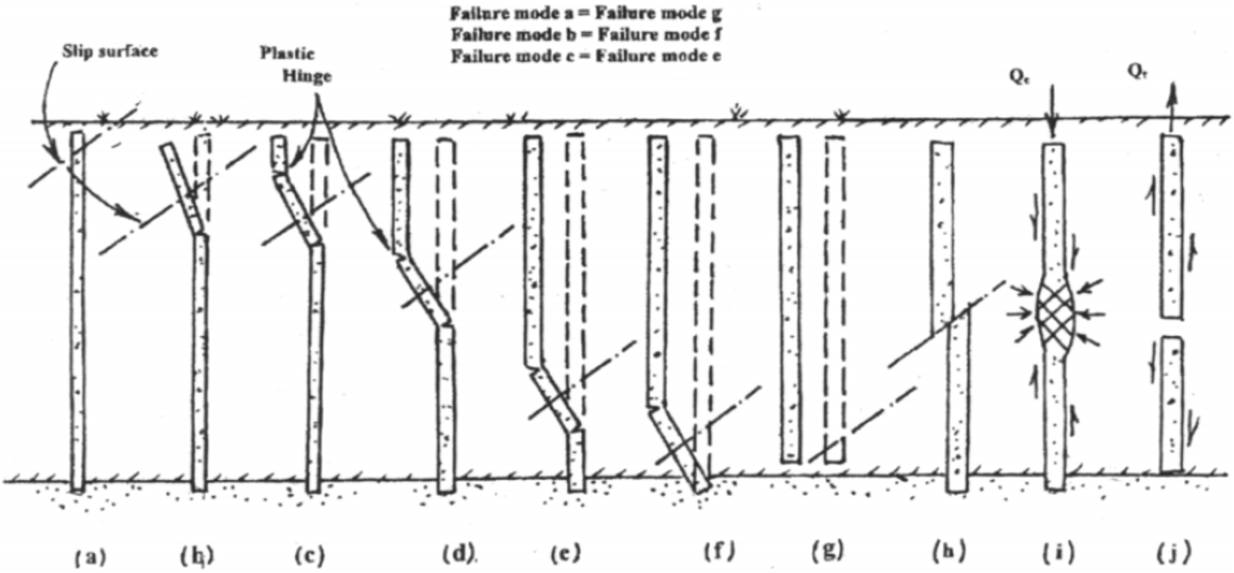

Figure 2.25 Possible failure modes for single columns (Broms, 2000)

2.2.5.1.1. *Single column*

Broms (Broms, 2000) reported ten possible modes of failure for a single SM column (Figure 2.25). Each mode can be described (Fang, 2006):

- *Type a* - a shallow slip, sufficient moment capability to resist the lateral earth pressure depending on the relative displacement,
- *Type b* - a deeper slip, plastic hinge at the location of the maximum bending moment, moment resistance exceeded,
- *Types c, d, e* - two plastic hinges, moment resistance exceeded,
- *Type f* - extension to the firm layer, deep slip closed to the bottom,
- *Type g* - extension to the firm layer, deep slip closed to the bottom, moving through the soil as a rigid member,
- *Type h* - governed by the shear resistance of the column section,
- *Type i* - compression failure, governed by the load carried,
- *Type j* - passive zone, dominated by tensile strength.

2.2.5.1.2. *Group of columns*

Kitazume et al. (Kitazume, et al., 1996) carried out a number of centrifugal model tests to investigate the vertical bearing capacity and the bearing capacity factor of a group of SM columns. Figure 2.26 illustrates, failure patters of soil reinforced by a group of columns. Behaviour of columns, can be concluded, that the vertical bearing capacity of the improved soil is dominated by the shear strength of the columns.

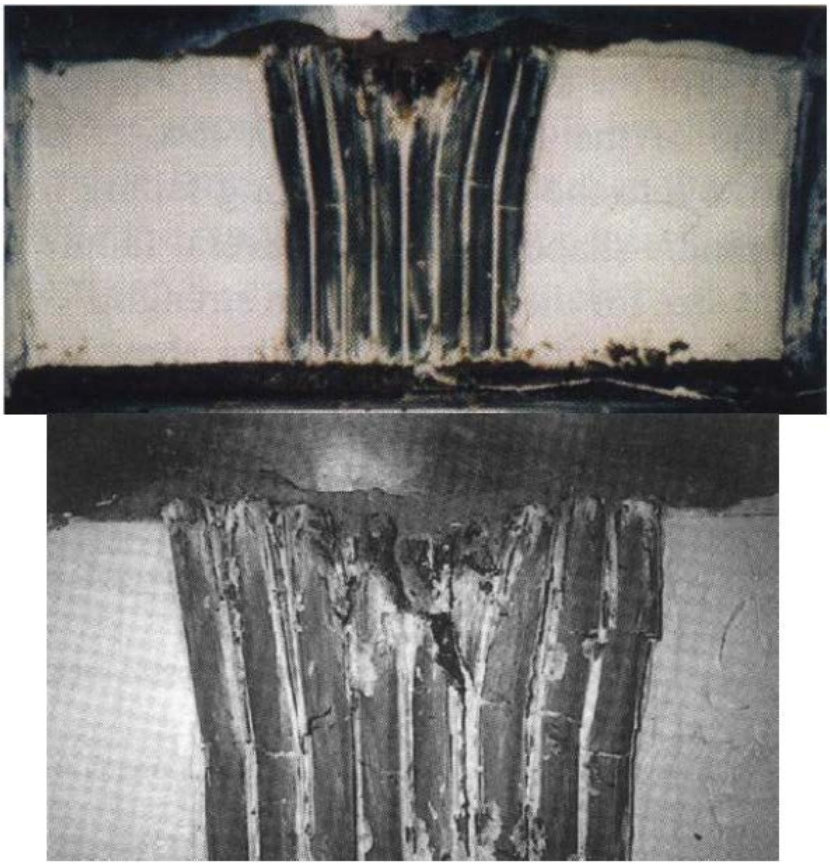

Figure 2.26 Failure pattern of the improved soil; a) the post-test whole section of the improved model, b) failure of the columns(Kitazume, et al., 1996)

2.2.5.2. Design

Despite the large number of projects, where SM technique is applied for various purposes around the world, the design of this kind of improvement is still highly empirical. Some of research, which are needed to design SM treatment, can be outlined as follows (Porbaha, 2000):

- understanding the soil-structure interaction,
- investigation the effect of relative stiffness (treated and untreated) on the behaviour of the improved ground,
- investigation the flexural rigidity of column-type SM subject to the bending failure mechanism,
- reports of case histories with the aim of improvement of the empirical coefficients currently being used in the analysis,
- development of a reliability-based design methodology,
- elaboration on the analysis of SM based on the limit state design (LSD) principle.

2.3. Numerical modelling of the Soil Mixing

Until now, no specific algorithm for engineers, who want to calculate SM elements has been proposed. Even though, Porbaha (Porbaha, 2000) and Topolnicki (Topolnicki, 2004) give some general guides and examples of applications of the method, they insist on the investigation by field loading tests. Unfortunately, this type of measurements significantly increases project costs. In this context, numerical approach can be complementary solution which is able to limit number of loading tests to necessary minimum.

Many studies have been performed to investigate the behaviour of soil treated by SM method. Two methods of analyses are the most commonly used by researchers: the finite element method (FEM) and the finite difference method (FDM). Both are powerful numerical techniques that are widely applied for solution of various engineering problems.

2.3.1. Software

A range of problems in soil mechanics are being investigated using numerical methods, primarily FEM and FDM. Both commercial and in-house software packages are used as a tool in studies of SM elements:

- PLAXIS and PLAXIS 3D (FEM), for example Figure 2.28a and Figure 2.29b and c,
- FLAC and FLAC 3D (FDM), for example Figure 2.28c,
- CESAR-LCPC (FEM), for example Figure 2.27a and Figure 2.29a,
- ABAQUS (FEM), for example Figure 2.27b and Figure 2.28b,
- GEFDyn (FEM), (Cuira, et al., 2013),
- Cast3m (FEM), (INNOTRACK, 2010),
- FOXTA (semi-analytical method), (Cuira, et al., 2013).

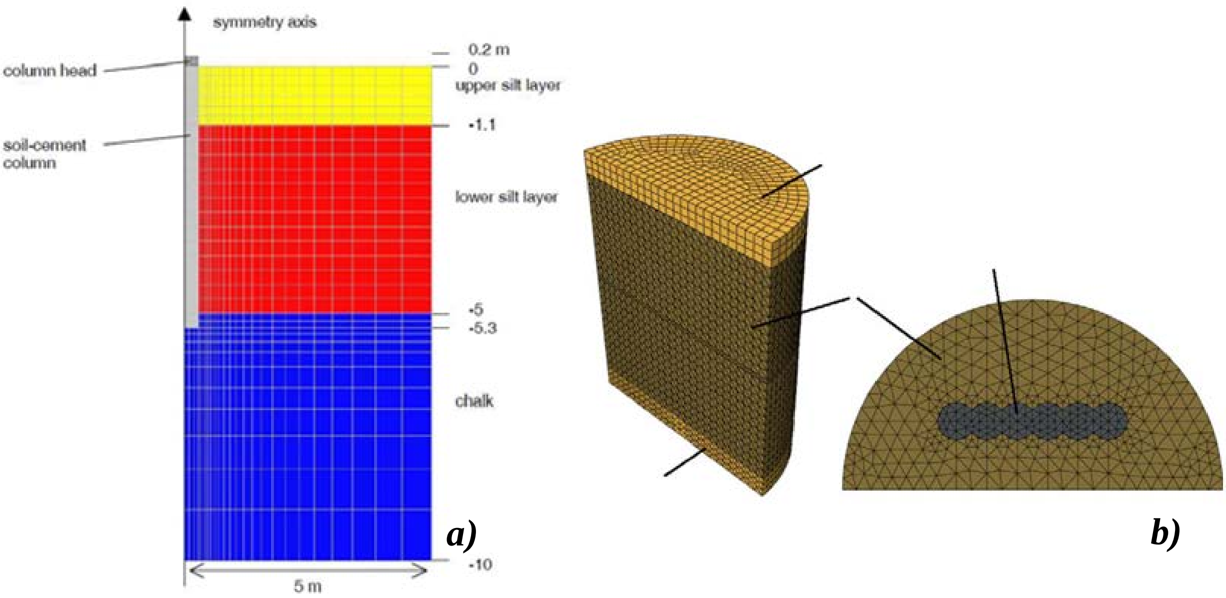

Figure 2.27 Models used in the numerical simulations: a) loading test of SM column (Le Kouby, et al., 2010), b) shear test of lime-cement columns (Larsson, et al., 2012)

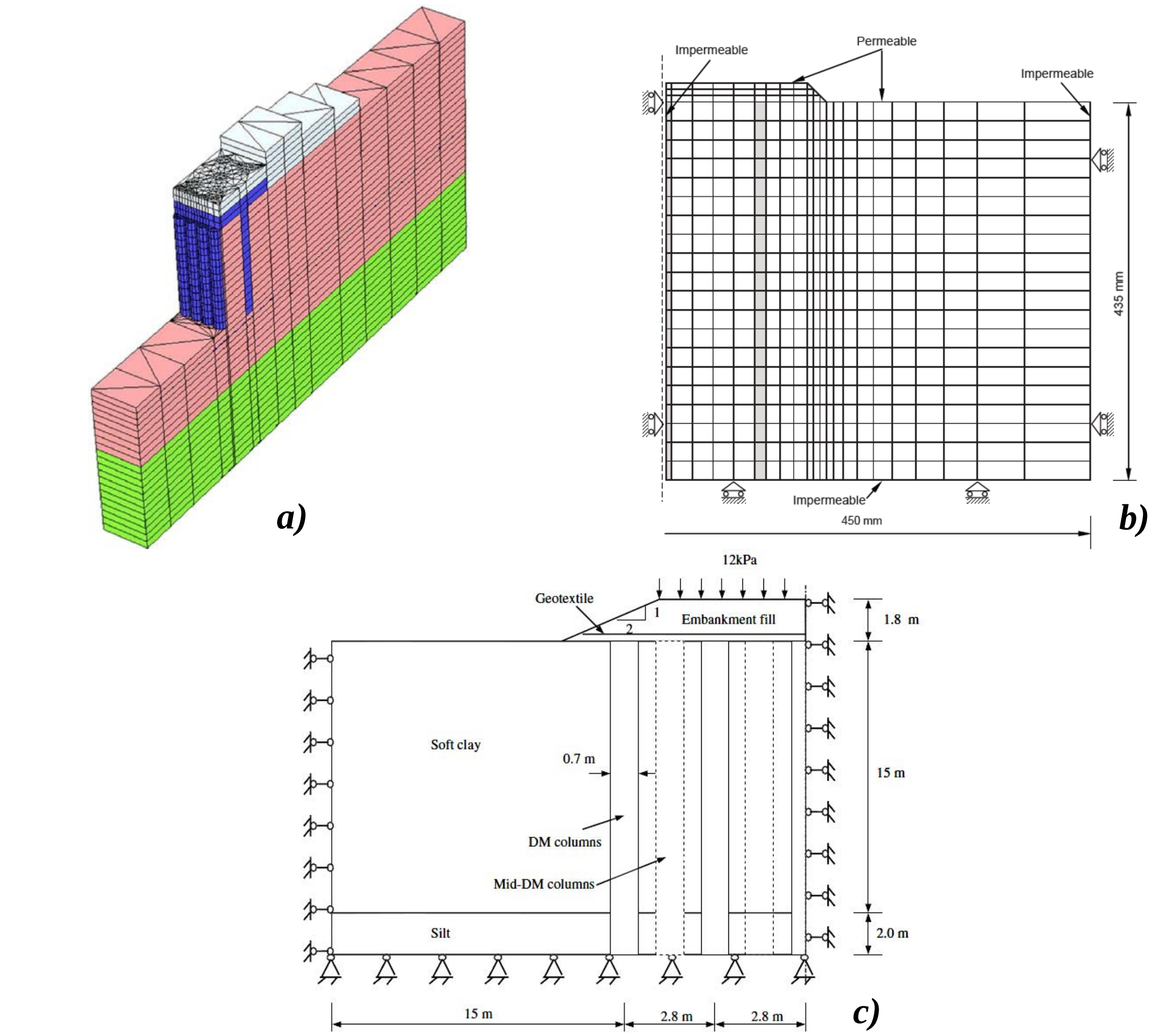

Figure 2.28 Models used in numerical simulations: a) SM wall in sand (Mun, et al., 2012), b) soft ground treated by SM method (Fang, 2006), c) stability of reinforced embankment (Han, et al., 2008)

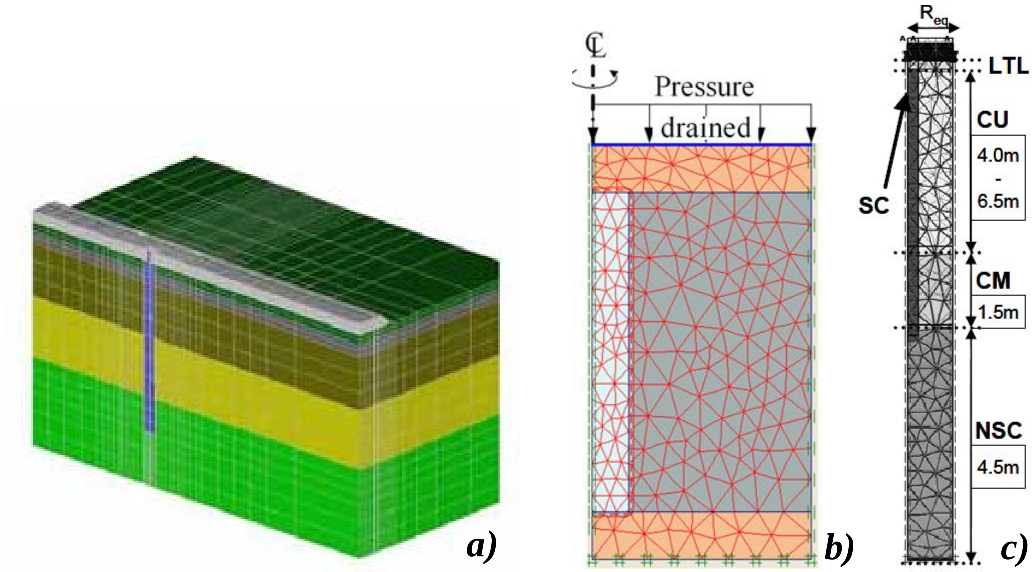

Figure 2.29 Finite element mesh used in the numerical simulations: a) reinforcement of the subgrade of an existing track (Le Kouby, et al., 2010), b) consolidation behaviour of SM column improved ground (Horpibulsuk, et al., 2012), c) underpinning of a floor slab (Melentijevic, et al., 2013)

Table 2.5 Summary of examples of cases analysed by numerical modelling reported by various authors.

Reference	Modelled case
Babasaki, et al. (Babasaki, et al., 1992)	liquefaction prevention of improved ground
Fukutake and Ohtsuki (Fukutake & Ohtsuki, 1995)	liquefaction prevention of improved ground
Ou, et al. (Ou, et al., 1996)	SM column type of ground improvement to minimize the ground settlement caused by deep excavation
Lambrechts and Roy (Lambrechts & Roy, 1997)	tunnel support
Nicholson et al (Nicholson, et al., 1998)	SM composite gravity wall
Broms (Broms, 1999)	reinforced embankment
Bergado et al. (Bergado, et al., 1999)	reinforced embankment
Fang (Fang, 2006)	consolidation behaviour of soft soil
Han et al. (Han, et al., 2007)	stability of reinforced embankment
Zheng, et al. (Zheng, et al., 2008)	composite foundation
Abusharar, et al. (Abusharar, et al., 2009)	consolidation behaviour of multi-column supported road embankment
Kitazume (Kitazume, 2009)	treated soft soil - centrifuge model
Le Kouby, et al. (Le Kouby, et al., 2010)	loading test of SM column and reinforcement of the subgrade of an existing track
Voottipruex et al (Voottipruex, et al., 2011)	SM column axially and laterally loaded
Venda Oliveira, et al. (Venda Oliveira, et al., 2011)	reinforced embankment on soft soil
Archeewa et al (Archeewa, et al., 2011)	support of the bridgehead
Larsson et al (Larsson, et al., 2012)	shear test of lime-cement columns
Horpibulsuk et al (Horpibulsuk, et al., 2012)	consolidation behaviour of reinforced embankment
Mun et al (Mun, et al., 2012)	SM wall in sand
Cuira et al (Cuira, et al., 2013)	static loading test of single SM column
Melentijevic, et al. (Melentijevic, et al., 2013)	underpinning of the existing floor slab

2.3.2. Modelled cases

Static loading test of SM column and its numerical simulations were studied by Cuira et al. (Cuira, et al., 2013). Three independent finite element simulations and two attempts by the semi-analytical method well represented observed behaviour of the column. Le Kouby, et al. (Le Kouby, et al., 2010) also analysed behaviour of SM column subjected to static, axial load. Their numerical model (Figure 2.27a) was able to correctly reproduce results of the *in situ* test in terms of total and shaft bearing capacity.

Fang (Fang, 2006) in his physical and numerical modelling focused on the consolidation behaviour and vertical bearing capacity of soft soil improved by SM method. In numerical part of the study, settlement and excess pore pressure, measured during the laboratory tests, were reproduced without significant discrepancies. It was found that soil modelled in the study might support relatively light structures, reclaimed fills or road embankments. Venda Oliveira, et al. (Venda Oliveira, et al., 2011) analysed numerically behaviour of an embankment built on soft soil reinforced with SM columns. In their study it was proven that this kind of reinforcement is extremely efficient while soil's consolidation time is significantly reduced. Similar conclusions can be found in work of Horpibulsuk et al (Horpibulsuk, et al., 2012). In his laboratory study and numerical simulation of the consolidation behaviour of composite ground, settlements observed for the treated soil were notably smaller and consolidation faster when the applied vertical stress was far below the failure stress.

Another way of using SM technique is presented by Le Kouby, et al. (Le Kouby, et al., 2010). They used it as a reinforcement of the subgrade of an existing track. The experimental and numerical studies confirmed that it is possible to improve soil without having to remove the track while, the ballast and subballast layers were not polluted by the grout.

Melentijevic, et al. (Melentijevic, et al., 2013) analysed numerically, the case history of the application of wet SM columns, executed by Springsol device, for underpinning of the existing floor slab. The slab of an industrial building settled due to different encountered post-constructive pathologies related to ground conditions.

The behaviour of excavations with the SM column type of ground improvement can be evaluated by simulating the actual distribution of the soil, columns and the excavation sequence using a 3D finite-element method (Ou, et al., 1996). However, this generally requires a large amount of computer storage and computation time because a fine finite element mesh is required. For this reason, a method for evaluating the overall material properties of the treated soil mass was proposed by Ou, et al. (Ou, et al., 1996), in which the treated soil volume was replace by a single material during analysis. By this means, the 3D analysis was then performed with less computer storage and computation.

Summary of examples of cases of ground, improved by SM, analysed by numerical modelling is presented in Table 2.5.

2.3.3. Constitutive models used to describe the Soil Mixing elements

It is very common to describe SM as isotropic elastic material, as it is usually assumed for concrete and steel elements in geotechnical analysis. It is important to emphasize that this type of constitutive model exhibits some important limitations. It does not allow simulating the yielding of the top of the SM element due to low confining stress and high loads and the bending failure caused by lateral movements of the columns, that appears at the elements located under the foundation or toe of the embankments ((Broms, 1999), (Kitazume, 2009)). Despite that, this model is usually adopted:

- Zheng et al. 2008 (Zheng, et al., 2008),
- Abusharar et al. 2009 (Abusharar, et al., 2009),
- Le Kouby et al. 2010 (Le Kouby, et al., 2010),
- Venda Oliveira et al. 2011(Venda Oliveira, et al., 2011).

Another approach, is to analyze SM elements with the Mohr-Coulomb failure criterion, since they have their origin in soil. However, this criterion also manifests some limitations, such as correct reproduction of the brittle mode of failure and post failure behaviour. The Mohr-Coulomb criterion was used by:

- Han et al. 2007(Han, et al., 2007),
- Voottipruex et al. 2011 (Voottipruex, et al., 2011),
- Horpibulsuk et al. 2012 (Horpibulsuk, et al., 2012),
- Mun et al. 2012 (Mun, et al., 2012),
- Melentijevic et al. 2013 (Melentijevic, et al., 2013),
- Cuira et al. 2013 (Cuira, et al., 2013).

An alternative approaches are to model SM columns with the Hardening Soil Model (Cuira, et al., 2013) or the Concrete damage plasticity model (Larsson, et al., 2012).

3. Constitutive models of soil

3.1. Introduction

Soils are, in general, heterogeneous materials. To understand the behaviour of any natural soil found in the world it is necessary to obtain several values by means of different procedures. These ones can be achieved either *in situ* or in laboratories. Soils' behaviour is strongly dependent on physical characteristics like: mineralogy, structure and grain size. The crucial factor that governs the behaviour of loose granular materials under low stresses is strain hardening. The behaviour of dense granular materials under high stresses is governed by stress-dilation (an ability to change volume due to stresses). A plasticity theory, developed by Dorris and Nemat-Nasser (Dorris & Nemat-Nasser, 1982), for finite deformation of granular materials, accounts for the true stress triaxiality, pressure sensitivity and dilation. They captured the effect of stress triaxiality by including the third deviatoric stress invariant in the yield function and the flow potential (DorMohammadi & Khoei, 2008). Furthermore, soils exhibit time dependent modifications, that makes them significantly rheological materials.

Various models and criteria, like: the Mohr-Coulomb, the Drucker-Prager, the Duncan Chang as well as the Cam Clay, have been proposed to describe accurately different aspects of soil behaviour. Some of them have been also applied in the finite element modelling for geotechnical engineering applications. It must be emphasized that none of available soil constitutive models is able to completely describe the complex behaviour of real soils under all conditions. The decision of using one or another constitutive law should be taken carefully considering its crucial impact on results of the modelling, in terms of obtained values and mode of failure. It is fundamental to know and take into account all model's limitations. Furthermore, a choice must be made in accordance with: the soil type, type of geotechnical problem and, most of the time, the possibilities of estimating constitutive parameters (Popa & Batali, 2010).

In this chapter attention is paid to the choice of constitutive laws which are relevant for the modelling of soils. The elastoplastic models with four failure criterions (the Mohr-Coulomb, the Classical Drucker-Prager, the Modified Drucker-Prager and the Modified Drucker-Prager with cap) are considered with their respective advantages and drawbacks. Afterwards, an example of loading test of a small scale shallow foundation is used in order to visualised differences in results obtained by simulations with some of the criterions.

3.2. The elastoplastic models

Modelling of geomaterials requires taking into consideration their plastic behaviour. It is usually done based on the concept of yield surface. Experimentally, the presence of the yield surface demonstrates at certain point by the lack of the linear stress-strain relation. In the stress space, it is represented by an impassable bound. Lanier (Lanier, 1988) has studied experimentally the shape of the yield surface in deviatoric plane. His findings have empirically confirmed theory formulated about two centuries before by Coulomb (Coulomb, 1776), where a linear relation exists between tangential stress τ and normal stress σ_N. Comparison between experimentally determined limit surface and Mohr-Coulomb surfaces is presented in Figure 3.1.

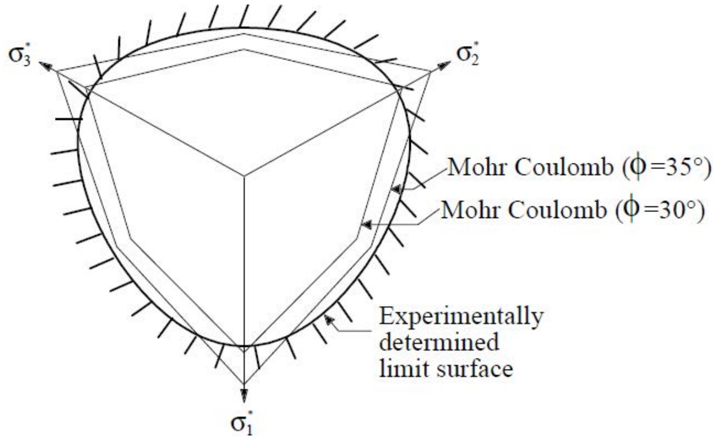

Figure 3.1 Deviatoric stress path with the Mohr-Coulomb criterion for ϕ = 30°and ϕ = 35° and limit surface determined by Lanier (Lanier, 1988), after (Barnichon, 1998)

3.2.1. The Mohr-Coulomb criterion (MC)

The elastic perfectly plastic model with the Mohr-Coulomb failure criterion is one of the most commonly used strength theory in geotechnical analysis, mainly for analyses of stability of slopes and foundations. The Mohr-Coulomb criterion can be considered as a contribution from Mohr and Coulomb (Nadai, 1950). Mohr's condition is based on the assumption that failure depends only on major σ_1 and minor σ_3 principal stresses. He proposed a criterion for the failure of materials on a plane which has a unique function with the normal stress on that plane of failure (Equation 3.1), where τ_{ff} is the shear strength and σ_{ff} the normal stress on the failure plane. With the use of the Mohr's circles, which is a two dimensional graphical representation of the state of stress at a point and the circumference of the circle is the location of points that represent the state of stress on individual planes, the failure criterion envelope was proposed. The Mohr envelope (Figure 3.2) is a line tangent to the maximum possible circles at different stresses and no circle could have part of it above that tangent curved line (Mohr, 1900).

$$\tau_{ff} = f(\sigma_{ff}) \qquad 3.1$$

Coulomb (Coulomb, 1776), in his investigations of retaining walls observed that soil shear strength was composed of two parameters cohesion c and internal friction angle ϕ. By plotting these data on a τ-σ diagram he obtained the straight line denoted by the Equation 3.2 and illustrated in Figure 3.3.

$$\tau = c + \sigma \tan \phi \qquad 3.2$$

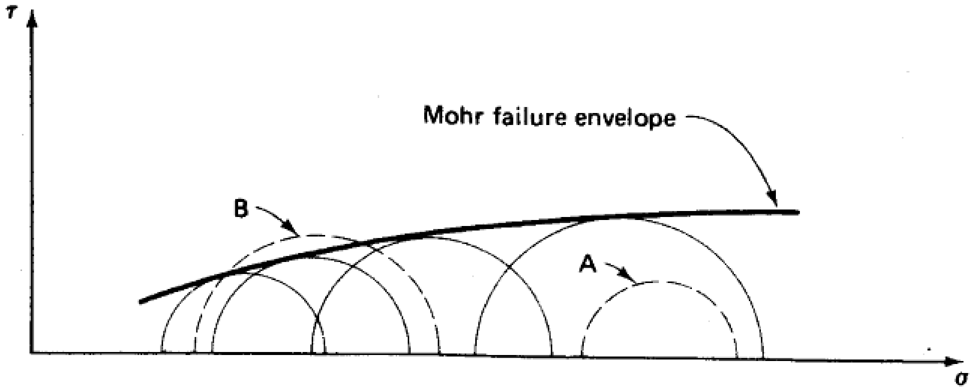

Figure 3.2 The Mohr circles at failure define the Mohr failure envelope (Holtz & Kovacs, 1981, p. 451)

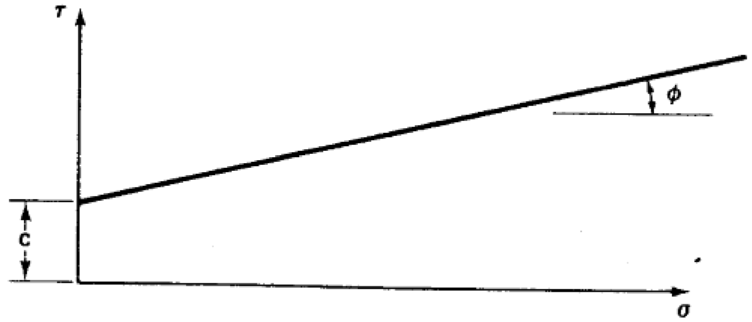

Figure 3.3 The Coulomb strength equation presented graphically (Holtz & Kovacs, 1981, p. 453)

It is unknown who combine these two theories as the first one. To avoid complications related to higher than first order equations, straight line was adopted to the theory. So, the curved Mohr failure envelope was approximated by the best fitting straight line over given stress range. Then the equation for that line in terms of the Coulomb strength parameters could be written. Thus, the Mohr-Coulomb criterion (MC) looks as in Equation 3.3. It can be expressed in a more general form, in terms of principal stresses at failure, as it is presented in Equation 3.4. Stresses in the soil element at failure and failure plane are presented in Figure 3.4b. The equation is acquired from relation illustrated in Figure 3.4a, namely sin ϕ = R / D. The Figure 3.4 shows that the location of the point of tangency of the Mohr failure envelope and the Mohr circle (τ_{ff} and σ_{ff}) are the stresses on the plane of maximum slope in the soil element. In the other words the ratio τ_{ff} / σ_{ff} is a maximum on this plane (Holtz & Kovacs, 1981).

$$\tau_f = c + \sigma_f \tan\phi \qquad 3.3$$

$$(\sigma_{1f} - \sigma_{3f}) = (\sigma_{1f} + \sigma_{3f}) \sin\phi + 2c \cos\phi \qquad 3.4$$

Analysing three dimensional state of stress it needs to be remembered that in MC criterion, the intermediate principle stress σ_2 has no effect on conditions at failure. Since by definition σ_2 lies between the major and minor principal stresses, the Mohr circles for the three principal stresses look like those shown in Figure 3.5. No matter what is the value of the σ_2, it has no influence on conditions at failure.

Geometrical representation of criterion in the principal stresses space is an irregular hexagonal pyramid (Figure 3.6). The shape of the surface in deviatoric plane is controlled by the friction angle of the material (Figure 3.7). For all materials, the range of its friction angles is varied between 0° and 90°. In case of ϕ = 0° the MC reduces to the pressure-independent Tresca model with a perfectly hexagonal deviatoric section. In the case of ϕ = 90° the criterion reduces to the "tension cut-off" Rankine model with a triangular deviatoric section.

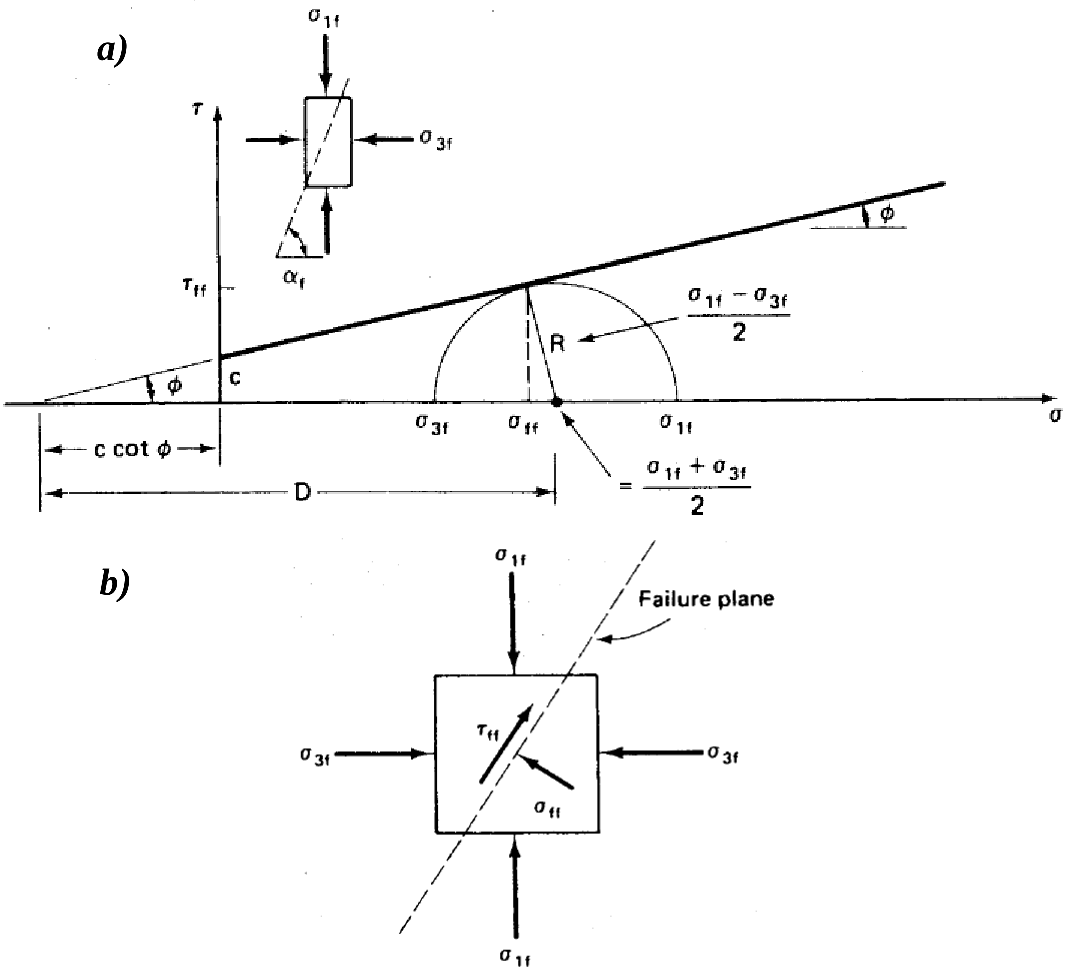

Figure 3.4 a) The Mohr-Coulomb strength envelope with one Mohr circle at failure (Holtz & Kovacs, 1981, p. 456), b) soil element at failure, showing the principal stresses and the stresses on the failure plane (Holtz & Kovacs, 1981, p. 450)

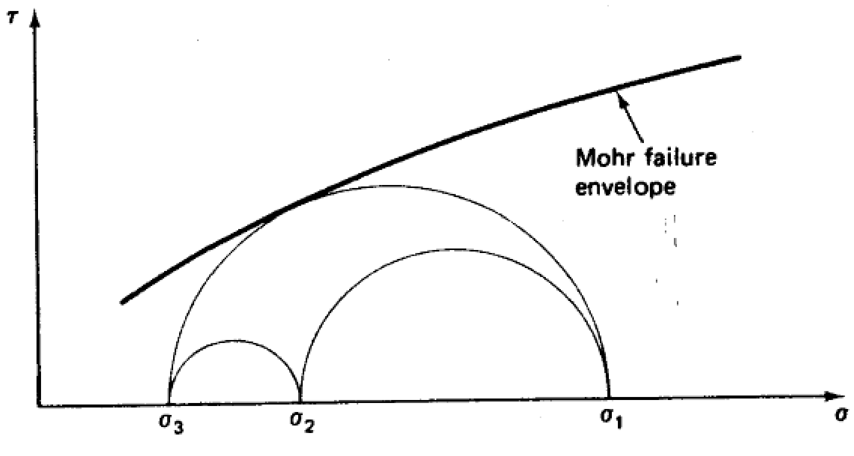

Figure 3.5 Mohr circles for a three dimensional state of stress (Holtz & Kovacs, 1981, p. 457)

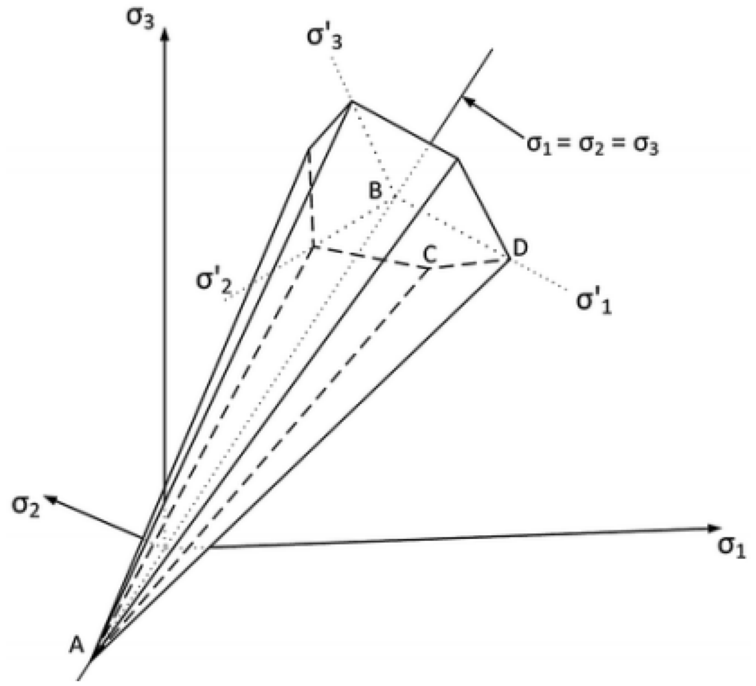

Figure 3.6 Limit surface for the Mohr-Coulomb criterion in deviatoric plane (Labuz & Zang, 2012)

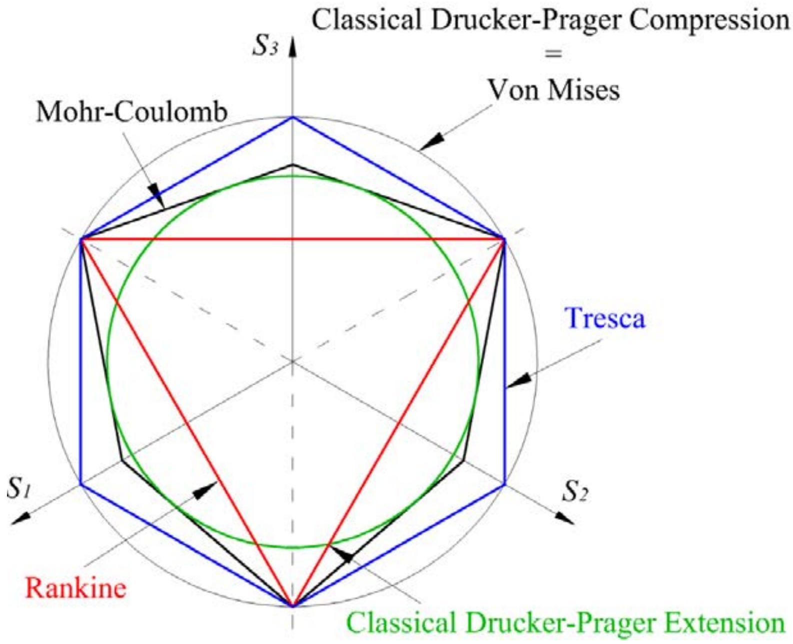

Figure 3.7 The Mohr-Coulomb yield surface in deviatoric plane after (ABAQUS, 2010)

The main benefits coming from usage of MC criterion are: simplicity of its equation, small number of parameters whilst provided results are keeping reasonable accuracy. Apart of advantages of the criterion, its user needs to deal with two important limitations, which limits its wider application. Firstly, the major principal stress σ_1 is independent of the intermediate principal stress σ_2. As mentioned before, only the major and the minor principal stresses are taken into consideration in analyses. It leads to underestimation the yield strength of material due to the fact that the biaxial compressive strength is always higher than the uniaxial compressive strength for geomaterials. It has been proven by the experimental investigation. Results reflecting the influence of σ_2 on the behaviour of material in many cases, have been presented by Kikumoto et al. (Kikumoto, et al., 2008), Mongi (Mogi, 1971), Al-Ajmi and Zimmerman (Al-Ajmi & Zimmerman, 2005) and Colmenares and Zoback (Colmenares & Zoback, 2002). Secondly, an irregular hexagonal section of the yield cone in deviator plane induces the convergence problems in flow theory, due to its six sharp corners (Jiang & Xie, 2011).

3.2.2. The Drucker-Prager criterion (DP)

An alternative solution to overcome difficulties related to limitations of MC criterion has been proposed by Drucker and Prager. In this section two kinds of the Drucker-Prager criterion are presented: the classical formulation and the modified one.

3.2.2.1. Classical criterion

In 1952, the Drucker-Prager criterion (DP), known also as the Extended Von Mises criterion has been proposed (Drucker & Prager, 1952). Since then, it is widely used in geotechnical engineering calculations to predict failure strength. It is also employed for plastic potential in continuum damage mechanic model. Its undeniable advantage is taking into account intermediate principal stress σ_2. The yield function of the linear DP can be expressed as a linear relationship between the first stress tensor invariant I_1 and the second deviatoric stress tensor invariant J_1 (Appendix A).The formula can be found in Equation 3.5. Where α and k are material constants. Their values can be established by the relations to friction angle and cohesion. Basically, there are two possibilities of approximation of the Mohr-Coulomb hexagonal section: internal circle corresponds to triaxial extension conditions and external circle corresponds to triaxial compression (Figure 3.8). Also, exist some other ways of approximation. They can be find in paper presented by Jiang and Xie (Jiang & Xie, 2011), however they are not the most commonly used and are not going to be analysed in this thesis.

By choosing the compression circle, the material friction angle is assumed to be equalled to its value in compression conditions $\phi = \phi_C$. The criterion parameters are calculated according to Equation 3.6 and Equation 3.7.

$$F = \sqrt{J_2} - \alpha I_1 - k \qquad 3.5$$

$$\alpha = \frac{2\, sin\, \phi_c}{\sqrt{3}(3 - sin\, \phi_c)} \qquad 3.6$$

$$k = \frac{6c\, cos\, \phi_c}{\sqrt{3}(3 - sin\, \phi_c)} \qquad 3.7$$

Several studies of DP criterion, like Barnichon (Barnichon, 1998), Desrues (Desrues, 2002), Cudny and Binder (Cudny & Binder, 2005), have been carried out. It is proven that the difference between approximations (Figure 3.8) leads to situations when material shear strength is overestimated or underestimated (Cudny & Binder, 2005). To visualise the scale of the problem material with friction angle equal to 30.0° is investigated. The shear strength value, approximated with compression circle (Figure 3.8, external one), is overestimated in all cases other than triaxial compression. In the extreme case, triaxial extension; its value corresponds to shear strength calculated with frictions angle equals to 48.6°. In case of taking extension circle (Figure 3.8, internal one), the shear strength is underestimated in all cases except triaxial extension. The value of strength for the extreme case corresponds to friction angle equal to 22.0° (Cudny & Binder, 2005). It agrees with analytical studies carried out by Desrues (Desrues, 2002), who came out with Equation 3.8 where ϕ_E and ϕ_C are soil friction angles for triaxial extension and triaxial compression, respectively. As it is known, the material friction angle must be a number between $0° \leq \phi_{E/C} \leq 90°$, what implies $0 \leq \sin \phi_{E/C} \leq 1$. In order to calculate maximal value $\sin \phi_E = 1$ is used in Equation 3.8. It leads to $\sin \phi_C = 3/5$, where $\phi_C \approx 36.8°$. Relations presented in Figure 3.9 can be concluded that difference between approximations increases with the increase of friction angle and DP criterion cannot be used for materials with friction angle $\phi > 36.8°$ and, to avoid over/underestimation, should not be used for friction angle $\phi > 10°$.

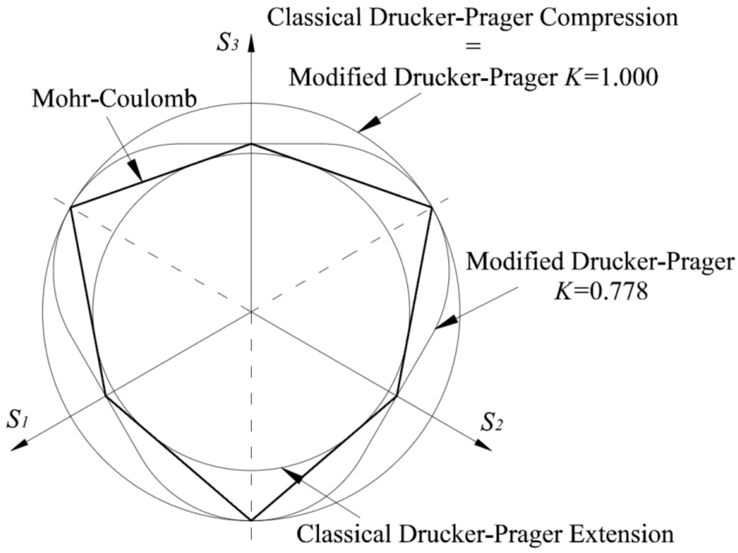

Figure 3.8 Yield surfaces in the deviatoric plane

$$sin\,\phi_E = \frac{3\,sin\,\phi_c}{3 - 2\,sin\,\phi_c} \quad 3.8$$

$$\phi_E = sin^{-1}\left(\frac{3\,sin\,\phi_c}{3 - 2\,sin\,\phi_c}\right) \quad 3.9$$

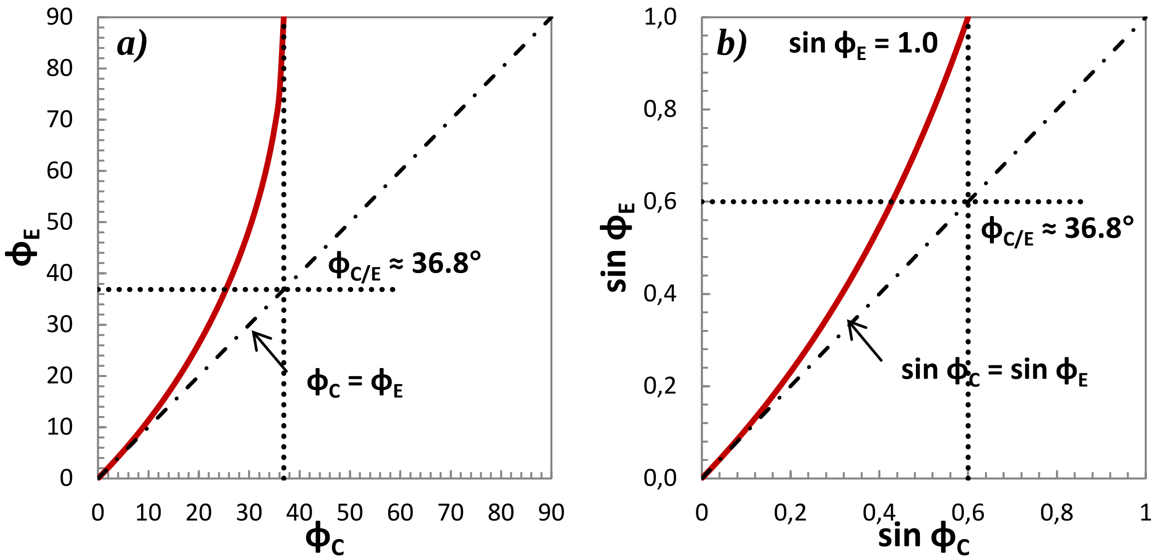

Figure 3.9 a) evolution of ϕ_E as a function of ϕ_C – relation according to Equation 3.9, b) evolution of sinϕ_E as a function of sinϕ_C – relation according to Equation 3.8, after (Desrues, 2002)

3.2.2.2. The modified criterion

3.2.2.2.1. *Formulation and parameters*

The reason of using modification, which brings on additional parameter, added to the classical criterion, is connected with mentioned above significant divergence. In ABAQUS (ABAQUS, 2010), the modified Drucker-Prager criterion (MDP) is introduced. It is defined by Equation 3.10 and can be illustrated in p-t plane (Figure 3.10) and in deviator plane (Figure 3.8). The *p* parameter is the equivalent pressure stress, *β* and *d* are MDP shear parameters and *t* is defined by Equation 3.11. Where *q* is the von Mises equivalent stress, J_3 is the third invariant of the deviator stress and *K* is the modification – flow stress ratio.

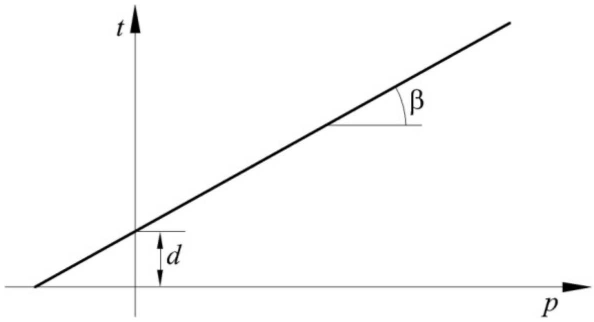

Figure 3.10 The modified Drucker-Prager yield surface in p-t plane (ABAQUS, 2010)

$$F_S = t - p\,tan\,\beta - d \qquad 3.10$$

$$t = \frac{q}{2}\left[1 + \frac{1}{K} - \left(1 - \frac{1}{K}\right)\left(\frac{J_3}{q}\right)\right]^3 \qquad 3.11$$

The flow stress ratio K, represents the ratio between the yield stress in triaxial tension to the yield stress in triaxial compression (Figure 3.11). It controls the dependence of the yield surface on the value of the intermediate principal stress. To ensure that the yield surface remains convex, it is required that $0.778 \leq K \leq 1.000$ (Figure 3.8). The $K = 1.000$, when the triaxial tension is assumed to be equal to the triaxial compression.

The MDP shear parameters β and d can be obtained from MC parameters, cohesion c and friction angle ϕ. Equations 3.12 and 3.13 express formulas for two dimensional, plane strain models. Formulas for parameters in three dimensional and axisymmetric types of modelling are presented by Equations 3.14 and 3.15. The ψ stands for a dilation angle.

$$tan\,\beta = \frac{9\,sin\,\phi}{tan\,\psi\,sin\,\phi + \sqrt{3(9 - tan^2\psi)}} \qquad 3.12$$

$$d = \frac{c\,cos\,\phi\,(9 - tan\,\beta\,tan\,\psi)}{\sqrt{3(9 - tan^2\psi)}} \qquad 3.13$$

$$tan\,\beta = \frac{6\,sin\,\phi}{3 - sin\,\phi} \qquad 3.14$$

$$d = \frac{18c\,cos\,\phi}{3 - sin\,\phi} \qquad 3.15$$

3.2.2.2.2. *Influence of the flow stress ratio K*

In order to explain in a better way the influence of this parameter, an axisymmetric study has been carried out. Geometry and mesh of the analysed shallow foundation can be found in Figure 3.12a. Properties of used soil, 'dense', dry Hostun sand, are presented in Chapter 4 in Table 4.16 and Table 4.17. Studied foundation has been loaded by imposed displacement. The example illustrates results, obtained for two edge values of K: 0.778 and 1.000. As it can be seen in Figure 3.12b, the flow stress ratio has significant influence on final results. For $K = 1.000$, which refers to compression approximation circle, the more the displacement increase, the greater the difference between two predictions. The value of force is overestimated and the difference increase with the increase of displacement. Initially, till about 3 mm displacement, the bearing capacities predicted by both cases are identical. According to this results, concerning behaviour of granular materials and limitation presented in previous section, the only possibility for soil is using $K = 0.778$.

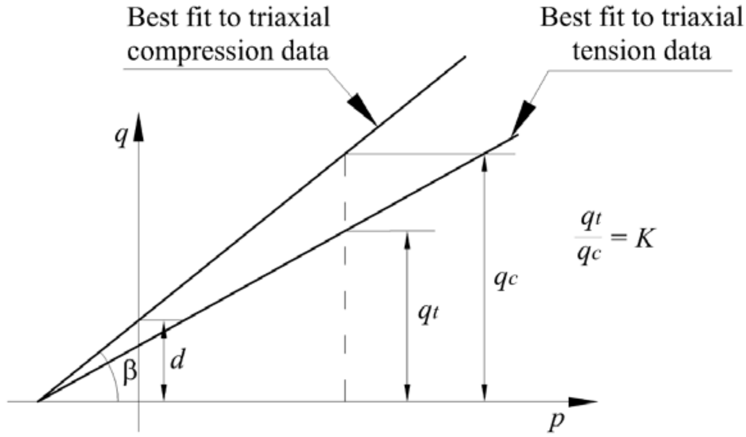

Figure 3.11 Influence of the modification - flow stress ratio K (ABAQUS, 2010)

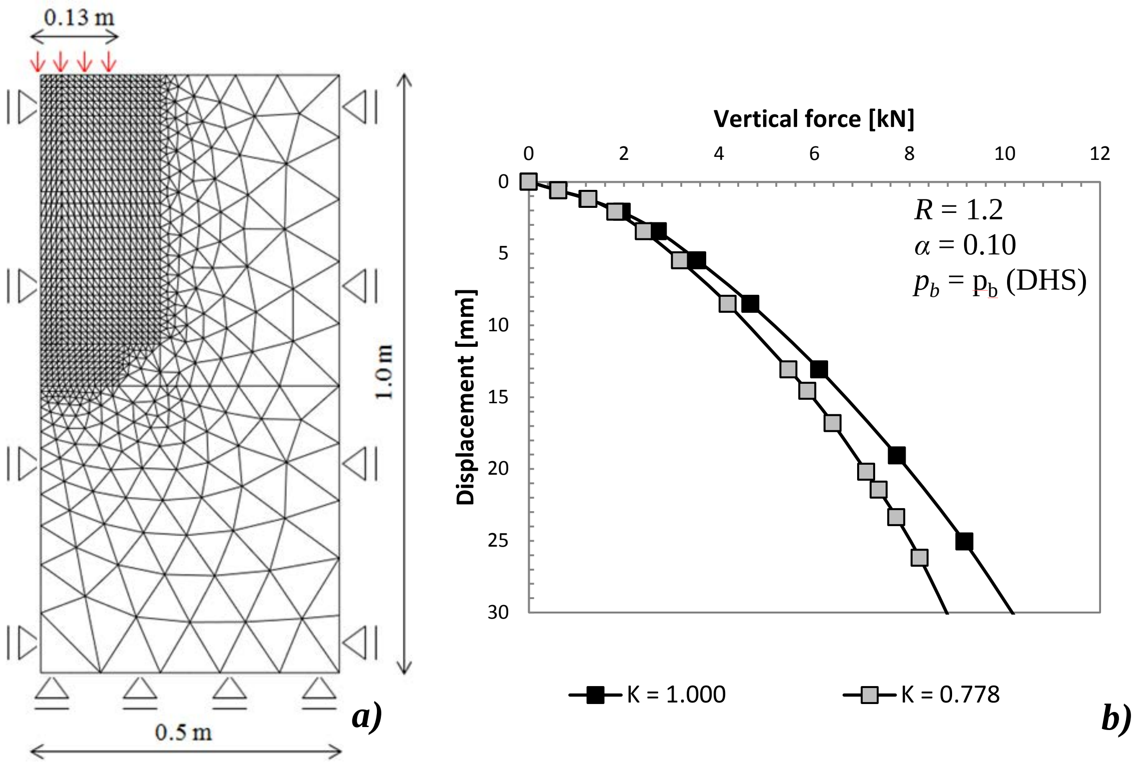

Figure 3.12 a) geometry and mesh of the numerical model used to investigate influence of flow stress ratio K, b) results of the modelling

3.2.2.2.3. *Verification study of transition equations*

In order to verify the provided equations (Equations 3.12 - 3.15), a simple study has been carried out in accordance with Carter, et al. (Carter, et al., 1977) analysed case. An inelastic response of a homogeneous granular material subjected to uniform extension or compression in plane strain has been performed in ABAQUS finite element code. Results for these cases were afterwards compared with results given in the paper (Carter, et al., 1977). The two dimensional model, presented in Figure 3.13, has been analysed for two sets of parameters (Table 3.1). The specimen has been initially stress-free and made of an elastic, perfectly plastic material. It has been also assumed that the cohesion is twice the Young's modulus for the extension test and 10% of the Young's modulus in the compression test. It has been necessary to relate ϕ and c to the material parameters used in model with the MDP criterion by Equations 3.12 and 3.13. The first equation gives β = 40°. The second equation results with d = 86.47 MPa (for 60 MPa) for the extension case and d = 4.32 MPa (for 3 MPa) for the compression case. Considered material has been analysed with: associated MC and associated MDP criteria. Uniform extension / compression of the soil sample has been specified by displacement boundary conditions. In all analysed cases, flow stress ratio has been assumed as K = 0.778.

The results of calculations are shown in Figure 3.14a, for extension and in Figure 3.14b for compression. The solutions obtained with MDP agree well with the results presented by Carter, et al. (Carter, et al., 1977). This has been expected since the MDP parameters are matched to the MC parameters under plane strain conditions. The differences between the associated ABAQUS MC solutions and Carter's solutions are due to the fact that the ABAQUS model with MC criterion uses a different flow potential – in order to deal with, mentioned in previous paragraph, sharp corners of the yield surface. The numerical model with MC uses a smooth flow potential that matches the theoretical Mohr-Coulomb surface only at the triaxial extension and compression meridians (not in plane strain).

Table 3.1 Parameters of the granular material used in verification study (Carter, et al., 1977)

Parameter	Compression	Extension
Young's modulus E [MPa]	30	30
Poisson's ratio ν [-]	0.3	0.3
Friction angle ϕ [°]	30	30
Dilation angle ψ [°]	30 ; 22	30 ; 22
Cohesion c [MPa]	10% E = 2	2 x E = 60

However, ABAQUS MC solution that match exactly Carter's plane strain solution have been also obtained. The model with the theoretical MC criterion can be matched under plane strain conditions to an associated model with the linear MDP criterion with the flow potential defined by Equation 3.16. This match implies that under plane strain conditions the flow of the model with the theoretical MC criterion can be alternatively calculated by the corresponding flow of the MDP with the dilation angle $\psi = \beta$, as computed before. Therefore, we can match the flow potential of the ABAQUS MC criterion to that of the MDPC one. Matching between these two forms of flow potential can be done by the relation presented in Equation 3.17 (ABAQUS, 2010). Using the equation leads to dilation angle ψ = 22° in the ABAQUS MC criterion.

$$G = q - p\, tan\, \beta \tag{3.16}$$

$$tan\, \psi = \frac{3 - sin\, \phi}{6\, cos\, \phi} tan\, \beta \tag{3.17}$$

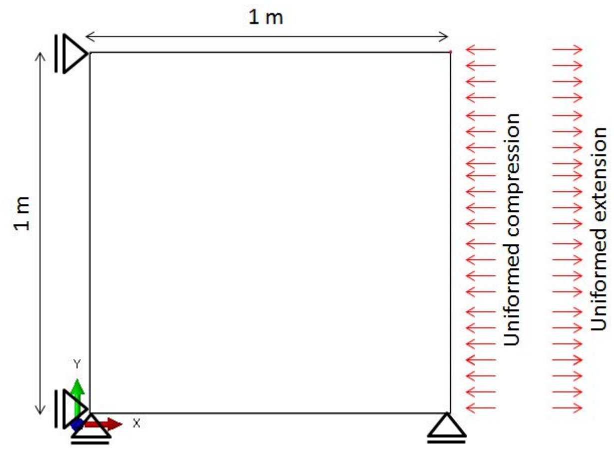

Figure 3.13 The one element model of a study performed in order to verify transition equations between MC and MDP parameters

Results of the modelling are presented in Figure 3.14. Both cases, extension and compression, are presented in a way, where P refers to applied force, l_0 = 1 m is a dimension of the soil sample and p stands for reduction ratio. The p takes value between 1 and 30 for extension, and between 1.00 and 0.48 for compression test. In both tests, a solid line with black markers and a black solid line represent results obtained with associated MC when $\psi = \phi$ = 30°. The first one is a result from the literature. The second one is obtained from calculations. Difference between them illustrates influence of the flow definition. After modification of the dilation angle, ABAQUS MC solution matches well with Carter's result as well as values obtained from model with MDP criterion. It proves that transition equations for β and d are correct and bring parameters which must be used in modelling with this criterion.

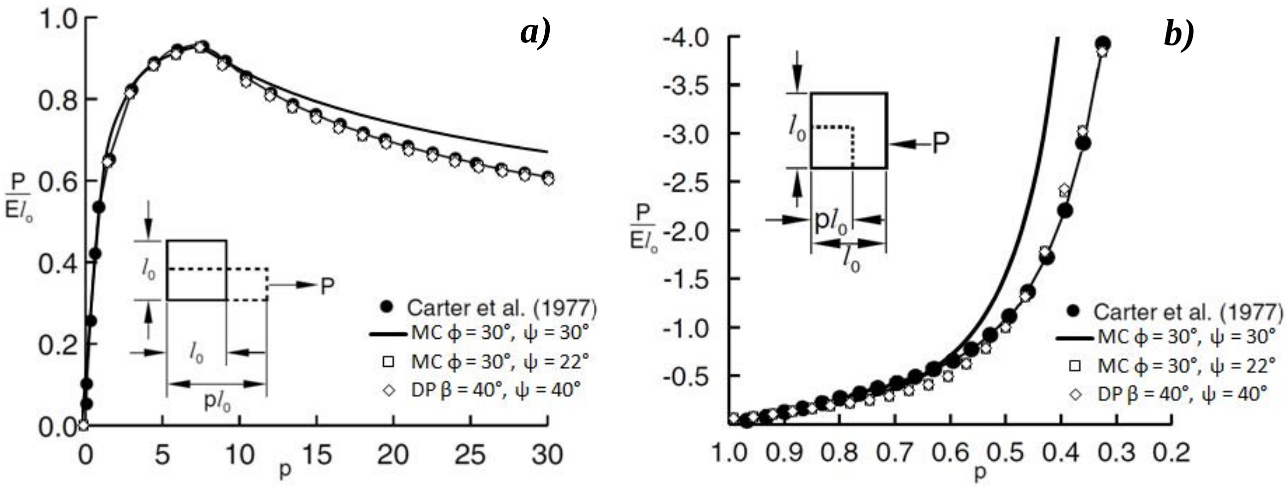

Figure 3.14 Results of a transition equations verification study: a) extension, b) compression

3.2.3. Modified Drucker-Prager criterion with cap

3.2.3.1. Cap

Studies of the behaviour of sands and silts like Kohler and Hofstetter (Kohler & Hofstetter, 2007) or investigations of sands by Pestana, et al. (Pestana, et al., 2002), show that to be able to reproduce correctly soil behaviour, adding cap and its evolution, defined by strain hardening law, seems to be the only solution. The cap in the model serves two main purposes. Firstly, it bounds the yield surface in hydrostatic compression, thus providing an inelastic hardening mechanism to represent plastic compaction. Secondly, it helps to control volume compaction when the material yields in shear by providing hardening as a function of the inelastic volume increase created as the material yields on the shear failure and transition yield surfaces. The cap surface hardens or softens as a function of the plastic volumetric strain: volumetric plastic compaction (when yielding on the cap) causes hardening, while volumetric plastic dilation (when yielding on the shear failure surface) causes softening (Helwany, 2007).

Models, where a cap is included, like the most commonly used Hardening Soil Model (Schanz, et al., 1999), consist of two yield surfaces; a shear surface and cap surface, which has an elliptical shape. The first one controls the ultimate shear strength of material and the cap surface captures the hardening behaviour of material under compression. These models can be utilized to construct the suitable phenomenological constitutive models which capture the major features of the response of geological and frictional materials (DorMohammadi & Khoei, 2008).

3.2.3.2. Formulation of the model

The cap criterion has been transformed and upgraded over years ((Chen & Mizuno, 1990) and (Sandler, 2005)). One of the most commonly used version of the model, the Modified Drucker-Prager with cap (MDPC) (Resende & Martin, 1985), has been implemented into ABAQUS software. The yield surface of this constitutive law consists of three parts (Figure 3.15): a shear failure surface, alike as in classical criterion, an elliptical cap, which intersects p axis at a right angle and a smooth transition region between the shear failure surface and the cap, purely for helping the numerical implementation (ABAQUS, 2010).

The constitutive equations for the cap (Equation 3.18) describe behaviour in hydrostatic compression, with hardening occurring when plastic deformation takes place. If, however, the Modified Drucker-Prager cone and the cap are coupled through the plastic volumetric strain, the cap softens when plastic volumetric strain occurs on the cone. When the cap-cone vertex overtakes the stress point, plastic deformation in pure shear becomes possible. The introduction of the cap thus overcomes, to some extent, the principal difficulties in MDP criterion. The major concern is behaviour when yielding occurs simultaneously on MDP cone and the cap. The yield surfaces are coupled, in the sense that the cap position depends on the total plastic volumetric strain produced on MDP and cap surfaces, among other parameters. The functional form of the yield surfaces, with full coupling and the assumption of an associated flow rule, is sufficient to permit the complete behaviour during simultaneous yielding to be derived.

The law uses associated flow ($\psi = \beta$) in the cap surface and non-associated flow ($\psi \neq \beta$) in the shear failure and transition region. Each part of the yield surface is described by the separated equation. Hence, the shear surface – Equation 3.10, the cap – Equation 3.18 and transition region – Equation 3.19. Parameters of the MDPC criterion are presented in sections below. The yield surface in deviatoric plane, in terms of cross section, stays the same as the one for MDP (Figure 3.8). Three and two dimensional visualisation of the density dependent model's yield surface is presented in Figure 3.16.

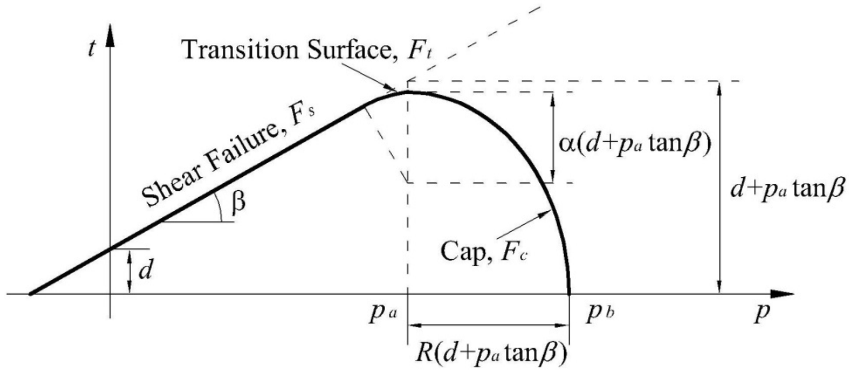

Figure 3.15 The Modified Drucker-Prager with cap criterion yield surface (ABAQUS, 2010)

$$F_c = \sqrt{(p-p_a)^2 + \left(\frac{Rt}{1+\alpha-\dfrac{\alpha}{cos\,\beta}}\right)^2} - R(d + p_a\, tan\,\beta) \qquad 3.18$$

$$F_t = \sqrt{(p-p_a)^2 + \left[t - (d + p_a\, tan\,\beta)\left(1-\frac{\alpha}{cos\,\beta}\right)\right]^2} - \alpha(d + p_a\, tan\,\beta) \qquad 3.19$$

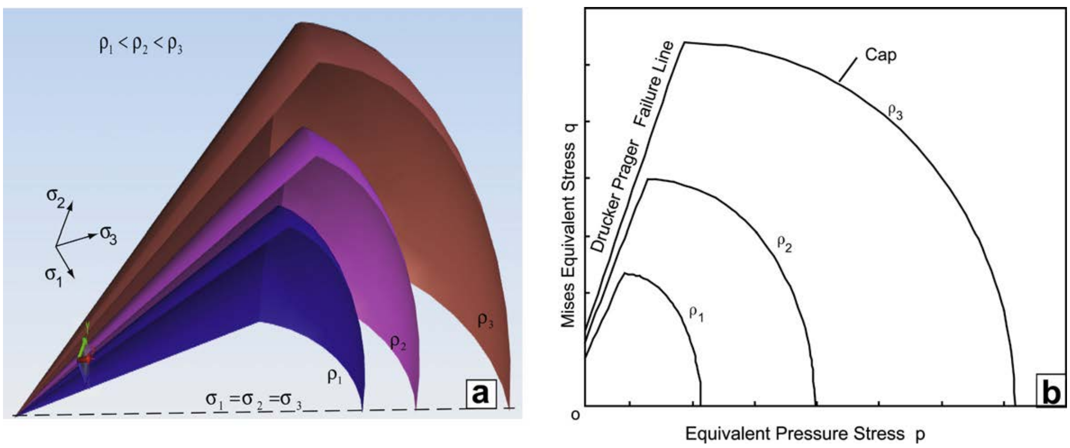

Figure 3.16 Schematics of a density-dependent the Modified Drucker-Prager with cap model: a) 3D yield surfaces in principal stress plane b) 2D representation (Han, et al., 2008)

3.2.3.3. Model parameters

The MDPC criterion is characterized by 7 parameters. Three of them are in common with MDP: shear parameters β and d (calculated base on the material friction angle and cohesion – Equations 3.12 - 3.15), and flow stress ratio K. Four other independent parameters are: cap eccentricity R, parameter of transition zone α, an initial cap yield surface position $\varepsilon^{pl}{}_{vol|0}$ and hydrostatic compression yields stress p_b. There is one more additional dependant parameter p_a, defined by Equation 3.20. It determines the beginning of the cap (Figure 3.15). The impact of each parameter on the numerically predicted borne by the soil force is illustrated by the example. The same axisymmetric model as in demonstration of the influence of the flow stress ratio case has been used in parametric study (Figure 3.12a). Properties of 'dense', dry Hostun sand, are presented in Table 4.16 and Table 4.17. In all analysed cases parameter K is assumed to be 0.778.

$$p_a = \frac{p_b - Rd}{1 - R \tan \beta} \tag{3.20}$$

3.2.3.3.1. *Cap eccentricity R*

The parameter R, cap eccentricity, represents the curvature of the elliptic cap part of the yield surface. The R's value must be taken between 0.0001 and 1000.0. Results of the study on the influence of different cap eccentricity on borne force are presented in Figure 3.17. The R varies between 0.8, 1.2 and 2.0. Another model parameters are assumed as: α = 0.10, $\varepsilon^{pl}{}_{vol}|_0$ = 0 and p_b is defined as a function of plastic volumetric strain according to soil hardening curve for analysed 'dense' Hostun sand ρ_d = 1500 kg/m^3 (DHS) (Figure 4.16). Figure 3.17 depicts three curves. As can be seen, in case of R = 2.0 the increase of force is the slowest. The lowest value of final borne force is obtained for this case. The quickest force increases for R = 0.8. The more the displacement increases, the greater the difference between results obtained with R = 2.00 and the other ones appears. At the beginning of the loading process, till about 1 mm, all three curves are indistinguishable, after nonlinearities start to appear in case of R = 2.0. Curves representing models with R = 0.8 and R = 1.2 are exact till about 3 mm and then the less steep curve shape can be observed for R = 1.2. It can be concluded that the higher the value of R, the more flat the curve shape, what corresponds to lower value of borne force.

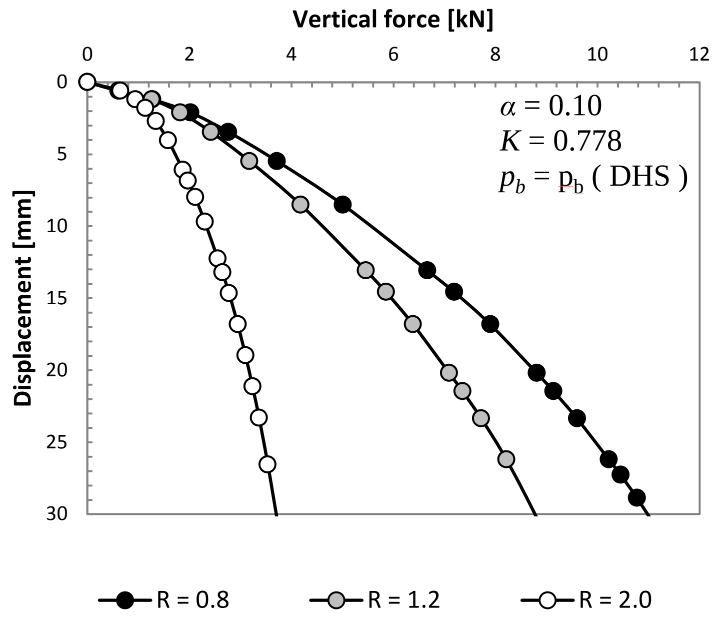

Figure 3.17 The influence of different cap eccentricity, R, on behaviour of loaded soil

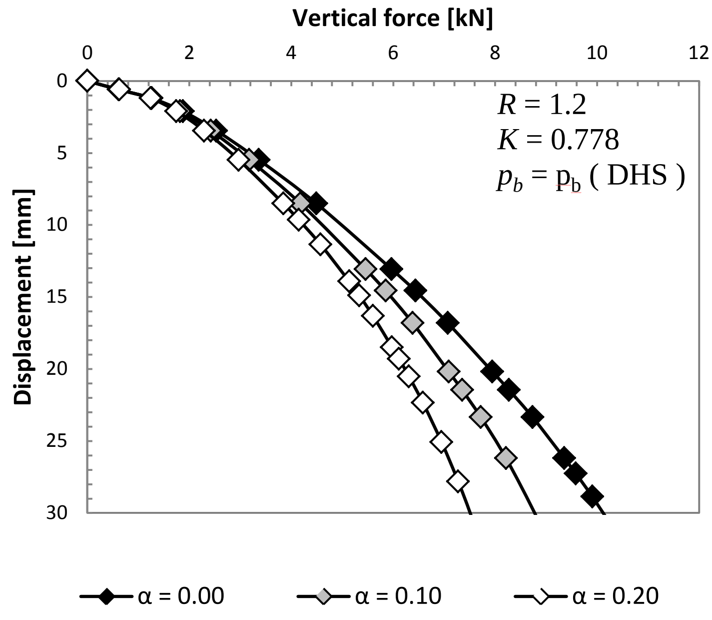

Figure 3.18 The influence of different transition region parameter, α, on behaviour of loaded soil

3.2.3.3.2. *Transition region parameter α*

The α is a parameter used to define a smooth transition region. It is a small number, typically varies between 0.01 and 0.1. The influence of its different values is presented in Figure 3.18. Rest of model's parameters are assumed as previously. This time also three different values of the parameter have been investigated: α = 0.00, α = 0.10 and in order to emphasise the impact α = 0.20. The beginnings of all curves are almost the same until about 5 mm, afterwards, the increase of force, for α = 0.00, starts to be faster than for the others. The more the displacement increases, in case of the calculation with α = 0.20, the greater the difference between this one and other numerical predictions. Firstly, the plastic behaviour appears for the highest α. It is illustrated in the graph by the earliest achieved plateau. The highest values of force are obtained for α = 0.00. In this case additional difficulty needs to be kept in mind. The α equals to 0.00, means lack of transition region, what implies direct contact between the shear surface and the cap. This sharp connection is highly unnatural, moreover creates problems with integration, which leads to convergence problems. Due to these obstacles, case when α = 0.00 is not recommended. According to obtained results, it can be deduced that predictions are sensitive to even very small changes of the transition region parameter. Furthermore, the increase of α causes a decrease of the final value of the borne force.

3.2.3.3.3. *Hardening parameters*

The last but not least analyzed parameter is hydrostatic compression yield stress, p_b. It can be visualised as a forehead of the cap surface (Figure 3.15). p_b is an evolution parameter that is defined by hardening/softening of a material. The hardening law has been chosen in accordance with the findings presented by White and Bolton (White & Bolton, 2004). Their investigation of the penetration mechanism of a displacing pile in two kinds of sand corresponds qualitatively with predictions based on strain path method, proposed by Baligh (Baligh, 1985). Moreover, the volumetric behaviour associated with sand has been captured. It has been found that a consequence of the piles penetration is a highly compressed region of soil below the pile tip (Figure 3.19a), called by the authors a 'nose cone' (Figure 3.19b). Stress–volume paths of sand beneath pile tip are presented in Figure 3.19c.

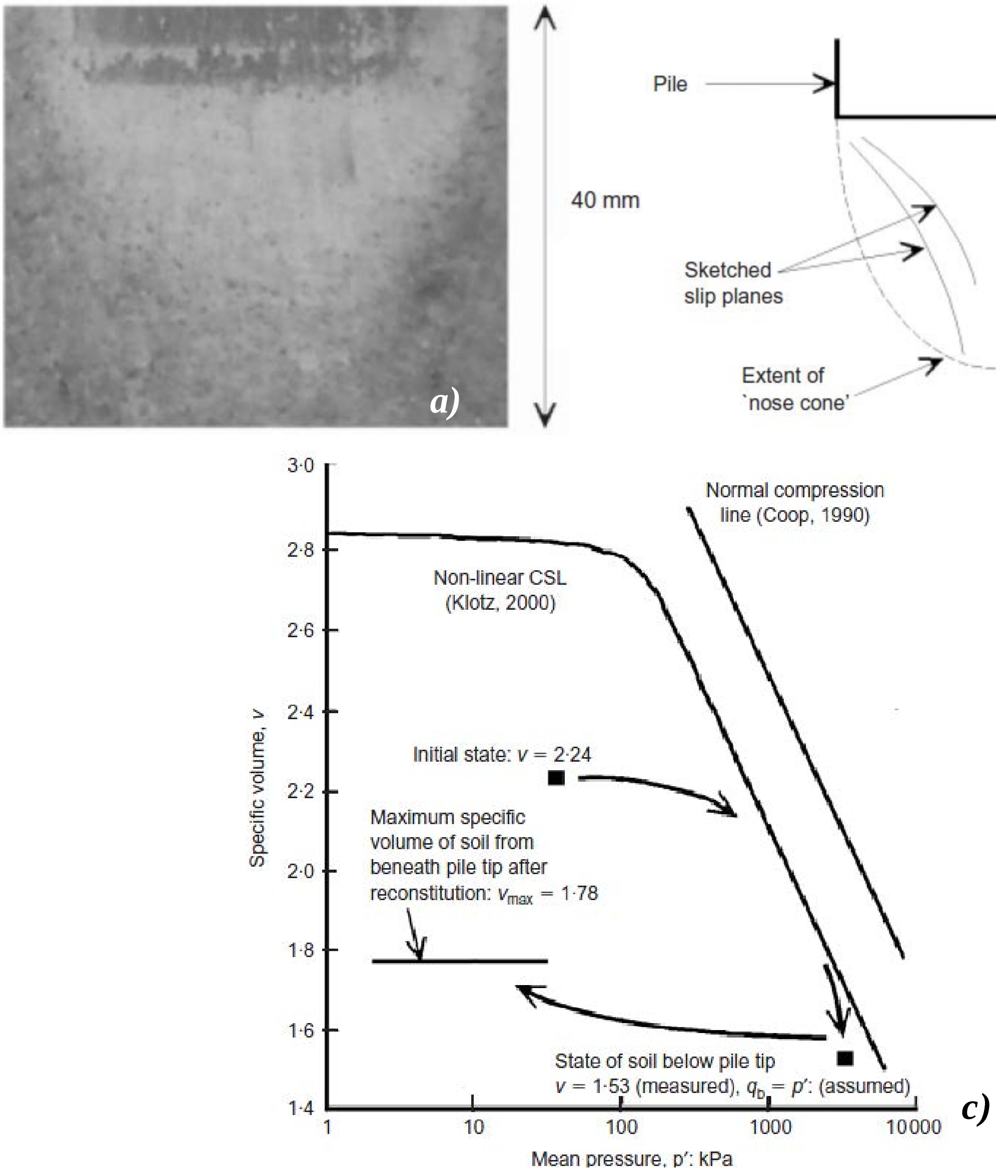

Figure 3.19 Post-mortem sampling of soil below pile tip: a) 'nose cone' of soil beneath pile tip, b) slip planes observed within nose cone c) stress–volume paths of sand beneath pile tip (White & Bolton, 2004)

Therefore, the hydrostatic compression yield stress is defined, as a relation, which associates it with the plastic volumetric strain $\varepsilon^{pl}{}_{vol}$, as it is presented by Equation 3.21. The $\varepsilon^{pl}{}_{vol}|_0$ is another cap parameter, namely, the initial cap yield surface position. The graphic illustration of the function can be found in Figure 3.20. The $\varepsilon^{pl}{}_{vol}$, plastic volumetric strain, can be expressed as a function of few parameters. The formula is presented in Equation 3.22, where: C_C is compression index, C_S is swelling index and e_0 is void ratio.

$$p_b = p_b\left(\varepsilon_{vol}^{pl}\big|_0 + \varepsilon_{vol}^{pl}\right) \qquad 3.21$$

$$\varepsilon_{vol}^{pl} = \frac{C_C - C_S}{2.3(1+e_0)}\, ln\left(\frac{p`}{p`_0}\right) \qquad 3.22$$

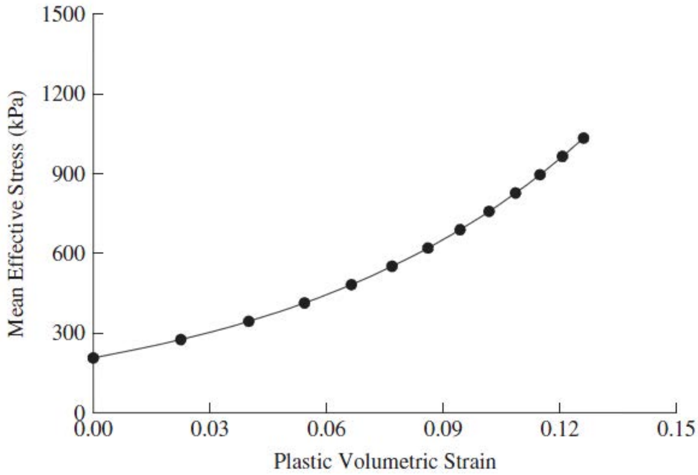

Figure 3.20 The MDPC criterion hardening curve (Helwany, 2007, p. 67)

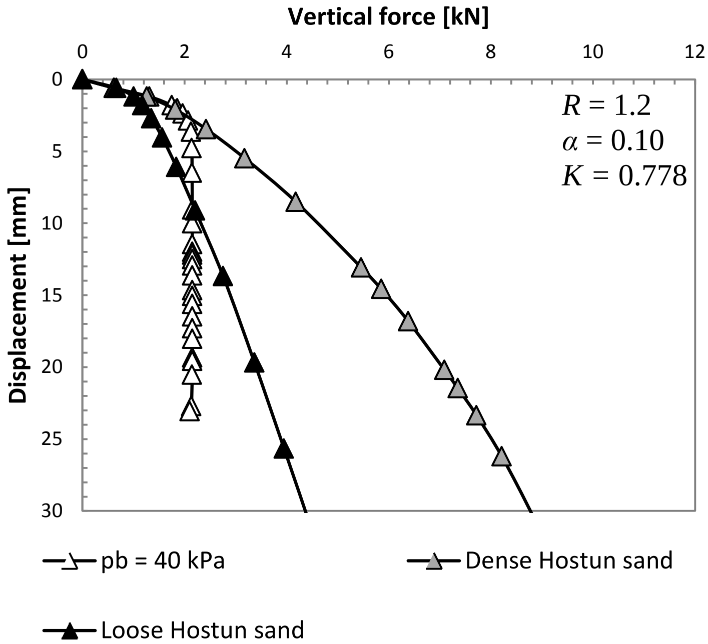

Figure 3.21 The influence of different definitions of a hydrostatic compression yields stress p_b, on behaviour of loaded soil.

An influence on force borne by soil and sensitivity of results to this parameter have been examined. Calculations with three different definitions of the p_b have been carried out. Specification of the hydrostatic compression yields stress can be divided into two categories: p_b is defined as constant or p_b is expressed as a function. Results of the modelling of both cases are presented in Figure 3.21. Case, which belong to first category, p_b = 40 kPa, is characterised by early plastic failure, represented by a sudden drop - increase of displacement whereas force stayed constant. In the second category, soil is described by a hardening function. Both hardening curves for: 'dense' Hostun sand, ρ_d = 1500 kg/m^3 and 'loose' Hostun sand, ρ_d = 1380 kg/m^3 are presented in Figure 4.16. The shape of curves (Figure 3.21) recalls the behaviour of natural soils that is why, this way of defining cap evolution seems to be the correct one. A line with grey markers represents behaviour of soil with proper hardening curve for 'dense' Hostun sand. A line with black markers corresponds to results acquired with 'loose' sand hardening. Their shapes are similar, moreover the tendency in the soil's behaviour is alike. Despite that, these two curves visualise how important is proper calibration of the hardening law. Strain hardening curve of other density or even kind of sand can be used for the preliminary, general calculations while précised data from oedometer test are not available. However, it is highly recommended to perform this test for better material characterization because it leads to significant improvement of the final results of the calculations.

3.3. Comparison between criteria

The choice of constitutive law, which is relevant for modelled soils, is a significant decision. Loading test of a small scale shallow foundation, which helped to explain influence of each parameter of MDPC criterion, is used in order to visualised differences in results obtained by simulations with some of models and criteria. The elastic and elastoplastic models with three failure criteria: the Mohr-Coulomb, the Modified Drucker-Prager and the Modified Drucker-Prager with cap are considered.

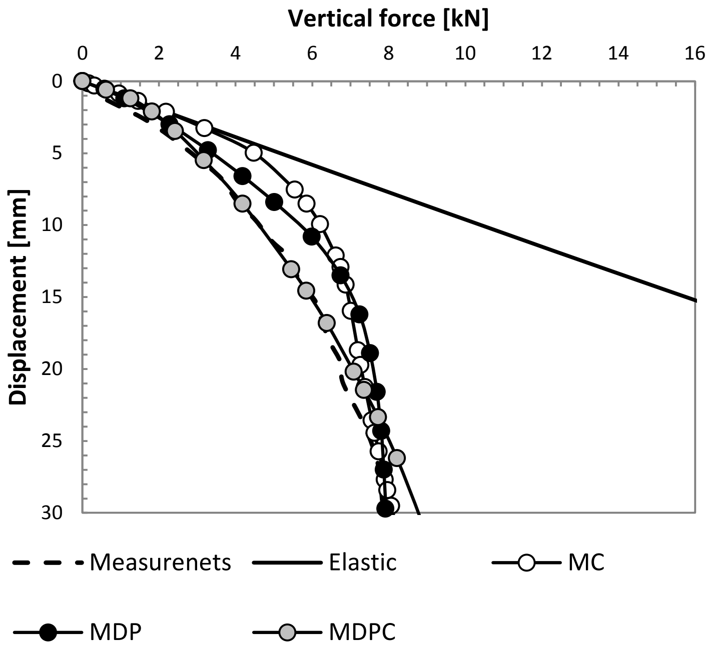

Figure 3.22 Comparison between measurements and results of calculations carried out with models: elastic and elastoplastic with the Mohr-Coulomb, the Modified Drucker-Prager and the Modified Drucker-Prager with cap criteria

Figure 3.22 depicts results of the loading test of a shallow foundation tested on layer of dry, 'dense' Hostun sand (ρ_d = 1500 kg/m^3), calculated with different constitutive laws and compared with measured behaviour. Results obtained with elastic model proves, that, as it is explained in previous paragraphs, soil with its whole complexity, which makes it highly heterogeneous, should not be defined as purely elastic material. The predicted behaviour is linear and does not correspond to the measurements. The elastoplastic model with MC failure criterion have been also used to describe soil under the foundation. Due to introduction of the failure surface, reply of the calculated foundation and the observed behaviour look more alike. Nevertheless, model is not capable of well reproduction of the measurements. The results obtained with MDP criterion are very close to the one calculated with MC. Even though, criteria base on the same mechanism, which is added shear failure surface, MDP varies a bit in its definition from MC. Difference mainly manifests itself in taking into account intermediate principal stress. Thank to transition equations, parameters of MDP criterion can be correlated with the most common soil characteristics, namely internal friction angle and cohesion. In order to ensure properly chosen parameters of MDP and MDPC, it is necessary to start modelling with preliminary calculations with basic criterion – MC. The last curve represents behaviour of soil subjected to imposed displacement calculated with MDPC. All curves representing numerical predictions with elastoplastic models, show relatively good agreement with each other for lower values of displacement. However, between 3 mm and 21 mm the difference appears. Elastic domain predicted by model with MC is longer and its end results directly in plastic plateau. As it can be seen, the increase of force in MDP and MDPC cases is slower and closer to the measured one between about 3 mm till and 15 mm, and 3 mm and 21 mm for MDP and MDPC respectively. It can be observed that simulation carried out with the most advanced constitutive law, MDPC, is the most successful attempt. It can be explained by fact that it is the only case, where failure surface is limited not only by shear failure but also cap.

3.4. Conclusions

All natural soils, which can be found in the world, have one common feature - they are highly heterogeneous materials and their behaviour is strongly dependent on mineralogy, structure and grain size. Furthermore, they are governed by stress-dilation, which manifests in ability to increase in volume. Therefore, finding one mathematical equation, capable to consider all soils' characteristics till now is impossible. Numerous constitutive laws have been proposed and decision which one should be used in modelling is crucial. It must be taken according to type of soil, structure, applied loading and possibility to obtain model's parameters.

Four failure criteria, commonly used in geotechnical analyses, were discussed: the Mohr-Coulomb, the Classical Drucker-Prager, the Modified Drucker-Prager and Modified Drucker-Prager with cap surface. Their advantaged and disadvantages were presented. Even thought, the Drucker-Prager criterion takes into account intermediate principal stress, it was shown that its Classical definition can lead to significant under and over predictions. The shear strength is overestimated in all cases other than triaxial compression, when approximation by outer, circle is used. Whereas, its value is under predicted in all cases except triaxial extension, when inner, one is chosen. Hence, DP criterion, in its classical form, is not highly recommended law for soils, unless load is executed by pure triaxial compression or extension.

The modification, flow stress ratio K, added to criterion reduces the negative influence of approximations, when K = 0.778. The influence of K was presented by an example – loading test of the shallow foundation. Furthermore, proper calibration of the criterion's parameters is possible by the transition equations. Model consisting of one finite element was tested according to theoretical studies presented by Carter, et al. (Carter, et al., 1977). Three, single element models, were subjected to uniformed compression and uniformed extension. Associated MC, non-associated MC and associated MDP criteria were used in order to verify provided transition equations. Afterwards, results of the modelling were successfully compared with theoretical ones.

The next modification added the MDP criterion, discussed in this chapter, was cap surface and its evolution defined by material hardening/softening. It brought further four independent parameters: cap eccentricity, R, transition region parameter, α, hydrostatic compression yield stress, p_b and initial cap yield surface position $\varepsilon^{pl}{}_{vol}|_{0}$, which in majority of cases should be assumed as zero. The influence of three of them was illustrated by the same loading test, used to explained the importance of flow stress ratio. It was found that the most significant parameter is hydrostatic compression yield stress, which is directly related to hardening phenomena. The slightly smaller impact on the result has cap eccentricity. The transition region parameter seems to be relatively less influential.

The need of using more advanced constitutive law was clearly highlighted by analysing results, obtained from numerical modelling with four constitutive models. It can be concluded that, if a limit, which changes soils properties under the applied load, is not imposed, the prediction is unable to properly reproduce soil behaviour.

4. Behaviour of a Soil Mixing column

4.1. Introduction

Knowledge of the properties of the SM material is crucial, nevertheless it is not sufficient. Without a complete analysis of the behaviour of the element under loading, it is not possible to capture all the characteristics.

SM elements can be formed in different shapes (Chapter 2), however in this thesis only columns are analysed. Hence, in order to examine column itself and its interaction with surrounding soil, two types of a static loading test have been performed: full scale and small scale tests.

In this chapter the full scale test performed on heterogeneous SM column is presented. Column was created in Vernouillet, France by Soletanche Bachy by their Springsol mixing tool. The stratigraphy of the ground as well as the column's properties are given. Numerical, finite element, study performed in ABAQUS is divided in to two steps. Firstly, the preliminary calculations, based on the received from Soletanche Bachy and IFSTTAR data (Soletanche Bachy, 2013), are carried out. Six sets of properties are tested by parametric study in order to define the appropriate ones. Secondly, with the modified, more accurate data, numerical calculations are repeated. The loading test was analysed by modelling with three constitutive laws for soils. Due to lack of necessary parameters of both soil layers existing in the Vernouillet site, the advanced constitutive model is used for only one layer of soil. Missing parameters are assumed according to literature. Numerical predictions, especially the one obtained from a model with advanced constitutive law for soil, show good agreement with the observed behaviour.

In subsequent sections of this chapter, small scale static loading tests are presented according to results of tests performed in Laboratoire de Génie Civil et l'Ingénierie Environnementale (LGCIE), INSA Lyon, by Dhaybi (Dhaybi, 2015).

Firstly, materials and interactions are presented. Experimental testing program consists of tests performed on Hostun sand with two densities: 'loose' and 'dense'. Results of the laboratory tests of soil such as grain size test, direct shear test, oedometer test are presented and according to them, numerical calculations properties are chosen. Modulus of deformation is assumed in agreement with literature, due to lack of triaxial test. Also, some of missing parameters of an advanced constitutive law are chosen according to literature and parametric study. Properties of SM mixture are analysed in terms of cement ratio and the age of the material. Comparison is made according to results of unconfined compression tests. Static and dynamic modulus of deformation are indicated. Two, 7 and 14 days old, SM columns are tested in the study. Their Mohr-Coulomb criterion's shear properties are assumed according to literature.

Secondly, the experimental setup and method of the creation of the column in laboratory conditions are described.

The next part of the chapter concentrates on numerical modelling of the loading tests of the single and group of SM columns tested in 'loose' and 'dense' sand. Obtained columns' behaviour is compared with measured one with satisfactory results. All discrepancies are indicated and their sources explained.

The last section of this chapter concludes and sums up all observations collected during analyses.

4.2. Full scale static loading test of a Soil Mixing column

As it was mentioned before, the Soil Mixing is a technology that mixes *in situ* soils with binding materials to form a stiff vertical element in the ground. In order to investigate the behaviour of a Soil Mixing column in its natural (field) working conditions a full scale static loading test (Figure 4.2a) was performed in September 2011 by Soletanche Bachy in Vernouillet, France (Figure 4.1a) (Soletanche Bachy, 2013). Column was installed by the Springsol mixing tool (Figure 4.1b) in the SNCF experimental site 90 days before testing. 180 days after the loading, column was excavated and obtained samples were subjected to laboratory tests in order to analyse its homogeneity and mechanical properties.

According to provided characteristics of the materials, the numerical finite element simulation in ABAQUS was performed. It allowed simulating and recreating the loading process and an answer of the column.

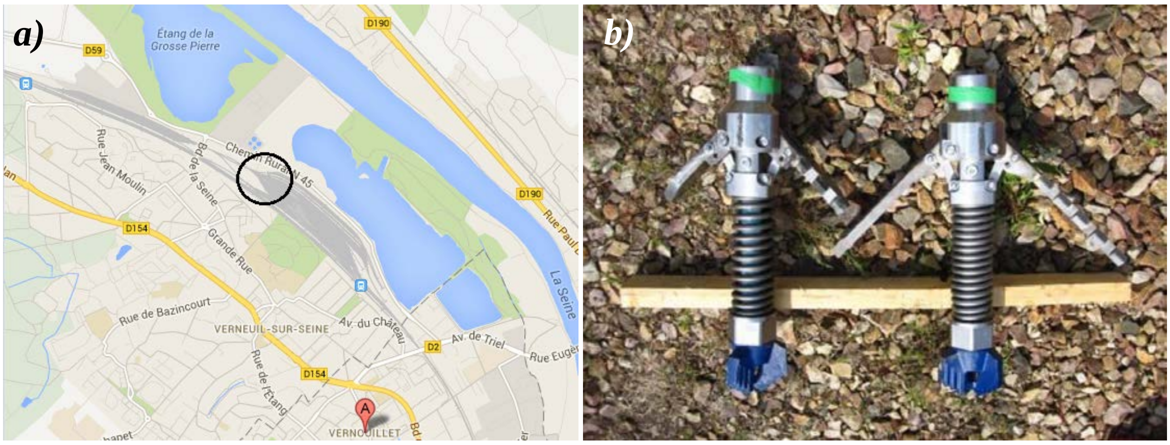

Figure 4.1 a) site location, b) Springsol mixing tools. Left 0.4 m and 0.6 m diameters (Guimond-Barrett, et al., 2012)

Figure 4.2 Loading test of the Soil Mixing column in Vernouillet, France: a) testing apparatus, b) excavated Soil Mixing column after loading, c) section of the excavated column (Soletanche Bachy, 2013)

4.2.1. Received data

The loading test setup, including the stratigraphy of the ground, was provided by Soletanche Bachy and IFSTTAR (Figure 4.3a) (Soletanche Bachy, 2013). Three layers of soil were found. The first one was fill (remblais) which was not considered as a bearing layer. The second one was sandy silt (limons sableux). The last observed layer was gravelly sand (sable graveleux). Analyzed column diameter was D = 0.4 m. Column was installed with the Springsol rotary tool. The slag cement CEM III/C 32.5 was used as a binder. It was introduce into the soil as slurry – wet method. Some bentonite was added to stabilise the cement grout. The cement content of the slurry injected into the column was 230 kg/m^3. By the cement content is understood the mass of dry binder per cubic meter of soil. Field and laboratory tests on collected samples of the soils and column were carried out in IFSTTAR laboratory. Acquired with dynamic penetrometer (PANDA) test, pressiometer test and direct shear test (σ = 50 kPa, 100 kPa, 200 kPa), properties of each layer of soil are presented in Table 4.1 (Soletanche Bachy, 2013). Excavation and analyzes of the shape and structure of the column showed that due to mixing, it was possible to obtain almost homogeneous material consisted of soil at the certain layer and cement (Figure 4.2b and Figure 4.2c). Because of more than one layer of soil, the Soil Mixing column is inhomogeneous in the vertical sense. Its characteristics, obtained by the unconfined compression test and the Brazilian test, are gathered in Table 4.2 and presented as a function of depth.

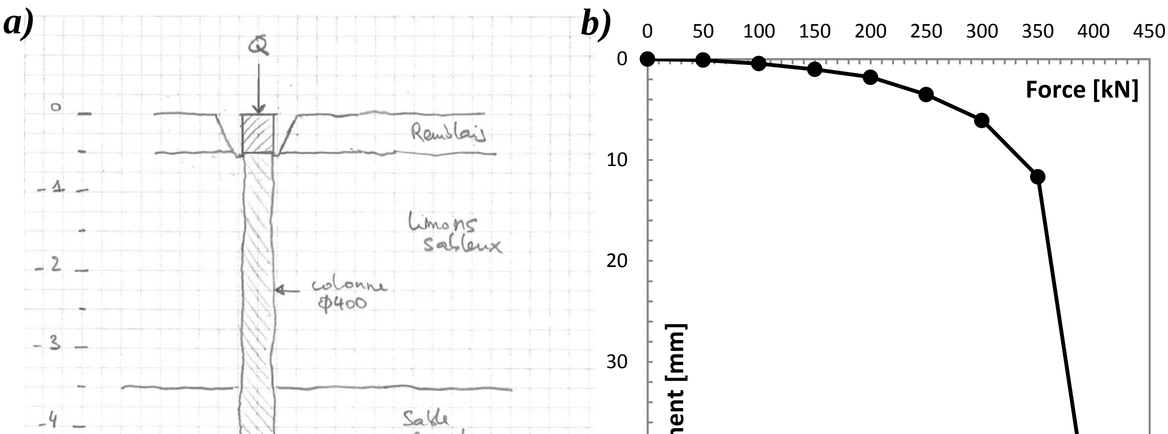

Figure 4.3 a) dimensions of the full scale loading test of the Soil Mixing column, b) results of the test (Soletanche Bachy, 2013)

The loading process was performed in 8 steps. In each step, the load applied to the head of the column, was increased by 50 kN, until 400kN, when displacement exceeded 40 mm. This displacement corresponds to 1/10 of the diameter. 30 minutes was accepted as a time necessary for stabilization of the vertical displacements. Results of the test, vertical force versus vertical displacement of the head of the column, are illustrated in Figure 4.3b and precise values of displacements can be found in Table 4.3.

Table 4.1 Properties of soil obtained from field and laboratory tests (Soletanche Bachy, 2013)

Layer	Fill (Remblais)	Sandy silt (Limon sableux)	Gravelly sand (Sable graveleux)
Depth [m]	0 – 0.5	0.5 – 3.5	3.5 - > 9.0
Classification GTR	/	A1	B5 to C1B5
Dynamic penetration resistance q_d [MPa]	7	4	16
Limit pressure $pl*$ [MPa]	/	1	2.5
Presiometric modulus E_m [MPa]	/	10	20

Table 4.2 Properties of the Soil Mixing column obtained from field and laboratory tests (Soletanche Bachy, 2013)

Layer	Head of column	Reinforced silt	Reinforced sand
Depth [m]	0 – 0.5	0.5 – 3.5	3.5 – 5.0
Unconfined compressive strength q_u [MPa]	/	2.5	5.0
Modulus of deformations E_{50} [MPa]	/	$\geq 200\ q_u$	$\geq 200\ q_u$
Friction angle ϕ [°]	/	36°	41°
Cohesion c [kPa]	/	700	1200

Table 4.3 Results of the loading test (Soletanche Bachy, 2013)

Step [30 min]	Loading on column [kN]	Displacement of the head of column [mm]
0	0	0.00
1	50	0.09
2	100	0.44
3	150	1.02
4	200	1.79
5	250	3.52
6	300	6.07
7	350	11.66
8	400	48.18

4.2.2. Preliminary calculations

The Soil Mixing column bearing capacity has been analyzed by an axisymmetric model. The acquired results have been compared with the measurements obtained from static loading test. Parametric study has led to correct properties of the material.

4.2.2.1. Model geometry and material properties

The numerical simulation, in accordance with the field tests, has consisted of three soil layers: fill, sandy silt and gravelly sand; and an inhomogeneous column (Figure 4.4). No water table was detected during site investigation. The first layer – fill, has been replaced by equivalent pressure σ_{v0}, due to lack of contact between the first 0.5 m of the column and soil Figure 4.3a. The equivalent pressure, σ_{v0}, has been determined by Equation 4.1, where h_{fill} is thickness of the layer and γ_{fill} stands for unit weight of the layer. The unit weight has been assumed as γ_{fill} = 20 kN/m^3 and h_{fill} = 0.5 m, so σ_{v0} = 10 kPa.

$$\sigma_{v0} = h_{fill}\gamma_{fill} \qquad 4.1$$

Moreover, the last layer has been divided into two sub layers according to their location relatively to the column: gravelly sand – friction and gravelly sand – tip. It is assumed that the last 0.2 m of the column is placed in layer gravelly sand – tip. As mention before, due to two different soil layers, the Soil Mixing column is inhomogeneous (Figure 4.4). Three parts of column can be noticed. The first one, between surface and 0.5 m depth, is a section without contact with surrounded soil (layer of fill). The second, 0.5 m – 3.5 m, and the third, 3.5 m – 5 m, parts are in contact with sandy silt and gravelly sand, respectively. The column's properties in each section are different and related to the soil parameters. All materials have been characterized by the elastic perfectly plastic model with the Mohr-Coulomb failure criterion. Six sets of parameters, for the preliminary modelling to be able to obtain appropriate material properties. Properties were determined according to filed and laboratory tests, literature (Table 4.4). Where: q_u stands for unconfined compressive strength, E is Young's modulus, ν is Poisson's ration, c is cohesion, ϕ stands for friction angle, K_0 is lateral earth pressure coefficient and γ stands for unite weight. Poisson's ratio of SM column was chosen as 0 with the assumption that column works as a truss element.

The mesh consists of 6-node modified quadratic axisymmetric triangle elements (CAX6M) is presented in Figure 4.4.

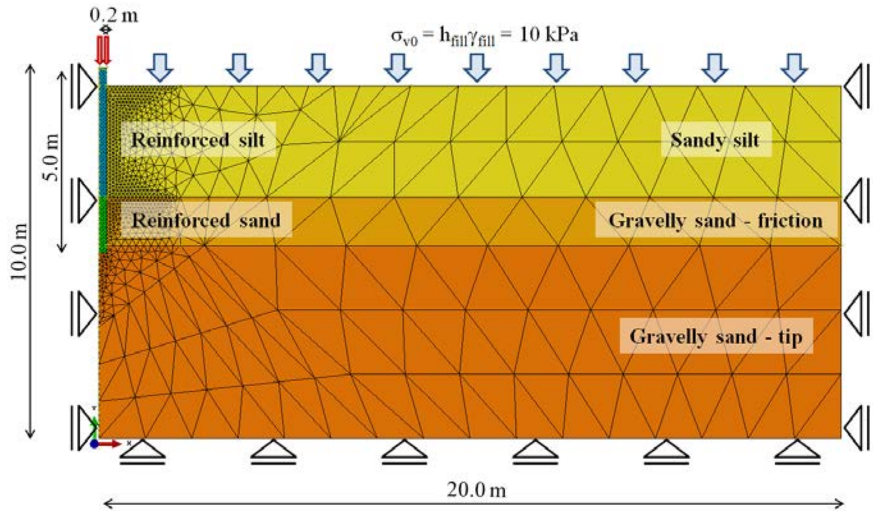

Figure 4.4 Numerical model of the static loading test

When we analyze the reply for loading of the SM columns, the analogy to pile foundation can be seen. It means that column should not be investigated as layer of soil with high elastic properties, but as pile element. Hence, it is assumed that the interactions between SM column and surrounding soil and piles with soil are similar. Therefore, contact between column and soil needs to be introduced. It has been found (Lee, et al., 2002), that the behaviour of pile in homogenous soil is governed mainly by the interface behaviour, hence in this study, the interface elements with zero initial thickness, obeying the Coulomb failure criterion, are used. The law bases on the interface friction coefficient μ_f and a limiting displacement γ_{crit} (Figure 4.5). The criterion considers frictional shear stress between two contact surfaces as a normal stress, 'in contact', multiplied by the friction coefficient ($\mu_f\sigma$'). If the shear stress applied along the shaft was less than $\mu_f\sigma$', the surfaces would stick. The nodes of the soil elements in contact with a pile could slide along it when soil slip occurs. Figure 4.5 presents the relationship of shear stress, displacement and soil slip. In this study, a limiting displacement γ_{crit}, of 0.5 cm was assumed to achieve full mobilisation of skin friction. According to field measurements reported by (Broms, 1976) displacement should be between 0.1 and 0.8 cm. The friction coefficient, μ_f, is taken as 2/3 of a tangent of the layer friction angle(Burland, 1973). The column is in contact with two layers; hence two friction coefficients have been used. The friction coefficient for sandy silt equals to μ_f = 0.36 what refers to about 20° (ϕ = 30°), for gravelly sand equals to μ_f = 0.45 which refers to about 24° (ϕ = 35°).

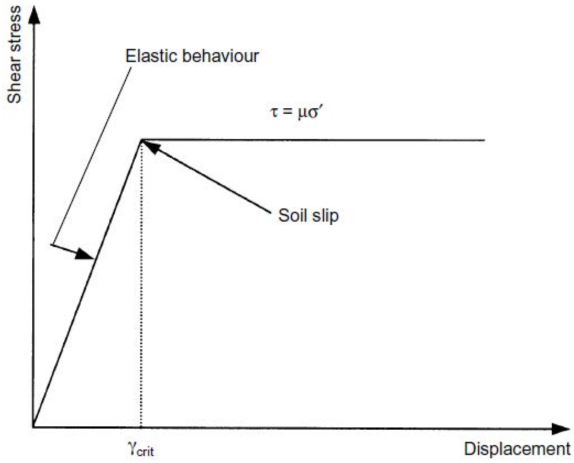

Figure 4.5 Behaviour of interface element (Lee, et al., 2002)

4.2.2.2. Loading and boundary conditions

The numerical model's vertical edges boundary conditions are symmetric boundary on the left hand side of the model (axis of symmetry) and no horizontal displacement at the right hand side. In the bottom boundary, displacements are restricted in vertical direction (Figure 4.4). Column is loaded by imposed displacement to its top. The soil surface is loaded by the equivalent pressure σ_{v0} = 10 kPa, previously presented.

4.2.2.3. Parametric study and results

The preliminary calculations have been carried out for 6 cases (Table 4.4) to be able to define the most appropriate material parameters. Cases can be organised into two groups. The first one, where the Young's modulus of the Soil Mixing column is modified (Figure 4.6 and Table 4.5) and the second where soils shear parameters are changed (Figure 4.7 and Table 4.6).

For the first group of cases, it can be observed, that the closes to measurements result was obtained from Case 02, where Young's modulus of the column is assumed to be 2000 q_u. However, calculations for this case ends as the first one, maximum value of force F = 320 kN (loading to the columns is applied as a displacement). The worst agreement has been obtained from Case 01, where E = 500 q_u. Summing up, the higher value of the Young's modulus, the better agreement between prediction and measurements.

Table 4.4 Preliminary calculations parameters

Layer	q_u [MPa]	E [MPa]	ν [-]	c [kPa]	ϕ [°]	K_0 [-]	γ [kN/m³]
Case 00							
Sandy silt	--	25	0.3	10	30°	0.5	18
Gravelly sand	--	100	0.3	0	35°	0.5	20
Reinforced silt	2.5	1000 q_u	0.0	700	36°	0.5	18
Reinforced sand	5.0	1000 q_u	0.0	1200	41°	0.5	20
Case 01							
Sandy silt	--	25	0.3	10	30°	0.5	18
Gravelly sand	--	100	0.3	0	35°	0.5	20
Reinforced silt	2.5	500 q_u	0.0	700	36°	0.5	18
Reinforced sand	5.0	500 q_u	0.0	1200	41°	0.5	20
Case 02							
Sandy silt	--	25	0.3	10	30°	0.5	18
Gravelly sand	--	100	0.3	0	35°	0.5	20
Reinforced silt	2.5	2000 q_u	0.0	700	36°	0.5	18
Reinforced sand	5.0	2000 q_u	0.0	1200	41°	0.5	20
Case 03							
Sandy silt	--	25	0.3	10	30°	0.5	18
Gravelly sand - friction	--	100	0.3	0	35°	0.5	20
Gravelly sand - tip	--	200	0.3	0	35°	0.5	20
Reinforced silt	2.5	1000 q_u	0.0	700	36°	0.5	18
Reinforced sand	5.0	1000 q_u	0.0	1200	41°	0.5	20
Case 04							
Sandy silt	--	25	0.3	5	25°	0.5	18
Gravelly sand - friction	--	100	0.3	0	35°	0.5	20
Gravelly sand - tip	--	100	0.3	0	35°	0.5	20
Reinforced silt	2.5	1000 q_u	0.0	700	36°	0.5	18
Reinforced sand	5.0	1000 q_u	0.0	1200	41°	0.5	20
Case 05							
Sandy silt	--	25	0.3	5	25°	0.5	18
Gravelly sand - friction	--	100	0.3	0	30°	0.5	20
Gravelly sand - tip	--	100	0.3	0	30°	0.5	20
Reinforced silt	2.5	1000 q_u	0.0	700	36°	0.5	18
Reinforced sand	5.0	1000 q_u	0.0	1200	41°	0.5	20

The second group of calculations, where soils shear parameters are varied, are presented in Figure 4.7 and Table 4.6. The beginning of all three curves, representing the numerical predictions, is the same. The first differences start to appear for Case 05, which refers to silt characterised by ϕ_{silt} = 25° and c_{silt} = 5 kPa, and sand characterised by ϕ_{sand} = 30° and c_{sand} = 0 kPa. The final value of the bearing capacity acquired from Case 04 is the same as the one obtained from Case 05 but the displacement is significantly lower for the 04 one. The most appropriate approximation of the loading test, out of this three, seems to be Case 00.

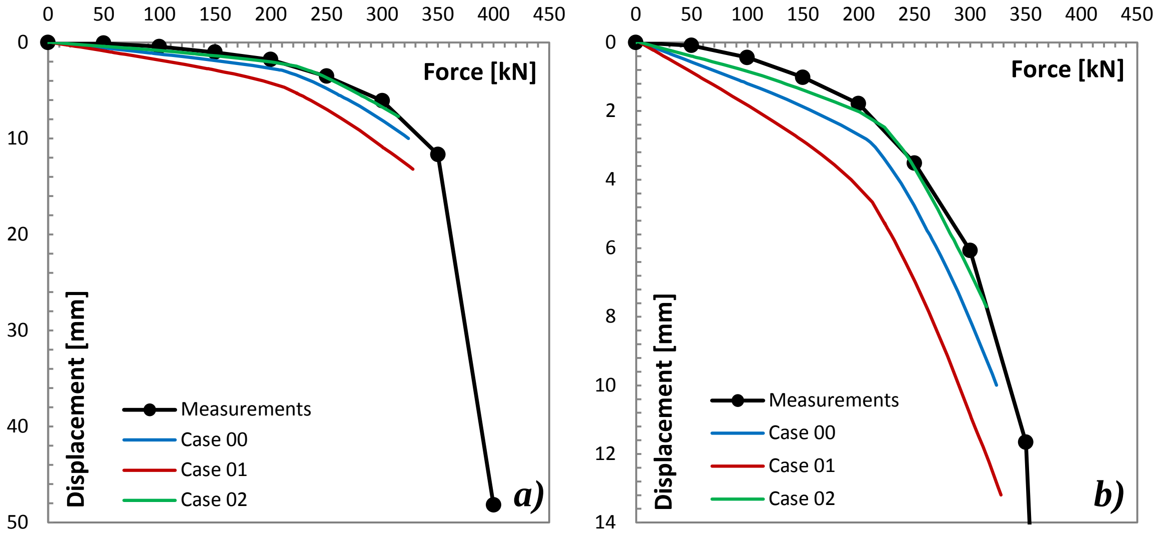

Figure 4.6 The influence of column Young's modulus, on its bearing capacity. Results of a) the whole loading test, b) test till 14 mm displacement

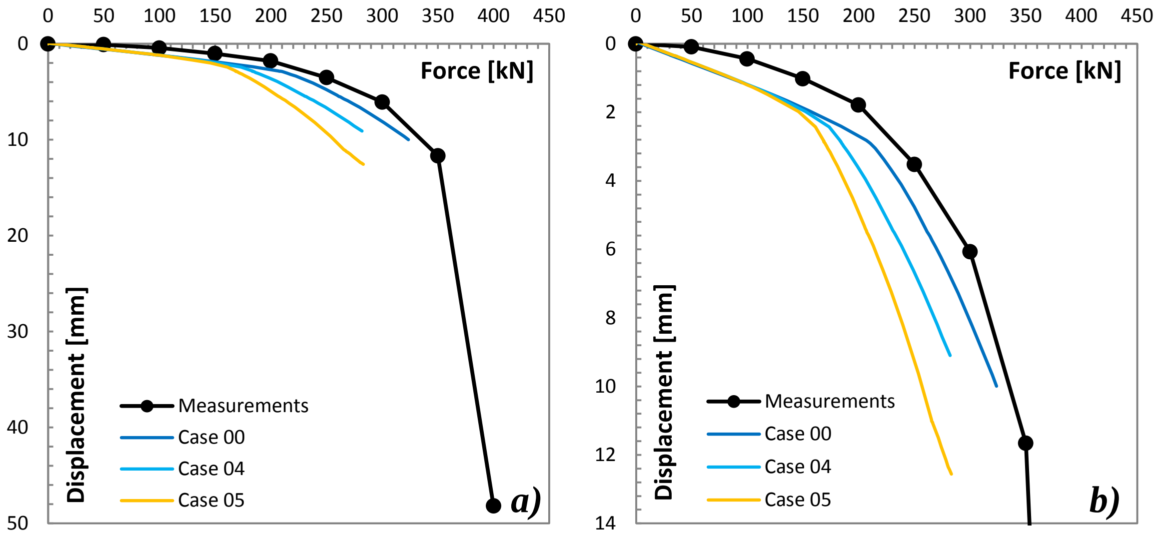

Figure 4.7 The influence of soils shear parameters, ϕ and c, on column's bearing capacity. Results of a) the whole loading test, b) test till 14 mm displacement

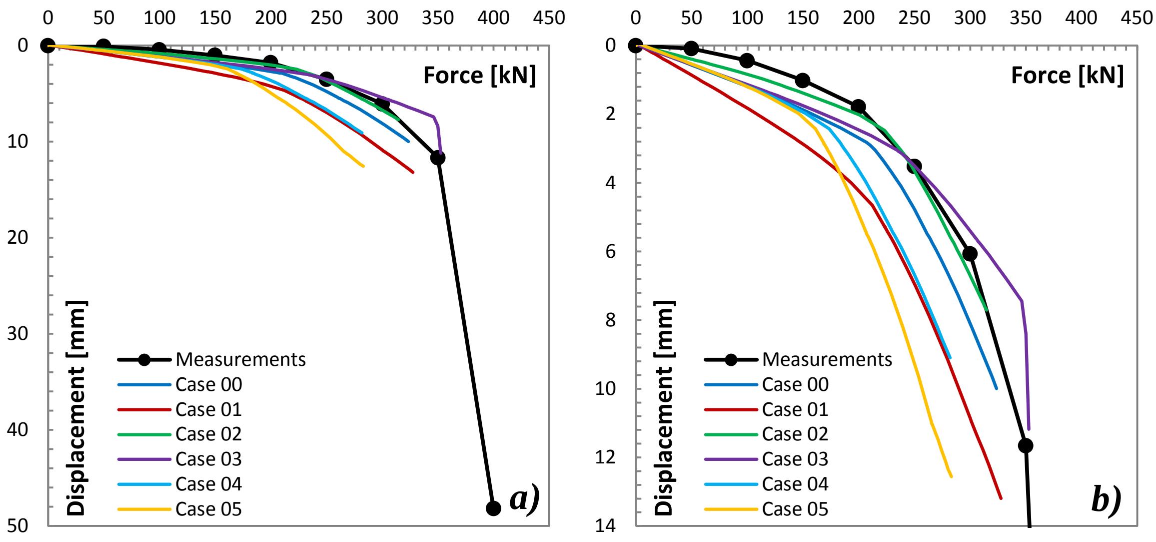

Figure 4.8 Results of the preliminary calculations Results of a) the whole loading test, b) test till 14 mm displacement

Table 4.5 Material properties used in parametric study to investigate the influence of column Young's modulus on bearing its capacity

Case	Young's modulus	
	Reinforced silt	Reinforced sand
Case 00	1000 q_u	1000 q_u
Case 01	500 q_u	500 q_u
Case 02	2000 q_u	2000 q_u

The results of all six calculation cases are gathered in Figure 4.8. The violet curve, which represents Case 03, has not been presented before. The uniqueness of this case is based on the separation of layers of gravelly sand into gravelly sand – friction and gravelly sand – tip. The Young's modulus has been defined as 100 kPa for the 'friction part' and 200 kPa for the 'tip part'. The beginning of the curve differs from the measurements but it is the only case where plastic failure is obtained that clearly and its value correlates to the reality. At this point, as the best fit solution, Case 03 is chosen.

Table 4.6 Material properties used in parametric study to investigate the influence of soils shear parameters, ϕ and c, on column's bearing capacity

Case	Sandy silt		Gravelly sand	
	c [kPa]	ϕ [°]	c [kPa]	ϕ [°]
Case 00	10	30	0	35
Case 04	5	25	0	35
Case 05	5	25	0	30

4.2.3. Advanced calculations

The numerical modelling of the behaviour of the Soil Mixing subjected to the static loading on its top has been carried with the more precise data. The modifications of the previously presented data are: one meter thick transition zone in the Soil Mixing column (Figure 4.9), properties of the soils (Table 4.7) and properties of the Soil Mixing column (Table 4.8).

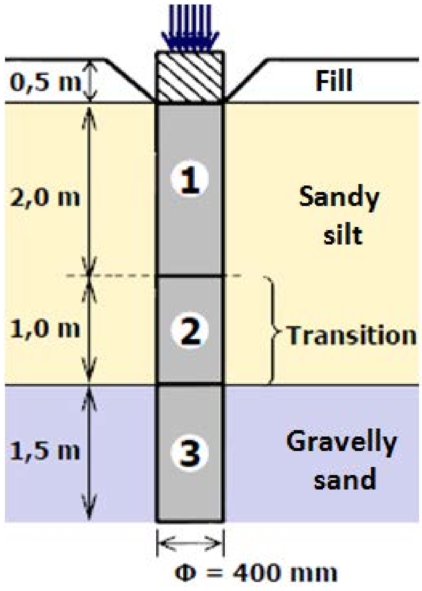

Figure 4.9 Schema of the full scale loading test of the Soil Mixing column with updated data (Soletanche Bachy, 2013)

Table 4.7 Updated properties of soil obtained from field and laboratory tests (Soletanche Bachy, 2013)

Layer	Fill (Remblais)	Sandy silt (Limon sableux)	Gravelly sand (Sable graveleux)
Depth [m]	0 – 0.5	0.5 – 3.5	3.5 - > 9.0
Classification GTR	/	A1	B5 to C1B5
Dynamic penetration resistance q_d [MPa]	7	4	16
Limit pressure $pl*$ [MPa]	/	1	2.5
Presiometric modulus E_m [MPa]	/	10	20
Friction angle ϕ [°]	/	27°	37°
Cohesion c [kPa]	/	2	0

Table 4.8 Updated properties of the Soil Mixing column obtained from field and laboratory tests (Soletanche Bachy, 2013)

Layer	Head of column	Reinforced silt	Transition zone	Reinforced sand
Depth [m]	0 – 0.5	0.5 – 2.5	2.5 – 3.5	3.5 – 5.0
Unconfined compressive strength q_u [MPa]	/	3.7	7.6	11.9
Modulus of deformations E_{50} [MPa]	/	1280 q_u	1280 q_u	1280 q_u
Friction angle ϕ [°]	/	42°	42°	42°
Cohesion c [kPa]	/	700	1700	2800

4.2.3.1. Model geometry and material properties

The numerical simulation, in accordance with the new data obtained from field tests (Soletanche Bachy, 2013), leads to the new mesh, presented in Figure 4.10. This time, three kinds of constitutive models have been used. All parts of the Soil Mixing column and sandy silt layer have been analysed with the elastoplastic model with the Mohr-Coulomb (MC) failure criterion. The gravelly sand layer has been modelled with constitutive model with three criteria. Firstly, calculations have been run with MC criterion with parameters according to the new data (Table 4.9). The cohesion for sand was assumed 0.5 kPa. The change has been introduced to avoid problems with the numerical convergence.

The numerical model boundary conditions and way of loading have been kept the same as for the preliminary modelling.

According to Equations 3.14 and 3.15, parameters of the Modified Drucker-Prager (MDP) and the Modified Drucker-Prager with Cap (MDPC) criteria have been calculated (β = 56.41 and d = 3.00 kPa). The cap parameters used in calculations are: R = 0.1, α = 0.01, $\varepsilon^{pl}{}_{vol}|_0$ = 0.0 and K = 0.778. Due to lack of needed hardening parameters, no oedometer test for gravelly sand has been carried out, the hardening law for Ottawa sand (Helwany, 2007) has been used. Details of the hardening used in calculation are presented in Figure 4.11.

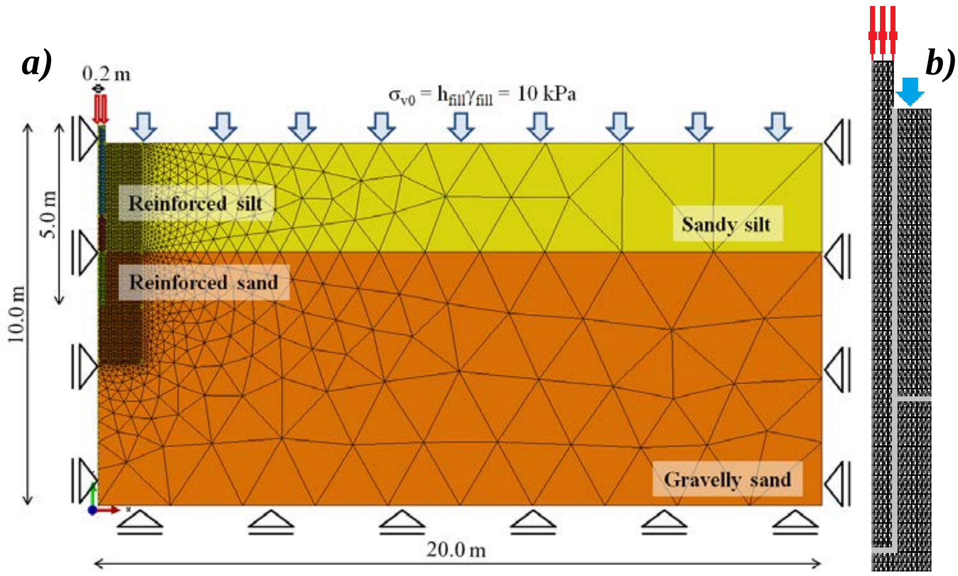

Figure 4.10 a) the mesh and boundary conditions used in numerical modelling b) zoom on the mesh of the column

Table 4.9 Parameters of the materials used in numerical calculations

Soil	Depth [m]	q_u [MPa]	E [MPa]		ν [-]	c [kPa]	ϕ [°]	ψ [°]	K_0 [-]	γ [kN/m³]
Sandy silt	0.5 - 3.5	--	25		0.3	2.0	27	10	0.5	18
Gravelly sand	3.5 - 10.0	--	100		0.3	0.5	37	10	0.5	20
Reinforced silt	0.5 - 2.5	3.7	$1280q_u$ =	4736	0.0	700.0	42	5	0.5	21
Transition zone	2.5 - 3.5	7.6	$1280q_u$ =	9728	0.0	1700.0	42	5	0.5	21
Reinforced sand	3.5 - 5.0	11.9	$1280q_u$ =	15232	0.0	2800.0	42	5	0.5	21

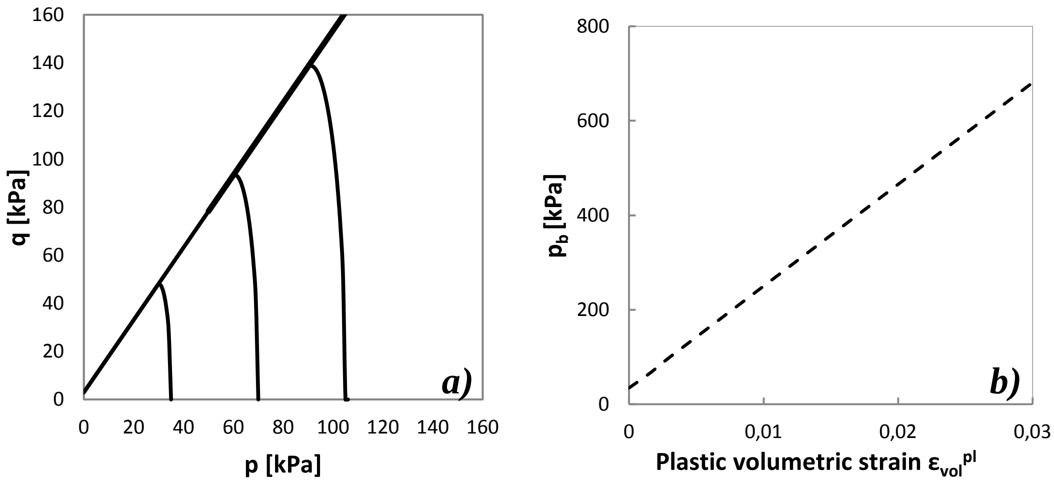

Figure 4.11 a) the Modified Drucker-Prager yield surface for gravelly sand, b) hardening law of Ottawa sand (Helwany, 2007) used in calculation for gravelly sand

4.2.3.2. Results

The numerical predictions and measurements are presented in Figure 4.12. As it was expected, predictions obtained by the calculations with MC and MDP criteria matches to each other. The beginning of all three curves, representing the numerical predictions, is the same. The difference starts to appear for MDPC case about 200 kN and it is caused by the strain hardening of the sand (Figure 4.11). The numerical prediction underestimates the force until 310 kN, afterwards situation inverses. Similarly, the behaviour of the Soil Mixing column is modelled with MC and MDP criteria, but the overestimation starts after 250 kN. The final value of the bearing capacity acquired by the numerical predictions is lower than measured one. However, displacements, for which it is obtained, are lower in case of MDPC and significantly lower for MC and MDP. In case of calculation with MDPC criterion, commanding plastic failure in the head of column, visualised by plateau, has been achieved. It can be observed that the advanced constitutive law (MDPC) significantly improved results of the numerical prediction.

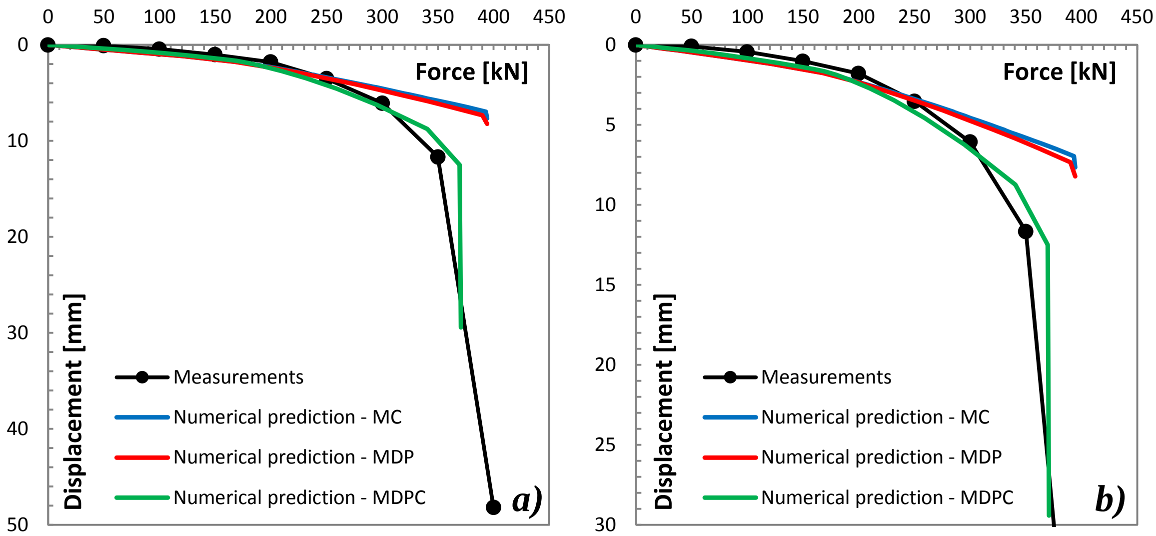

Figure 4.12 Comparison between numerical predictions and measurements. Results of a) the whole loading test, b) test till 30 mm displacement

4.2.4. Conclusions

The aim of the study was to recognize behaviour of a SM column by the full scale static loading test. Taking into account, the economical aspect of this kind of field tests, the numerical method, able to predict results of the test, is needed. The finite element axisymmetric analyse provided good agreement with the measurements. The obtained results from both preliminary and advanced calculations were presented. The results lead us to conclude that the more advanced constitutive law needs to be used. Since more detailed soil properties, like result of the oedometer test, are unknown, the advanced constitutive model was used for only one layer. Its parameters were chosen by the parametric study in accordance with the measurements. The hardening law was defined in consonance with example in literature (Helwany, 2007). As, it was examined previously, the results obtained with the hardening curve for other kind of sand (Figure 3.21), than the analyzed one, is able to approximate quite well the behaviour of the soil.

4.3. Small scale modelling

The use of a scale models in geotechnical engineering allows simulating complex systems under controlled conditions. It gives opportunity to investigate mechanisms guiding in these systems. A scale model of a static loading test of pile may offer a more economical option than the corresponding full-scale test. Moreover, conducting parametric studies with these kind of models can be used to explore phenomenon where case histories and prototype tests provide limited data.

This paragraph will first briefly describe the experimental study performed in Laboratoire de Génie Civil et l'Ingénierie Environnementale (LGCIE), INSA Lyon, by Mahmoud Dhaybi (Dhaybi, 2015). Then all used materials are going to be characterized.

Afterwards, the finite element modelling of carried out physical tests will be presented. All numerical predictions are compared with the measurements and the appearing differences are discussed. The model calibrated in accordance with the laboratory material and loading tests is used to make perditions of the additional tests.

4.3.1. Laboratory test

Between September 2010 and August 2013 in LGCIE an advanced experimental study of the behaviour of the Soil Mixing column has been carried out by Dhaybi (Dhaybi, 2015). The main objective of the research was to investigate properties of the Soil Mixing as a material and its usage as a reinforcement of soil and shallow foundation.

4.3.1.1. Characteristics of the materials

In order to understand behaviour of the small scale SM columns, profound investigation of the material properties has been needed. The Hostun sand, with two densities, have been examined by direct shear and oedometer tests. The material analysis of the Soil Mixing consisted of: slam and flow tests, static and dynamic Young's modulus tests, and unconfined compressive strength (UCS) test with varied cement ratio. The unconfined compressive strength, as well as static and dynamic Young's modulus, has been investigated as a function of the curing time of the mixture. Three different cement ratios have been taken into consideration. Contact between soil and column was also a subject of the study. Properties of this interaction have been obtained by shear test.

Results of the empirical investigation provided data for the numerical calculations are presented below.

4.3.1.1.1. *Hostun sand HN 31*

The origin of Hostun sand HN 31 is Hostun located in the area of Drôme in the south-east of France. The sand is a silica one, which consists of high (~98.76 %) siliceous amount (SiO_2). The grain shape varies from angular to sub-angular. Their size distribution curve can be found in Figure 4.13.

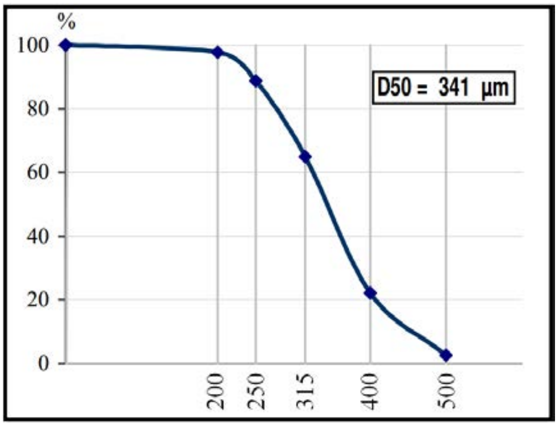

Figure 4.13 Grains size distribution curve for Hostun sand (Sibelco, 2012)

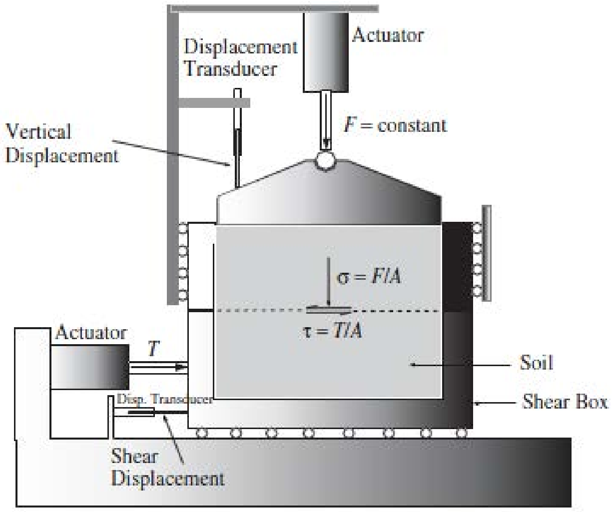

Figure 4.14 Direct shear test apparatus (Helwany, 2007, p. 167)

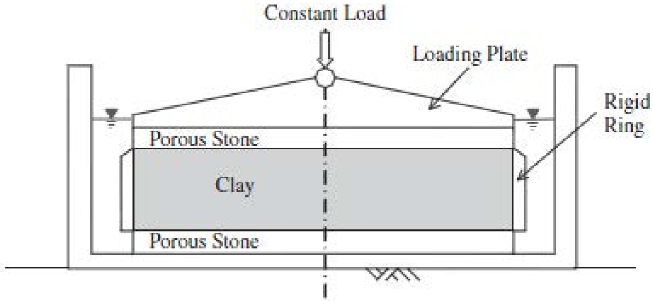

Figure 4.15 Oedometer apparatus (Helwany, 2007, p. 128)

This sand has been subject of many studies in recent years like: Combe (Combe, 1998), Sunyer Amat (Sunyer Amat, 2007), Flavigny, et al. (Flavigny, et al., 1990), etc. Moreover, for a long period of time it has been used as the reference sand in France. Hence many information can be found in the literature under the previous name - Hostun sand RF. According to Colliat (Colliat, 1986) the maximal and minimal unit weights of this type of sand are γ_{max} = 15.99 kN/m^3 and γ_{min} = 13.24 kN/m^3, respectively. The unit weight of the soil solids (soil skeleton) is equal to γ_s = 25.97 kN/m^3. The void ratio of the Hostun sand varies between its maximal e_{max} = 0.961 and minimal value e_{min} = 0.626.

In the experimental study, performed by Dhaybi (Dhaybi, 2015), the dry sand with two densities was analyzed. The first one $\gamma_{loose} = \gamma_d \approx 13.80$ kN/m^3 and in the study is called 'loose'. The second density was about $\gamma_{dense} = \gamma_d \approx 15.00$ kN/m^3, which in this study is called 'dense'.

A direct shear test apparatus (Figure 4.14) was used in order to investigate shear properties of the sand. The friction angle is equal to ϕ_{dense} = 35.2° and ϕ_{loose} = 29.0° for 'dense' and 'loose' sands, respectively. According to theory, dry sand is considered as cohesionless material. Despite many repetitions of the test, it was not possible to reach the zero value of cohesion. The obtained average values are c_{dense} = 0.16 kPa and c_{loose} = 0.44 kPa for 'dense' and 'loose' sands, respectively.

Properties of both sands obtained from laboratory tests are presented in Table 4.11. Concerning hardening behaviour of the soil, oedometer test apparatus was used (Figure 4.15). Oedometer test was performed for three densities. Two of them represent dense sand, ρ^{I}_{dense} = 1500 kg/m^3, ρ^{II}_{dense} = 1526 kg/m^3. The third tested density was ρ_{loose} = 1380 kg/m^3. Obtained values of void ratio, e_0, compression index, C_C and swelling index, C_S, are presented in Table 4.10.

The hardening phenomenon is defined in accordance with the oedometer test results. Hardening obeys the law presented by Equation 3.22. The p_b as a function of plastic volumetric strain is presented in Figure 4.16. All properties obtained for dense and loose sands are gathered in Table 4.11. According to this average values, parameters of the numerical models were assumed.

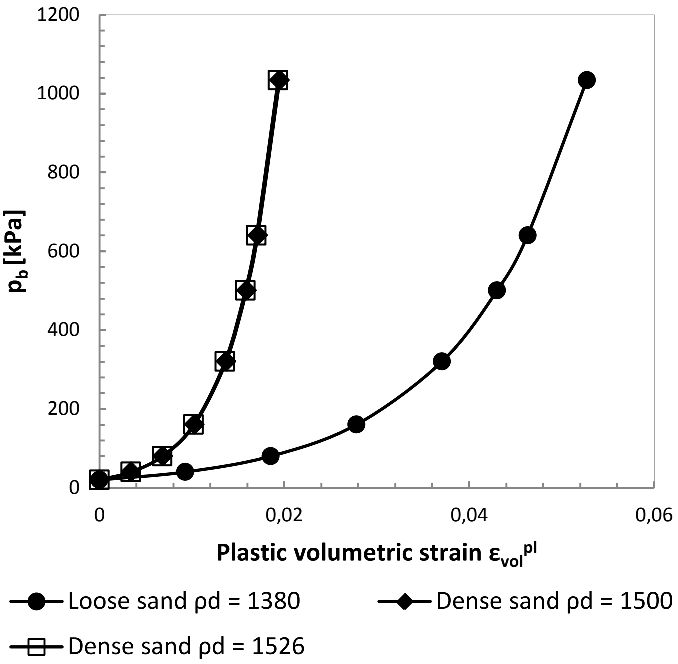

Figure 4.16 Hardening curves for different densities of the Hostun sand obtained from oedometer test

Table 4.10 Results of oedometer tests carried out for four densities of the Hostun sand (Dhaybi, 2015)

Parameter	Density [kg/m^3]		
	ρ^{I}_{dense} = 1500	ρ^{II}_{dense} = 1526	ρ_{loose} = 1380
Void ratio e_0 [-]	0.74	0.76	0.92
Compression index C_C [-]	0.0325	0.0320	0.0820
Swelling index C_S [-]	0.0129	0.0120	0.0230

Table 4.11 Properties of Hostun sand obtained during laboratory tests (Dhaybi, 2015)

Parameter	Unit	Hostun sand 'loose'	Hostun sand 'dense'
Density	ρ [kg/m^3]	1380	1500
Void ratio	e_0 [-]	0.92	0.76
Friction angle	ϕ [°]	29.0	35.2
Cohesion	c [kPa]	0.44	0.16

Small scale, 1g model analyzed in the laboratory conditions results with very low confining pressure. Due to that, value of the Young's modulus of sand is significantly lower than one which can be found in the *in situ* conditions. Due to lack of results of the triaxial test performed with appropriate confining pressures the value of Young's modulus was approximated according to equation proposed by Janbu (Janbu, 1963) (Equation 4.2), where: E_{ref} is the reference Young's modulus corresponding to the reference pressure, p_{ref} stands for atmospheric pressure (p_{ref} = 100 kPa), σ_{conf} is confining pressure and n is an exponential coefficient. According to Janbu investigation, value of coefficient n varies between 0.33 and 1.00.

$$E = E_{ref}\left(\frac{\sigma_{conf}}{p_{ref}}\right)^{n} \qquad 4.2$$

Table 4.12 Parameters of the Janbu (Janbu, 1963) equation for 'loose' Hostun sand HN31 (RF) proposed by several researchers

Parameter	Lancelot et al.	Colliat	Flavigny	Gay
E_{ref} 'loose' sand [kPa]	31700	9050	9650	14000
n 'loose' sand	0.76	0.60	0.83	0.97

Table 4.13 Parameters of the Janbu (Janbu, 1963) equation for 'dense' Hostun sand HN31 (RF) proposed by several researchers

Parameter	Lancelot et al.	Colliat	Flavigny	Gay
E_{ref} 'dense' sand [kPa]	62600	27700	33200	40000
n 'dense' sand	0.68	0.45	0.83	0.86

Several studies were carried out in order to define properly constant parameters for Hostun sand. It was noticed that not only value of confining pressure changes with density of the soil but also E_{ref} and n. Parameters, proposed by Lancelot et al. (Lancelot, et al., 1996), Colliat and Flavigny (Branque, et al., 1997) and Gay (Gay, 2000) are presented in Table 4.12 and Table 4.13.

In order to calculate the Young's modulus for both densities of sand value of σ_{conf} is calculated as the average value of horizontal stress, σ_h, in the 1 m deep tank filled with sand (Equation 4.3). The horizontal stress is obtained as the average vertical stress, σ_v, in the tank multiplied by the coefficient of earth pressure at rest K_0. The coefficient is defined according to Jaky (Jaky, 1944) equation and is a function of the internal friction angle of the material (Equation 4.4). The average value of the vertical stress is calculated as a value at the half depth of the tank, h = 0.5 m. Hence, vertical and horizontal stresses for both densities of sand are presented in Table 4.14, where g is gravity (g = 9.81 m/s^2). The confining pressure equals to 3.70 kPa and 3.24 kPa for 'loose' and 'dense' sand respectively is used to calculate the modulus of deformation according to the Janbu equation while having regard to the findings of the Lancelot, Colliat, Flavigny and Gay concerning Hostun sand (Table 4.12 and Table 4.13). Values of Young's modulus, E, are presented in Table 4.15. As it can be noticed the spectrum of values is significant. Modulus varies between 0.56 and 2.53 MPa for 'loose' sand and 2.10 and 6.08 MPa for the 'dense' one. The obtained values prove that the Young's modulus in 1g laboratory modelling is considerably lower than the one which can be found in *in situ* conditions. Acquired values of Young's modulus are used as a starting data for parametric study performed on numerous of experimentally investigated cases. According to its results the modulus of sand for numerical calculations is chosen as 3.00 MPa and 7.00 MPa for 'loose' and 'dense' sand respectively.

$$\sigma_{conf} = \sigma_h = K_0 \sigma_v \tag{4.3}$$

$$K_0 = 1 - sin\,\phi' \tag{4.4}$$

Table 4.14 Average values of vertical and horizontal stresses in tank for both densities of Hostun sand

Density	ϕ [°]	K_0 [-]	$\sigma_v = hg\rho_d$ [kPa]	$\sigma_{conf} = \sigma_h$ [kPa]
'loose' sand	28	0.53	6.77	3.59
'dense' sand	34	0.44	7.36	3.24

Table 4.15 Young's modulus calculated for 'loose' and 'dense' sands

Density	Lancelot et al. [MPa]	Colliat [MPa]	Flavigny [MPa]	Gay [MPa]
'loose' sand	2.53	1.23	0.61	0.56
'dense' sand	6.08	5.92	1.93	2.10

In the numerical study of the small scale Soil Mixing column, the soil is assumed as a material following, presented in Chapter 3, MDPC criterion. Its parameters have been obtained according to laboratory tests and parametric studies in accordance with all experimental results (18 tests) presented in Chapter 4 and Chapter 5. Properties of sand have been calibrated mainly according to results of the loading test of shallow foundations:

- 'loose' sand (ρ_d = 1380 kg/m^3) – loading test of a shallow foundation (0.35 m x 0.35 m),
- 'dense' sand (ρ_d = 1500 kg/m^3) – loading test of a shallow foundation (0.20 m x 0.25 m).

The properties of both soils are presented in Table 4.16. The cap parameters can be found in Table 4.17. The hydrostatic compression yield stress, p_b, is defined as a function of plastic volumetric strain (Figure 4.16 – 'loose' sand ρ_d = 1380 kg/m^3 and 'dense' sand ρ_d = 1500 kg/m^3.

Table 4.16 Properties of Hostun sand used in numerical studies

Parameter	Unit	Hostun sand 'loose'	Hostun sand 'dense'
Density	ρ [kg/m^3]	1380	1500
Young's modulus	E [MPa]	3	7
Poisson's ratio	ν [-]	0.3	0.3
Friction angle	ϕ [°]	28	34
Dilation angle	ψ [°]	3	4
Cohesion	c [kPa]	0.5	0.4

Table 4.17 MDPC parameters for parameters of 'loose' and 'dense' Hostun sand used in numerical studies

Parameter	Hostun sand 'loose'	Hostun sand 'dense'
Cap eccentricity R [-]	0.6	1.2
Transition zone parameter α [-]	0.05	0.1
Initial cap yield surface position $\varepsilon^{pl}{}_{vol}\|_0$ [-]	0.0	0.0
Hydrostatic compression yields stress p_b [kPa]	According to Figure 4.16 'loose' sand ρ_d = 1380	According to Figure 4.16 'dense' sand ρ_d = 1500

4.3.1.1.2. *Soil Mixing columns*

According to experimental testing (Dhaybi, 2015), SM column was prepared in laboratory conditions as a mixture of the Hostun sand HN 31, water and cement CEM III/C 32.5N. Before taking decision concerning expected mechanical properties, the characteristics of mixture with three different cement contents were studied. Materials containing 140 kg/m^3, 210 kg/m^3 and 280 kg/m^3 of cement were analyzed. The cement – soil (*C/S*) and cement – water (*C/W*) ratios of mixtures are presented in Table 4.18. In order to characterize properties of mixtures, the unconfined compression test was carried out on specimens (45 mm diameter and 90 mm height) prepared in accordance with RUFEX protocol (Guimond-Barrett, 2011).

SM specimens at the age of 7, 14, 21 and 28 days were tested in order to indicate an influence of curing time on the behaviour of the material. Three specimens were tested for each age of the mixture to ensure reliability of the obtained results. The effect of curing time on specimen's unconfined compressive strength q_u of the material, is presented in Figure 4.17. Results show that the mixture with the highest cement content can reach unconfined compressive strength equal to q_u = 7.03 MPa after 28 days. In contrary, specimens containing the lowest cement content reach just q_u = 1.20 MPa after 28 days. Taking into account mechanical and economical factors, mixture II was chosen for the further study.

Table 4.19 shows the variation of unconfined compressive strength, tangent (*E_{50} tangent)* and secant (*E_{50} secant)* Young's modules as a function of age.

Table 4.18 Properties of tested mixtures (Dhaybi, et al., 2012)

Mixture	Cement content [kg/m^3]	Cement – soil ratio C/S [-]	Cement – water ratio C/W [-]
Mixture I	140	0.10	0.70
Mixture II	210	0.15	0.55
Mixture III	280	0.20	0.40

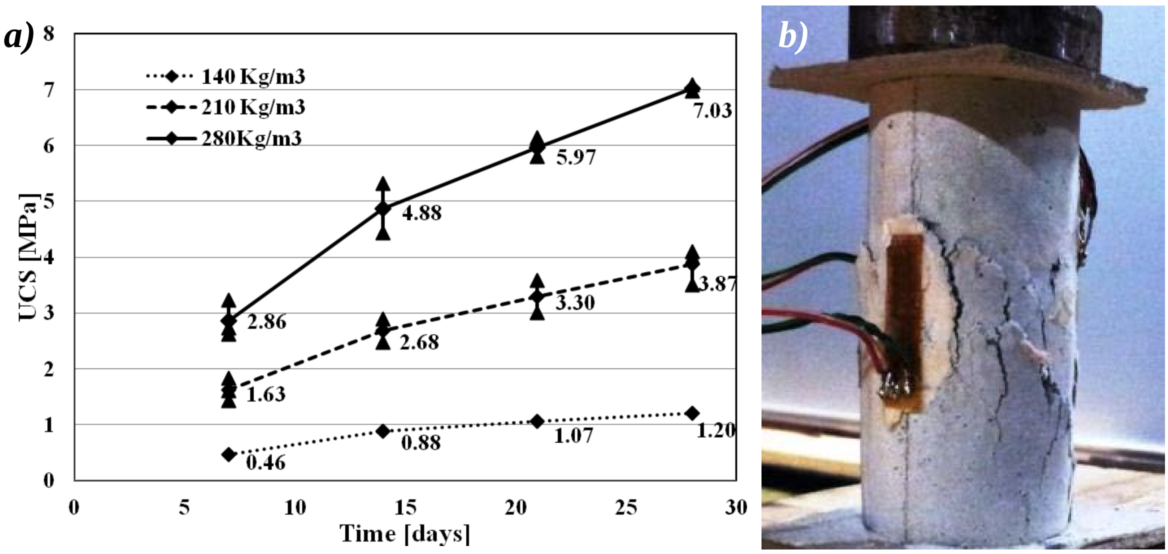

Figure 4.17 a) evolution of unconfined compressive strength, q_u = UCS, of SM specimens as a function of time, b) specimen equipped with sensors during the test (Dhaybi, et al., 2012)

Table 4.19 Evolution of the unconfined compressive strength, tangent and secant Young's modules with age (Dhaybi & Pellet, 2012)

Age [days]	q_u [MPa]	E_{50} tangent [GPa]	E_{50} secant [GPa]
7	1.6	2.2	2.8
14	2.6	3.3	4.0
21	3.3	3.8	4.5
28	3.8	4.3	4.9

Several numerical studies (Paragraph 2.3.2) have been performed to investigate the behaviour of soil treated by the SM method. In this thesis, two columns, after 7 and 14 days of curing, prepared in laboratory conditions are modelled with the elastic perfectly plastic model with the MC criterion. Their elastic properties are assumed to be as E_{50} secant obtained from the laboratory tests. Therefore, modulus of deformation E equals to 2.8 GPa and 4.0 GPa for 7 and 14 days old columns. The Poisson's ratio is taken as $\nu = 0.2$ in both cases.

Table 4.20 Mohr-Coulomb parameters of the SM columns presented in the literature

Reference	Type of reinforced soil	c [kPa]	ϕ [°]	E [MPa]
(Han, et al., 2007)	soft clay, silt	0	45	30
(Horpibulsuk, et al., 2012)	soft Bangkok clay	600	25	120
(Mun, et al., 2012)	clay	2800	0	330
(Voottipruex, et al., 2011)	clay	200-300	30	30-60
(Melentijevic, et al., 2013)	granular fill	500	35	300

Performing triaxial test for the SM material was impossible due to its high resistance. Consequently, plastic properties of the columns needed to be determined accordingly to examples presented in the literature and parametric studies. Some of studies, where SM column was analysed with MC criterion are presented in Table 4.20. Huge variation of properties can be observed. Cohesion changes between 0 and 2800 kPa, whereas friction angle between 0 and 45°.

As it was presented previously (Chapter 2), type of soil, cement ratio, mixing technique, age, etc. are factors with significant influence on properties of the SM elements. In this study, SM columns are created as a mixture of fine sand and slurry, that is why results presented by Melentijevic, et al. (Melentijevic, et al., 2013), seem to be the most relevant (Table 4.20). In their study SM columns were created by the Springsol technique in granular fill.

Table 4.21 Mohr-Coulomb parameters for concrete with characteristic compressive strength f_{ck} = 15 MPa (Ardiaca, 2009)

Parameter	Jimenez Montoya method	EHE-98	Eurocode-2
c [kPa]	712	365	387
ϕ [°]	54.9	35	9
E [MPa]	24.173	24.173	24.173

Table 4.22 Mohr-Coulomb parameters for concrete with characteristic compressive strength f_{ck} = 25 MPa (Ardiaca, 2009)

Parameter	Jimenez Montoya method	EHE-98	Eurocode-2
c [kPa]	1186	513	500
ϕ [°]	54.9	35	9
E [MPa]	27.264	27.264	27.264

Table 4.23 Properties of the 7 and 14 days old SM columns used in numerical studies

Parameter	Unit	Soil Mixing 7 days old	Soil Mixing 14 days old
Density	ρ [kg/m^3]	2000	2000
Young's modulus	E [MPa]	2800	4000
Poisson's ratio	ν [-]	0.2	0.2
Friction angle	ϕ [°]	35	35
Dilation angle	ψ [°]	5	5
Cohesion	c [kPa]	350	680

Taking into account results of the unconfined compressive strength test, SM material can be analysed as very weak concrete. In this case, cohesion and friction angle can be chosen according to properties of concrete presented by Ardiaca (Ardiaca, 2009). In this paper properties of two kinds of concrete (characteristic compressive strength f_{ck} = 15 MPa and f_{ck} =- 25 MPa) were determined according to three different methods (Jimenez Montoya method, EHE-98 and Eurocode-2). Obtained results are presented in Table 4.21 and Table 4.22. It can be noticed that friction angle in all methods is a constant value, independent from compressive strength. However, proposed values are considerably different from each other. The same tendency can be seen in case of cohesion.

Due to similarities between shear properties obtained for f_{ck} = 15 MPa according to EHE-98 and results presented by Melentijevic, et al. (Melentijevic, et al., 2013), c = 350 kPa and ϕ = 35° are used as the staring data for the parametric study. The final set of elastic and shear parameters of both columns have been obtained according to parametric study carried out in accordance with results of all 18 tests presented in Chapter 4 and Chapter 5 but mainly results of loading tests of columns in tubes.

Set of elastic and shear properties of 7 and 14 days old columns, used in numerical modelling, is presented in Table 4.23.

4.3.1.1.3. *Contact between soil and column*

As explained in the previous section, contact between soil and SM column can be compared to the one between soil and pile. In this case, the crucial role, in the definition of the interaction, plays correct determination of the interface friction angle ϕ^{int} and friction coefficient μ_f. Therefore, interaction between SM column and soil was topic of the experimental study. In order to characterize it properly, direct shear test between surface of the treated soil and soil was performed. The apparatus with a box (20 cm x 20 cm) was used. Figure 4.18a presents the apparatus. The lower box was filled with the treated soil prepared as presented in the previous paragraph. The surface of the mixture was roughed in order to make it similar to the shaft of a real column (Figure 4.18b). After 7 days, when the mixture solidified and gained resistance, the upper box was completed with sand. Test was carried out for 'loose' and 'dense' sands. Each test was repeated four times to confirm the result. The varying parameter was normal stress, 28 kPa, 43 kPa, 57 kPa, 88 kPa for 'loose' sand and 57 kPa, 102 kPa, 118 kPa, 148 kPa for 'dense' sand. Obtained results lead to conclusion that the friction angle between surfaces is about ϕ^{int}_{loose} = 27° for 'loose' and ϕ^{int}_{dense} = 30° for 'dense' sand. Hence, friction coefficient equals to μ_{floose} = tan 27° = 0.50 and μ_{fdense} = tan 30° = 0.58. It means that friction coefficient accounts for 89% and 82% of the internal friction between grains. All properties are presented in Table 4.24.

Figure 4.18 a) direct shear test apparatus used to analyze the interface between soil and Soil Mixing material (Dhaybi, 2015), b) roughed surface of the treated soil

In numerical calculations, the friction coefficient is taken as: μ_f = 0.46, that refers to about 25° (~87%) for 'loose' and μ_f = 0.55, what is about 29° (~82%) for 'dense' sand. Values used in the calculations are presented Table 4.25.

Table 4.24 Results of experimental study of an interface between soil and SM column carried out for densities of the Hostun sand (Dhaybi, 2015)

Parameter	Unit	Hostun sand 'loose'	Hostun sand 'dense'
Friction angle of soil	ϕ [°]	29.0	35.2
Interface friction angle	ϕ^{int} [°]	27.0	30.0
Friction coefficient	μ_f [-]	0.50	0.58
Interface friction / Internal friction tan ϕ^{int} / tan ϕ^{soil}	[%]	89	82

Table 4.25 Properties of interface between soil and SM column used in numerical studies

Parameter	Unit	Hostun sand 'loose'	Hostun sand 'dense'
Friction angle of soil	ϕ [°]	28	34
Interface friction angle	ϕ^{int} [°]	25	29
Friction coefficient	μ_f [-]	0.46	0.55
Interface friction / Internal friction $\tan \phi^{int} / \tan \phi^{soil}$	[%]	87	82

4.3.1.2. Experimental setup

The small scale experimental study of SM columns, was performed in Laboratoire de Génie Civil et l'Ingénierie Environnementale (LGCIE), INSA Lyon, by Dhaybi (Dhaybi, 2015). It was an attempt to investigate mechanisms guiding the behaviour of the SM element under controlled, laboratory conditions. Due to model's dimensions, it was possible to perform parametric studies to capture phenomenon of column's behaviour. However, small scale, and especially 1g conditions, makes this kind of experimental studies unable to be extrapolated to the real, full scale cases. Thus, obtained results need to be consider as qualitative, not quantitative.

A tank and tubes used in laboratory experimental program, as well as a method of creation of SM columns, created by Dhaybi, is provided in following paragraphs.

4.3.1.2.1. *Tank and creation of column*

As mention before, in order to analyze the behaviour of SM column, an experimental setup was built in LGCIE, INSA Lyon (Dhaybi, 2015). It consists of a tank (2 m x 1 m x 1 m) divided into two chambers - 1 m^3 each. The division let setting up simultaneously two tests. The tank (Figure 4.19) was filled by 10 cm thick layers of dry Hostun sand to ensure appropriate homogeneity and compaction of the soil. The uniformity of the soil was tested by dynamic penetrometer PANDA 2® (Benz Navarrete, 2009). Detailed results of the performed tests can be found in report prepared by Sol Solution (Sol Solution, 2012). For the survey, both chambers of the tank have been filled with soil. The first one consisted of 'loose' and the second one of 'dense' Hostun sand. In order to well represent the whole volume of the tank's chamber, each soil has been tested by minimum 6 penetrations localized in the corners, in the centre and in the centre of one edge of the tank's chamber. Patterns of the performed tests are presented in Figure 4.20. Results of surveys are presented in Figure 4.21 and Figure 4.22. Density is presented as a function of tanks depth, for planes A-A' and B-B' for 'loose' and 'dense' sands. Maps of soils' density, acquired from tests, present relatively small variation inside the soil volume. The obtained values of density and relative density are presented in Table 4.26 and Table 4.27 respectively. The average value for 'loose' sand equals to 1430 kg/m^3 and is comparable with assumed in numerical calculations 1380 kg/m^3. In case of 'dense' sand, provided by PANDA 2® survey density equals to 1530 kg/m^3, which corresponds well to taken value 1500 kg/m^3.

Figure 4.19 Tank used by Dhaybi to study behaviour of a small scale SM column. (Dhaybi, et al., 2012)

Table 4.26 Density of the Hostun sand tested in tank by the PANDA 2® test (Sol Solution, 2012)

Density	Unit	Hostun sand 'loose'	Hostun sand 'dense'
Minimal	[kg/m^3]	1290	1410
Maximal	[kg/m^3]	1550	1660
Average	[kg/m^3]	1430	1530

Table 4.27 Relative density of the Hostun sand tested in tank by the PANDA 2® test (Sol Solution, 2012)

Relative density	Unit	Hostun sand 'loose'	Hostun sand 'dense'
Minimal	[%]	6	27
Maximal	[%]	76	113
Average	[%]	34	71

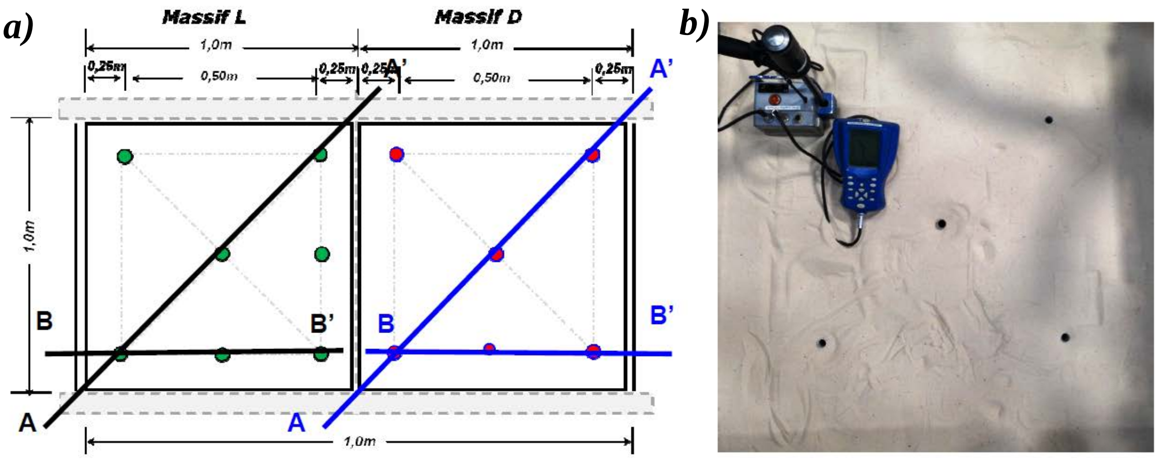

Figure 4.20 a) pattern of the penetrometer survey performed in the tank. The left hand side of the tank is filled with 'loose' sand and the right hand side with 'dense' sand, b) PANDA 2® test in 'dense' sand (Sol Solution, 2012)

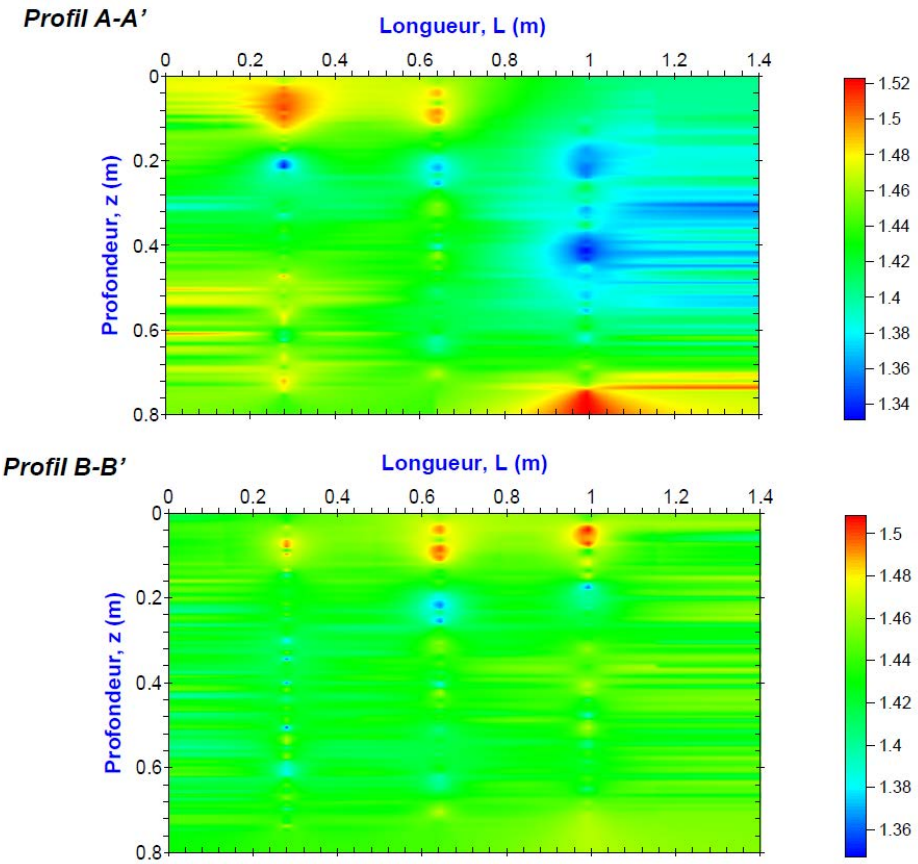

Figure 4.21 Variation of a density in the chamber filled with 'loose' Hostun sand. a) plane A-A', b) plane B-B' (Sol Solution, 2012)

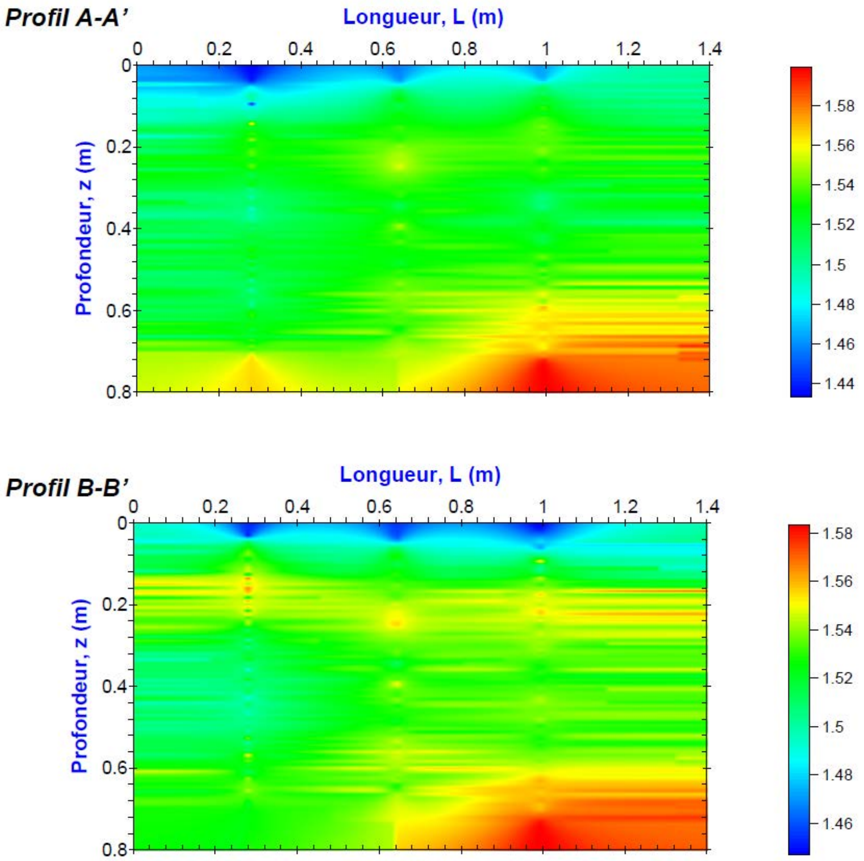

Figure 4.22 Variation of a density in the chamber filled with 'dense' Hostun sand. a) plane A-A', b) plane B-B' (Sol Solution, 2012)

In order to be able to perform tests on SM columns and shallow foundations, tank is equipped with hydraulic jack. It is installed on a special metal frame based on a guidance system on rails. The system allows the jack to be moved in the horizontal plane, covering the entire upper surface of the tank. The experimental setup can be found in Figure 4.19.

SM column in laboratory conditions needs to be installed in a different way than it is done in field. The main reason which prevents using real equipment is its size (Presented in Figure 4.1b, Springsol mixing tools have diameters: 0.4 m and 0.6 m). Due to this difficulty an alternative way of erecting columns was necessary to be invented. It must be mentioned, that technique needed to provide column with composition prepared in accordance with RUFEX protocol (Guimond-Barrett, 2011). The method chosen as the proper one is described in Figure 4.23. Installation procedure starts with pushing steel tube into the soil. Tube's internal diameter represents diameter of the created column. In the study, it is 0.07 m. The length of the column is 0.45 m and it is equal to the length of the tube. The next step is to remove by vacuum cleaner sand located inside the tube. This soil is afterwards used to prepare the SM. Then, empty tube is filled with prepared mixture layer by layer, each time compacted by a piston, which diameter corresponds to the internal diameter of the tube. After compaction, tube is slowly drawn out till its end achieves the top of the created layer of SM. Procedure is repeated continuously until the tube is completely removed from the soil. Formed in this way column is presented in Figure 4.24. Columns are left for 7 or 14 days before are tested. Obtained results are analysed together with the numerical ones in paragraph below.

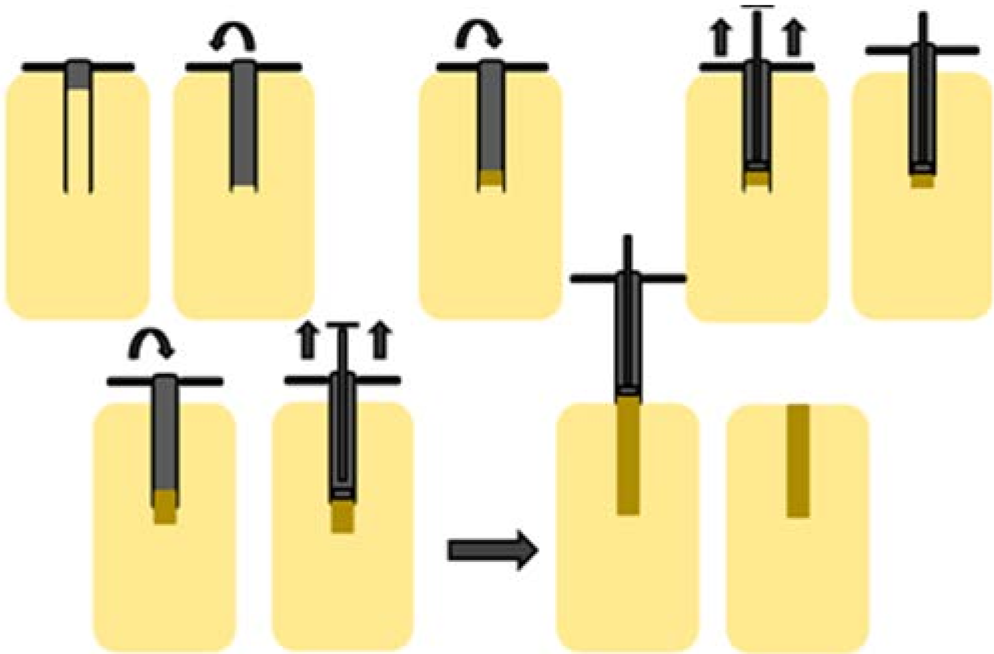

Figure 4.23 Laboratory technique of placing the SM column in soil (Dhaybi & Pellet, 2012)

Figure 4.24 Prepared in laboratory SM column (Dhaybi & Pellet, 2012)

4.3.1.2.2. *Tests in tubes*

The 2 m^3 tank offers one big or two smaller compartments to performer tests. Concerning the 1:10 scale of the model and size of the column, volume of the tank does not ensure enough space for the study of a bigger group of columns. Additional obstacle appears due to way of installation of a column in laboratory conditions. It is very difficult to create numerous columns inside the tank and simuntainesly guarantee their perpendicularity. As a solution for this problem, using blind steel tubes with different diameters was proposed. Hence, the behaviour of the SM columns in group has been analyzed with assumption that column placed in a non-deformable tube represents the central column in the group (Figure 4.25a). All tubes, regardless their diameter, were H = 0.8 m long. Four diameters, D, stand for spacing of columns were analysed: 0.26 m, 0.35 m, 0.45 m, 0.65 m. The column installation method was the same as in the tests in tank. With the non-deformable tube appeared additional and unwanted interaction. Loading test carried out on the centrally situated column generated difficult to measure friction between tube's shaft and soil. First loading tests of SM element in 'dense' sand were executed with the frictional contact between soil and the tube's shaft. The way of taking this interaction into account in numerical modelling is explained in details below. For tests in 'loose' sand, an efficient method of reduction soil-tube friction was applied. Interior of the tube was treated by an oil and afterwards padded with plastic film. Due to this slippery layer, friction could have been considered as zero or insignificantly low.

The aim of the loading tests in tubes was to investigate: the influence of the confining stress on the bearing capacity of a group of columns and failure mechanisms (Figure 4.25b). Studies concerning 'dense' sand included only one tube's diameter, D = 0.26 m, whereas for 'loose' sand columns were tested in all four tubes. However, only in 'dense' sand columns after 7 and 14 days of curing were loaded. The experimental testing provided more detailed study of the confining stress for the 7 days old column placed in 'loose' sand. Results of the executed tests and the numerical predictions are discussed below.

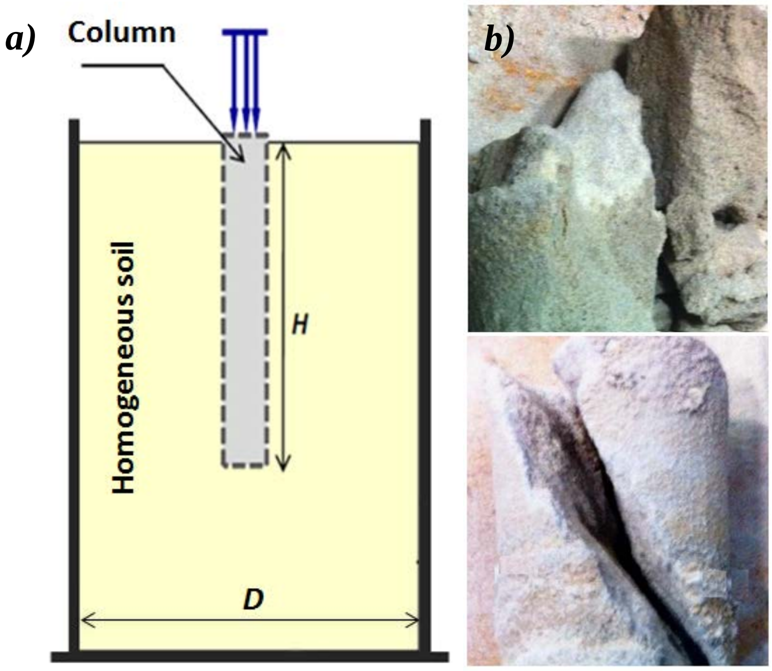

Figure 4.25 a) tube used to investigate behaviour of a group of SM columns, b) failure of column acquired from tests (Dhaybi, 2015)

4.3.2. Numerical calculations

The behaviour of the SM column was studied by the numerical finite element simulations in ABAQUS. In order to do it, axisymmetric type of model was used. Numerical models' dimensions were chosen according to the experimental setup. Parameters of all used materials are presented above in paragraph 4.3.1.1.

In this paragraph the static loading tests of the single and group of columns are presented.

4.3.2.1. Single column in 'dense' sand

As described previously, the loading test of a single column has been performed in 1 m^3 tank. The SM column has been centrally placed in the homogeneous layer of the 'dense' Hostun sand. Test was performed 14 days after column's installation.

The aim of the study is to reproduce the behaviour of the column by the numerical simulation and to assess its final bearing capacity, using an axisymmetric type of model. The numerical model geometry, mesh and boundary conditions are presented in Figure 4.26. The distance between column's axis and the boundary of the model is equal to half of the tank dimension (0.500 m). The 0.450 m long SM column with diameter d_{SM} = 0.070 m is a subject of the study. The mesh used in the modelling, consists of 6-node modified quadratic axisymmetric triangle elements (CAX6M).

The numerical model's boundary conditions are: symmetric boundary on the left hand side of the model (axis of symmetry) and no horizontal displacement at the right hand side. In the bottom, displacements are restricted in the vertical direction. The column is subjected to the loading modelled by imposed, to its head, displacement.

Soil is modelled with MDPC criterion. SM column is modelled with the elastoplastic constitutive law with MC criterion. The properties of soil are presented in Table 4.16 and Table 4.17. Column is modelled according to properties gathered in Table 4.23. As mentioned before, the contact between column and soil is simulated with the Coulomb friction criterion. Friction coefficient can be found in Table 4.25.

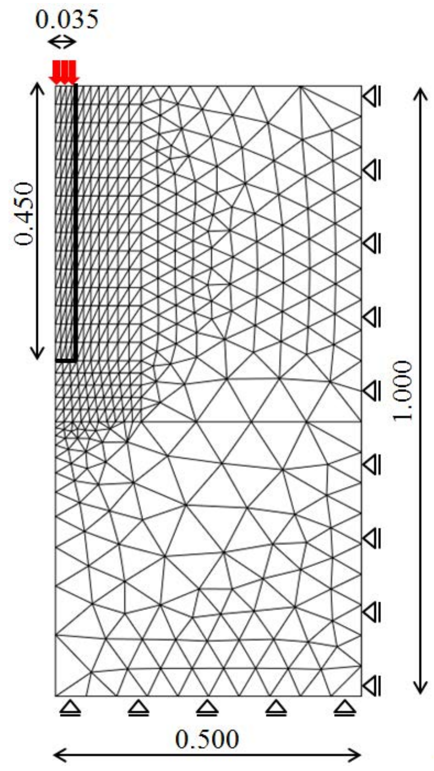

Figure 4.26 Finite element mesh and boundary conditions used in numerical modelling of a static loading test of a single SM column (all dimensions in meters)

4.3.2.1.1. *Results*

Results of the numerical modelling and the experimental test for 14 days old column are compared in terms of axial stress in Figure 4.27. Numerical prediction of the behaviour of 14 days old column corresponds to measurements. Some small but still acceptable differences appear at the beginning of the loading process. The predicted force is higher than the measured one till about 4.4 mm, where prediction is exact. First 1.6 mm of the loading, the difference between results increases. After this displacement, it starts to decreases till 4.4 mm. Then, the increase of force is slower for the numerical study. Hence, the more the displacement increases, the greater the difference between measurements and prediction till about 11.5 mm. From this displacement, dissimilarity starts to be constant with the difference about 1.1 kN. The value of axial force stabilizes respectively at about 5.7 kN and 6.8 kN for the numerical and the experimental results. In both analyses, the failure of the column takes place due to soil plasticity, which starts for the numerical test after about 2.6 mm. In spite of discrepancies, the predicted behaviour of 14 days old column corresponds well to the experimental observation.

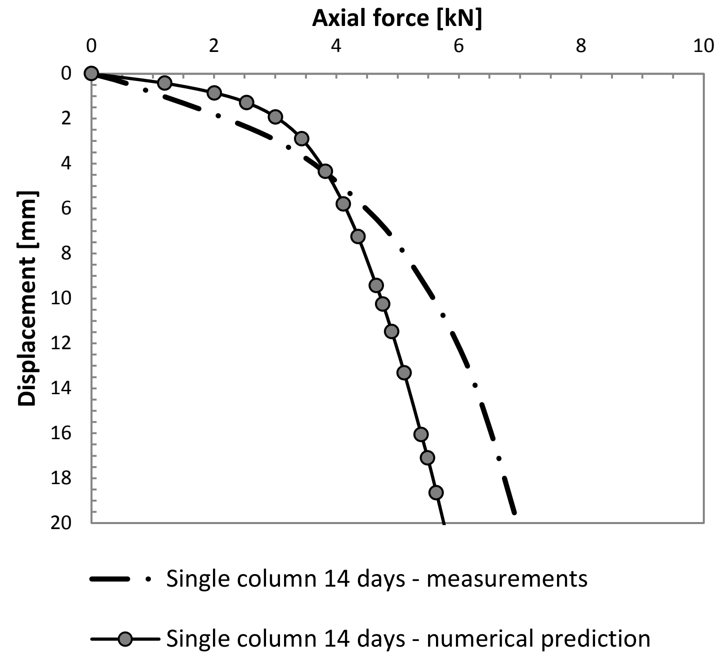

Figure 4.27 Results of the static loading test of the single SM column

4.3.2.2. 'Group of columns' in 'dense' sand

The behaviour of the SM columns in group has been analyzed with the assumption that column placed in a non-deformable tube represents the central column in the group (Figure 4.28a). The axisymmetric type of calculations has been used in order to predict the bearing capacity of the group of columns. Hence, the model has been reduced to the unique column (Figure 4.28b). The distance between its axis and the boundary of the model, simulates the half distance between columns.

The axisymmetric model consists of three parts: the SM column, soil around and steel tube, like in the physical test. The non-deformable, 0.800 m long, blind tube with internal diameter D = 0.260 m and wall thickness 0.010 m has been analyzed. It has been added to simulate the frictional contact between the tube shaft and the soil, which exists in reality. It would not be possible by defining the boundary conditions directly on the sand vertical side.

Also in this case, the mesh consists of CAX6M elements. The mesh and model dimensions are presented in Figure 4.28b. The boundary conditions are: no horizontal displacement at the right hand side, symmetric boundary on the left hand side of the model and restricted vertical displacement at the bottom. The steel tube is analyzed with the elastic model. Its parameters are: ρ = 7750 kg/m^3, E = 205 GPa and ν = 0.2. In order to simulate contact, between the soil and the tube (Figure 4.28c), the same kind of interface elements with zero initial thickness obeying the Coulomb failure criterion are used. The proper value of the coefficient has been chosen according to parametric study. The column-shaft friction coefficient has been kept identical as in previous modelling. The 7 and 14 days old columns are loaded by imposed displacement until failure.

4.3.2.2.1. *Parametric study*

The contact properties between steel tube and the Hostun sand was not studied in the laboratory. That is why, in order to approximate the value of friction coefficient parametric study has been performed. Acquired results have been compared with the measurements. Hereby, the most appropriate value of the coefficient of friction, μ_t, between the sand inside the tube and tube's wall, has been determined.

The 'dense' sand friction angle, used in the calculations, equals to ϕ_{dense} = 34°. Five values of the coefficient have been chosen as: tan ϕ_{dense} multiplied by 0.75, 0.50, 0.38, 0.25, hence coefficients taken into consideration are 0.506, 0.337, 0.256, 0.169 respectively. The influence of different friction coefficients is presented in Figure 4.29.

Figure 4.29a depicts four curves representing loading test of the 7 days old SM column. As can be seen, in case of μ_t = 0.506 the increase of displacement is the slowest. Additionally, the highest value of final force is obtained for this case. The quickest displacement occurs for μ_t = 0.169. In all cases values of borne force, for displacement equal to 7.6 mm, which corresponds to failure of column, are underestimated. Nevertheless, the value obtained by model with μ_t = 0.506 is the closest to empirical one. The more the displacement increases, the greater the difference between measurements and prediction for μ_t = 0.169 appears. Discrepancy between numerical results begins at about 2.0 mm, where force predicted with μ_t = 0.506 starts increasing faster than in the other three cases and force. The opposite situation can be observed for model with μ_t = 0.169. From 2.0 mm displacement, the increase of the force slows down and small differences in comparison with curves obtained for μ_t = 0.337 and μ_t = 0.256 appear. Whereas, inconsiderable small discrepancy between these two results starts to be visible after about 5.00 mm. In all four cases failure of loaded columns has been achieved by the plasticizing of the head of the column. The plastic failure manifests by significant slowing down the increase of the borne force with the increase of the displacement.

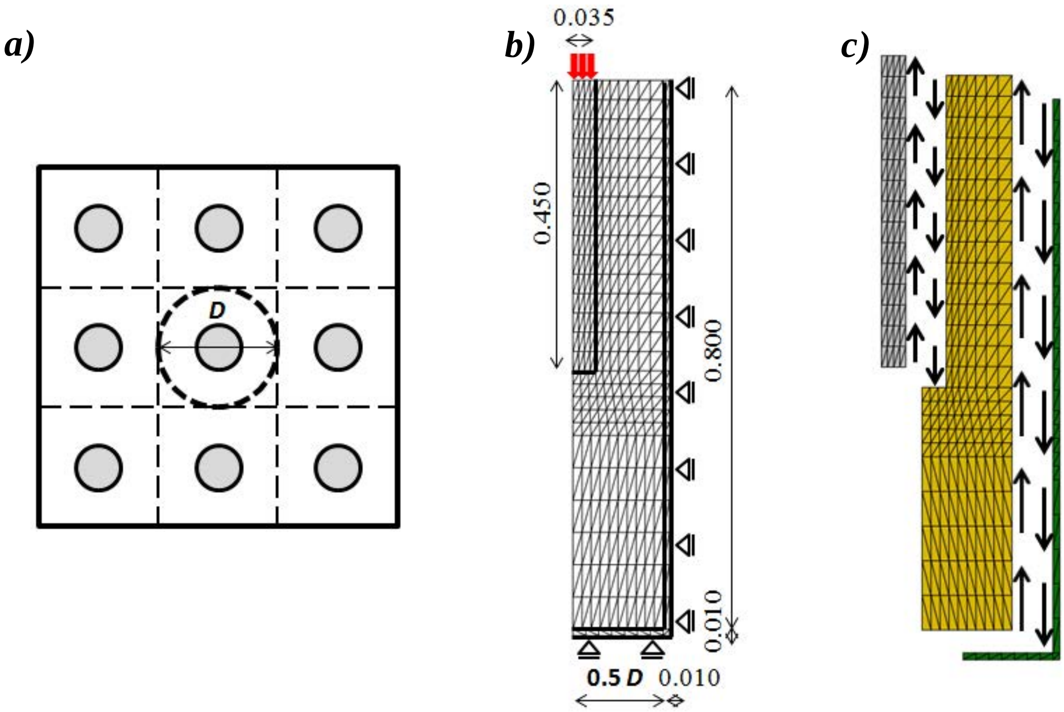

Figure 4.28 a) group of columns with the marked central column, b) finite element mesh and boundary conditions used in numerical modelling of a static loading test of the SM column working in a group (all dimensions in meters), c) two places of interactions in the model (soil-column and soil tube)

Similar tendency of curves can be observed for the older column. Figure 4.29b shows four curves illustrating loading test of the 14 days old SM column. Alike in case of the younger column, the fastest increase of force can be observed for μ_t = 0.506. Moreover, model with this friction coefficient results with the best matching to measurements curve. Additionally, the bigger displacement, the smaller discrepancy between numerical prediction and experimental result. Predicted beginning of the plasticity in column is equalled to the measured one.

Beginnings of all curves are the same until 1.0 mm where force for the highest friction coefficient starts to increase faster, Then, for μ_t = 0.337, μ_t = 0.256 and μ_t = 0.169 curves are almost the same until about 2.5 mm, afterwards, the increase of force, for μ_t = 0.337, begins to be faster than for the other cases. The plasticity of the column occurs for about 11.4 kN in all calculated cases, however, it can be observed for different displacement. Hence, failure has place for 8.2 mm, 9.0 mm, and 10.0 mm for μ_t = 0.337, μ_t = 0.256 and μ_t = 0.169 respectively.

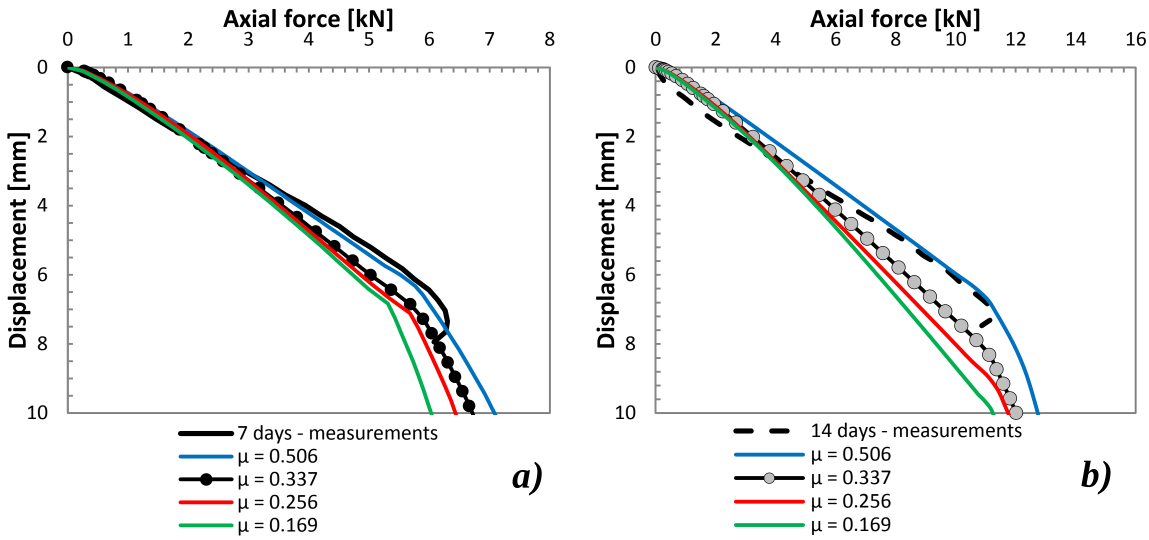

Figure 4.29 The influence of the friction coefficient between steel tube and sand around column on behaviour of: a) the 7 days old column, b) the 14 days old column

According to provided results it can be seen, that decrease of the friction coefficient reduces the slope of the force-displacement curve. As a consequence of friction, occurring between soil and the tube, results of the loading test cannot be analysed as the bearing capacity of the group of columns. However, performed parametric study in a clear way indicates the influence of the confining pressure on the behaviour of the column.

Concerning fact that friction coefficient between soil and steel is density dependant, it is assumed that the value of μ_t is the same for 7 and 14 days old columns. Presented results and findings of investigations of the friction between sand and steel presented by Brumund and Leonards (Brumund & Leonards, 1973) lead us to conclusion that the most appropriate friction coefficient is μ_t = 0.337. Even though the best fit curves in both cases are obtained for μ_t = 0.506 (75% of tangents of the internal friction angle). However, it appears to be inconsistent with the observations presented in the literature.

4.3.2.2.2. *Results*

Results obtained with friction coefficient μ_t = 0.337, which corresponds to tan ϕ_{dense} multiplied by 0.5, are presented in Figure 4.30. Comparison between experimental data and modelling, leads us to conclusion that numerical curves well reproduce the behaviour of columns. Both predictions slightly underestimate the axial force in the elastic phase of the loading. However, in case of the 7 days old SM column, the differences during the whole loading test are constant and negligibly small. For the 14 days old column, the higher value of the displacement becomes the smaller discrepancy between result of the numerical calculation and the measurements, till about 2.5 mm, can be seen. The maximal values of axial force predicted by modelling are: 6.20 kN and 11.52 kN, when measured ones are: 6.30 kN and 11.27 kN, for 7 and 14 days old columns, respectively. Despite the small differences, obtained results represent well the behaviour of the 'group' of the SM columns. The mentioned differences might be due to the definition of the interfaces between the column and sand or between sand and the steel tube. In both cases it is described by perfect frictional contact with constant friction coefficient.

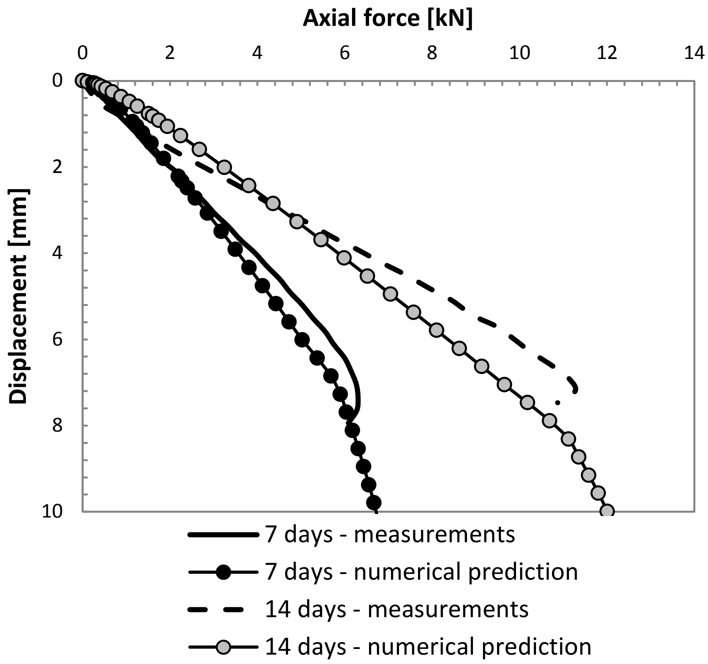

Figure 4.30 Loading test of the group of SM columns in dense sand

4.3.2.3. Conclusions

The behaviour of the small scale SM column was presented in this paragraph. Obtained numerical predictions showed quite good agreement with the measurements acquired by Dhaybi. The smallest discrepancy between results can be seen in case of loading test of 7 days old column in tube. In order to compare and conclude, results of all loading tests were presented in Figure 4.31. As mentioned before, due to presence of the friction between soil and the steel tube's wall, results of the loading test cannot be analysed as the bearing capacity of the group of columns. The final value of the friction coefficient was chosen as the constant value for both ages of columns, μ_t = 0.337. The choice was made based on the results of the parametric study and the findings presented in the literature. Both loading tests, in tank and tube, is a good opportunity to analyse the influence of the confining pressure on the behaviour of the column. Due to higher, than in case of single column, confinement, the values of axial force acquired from the 'tube tests' are much higher, about 11.52 kN instead of 7.50 kN for 14 days old. The second effect of the difference in confining stress is type of failure. The collapse occurs in the SM column. After elastic phase of behaviour, the head of column has been plasticized.

In case of experimental study of a single column, slope of the force-displacement curve is gentler. The same tendency has been predicted by the numerical modelling, however it starts after about 2.6 mm. The failure in case of test in tank is observed due to other mechanism – plasticity in the soil under the column's tip.

The predicted behaviour of columns is comparable with the measurements. It lead us to conclusion that properties of soil, column and both contacts (soil – column and soil – tube) are calibrated properly. Therefore parameters can be used for the simulations with different configurations of columns. However, in case of model carried out for the group of columns, presence of the friction between steel tube and soil generates uncertainty. It is advised, in order to ensure results to perform additional experimental and numerical tests where the friction coefficient is reduced to negligible value, where the most preferable on is zero. This kind of test was carried out for the group of SM columns in loose sand.

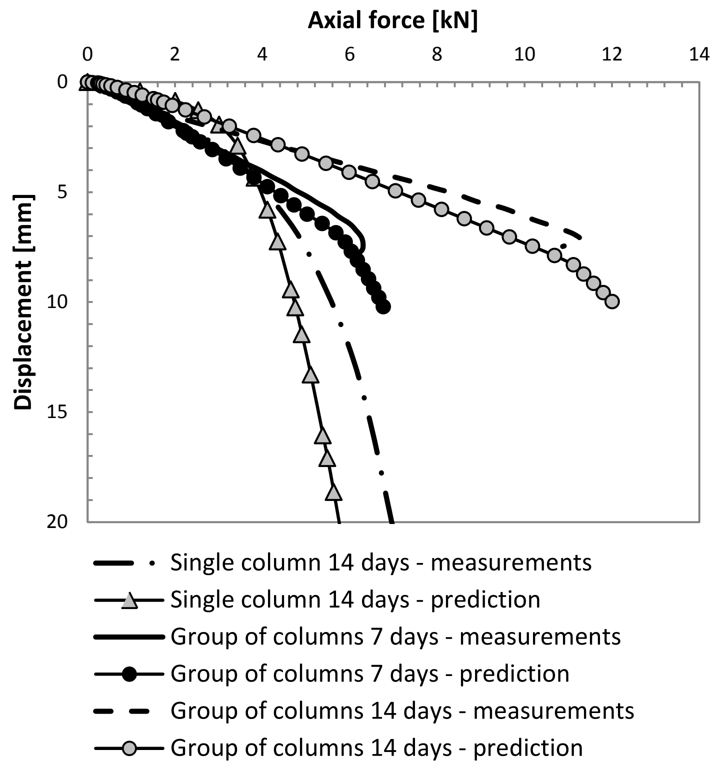

Figure 4.31 Loading test of the single and group of SM columns after 7 and 14 days of cure

4.3.2.4. Loading test of columns in 'loose' sand

The behaviour of 7 days old column in 'loose' sand was modelled according to the experimental setup. Loading tests were carried out in tank and four tubes. The aim of this study was to analyze the effect of the confining pressure. Different confinement was a consequence of the distance between axis of the column and the boundary of the model. In case of tubes, their diameters represented spacing between columns in a group. Similarly like in case of 'group of columns' in 'dense' sand, an axisymmetric type of numerical model was used. Also the assumption that the analysed column represents the central column in a group was taken into account. Since in experimental work walls of the tube were treated by oil and then covered by plastic film, the friction coefficient between soil and tube shaft was assumed to be equal to zero. Considering this, it was no longer necessary to model steel tubes. Therefore a vertical boundary condition on the right hand side was applied directly to the soil elements, like it was assumed in case of the single column loaded in the tank.

4.3.2.4.1. *Parametric study*

The parameter taken into consideration in this study is diameter of the tube, which defines the spacing between columns in the group, like it is presented in Figure 4.28a.

Mesh used in calculations, consists of CAX6M elements. Model's dimensions and mesh are presented in Figure 4.26 and Figure 4.32 for tests in tank and tubes respectively. As in the previous case dimensions of the column stay the same as well as the way of application of load – imposed displacement to the head of column. Properties of the loose soil, 7 days old SM column and interaction between column and soil are presented in Table 4.16, Table 4.17, Table 4.23 and Table 4.25, respectively. Boundary conditions are as presented in Figure 4.32. Axisymmetric conditions are applied to the left hand side vertical edge, horizontal displacement of the right vertical edge is prohibited and vertical displacement of the bottom of the model is blocked. As mentioned above, in these calculations contact between tube's wall and the soil is consider as frictionless.

Varied parameter is the diameter of the tube, *D*. It is assumed to be 0.26 m, 0.35 m, 0.45 m and 0.65 m. In order to complete the investigation of the confining stress and its influence on the columns bearing capacity, loading test of the column in tank has been performed as well.

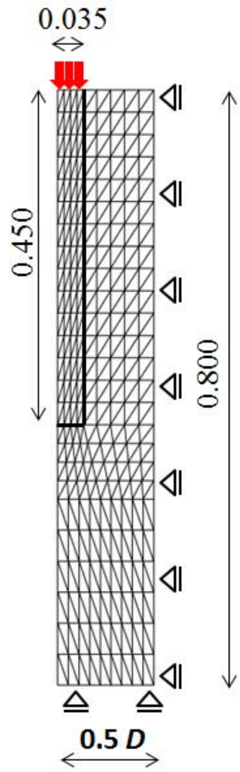

Figure 4.32 Finite element mesh and boundary conditions used in numerical modelling of a static test of the SM column working in a group installed in loose sand (all dimensions in meters)

Results of calculations and experiments carried out on 7 days old SM column are presented in Figure 4.33. The first three graph, Figure 4.33a, b ,c, illustrates predicted and measured axial force – displacement curves for a single column, column spaced each *D* = 0.65 m and *D* = 0.45 m, respectively. Loading test of the column performed in the tank ensures lack of additional horizontal pressure applied to the column. The confining stress in the tank is equal to horizontal stress caused by the weight of soil. In all three cases, numerically predicted behaviour of columns corresponds very well to the experimental observations. Small difference appears in the middle part of the loading tests. The same trend can be observed for all cases. Initially, the underestimation of the predicted value of force increases with the increase of the displacement. Afterwards, discrepancy between curves declines and results become identical. The decrease of correlation between measured and predicted force starts at 2 mm for all cases. Difference increases till about 3.2 mm, 6.0 mm and 5.5 mm for single column, *D* = 0.65 m and *D* = 0.45 m, respectively. Then, discrepancy declines till results start to be identical as the measured ones. It happens for displacement equal to 16.5 mm, 17.0 mm and 19.0 mm for single column, *D* = 0.65 m and *D* = 0.45 m, respectively. The final value of axial force, predicted for 20.0 mm, is comparable in all three cases. It changes between 2.8 kN for single column and 2.9 kN for both tests in tubes. This insignificant difference as well as type of failure, which occurs due to plasticizing soil under the column’s tip, proves that for spacing bigger than or equal to 0.45 m no additional confining stress is generated. The boundary of the model does not have an influence on the behaviour of the SM column installed in ‘loose’ Hostun sand.

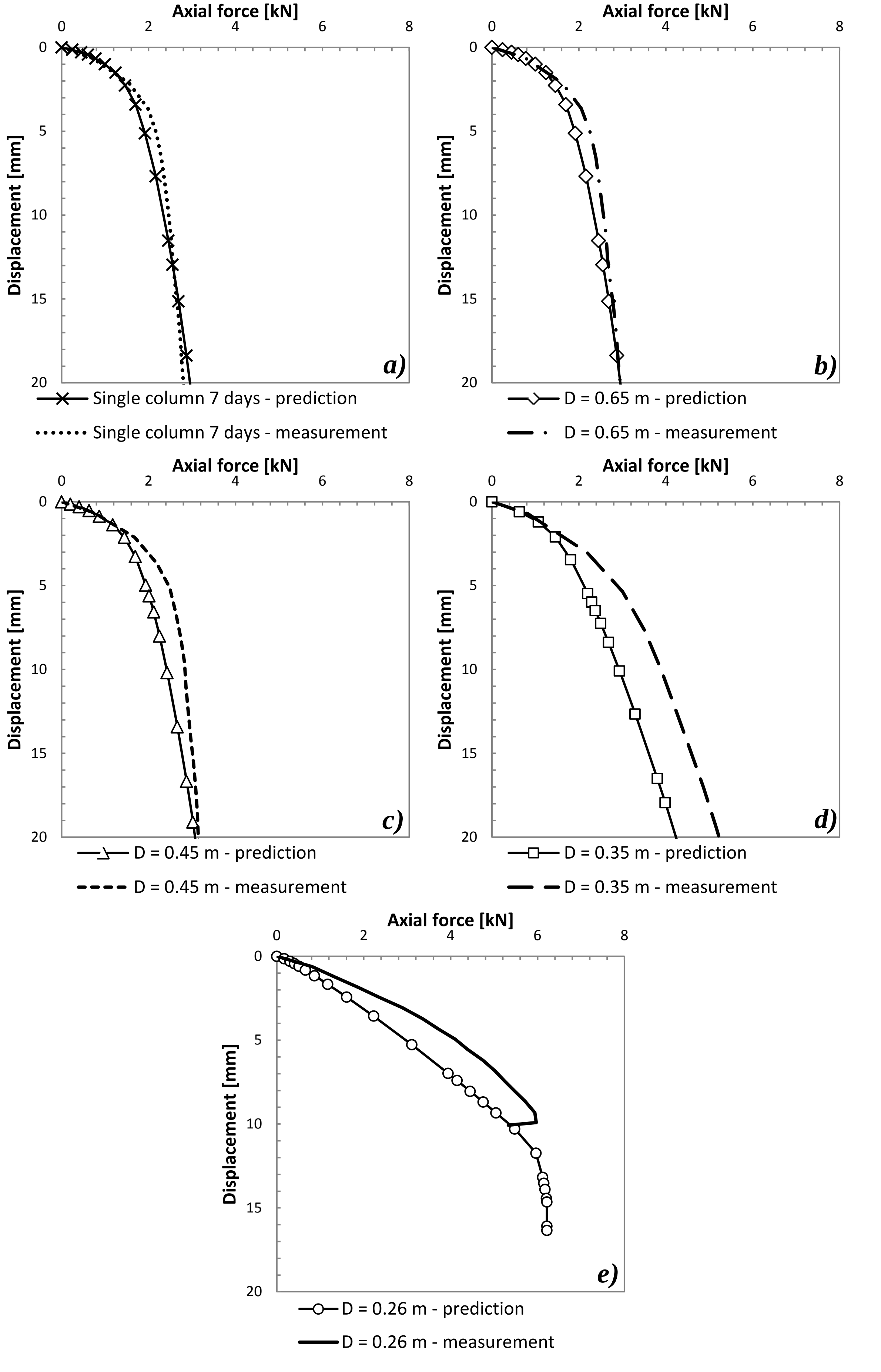

Figure 4.33 Results of the parametric study performed to investigate influence of the spacing of the column a), single column b) D = 0.65 m, c) D = 0.45 m, d) D = 0.35 m e) D = 0.26 m, on its bearing capacity in loose sand. Results compared with measurements

The behaviour of 7 days old column working in a group spaced each 0.35 m is presented in Figure 4.33d. The predicted values of force are significantly lower than the measured ones. The force obtained at the beginning of the loading test is identical as results of the experimental study, however situation changes at about 2.0 mm. From this value of displacement, the increase of the displacement leads to increase of the discrepancy but just until about 5.5 mm where it stabilizes. The 5.5 mm displacement is the moment when curves illustrating numerical prediction and measurement becomes parallel. The equal difference between predicted force is about 0.8 kN. Hence, the value of the borne force for 20.0 mm displacement equals 4.4 kN and 5.2 kN for numerical and experimental tests respectively. The last studied case, is presented in Figure 4.33e, test of a column in tube with the smallest diameter, D = 0.26 m. Similarly, as in case of D = 0.35 m, some differences between predictions and measurements can be seen. Although, the trend of both curves is the same. Initially, column answers in elastic way afterwards plastic behaviour starts. The failure in the column manifests by the increase of displacement and simultaneous insignificant increase of borne force. The predicted beginning of plasticization of the SM element has place at about 12.7 mm. The failure of column has been observed in physical study for about 10.0 mm displacement. The difference between numerical and experimental curves increases with the increase of the displacement.

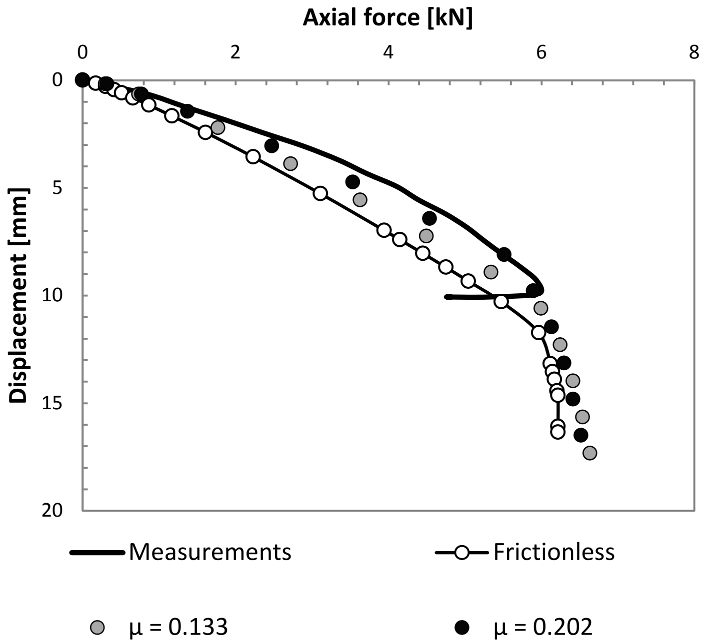

Figure 4.34 The influence of the friction coefficient between steel tube and sand around column on behaviour of the 7 days old column placed in 'loose' sand

One of the reasons of the underestimation of the force by the numerical model is the fact that contact between soil and the steel tube is assumed frictionless. As explained above, significant precautions have been taken to eliminate friction, but it is not impossible that in spite of used oil and plastic film, the friction manifested. In order to verify this hypothesis, additional numerical study has been performed. The loading test of the 7 days old column placed in the 'loose' sand has been studied by the model previously used for testing 'group of columns' in 'dense' sand (Figure 4.28b). Two friction coefficients, μ_t = 0.133 and μ_t = 0.202, which corresponds to tangent of ϕ_{loose} multiplied by 0.25, 0.38, respectively, have been analysed. Results of the parametric study have been compared with one obtained from the frictionless calculations. In Figure 4.34 obtained curves are confronted with measurements. The behaviour of the column during whole loading test differs between calculations. Discrepancies are not significant but clearly demonstrate that attempts to reduce to zero the friction between the soil and the tube were not completely successful. Similarly as in case of 'dense' sand, increase of the friction coefficient leads to higher value of the borne force achieved with lower displacement. All predictions underestimate axial force during the loading process, however the higher value of coefficient, the smaller discrepancy between prediction and measurement. The closes to column's observed behaviour is result of the calculation performed with μ_t = 0.202. In this case differences are negligible.

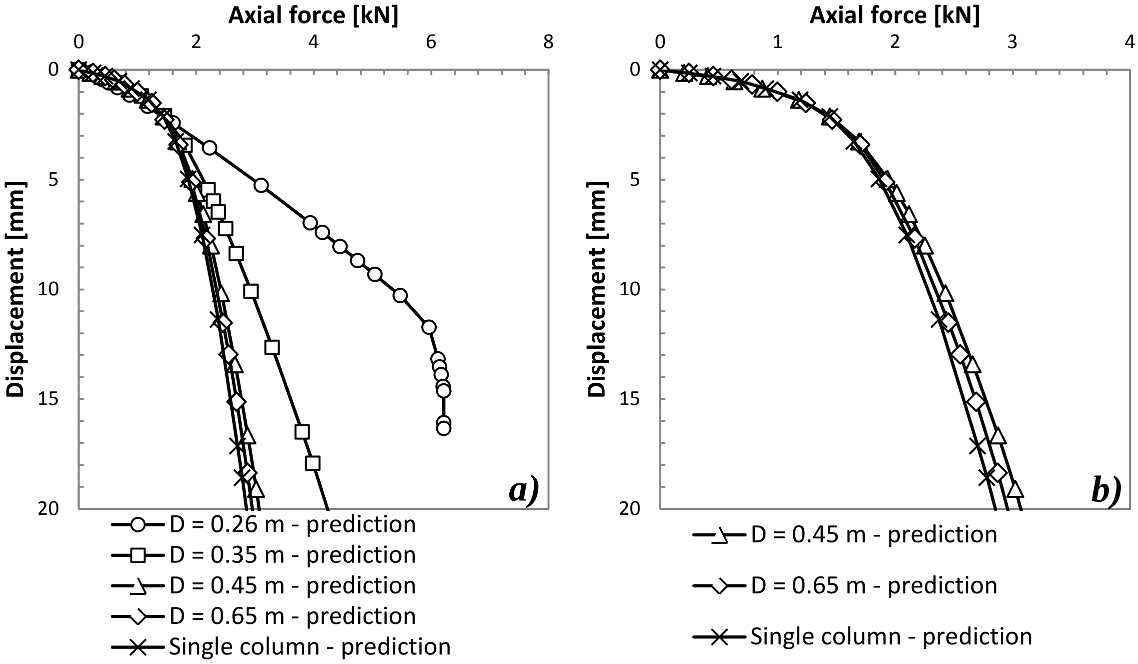

Figure 4.35 Results of the numerical calculations performed to investigate influence of the spacing of the column on its bearing capacity in 'loose' sand with the frictionless contact between soil and tube. a) tests carried out in tubes and loading test in tank, b) results acquired from loading tests in tubes

Results for all loading tests performed on 7 days old SM column in 'loose' sand with frictionless contact between soil and tube are presented in Figure 4.35a. As it is pointed out above, two modes of failure has been observed. The first one is failure in soil, which takes place for 0.35 m, 0.45 m, 0.65 m diameters and single column. Results from tests in the biggest tubes and the tank are almost the same. It proves that without higher confinement, column is able to bear about 2.8 kN after 20 mm of displacement. In Figure 4.36, the confining stress is presented as a function of distance from the column's shaft. Depth 0.2 m, roughly middle of the column, has been chosen to illustrate average value of stress. It can be seen that insignificant differences between curves representing behaviour of loaded columns (Figure 4.35b) do not come from the difference of confining stress. They are the consequences of mesh in the finite element model. Due to different dimensions of the axisymmetric model, size and number of elements slightly differs between cases. In the numerical prediction of the loading test in tube with diameter 0.35 m, similarly like in the experimental observation, influence of the confinement can be noticed, however its impact is much lower than in case of test in the smallest tube.

The second possible type of collapse, due to plasticity in the column's head, is acquired from test with D = 0.26 m. A considerable difference between predicted values of borne forces can be noticed (Figure 4.35a). In case of the failure in soil under the column, calculated capacity after 20 mm of displacement is about 2.8 kN (0.45 m, 0.65 m diameters and single column) and 4.4 kN (0.35 m), whereas the axial force predicted for case when the failure takes place in column is about 6.4 kN. In case of tube with diameter 0.26 m, confining pressure, caused by smaller distance between shaft of the column and tube's walls, revealed different than in previous cases mode of failure. Due to higher horizontal stress (Figure 4.36), shear strength of soil increases and capacity of SM material is mobilized. Hence, more important values of axial force can be borne.

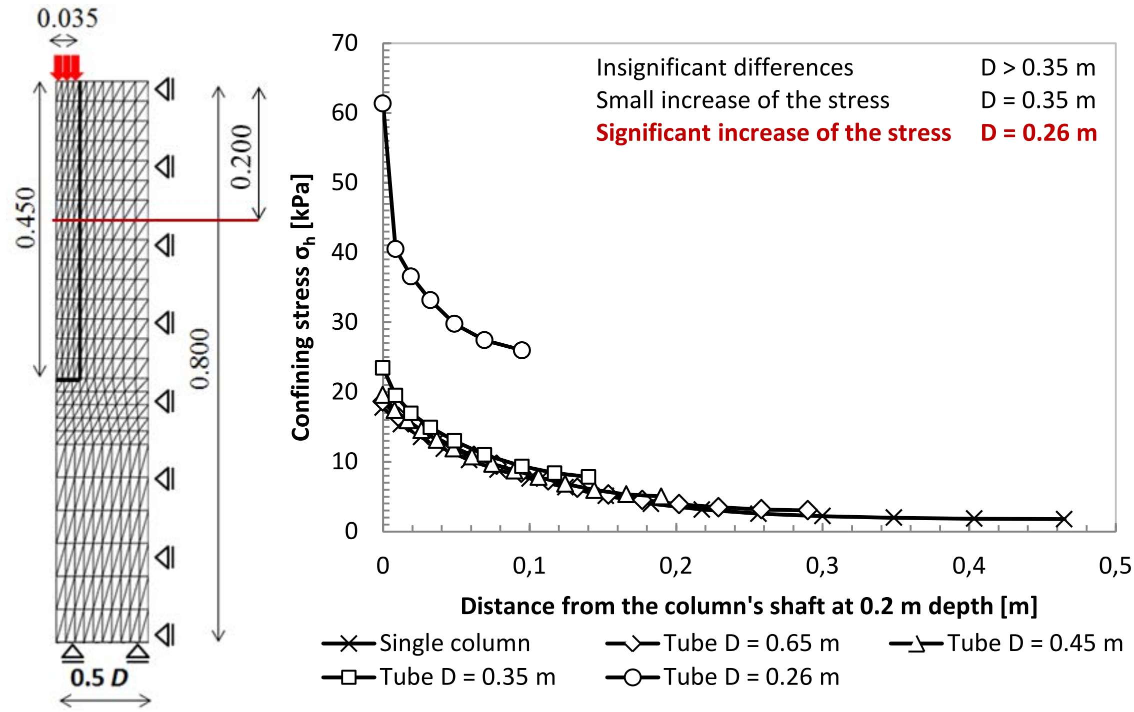

Figure 4.36 Confining stress at depth 0.2 m

4.3.2.4.2. *'Loose' versus 'dense' sand*

The Soil Mixing columns were tested in homogeneous layers of 'loose' and 'dense' Hostun sand. It can be noticed that shear and elastic properties change significantly with density of the material. In this paragraph the influence of the soil density on the behaviour of group of 7 days old SM columns, spaced each 0.26 m, is investigated. In Figure 4.37, results obtained for both densities are presented. In both cases friction between tube and soil is taken into account. Assumed friction coefficients are μ_t = 0.202 and μ_t = 0.337 for 'loose' and 'dense' respectively.

On the one hand, several similarities in the behaviour of tested columns need to be indicated. Firstly, failure mode in both cases is the same - the head of column has been plasticized. It leads to radical change of the slope of the force-displacement curves, after the elastic phase of loading. Secondly, final value of the bearing capacity is similar. The plastic behaviour starts when column achieves about 6.0 kN and after 10 mm force is equalled to 6.4 kN for 'dense' sand. In case of 'loose' sand the plastic behaviour begins with force about 5.8 kN and after 10 mm displacement its value is about 6.0 kN. The obtained value is directly related to the resistance of the 7 days old column. Unconfined compressive strength of this column is about 1.6 MPa (Table 4.19) what corresponds to 6.16 kN.

On the other hand, slopes of the force-displacement elastic phase are different between densities. As it was expected, the increase of borne force is faster for test in 'dense' sand. It can be explained by higher value of the Young's modulus – 7 MPa and 3 MPa for higher and lower densities respectively. Nonetheless, the tendency of curves is the same.

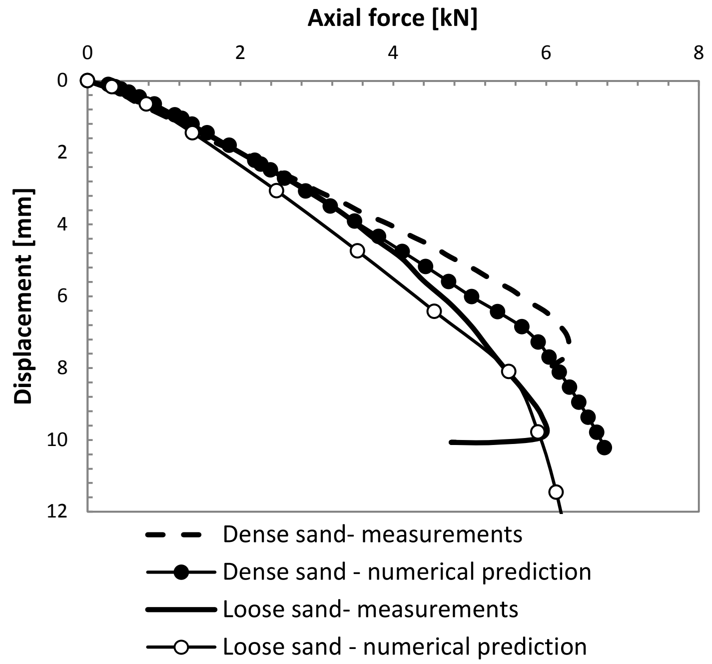

Figure 4.37 Influence of the soil density on the behaviour of the 'group' of 7 days old SM columns spaced each 0.26 m

4.3.3. Conclusions

In contrast to full scale *in situ* modelling, small scale laboratory models in geotechnical engineering allows simulating complex systems under controlled conditions in relatively easier way. Nonetheless, conducting parametric studies with these kind of models can be used to explore phenomenon where case histories and prototype tests provide limited data. However it needs to be remembered that due to considerable lower confinement (1g modelling), materials' properties and behaviour cannot be directly transferred to the real cases. Hence, acquired results should be consider as qualitative not quantitative.

A small scale model, built by Dhaybi, was presented in this section. According to its setup, axisymmetric calculations by finite element code ABAQUS were preformed. The aim of both numerical and experimental studies was to examine in details impact of parameters such as soil density, age and number of columns, on the behaviour of SM column. Laboratory investigation helped in correct calibration of the constitutive models. Soil was modelled with the elastoplastic model with the Modified Drucker-Prager with cap criterion. The 7 and 14 SM columns were described by elastic perfectly plastic model with the Mohr-Coulomb failure criterion. Similarly like in case of the full scale modelling of the SM column, the contact between soil and column's shaft was assumed as interaction obeying the Coulomb failure criterion.

Missing properties, which could not be obtained from laboratory analysis, were chosen according to literature and parametric studies. Using in experimental work Hostun sand HN31 (formerly RF) was on the one hand undeniable convenience. It was for many years used as the reference sand. Therefore considerable amount of information about its properties can be found in the literature. It significantly helped with proper calibration of the modulus of deformation and ensured that obtained values of density and shear parameters are correct. On the other hand, decision of using dry sand brought some difficulties with reference properties of the Soil Mixing material, since the method is mainly used to improve weak soils, such as clays or silts. Although, this obstacle was faced by precise laboratory tests (slam and flow tests, static and dynamic Young's modulus tests, unconfined compressive strength (UCS) test). Moreover the influence of the cement ratio and age on the strength of the material were investigated. Knowledge of the behaviour of the SM obtained from experimental work, leads to conclusion that this material can be considered as concrete with lower resistance. This observation considerably helped in choosing starting data to numerical analysis. Shear properties of the 7 and 14 days old columns were approximated according to Jimenez Montoya method, EHE-98 and Eurocode-2 and then verified by the parametric study. Moreover, due to similarity to the concrete, the contact between SM column and soil was assumed as following Coulomb criterion, as it is commonly used for piles. Friction coefficient, which is crucial parameter of the chosen criterion, was acquired from the shear test.

By numerous tests, behaviour of 7 and 14 days old columns was analysed. By both, experimental and numerical studies, it was proven that granular materials properties are highly dependent on density. The denser sand, the higher value of borne by column force. Moreover, the significant influence on the force has column’s age. The increase of age implies increase of modulus of deformation and cohesion of the SM material. The next studied factor was group effect. The impact of the spacing between column was studied by the loading tests performed in tubes. Loaded SM element represented central column in the group. This assumption created a problem in form of unwanted interaction, between soil inside tube and the tube’s shaft. In order to include the interaction in numerical calculations, additional steel element was added to the model. Thanks to that, it was possible to define friction between surfaces. Unwanted friction was present for both densities, even though, an attempt of the reduction of the friction by covering tube’s walls by oil and layer of plastic film was taken. Due to the presence of the additional interaction, it is not recommended to consider obtained results as the bearing capacity of the column in a group. However, the series of experiments in tubes in clear way visualised how significant impact on column’s behaviour has confining stress. By the behaviour, the values of axial force corresponding to the applied displacement and the mode of failure are understood. It was observed that for single columns collapse had placed in soil under the column. Similar behaviour was measured and predicted for columns tested in all tubes except the smallest one. For two tube D = 0.26 m, failure occurred in the column’s head. Analysis of the obtained force-displacement curves for 7 days old column tested in tube with diameter D = 0.26 m, let to conclude that density of the soil has considerable influence on the increase of force. Even though the final values of force are almost the same, the discrepancy appears in the slope of the column. It is explained by the different values of the Young’s modulus of soil – 7 MPa and 3 MPa for higher and lower densities respectively.

The behaviour of the loaded columns was predicted by the numerical models correctly. In case of appearing differences, like in case of loading test in tubes filled with ‘loose’ sand, they were explained and verified by the additional calculations. According to acquired reasonable results, constitutive models describing: sand with both densities, SM columns and contact between soil and column are considered as properly calibrated and used in tests of reinforced shallow foundation.

4.4. Conclusions

The concept of using the Soil Mixing method as reinforcement for soil and existing or designed foundations requires precise analysis of the behaviour of the Soil Mixing column.

In this chapter two attempts of analysing: full and small scale were presented. Their aim was to recognize column’s reply to applied load by performing the static loading test. The finite element analysis provided good agreement with the measurements. Data obtained from field and laboratory tests and preliminary calculations allowed calibration of the advanced model. It consisted on analysis of SM column, installed in multilayered ground, as inhomogeneous element (three parts). Moreover, constitutive model with MDPC criterion for the lower layer of soil was used. Acquired results lead to conclusion that the more advanced constitutive law is necessary to properly reproduce column’s behaviour. Since, result of the oedometer test, were not provided, MDPC criterion was used for only one layer. Its parameters were chosen by the parametric study in accordance with the measurements. The hardening law was defined in consonance with example in literature (Helwany, 2007). As it was examined in previous chapter, (3.2.3.3.3), results obtained with the hardening curve for other sand (Figure 3.21), than the analyzed one, is able to approximate quite well the behaviour of the soil.

The small scale, 1g, laboratory models were used to investigate behaviour of SM columns produced in the laboratory. According to experimental setup, successful, axisymmetric calculations were preformed. The aim of both numerical and empirical studies was to examine in details, impact of parameters such as soil density, age and number of columns, on the behaviour of SM element. Laboratory investigation helped in correct calibration of the constitutive models. Missing properties, which were not obtained from laboratory analysis, were chosen according to literature and parametric study.

By numerous tests, behaviour of 7 and 14 days old columns was analysed. It was found that significant influence on the axial force borne by the column had its age. Due to chemical processes inside the soil-cement mixture, its modulus of deformation and cohesion increase. Therefore SM element with higher resistance is capable of bearing higher force.

The impact of the confining pressure on the column's behaviour was studied by the loading tests in tubes. It was assumed that loaded SM element represented central column in the group and higher confinement came from interactions with other elements. The assumption caused additional obstacle, which manifested by unwanted friction, between soil inside tube and the tube's shaft. The proper friction coefficient, describing the friction, was found by parametric study. Its value was confronted with findings reported in literature. Even though, an attempt of the reduction of the friction by covering tube's walls by oil and layer of plastic film was taken for all tubes filled with 'loose' sand, unwanted friction appeared. That is why, it is not recommended to consider obtained results as the bearing capacity of the column in a group. However, the series of experiments in tubes and in tank clearly depicted significance of the confining stress. It was observed that not only column's behaviour was influenced by the confining stress by also mode of failure. For tubes with diameter bigger than 0.26 m collapse appeared in soil. In the smallest tube, failure occurred in the column's head.

Analyses of two soil densities, let to conclusion that density of the soil has considerable influence on the increase of force. According to acquired reasonable results, constitutive models describing: sand with both densities, SM columns and contact between soil and column are considered as properly calibrated and can be used in tests of reinforced shallow foundation.

5. Shallow foundation reinforced by a Soil Mixing column

5.1. Introduction

Reinforcement of shallow foundations is one of many fields of application of the Soil Mixing technique. Column or columns, installed directly below the base of the foundation influenced its behaviour by increase of the bearing capacity, with simultaneous reduction of the displacement.

In Chapter 4, behaviour of SM columns have been studied on full and small scale example. Results of this detailed investigation ensure that constitutive models used to described soils, columns and interactions between them are well calibrated and capable to capture specificity of the behaviour of the loaded columns. Moreover, these test provide necessary knowledge to perform loading tests of shallow foundations supported by the SM elements.

In the first part of this chapter, shallow type of the foundation is characterized. Then, behaviour of two small scale shallow foundations is examined. The interaction between foundations and reinforcement, resulting in significant improvement of the bearing capacity, is detailed. A rectangular, 0.20 m x 0.25 m, and a square, 0.35 m x 0.35 m, footings are modelled with the finite elements code ABAQUS. Afterwards, numerical predictions are compared with measurements obtained by the experimental tests performed in Laboratoire de Génie Civil et l'Ingénierie Environnementale (LGCIE), INSA Lyon by Dhaybi (Dhaybi, 2015).

The concept of using SM elements as reinforcement for shallow foundations is illustrated through two configurations of the reinforcing columns. The first one consists of single column, centrally situated under the footing. This configuration is applied to both foundations. The second one is executed by group of four columns. Due to dimensions of the foundation, only the bigger footing is analysed with four columns.

Moreover, the influence of: number of reinforcing columns, their age, soil's density and homogeneity on the bearing capacity of the footings is investigated and pointed out.

5.2. Shallow foundations

A foundation is a structural element that is expected to transfer load from a structure to the ground safely. The two major classes of foundations are: shallow foundations and deep foundations. A foundation is considered shallow, if it transfers the entire load at a relatively shallow depth. A common understanding, proposed by Terzaghi (Terzaghi, 1943), is that depth of shallow foundation D_f, must be less than its width, B, (Figure 5.1). Width is understood as the shorter of the two plan dimensions. However, it was also proposed, that foundations with greater depths (up to $4B$) can be considered as shallow (Helwany, 2007).

Shallow foundations include pad footings or just footings (for example square and circular), strip (or wall) footings and mat (raft) foundations, shown in Figure 5.2. Each of these shapes is suitable for a specific type of structure: a square foundation is used under a column, a circular foundation is used for cylindrical structures such as water tanks, a strip foundation is used under retaining walls, and a mat (raft) foundation is used under an entire building.

When designing a shallow foundation, two aspects must be considered: the applied foundation pressure should not exceed the bearing capacity of the supporting soil; and the foundation settlement should not be excessive due to the applied foundation pressure. The bearing capacity criterion ensures that there is adequate safety against possible bearing capacity failure within the underlying soil. This is done through provision of an adequate factor of safety of about 3 (Sivakugan & Pacheco, 2011). In other words, shallow foundations are designed to carry a working load of one-third of the failure load. For raft foundations, a safety factor of 1.7–2.5 is recommended (Bowles, 1996, p. 1024). The settlement criterion ensures that settlement is within acceptable limits. For example, pad and strip footings in granular soils generally are designer to settle less than 25 mm (Sivakugan & Pacheco, 2011).

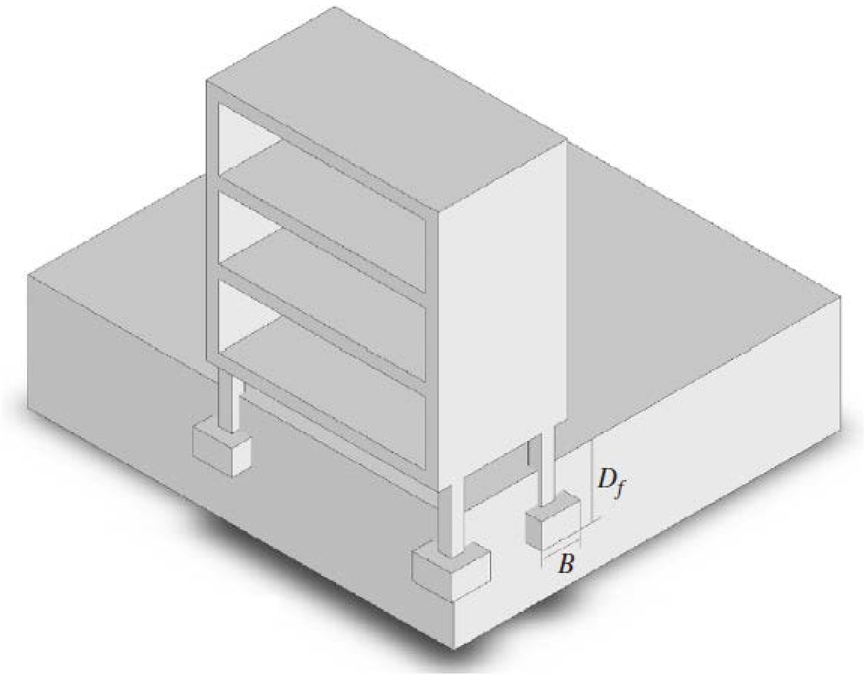

Figure 5.1 Shallow foundation after(Helwany, 2007, p. 210)

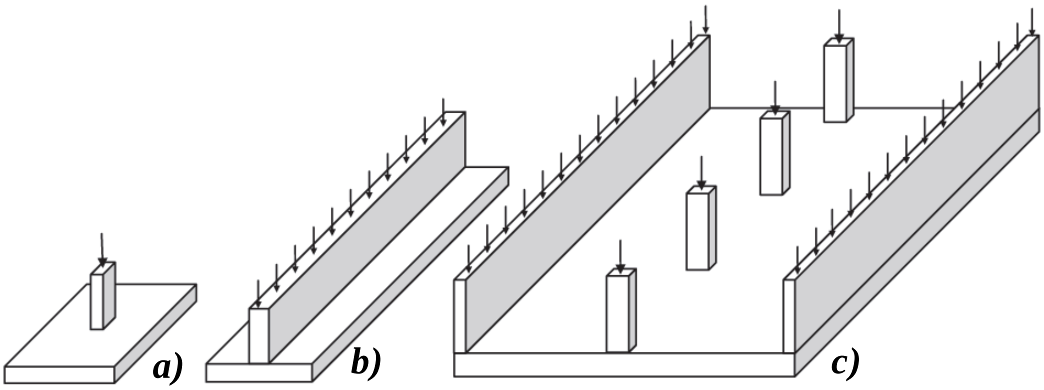

Figure 5.2 Types of shallow foundations: a) footing (pad footing), b) strip footing, c) mat or raft foundation after(Sivakugan & Pacheco, 2011, pp. 3-2)

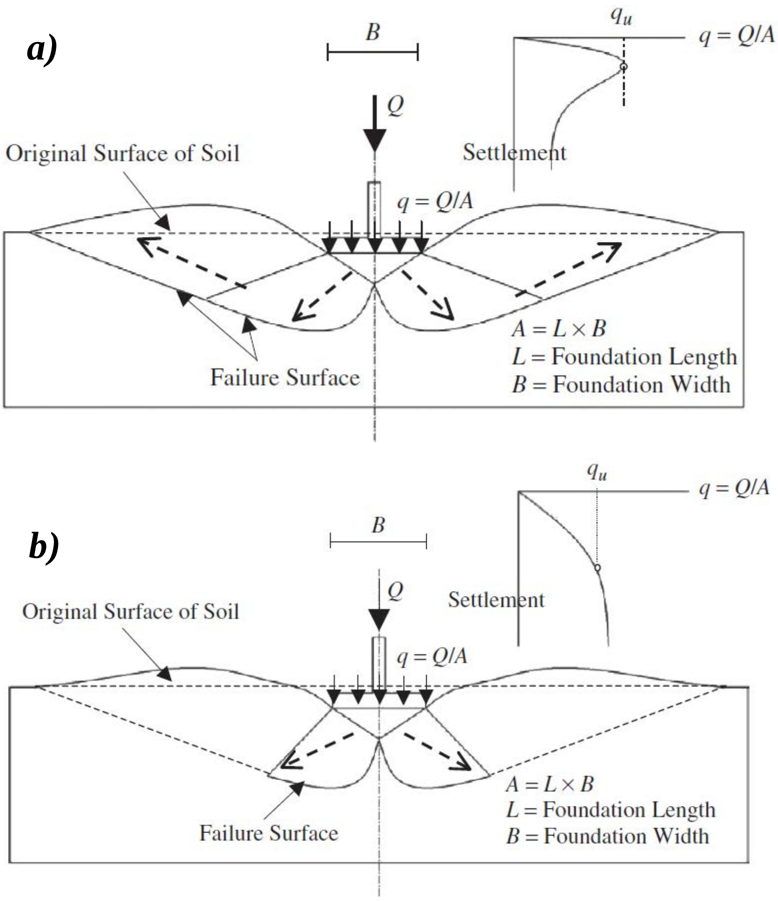

Figure 5.3 Modes of failure, a) general, b) local (Helwany, 2007)

5.2.1. Modes of failure

There are three possible modes of failure, depending on: soil type, foundation size and foundation's depth. The first mode, general shear failure, is usually encountered in dense sands and stiff clays underlying a shallow foundation. In reference to Figure 5.3a, when the load Q is increased gradually, the corresponding foundation pressure, q, increases. The foundation settlement also increases, with increasing pressure until the ultimate bearing capacity, q_u, is reached. A sudden increase in settlement is noted immediately after reaching q_u, indicating severe loss of support. The general shear failure mode is accompanied by the occurrence of a failure surface (Figure 5.3a) and the inability to maintain the applied pressure. There is a distinctive peak in the pressure versus settlement curve shown in the figure, which corresponds to the ultimate bearing capacity.

The second failure mode, local shear failure, is encountered in medium-dense sands and medium-stiff clays. It is characterized by the lack of a distinct peak in the pressure versus settlement curve, as shown in Figure 5.3b. In the case of local shear failure, determination of the ultimate bearing capacity is usually governed by excessive foundation settlements, as indicated in the figure. The local shear failure mode is accompanied by a progressive failure surface that may extend to the ground surface after q_u is reached (Figure 5.3b).

The third mode of failure, punching shear failure, usually occurs in weak, compressible soils such as very loose sands. This type of failure is accompanied by a triangular failure surface directly under the foundation and is not noticeable at the ground level. As in local shear failure, punching failure is also characterized by the lack of a distinctive ultimate bearing capacity. Thus, the ultimate bearing capacity in this case is taken as the pressure corresponding to excessive foundation settlements.

5.2.2. Bearing capacity

Prandtl (Prandtl, 1921) studied the process of penetration of hard bodies such as metal punchers into another soft homogenous isotropic rigid material. He assumed a rigid plastic body in his system where deformations have no effect on the level of stresses in the limit equilibrium analysis. He decided that at failure the material beneath the load could be divided into five regions consisting of Rankin's zones and fans. From Mohr's stress theory, Prandtl obtained a differential equation of a second order. The solution gives the analytical expression of the ultimate bearing capacity of soil. The Prandtl plastic limit equilibrium plane strain analysis was extended by Terzaghi (Terzaghi, 1943) to develop the first rational bearing capacity equation for strip footings embedded in soils. Terzaghi assumed the soil to be a semi-infinite, isotropic, homogeneous, weightless, rigid plastic material. The footing was consider as rigid and its base was sufficiently rough to ensure there is no separation between the footing and the underlying soil. Model assumed that the failure occurs in the general shear mode (Figure 5.4).

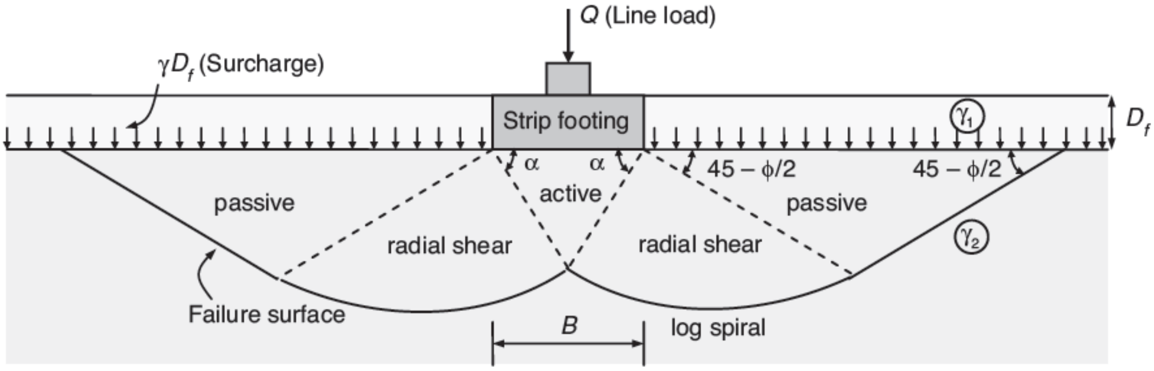

Figure 5.4 Failure surfaces and the soil during bearing capacity failure (Sivakugan & Pacheco, 2011)

Based on these assumptions, Terzaghi expressed general shear failure of a strip footing by Equation 5.1, where c is the cohesion, γ_1 and γ_2 stand for unit weights of the soil above and below the footing level, N_c, N_q and N_γ are bearing capacity factors, which are functions of the internal friction angle. The first term in the equation concerns the contribution of cohesion to the ultimate bearing capacity. The second term reflects the frictional contribution of the overburden pressure or surcharge. The third terms stands for the frictional contribution of the self-weight of the soil in the failure zone. Equation 5.1 can be modified to estimate the bearing capacity for a square and circular foundations, Equations 5.2 and 5.3, respectively.

$$q_{ult} = cN_c + \gamma_1 D_f N_q + 0.5B\gamma_2 N_\gamma \qquad 5.1$$

$$q_{ult} = 1.3cN_c + \gamma_1 D_f N_q + 0.4B\gamma_2 N_\gamma \qquad 5.2$$

$$q_{ult} = 1.3cN_c + \gamma_1 D_f N_q + 0.3B\gamma_2 N_\gamma \qquad 5.3$$

Terzaghi, in his equations, neglected the shear resistance provided by the overburden soil, which was treated as a surcharge. He also assumed that angle α (Figure 5.4.) under the foundation is equalled to internal friction angle, $\alpha = \phi$. Later studies performed by Vesic (Vesic, 1973) show that $\alpha = 45 + 0.5\phi$, which makes the bearing capacity factors different than ones originally proposed by Terzaghi. With Vesic definition of α, the bearing capacity factors N_q and N_c become as presented in Equations 5.4 and 5.5. In case of N_γ,, different equations have been proposed in the literature, some of them are presented in Table 5.1

$$N_q = e^{\pi \tan\phi} \tan^2\left(45 + \frac{\phi}{2}\right) \quad 5.4$$

$$N_c = \left(N_q - 1\right) \cot\phi \quad 5.5$$

Table 5.1 Expressions of Nγ after (Sivakugan & Pacheco, 2011)

Expression	Reference
$\left(N_q - 1\right)\tan(1.4\phi)$	(Meyerhof, 1963)
$1.5\left(N_q - 1\right)\tan\phi$	(Hansen, 1970)
$2.0\left(N_q - 1\right)\tan\phi$	(European Committee for Standardisation, 1995)
$2.0\left(N_q - 1\right)$	(Vesic, 1973)
$1.1\left(N_q - 1\right)\tan(1.3\phi)$	(Spangler & Handy, 1982)
Rough footing $0.1054e^{9.6\phi}$ Smooth footing $0.0663e^{9.3\phi}$	(Davis & Booker, 1971)

5.3. Foundation reinforced by a single column

A rectangular and a square shallow foundations (footings) have been subject to analyses. Small scale loading tests of foundations placed on the homogeneous layer of Hostun sand have been performed. Loading procedures have been continued until failure in order to obtain foundations' bearing capacities.

The results of the tests have been compared with measurements obtained by Dhaybi (Dhaybi, 2015) from a small scale models. In order to discuss improvement brought by the reinforcement, foundations with and without additional support have been studied.

5.3.1. Experimental setup

Experimental study of a small scale model has been performed in Laboratoire de Génie Civil et l'Ingénierie Environnementale (LGCIE), INSA Lyon (Dhaybi, 2015). Two shallow foundations have been examined in the 2 m^3 tank, the same one as used for loading tests of the single column described in paragraph 4.3.1.2. In order to model non deformable foundations in the laboratory, 1/10 scale, two steel plates have been used. Each analysed footing has been placed in a way that its central point covers up the central point of the tank's chamber. A 'small' rectangular, 0.20 m x 0.25 m (Figure 5.5a), and a square 'big', 0.35 m x 0.35 m (Figure 5.5b), shallow foundations (Table 5.2) have been loaded (static loading test) in two cases: with and without reinforcement.

The SM columns after 7 and 14 days of cure have been tested. Reinforcing columns have been created in the same way as in case of studies concerning bearing capacity of single and a group of SM columns (Figure 4.23). Loading tests have been performed for two densities of Hostun sand: 'loose' (ρ = 1380 kg/m^3) and 'dense' (ρ = 1500 kg/m^3). Obtained results are analysed together with the numerical ones in paragraphs below.

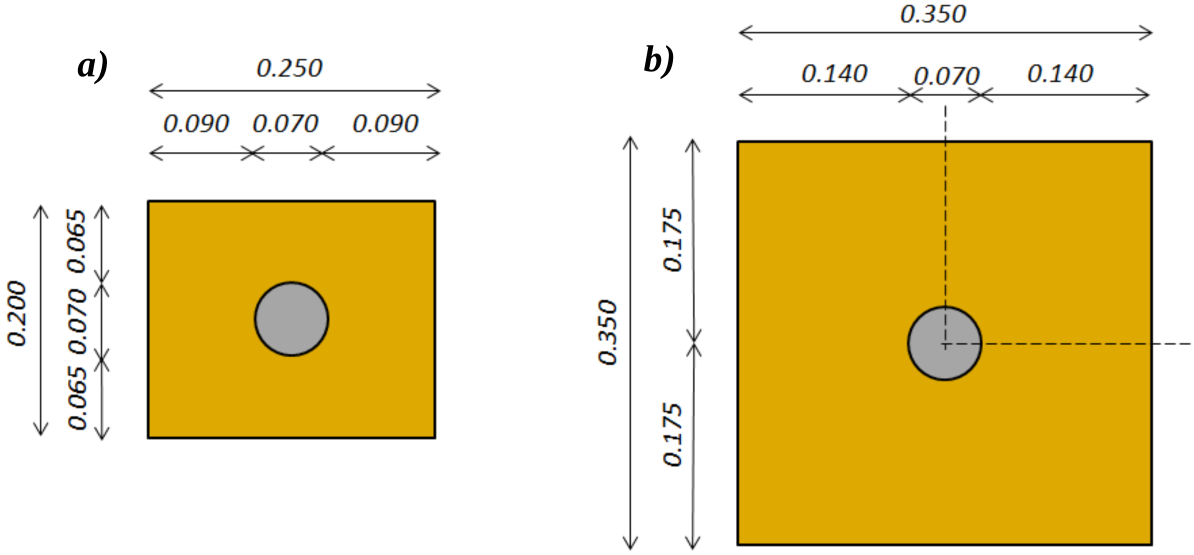

Figure 5.5 Small scale shallow foundations reinforced by single SM column, tested in the laboratory and modelled with finite element code; a) 'small' footing 0.20 m x 0.25 m and b) 'big' footing 0.35 m x 0.35 m (all dimensions in meters)

Table 5.2 Surface of 'small' and 'big' foundation and proportions between surface of the reinforcement and surface in contact with soil under the foundation

Foundation	Surface [m^2]	Reinforcement [m^2]	Surface in contact with soil [m^2]	Reinforcement [%]	Surface in contact with soil [%]
'Small' 0.20 m x 0.25 m	0.050	0.004	0.046	7.70	92.30
'Big' 0.35 m x 0.35 m	0.123	0.004	0.119	3.14	96.86

5.3.2. Numerical modelling

The numerical modelling of the small scale shallow foundation reinforced by a centrally situated SM column has been carried out to reproduce the physical test. The model's dimensions have been defined according to experimental setup. The reduced scale (1:10) model consisted in a vertically loaded shallow foundation, laying centrally on the surface of 1 m^3 of fine Hostun sand. Numerical calculations have been performed for: 7 and 14 days old columns and for two sand densities. The influence of the column's age and the density of soil on footings' behaviour has been reported and analysed.

5.3.2.1. 'Dense' sand

The bearing capacity of a shallow foundation situated on the layer of 'dense' Hostun sand has been analyzed by an axisymmetric model. Hence, 'small' (0.20 m x 0.25 m) rectangular rigid foundation (Figure 5.5a) has required to be modelled as a circular one. The equivalent radius, r_{eq} = 0.130 m, is calculated according to Equation 5.6, where S_m is the foundation cross section.

$$r_{eq} = \sqrt{\frac{4S_m}{\pi}} \tag{5.6}$$

Figure 5.6 shows dimensions and mesh, consisting of CAX6M elements, used in the analysis. Boundary conditions are assumed as symmetric boundary on the left hand side of the model (axis of symmetry) and no horizontal displacement at the right hand side. At the bottom, displacements are restricted in the vertical direction. Soil is modelled with MDPC criterion. Its parameters can be found in Table 4.16 and Table 4.17. Columns, 7 and 14 days old, are obeying law with MC criterion. Their properties are presented in Table 4.23. Contact between column and soil is simulated with the Coulomb friction criterion. Friction coefficient can be found in Table 4.25.

The rigid shallow foundation is modelled by displacement imposed to the sand surface, with equivalent radius (0.130 m). Dimensions of the 7 and 14 days old columns, are the same as ones of columns analyzed in Chapter 4, in case of small scale loading tests of the single and group of SM columns. Therefore, columns are 0.450 m long with diameter 0.070 m.

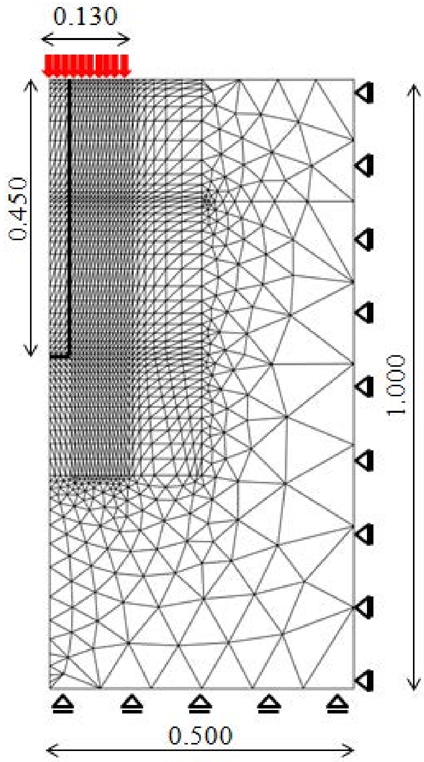

Figure 5.6 Finite element mesh and boundary conditions used in numerical modelling of a static loading test of a 'small' shallow foundation reinforced by SM column (all dimensions in meters)

5.3.2.1. Foundation without reinforcement

In order to discuss improvement brought by the reinforcement, foundation without additional support has been studied. Thus, loading test of the small scale shallow foundation has been accomplished and compared to measurements. Results of the test are presented in Chapter 3, where it has been used in order to visualise influence of each parameter of the Modified Drucker-Prager criterion with Cap. The comparison between numerical prediction and experimental observations can be found in Figure 5.7. The behaviour of the foundation is well reproduced by the numerical calculation. The borne force is insignificantly overestimated at the beginning of the loading test, till about 6 mm. After that displacement, predicted and measured behaviours of the foundation are alike. Since foundation is modelled by displacement applied directly to the soil, this slight discrepancy can be explained by perfect contact between footing and soil, which is assumed in calculation.

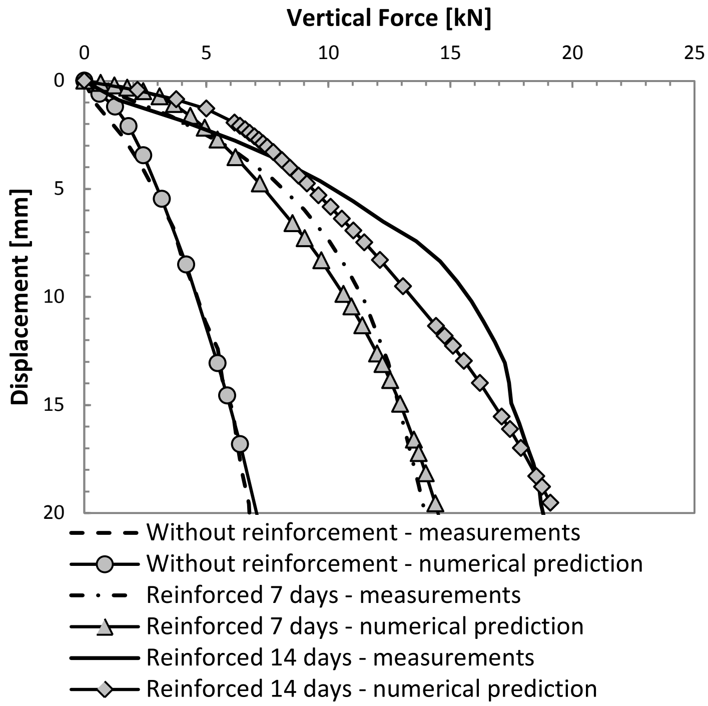

Figure 5.7 Comparison between numerical predictions and measurements for the shallow foundation situated on 'dense' sand

5.3.2.2. Reinforced foundation

As it is analysed in case of single and group of columns (Chapter 4), two SM columns, 7 and 14 days old, are examined. They have been used as a centrally situated reinforcement of the shallow foundation. Obtained results are compared with the foundation without support. The comparison between predicted and measured distributions of vertical force and vertical stress has been also taken into consideration in the study.

Figure 5.7 provides measurements and numerical predictions in terms of total vertical force and vertical displacement. The considerable improvement in terms of bearing capacity can be observed for both analysed columns.

Force borne by unreinforced foundations equals to 7.00 kN for 20 mm displacement. The use of supporting columns increases the bearing capacity to 14.50 kN and 18.70 kN for 7 and 14 days old columns respectively. Besides, the enhancement of the borne force, different kind of the behaviour can be observed. In both reinforced cases the elastic reply of the footing can be easily distinguished. Furthermore, much higher values of force are achieved with meaningfully reduced values of displacement. Small perturbation appears on the curve representing behaviour of the foundation reinforced by the older column. Non linearity can be observed for 15 mm displacement, however curve starts to bulge about 7 mm. The gibbosity can be explained by imperfections during laboratory test.

The numerical predictions of reinforced foundation present a good agreement with measurements. The numerical curve obtained from model with the 7 days old SM column fits with the measurements, despite the fact that prediction overestimates a little bit the force at the beginning of the test till about 2 mm. Then calculated force is slightly lower till about 14 mm, where numerical prediction is equal to measured one. Afterwards, predicted force is insignificantly overestimated. Displacements obtained by numerical analyses, between 0 and 1 mm, have almost the same values for both columns. In the case of the 14 days old column, prediction slightly overestimates the force for displacements between 0 to 3 mm and 18 to 20 mm and underestimates it between 3 and 18 mm.

The distribution of the vertical force and the vertical stress predicted by the numerical model are compared with measurements in Figure 5.8 and Figure 5.9. In Figure 5.8, analysis of the foundation reinforced by the 7 days old column can be found. For both distributions (forces and stresses) good agreement with measurements can be observed. As it is pointed out above, in case of total vertical force under the foundation, prediction underestimates force between 2 and

14 mm. Predicted values at the beginning of the loading process and after about 14 mm are almost the same as the measured ones. The discrepancy in the middle phase of the loading test can be explained by underestimation of the vertical force taken by the column. Force borne by the reinforcement is correctly reproduced at the beginning of the test, till about 2 mm. Afterwards, the difference between results increases till about 5 mm, where achieves its maximal value equals to about 1.20 kN. Then, discrepancy decreases till about 7 mm and force – displacement curves become parallel. From that point till the end of the loading, 20 mm, predicted force taken by the column is about 0.8 kN lower.

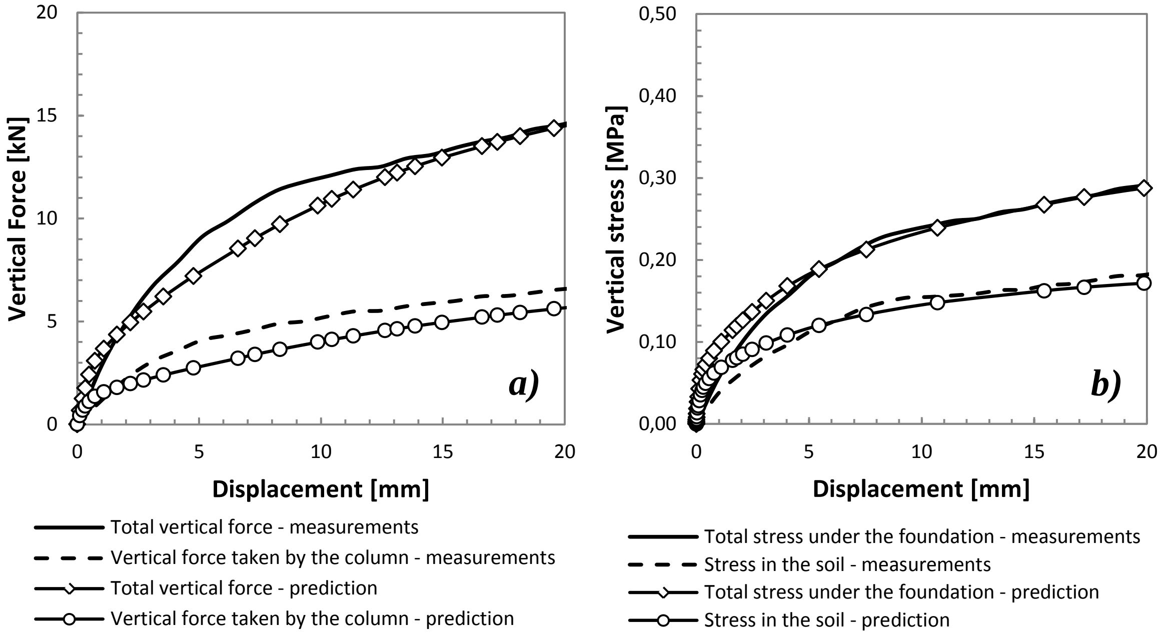

Figure 5.8 The distribution of a) force and b) stress predicted by model with the 7 days old column

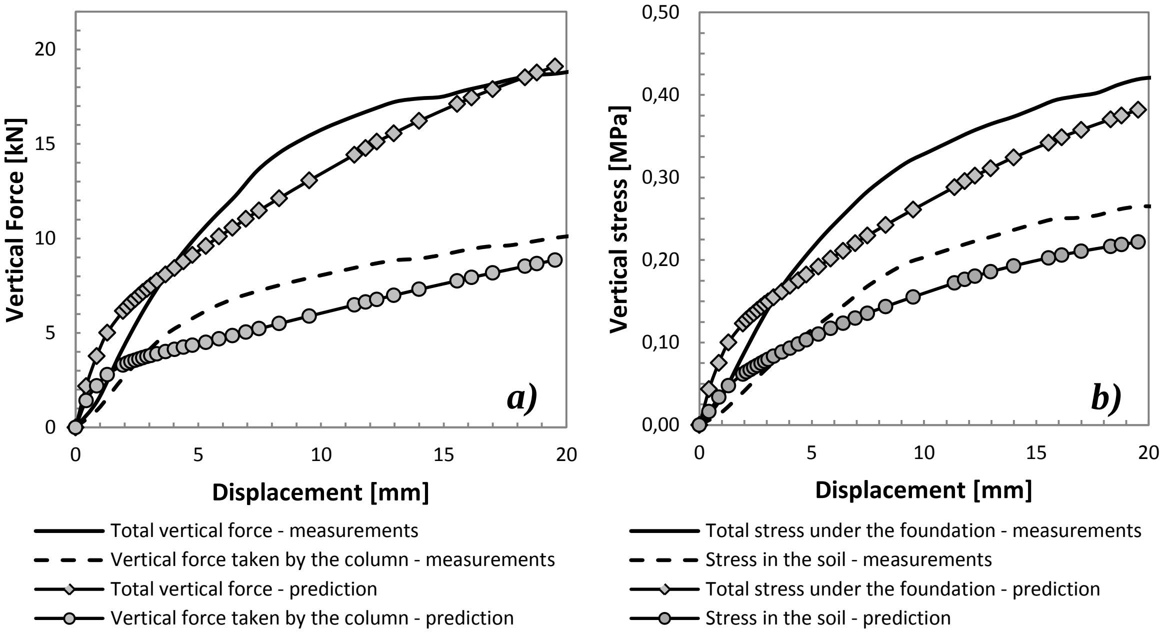

Figure 5.9 The distribution of a) force and b) stress predicted by model with the 14 days old column

In case of stresses, illustrated in Figure 5.8b, predictions correspond well to the measurements. Prediction of the stress in soil overestimates values till about 6 mm, then situation reverses and the stress is slightly underestimated. The same tendency can be observed for the total stress under foundation. However, in this case the numerical curve fits perfectly to the experimental one after 12 mm displacement.

For the foundation reinforced by the 14 days old SM column (Figure 5.9), some differences appear during the loading process but predictions are acceptable. The similar situation, as for the 7 days old column, takes place in the case of the vertical force distribution (Figure 5.9a). The force taken by the column is over predicted in the first phase of loading, till about 3 mm and afterwards underestimated till about 18 mm. Then, calculated total force is insignificantly higher than the measured one for the last part of the loading. The under predicted value of force is cause by lower force taken by the column.

The stress distribution can be found in Figure 5.9b. Total stress under the foundation, as it is in the case of the younger column, is overestimated at the beginning of the loading, till about 3 mm, then situation changes and the total stress is underestimated. As mentioned above, in case of foundation reinforced by 14 days old column, difference between prediction and measurements is due to underestimation contribution of column and soil. The total stress and the one taken by the soil presents the same tendency. Even though the stress is underestimated during the rest of the loading process, starting from 3 mm, the scale of under prediction changes with the increase of displacement. About 3 mm, curves illustrating predicted and measured stress, intersect. The difference increases and manifests its maximal value, 0.05 MPa at 10 mm displacement. Afterwards, it stays constant till the end of the loading.

5.3.2.3. Conclusions

The positive effect of using the SM method as reinforcement for the ‘small’ shallow foundation situated on a homogeneous layer of the ‘dense’ Hostun sand, has been clearly highlighted. The experimentally and numerically investigated case proved that, the value of the load borne by the foundation increased significantly, and its displacement is substantially reduced. The numerical simulations have been an attempt to identify the influence and the consequences of the SM method on the behaviour of the soil and the footing, hence total vertical force as well as vertical force and vertical stress distributions have been investigated. Despite the small differences, results obtained by axisymmetric modelling, represent well the behaviour of reinforced and unreinforced foundations. The mentioned differences might be due to the shape of the foundation (circular instead of rectangular one due to axisymmetric type of calculations), the interface between the Soil Mixing column and the sand or the idealized contact between the foundation and the soil layer (imposed displacement).

5.3.3. ‘Loose’ sand

The need of improving shallow foundations is more necessary in case of weaker soils. This study has been performed to examine influence of the soil density on the bearing capacity of the shallow foundation placed on a layer of homogeneous Hostun sand. In order to study it, the same ‘small’ foundation has been tested on the layer of ‘loose’ sand. Acquired results have been compared with ones obtained for denser sand.

Moreover, second series of tests have been carried out. The ‘big’ foundation, 0.35 m x 0.35 m, have been analysed. Both foundations, have been reinforced by the single, installed under its centre, SM column.

In this paragraph, behaviour of the foundations, obtained by axisymmetric and three dimensional models are compared with provided experimental results. The total vertical force and distribution of forces and stresses under the foundation are analysed.

5.3.3.1. ‘Small’ foundation

The 0.20 m x 0.25 m shallow foundation situated on a layer of ‘loose’ sand has been a subject of the axisymmetric study. Boundary conditions, mesh and dimensions of the model are the same as in case of the ‘small’ foundation on the layer of ‘dense’ sand (Figure 5.6). The foundation is modelled by displacement imposed to the soil. Due to axisymmetric analysis, rectangular foundation is replaced by the circular one with equivalent radius r_{eq} = 0.130 m (Equation 5.6). As previously, soil is obeying constitutive law with MDPC criterion (Table 4.16

and Table 4.17) and columns are described by MC (Table 4.23). The contact between column and soil is simulated with the Coulomb friction criterion (Table 4.25).

5.3.3.1.1. *Foundation without reinforcement*

The loading test of the small scale shallow foundation has been performed and compared to experimental findings. The bearing capacity of the analysed footing is presented in Figure 5.10. Lack of experimental result does not allow comparison, however a similar tendency as in case of foundation on the ‘dense’ sand, can be noticed. The maximal value of vertical force obtained for 20 mm displacement is 4.50 kN. The linear elastic behaviour can be observed until 2 mm and 1.60 kN, afterwards increase of the force slows down till the end of the loading test.

5.3.3.1.2. *Reinforced foundation*

The shallow foundation, reinforced by 7 and 14 days old centrally situated SM column has been analysed. The obtained, from numerical and experimental study, total vertical force as a function of displacement is presented in Figure 5.10. The considerable improvement in terms of bearing capacity can be observed for both analysed columns. Measured values of vertical force after 20 mm displacement are about 6.40 kN and 7.50 kN for younger and older SM column respectively. Similarly, as in case of a ‘dense’ sand, higher values of total force are achieved with meaningfully reduced values of displacements.

The predicted behaviour of reinforced foundation corresponds well to the experimental observations. In case of 7 days old column, predicted force is overestimated for the whole loading test. However, for the first 10 mm, discrepancy between results is insignificant, about 0.20 kN. Afterwards, difference increases up until 1.00 kN at the end of the test, 20 mm displacement. In case of the 14 days old column, prediction inconsiderably overestimates the force for displacements between 0 to 2 mm. Additionally, increasing overestimation can be observed after 12 mm, where illustrating curves intersect. The force is slightly underestimated between 2 and 12 mm. The maximal difference between prediction and measurement can be indicated for 20 mm displacement and equals to 0.50 kN.

Also, the distribution of forces and stresses under the foundation reinforced by the single column has been a subject of the study. As it is observed for denser sand, analysis of the contribution of the column and the soil separately, leads to better understanding of the reinforced foundation’s behaviour and sources of discrepancies. The distribution of the vertical force and the vertical stress predicted by the numerical model are compared with measurements in Figure 5.11 and Figure 5.12. In Figure 5.11, analysis of the footing reinforced by the 7 days old column is presented. The good agreement with measurements can be observed for both force and stress distributions. The total vertical force is overestimated during the whole test. However, it is not caused by overestimation of the force taken by the column. The column’s contribution is correctly reproduced, nonetheless about 3 mm displacement, slight underestimation appears. The overestimation of the total force and the total stress is caused by little overestimation of the stress in soil. Difference between numerical prediction and the measurements increases between 0 and 2 mm, where achieves its maximal value 0.010 MPa. Afterwards discrepancy decreases till the end of the loading test. Prediction of the total stress overestimates the measured values all along the test. However, in this case the numerical curve fits very well to the experimental one and the difference between stresses is about 0.003 MPa.

The force distribution in case of the reinforcement executed by the 14 days old column is presented in Figure 5.12a. The underestimation of the vertical force taken by the column explains the discrepancies between calculated and measured total force. Up until 2 mm predicted behaviour fits well, then difference increases with the increase of the displacement till about 6 mm. Afterwards, the higher value of the displacement becomes, the smaller discrepancy appears. At the end of the test, 20 mm displacement, dissimilarity is just about 0.15 kN. The predicted stress, presented in Figure 5.12b, shows good agreement with the results of laboratory tests. Calculated total stress under the foundation demonstrates the same relation to the measurement as in case of the total vertical force. Thus, for the small displacement, curves are alike, then the difference starts to appear about 2 mm. It increases till its maximum at about 6 mm and decreases until 15 mm, where curves again intersect. The final value of stress, at the end of the test is slightly, about 0.004 MPa, overestimated. In case of stress in soil, results of modelling and observations fit almost perfectly. Insignificant differences do not over pass 0.002 MPa.

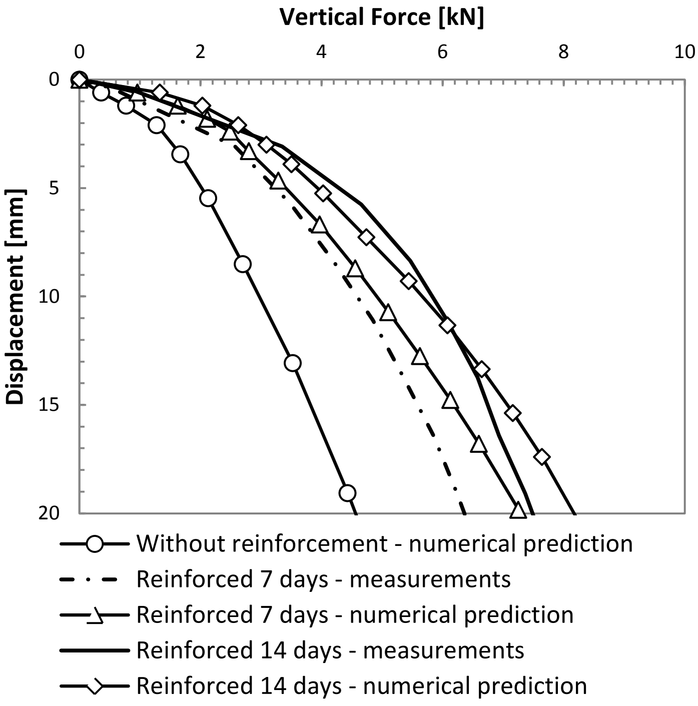

Figure 5.10 Comparison between numerical predictions and measurements for the shallow foundation situated on 'loose' sand

5.3.3.1.1. *Conclusions*

The positive effect of the reinforcement of the 'small' shallow foundation placed on 'loose' Hostun sand, was pointed out. The load borne by the foundation increased considerably whereas its displacement was substantially reduced. The total vertical force, vertical force and vertical stress distributions were successfully reproduced by the numerical modelling. In spite of small differences, the obtained results agree well with the observed behaviour of the foundation. As it was in case of 'dense' sand, the mentioned discrepancies might be caused by the shape of the different than in the reality foundation, its idealized non-deformability and contact with soil, and the interface between the Soil Mixing column and the sand.

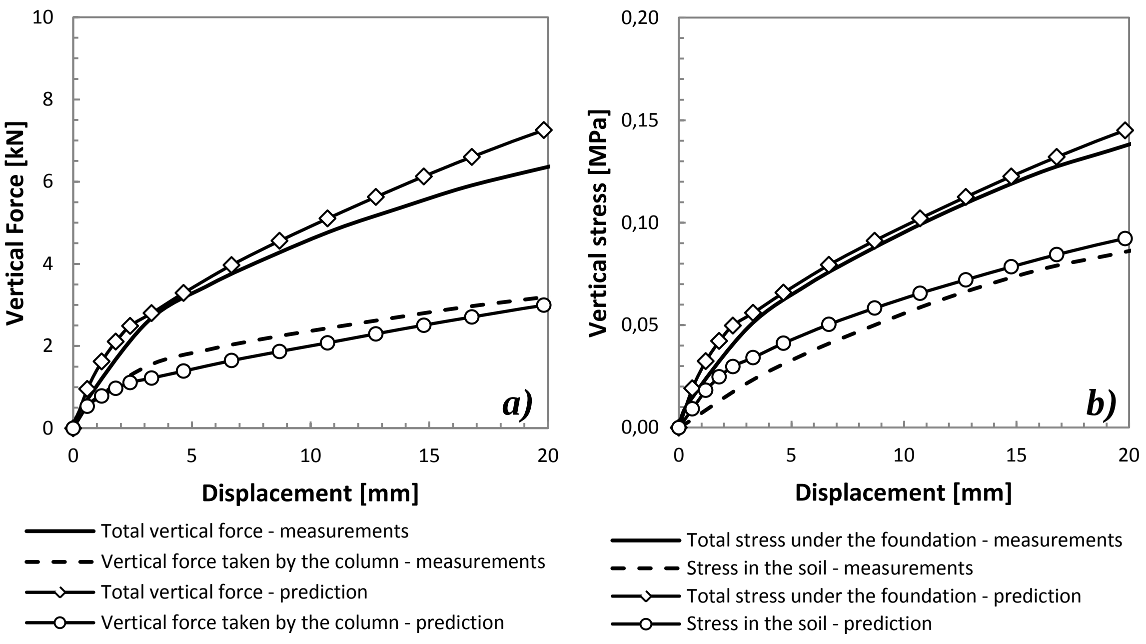

Figure 5.11 The distribution of a) force and b) stress predicted by model with the 7 days old column

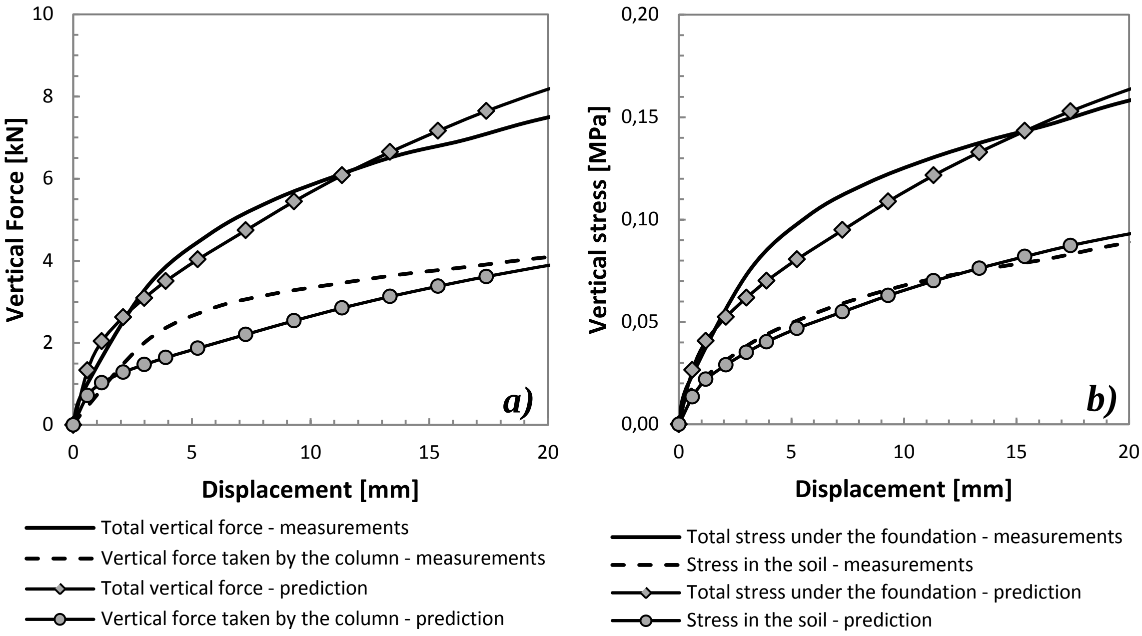

Figure 5.12 The distribution of a) force and b) stress predicted by model with the 14 days old column

5.3.3.1. Comparison between ‘dense’ and ‘loose’ sand

The ‘small’ foundation has been tested with both soils: ‘loose’ and ‘dense’. Obtained results are presented and compared with laboratory observations in previous paragraphs. In order to analyse influence of the soil’s density on the foundation performance, it is necessary to compare total vertical forces obtained for both densities. To be able to understand it better the force and stress distributions should be also compared. The investigation of percentage of total force taken by column and soil helps to compare performance of the footings. It brings information about improvement caused by the reinforcement and help to identify participation of each part of the mixed foundation (footing and reinforcing column).

5.3.3.1.1. *Total force*

Comparison of the total force borne by ‘small’ foundation on ‘loose’ and ‘dense’ Hostun sand, with and without reinforcement is presented in Figure 5.13.

Behaviour of the foundation without support can be found in Figure 5.13a. Force predicted for ‘loose’ sand is significantly lower than the one for denser soil. Additionally, due to different values of the modulus of deformation, 3 MPa and 7 MPa for ‘loose’ and ‘dense’ sand respectively, slopes of the force-displacement curves are not alike. In case of denser soil, increase of force is faster than in the other case. Discrepancy mounts up with increase of the displacement and achieves 2.3 kN, after 20 mm. The same tendency can be observed for reinforced foundation. Moreover, difference between predictions grows also as a function of column’s age. Hence, after 20 mm displacement, in case of younger one, foundation placed on denser sand sustains about 7.2 kN higher force. In case of 14 days old column, difference at the end of the test equal to about 11.1 kN. Additionally, it can be pointed out, that foundation without reinforcement on denser soil is capable of bearing comparable total vertical force as reinforced by 7 days old column one on the ‘loose’ layer, 7.1 kN and 7.5 kN respectively.

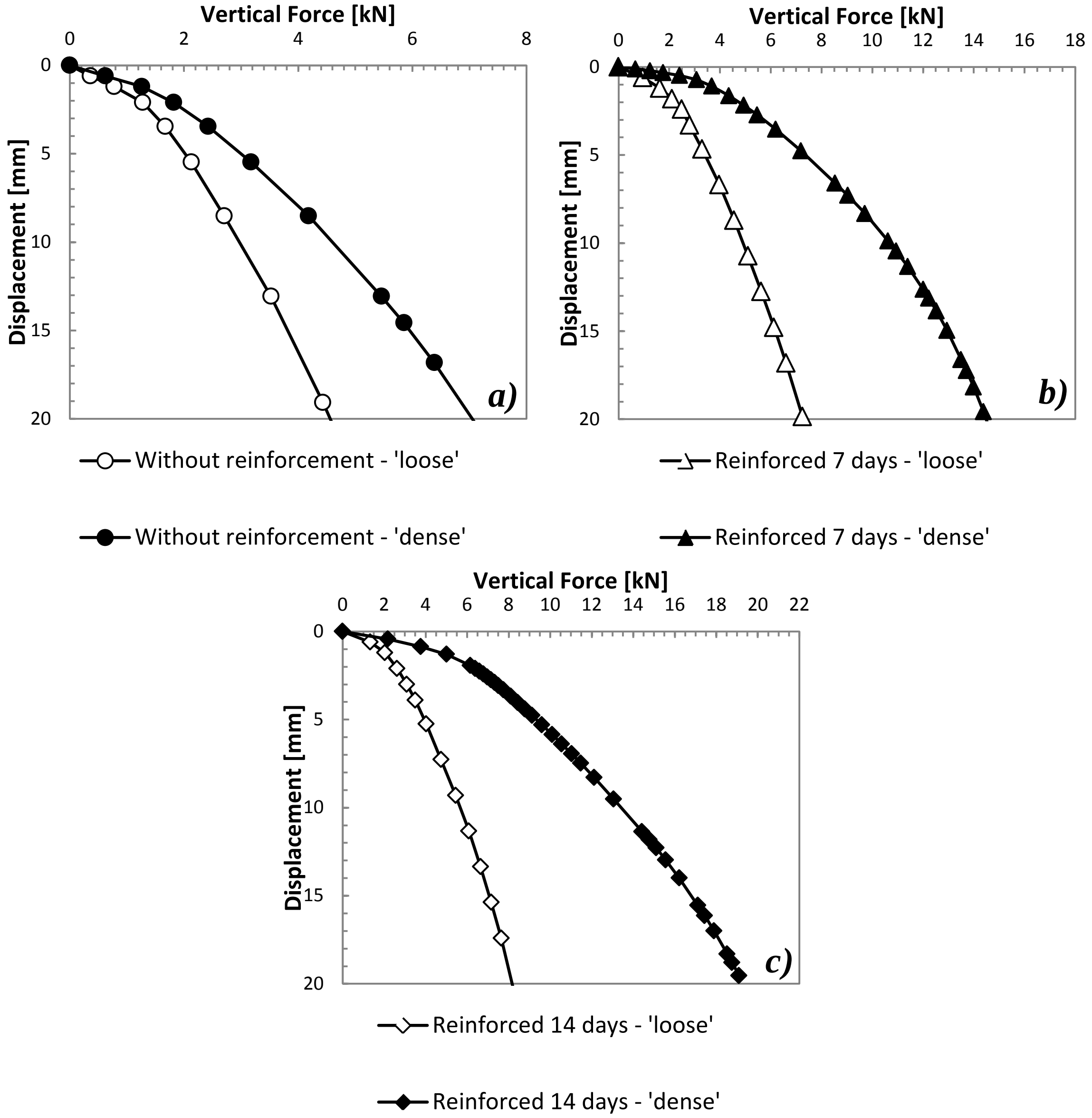

Figure 5.13 Total force borne by shallow foundation placed on 'loose' and 'dense' sand, a) without reinforcement, b) reinforced by single, 7 days old column, c) reinforced by single, 14 days old column

5.3.3.1.2. *Force and stress distribution*

Distribution of the vertical force is presented in Figure 5.14. As it is in case of the total force, also the force taken by the column is meaningfully influenced by the density of soil. Values of force taken by columns in denser sand are comparable with the total capacity of mixed foundation tested on 'loose' one.

The impact of the density on the total stress and stress in soil under the foundation can be found in Figure 5.15. Density of soil has influence not only on final value of stresses but also on the slope of illustrating curves. Steeper slopes of curves are result of higher modulus of deformation of denser sand, 7 MPa. Another properties, which change with density of soil are its shear parameters: internal friction angle and cohesion. In case of sands, the crucial role plays friction angle. It's value increases with the increase of density, thus the soil elastic answer to imposed displacement is extended and plastic failure takes place for the higher value of load.

For detailed investigation of an impact of the soil density on the mixed foundation performance, contribution of each part of the structure has been analysed, in order to discover some regularities.

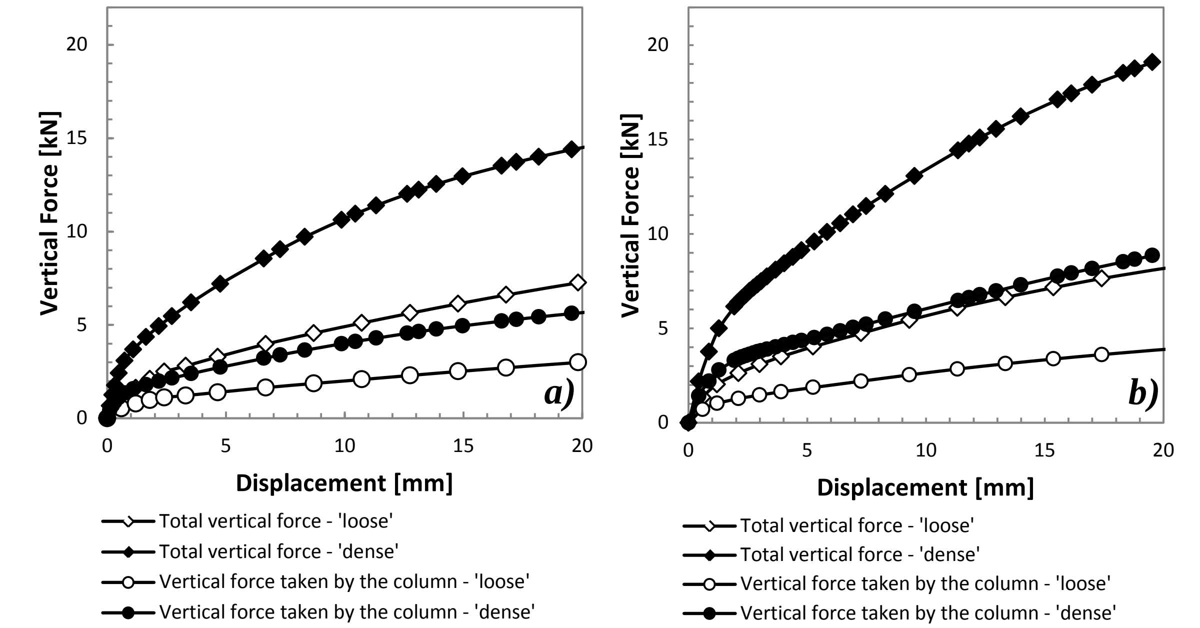

Figure 5.14 Distribution of vertical force under the shallow foundation placed on 'loose' and 'dense' sand reinforced by the a) 7 days old and b) 14 days old column

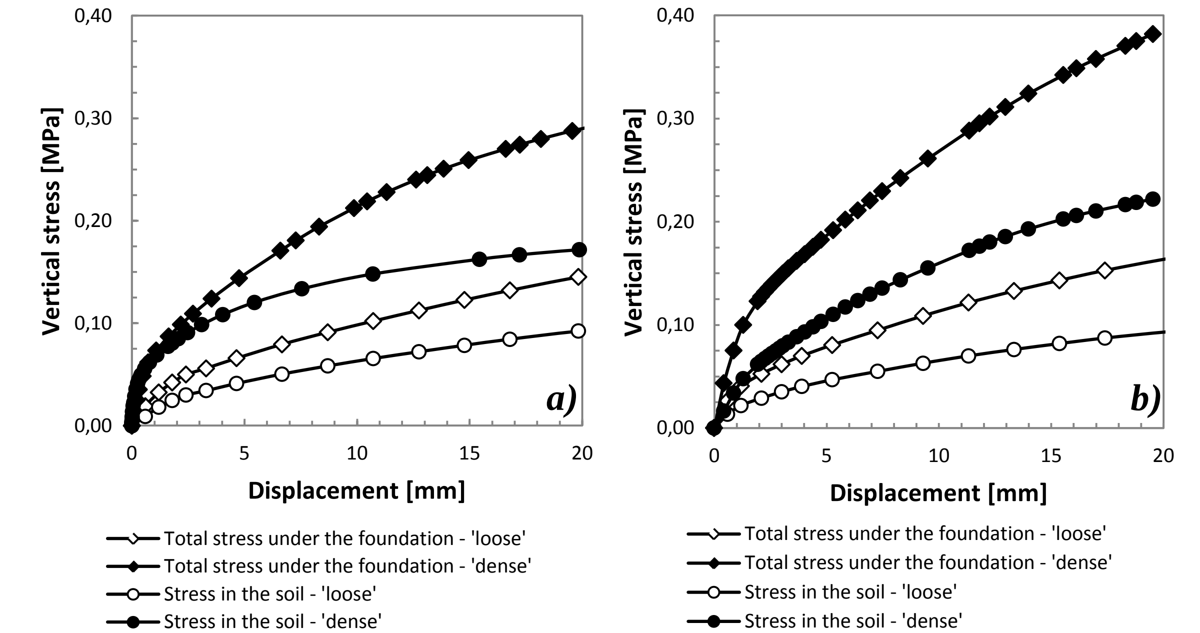

Figure 5.15 Distribution of stress under the shallow foundation placed on 'loose' and 'dense' sand reinforced by the a) 7 days old and b) 14 days old column

Figure 5.16 depicts participation of reinforcement and soil being in contact with the foundation in bearing applied load. The contribution of 7 days old column as a function of foundations displacement can be found in Figure 5.16a. The same trend of the behaviour have been observed regardless soil density. Even though, values of forces taken by columns, installed in 'loose' and 'dense' sands are significantly different, their participation in the whole borne force is comparable. The same tendency can be observed for soil's contribution. After 20.0 mm displacement, column takes about 39% and 42%, whereas contribution of sand, accounts for 60% and 58% for 'loose' and 'dense' sand respectively.

The contribution of soil and older column is presented in Figure 5.16b. In this case influence of the soils' density is visible at the beginning of the loading till about 3.5 mm. The participation of column in 'dense' sand decreases till about 11.0 mm, where it stabilises at about 44%. The contribution of soil is a mirror reflection of the column's one. So, it rises till 11.0 mm and becomes constant at about 56%. Similar trend is observed for 'loose' sand, however difference between contributions never overpasses 6%, while at it maximum, for 'dense' soil, difference achieves 26% (at the beginning of the loading test). Elements take the same load, 50% of the total force, after 1.0 mm and 3.5 mm displacement for looser and denser soil respectively. After 11 mm, when contributions for both soils are stabilised, percentages become comparable like in case of reinforcement executed by younger column. About 55% of the total force is taken by soil, whereas about 45% is borne by the SM element.

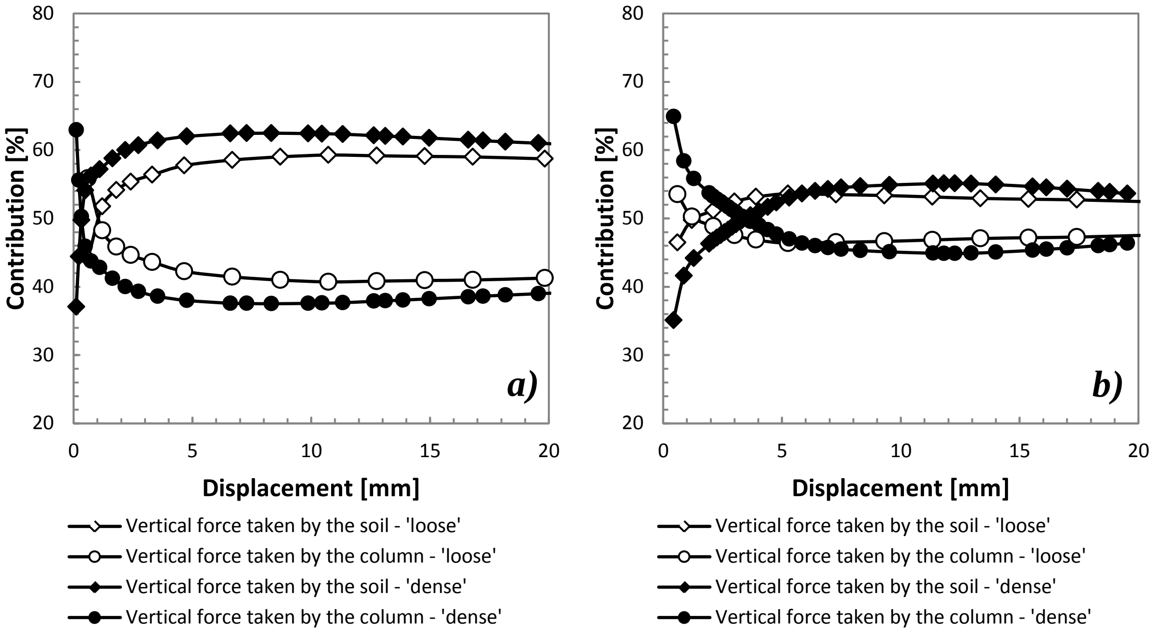

Figure 5.16 Contribution of each element of the mixed foundation in bearing vertical force applied to the foundation placed on layer of 'loose' and 'dense' sand. Reinforcement executed by a) the 7 days old and b) the 14 days old column

5.3.3.1.3. *Conclusions*

'Small' shallow foundation with and without support executed by single SM column have been analysed. Three loading tests for each density of soil have been accomplished in order to point out influence of the sand's density. Better compaction of soil leads to higher modulus of deformation and internal friction angle. Moreover, its impact has been observed not only on the capacity of soil but also columns regardless their age. Therefore, it has been proven, that the higher density becomes, the better performance of the footing can be expected. For instance, foundation built on 'dense' Hostun sand is able to sustain comparable force as the reinforced by 7 days old built on 'loose' soil.

Even though differences between forces and stresses borne by foundations placed on 'loose' and 'dense' sand are significant, similarities can be found. It has been observed that, contribution of soil, in bearing total force applied to the foundation has been found density independent.

5.3.3.2. 'Big' foundation

Static loading test of the 'big' shallow foundation (Figure 5.5b) situated on the layer of 'loose' Hostun sand, is a subject of this study. By the 'big' shallow foundation, footing modelled by a steel plate 0.35 x, 0.35 m x 0.01 m (length x width x height) is understood. Two cases have been studied: footing without reinforcement and one supported by single column. Mixed foundation consisting of footing and a single, 7 days old column installed under its centre has been calculated by three dimensional finite element model.

The three dimensional calculations have an advantage over the axisymmetric ones because there is no need to replace square foundation by a circular one with the equivalent radius. However, this kind of calculations are time consuming. To cope with this problem, only one, representative, quarter of the tank, where the loading test was performed, has been analysed. It has been possible because of two planes of symmetry dividing each edge of the plate into two parts.

Results of the modelling are compared with experimental findings in terms of total force and distribution of force and stress. Moreover, the improvement brought by the reinforcement is pointed out by comparison with unreinforced footing.

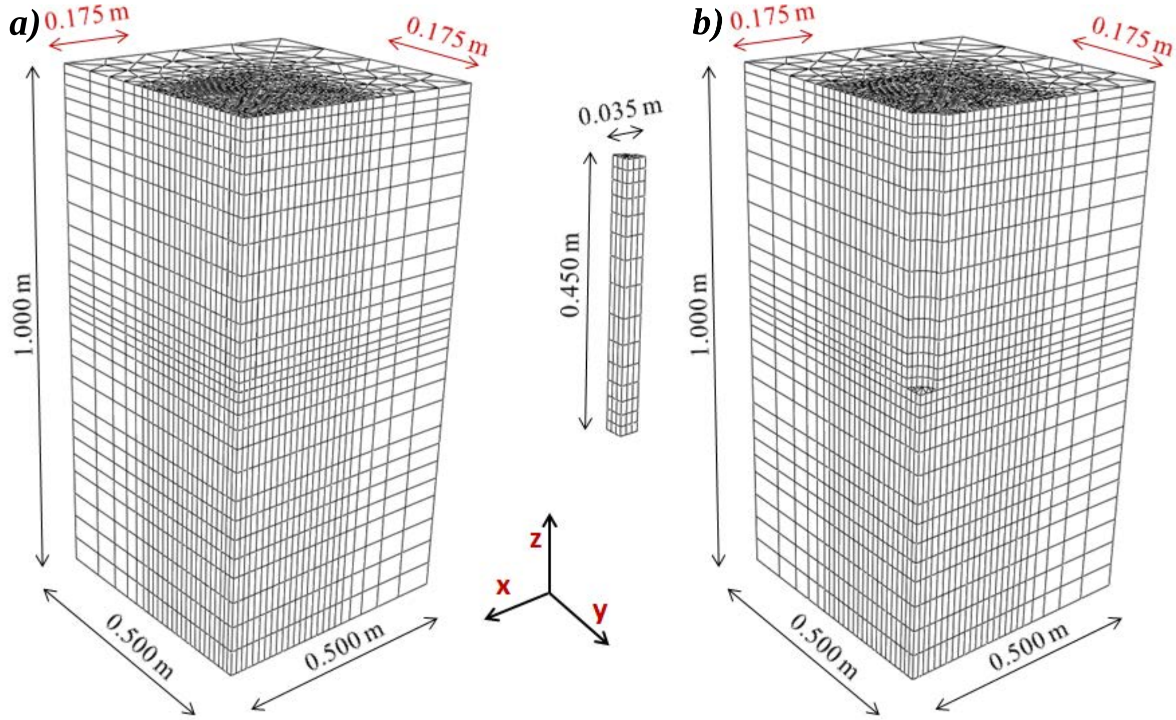

Figure 5.17 Three dimensional mesh and dimensions of the 'big' shallow foundation numerical model a) without reinforcement, b) reinforced by single 7 days old column (dimensions in meters)

5.3.3.2.1. *Without reinforcement*

Three dimensional modelling of a static loading test has been carried out to reproduce experiment. Dimensions and mesh of the calculated case are presented in Figure 5.17a. Mesh consists of 15-node quadratic triangular prism elements (C3D15). Model's boundary conditions are assumed as: symmetric boundaries on the planes of symmetry, no horizontal displacement in the X axis direction for the wall parallel to the YZ plane and no horizontal displacement in the Y axis direction for the one parallel to the XZ plane. At the bottom, displacements are restricted in the vertical direction

'Loose' sand has been modelled with MDPC criterion. Its properties are presented in Table 4.16 and Table 4.17. The 7 days old SM column, as in previously analysed cases, obeys constitutive law with MC criterion. Its properties can be found in Table 4.23. Model is loaded by the imposed displacement applied to the surface corresponding to dimensions of the one quarter of the footing. Results of the modelling is presented in Figure 5.18.

5.3.3.2.2. *Reinforced*

The shallow foundation, reinforced by 7 days old centrally situated SM column has been analysed. The mesh used in calculations can be found in Figure 5.17b. Quarter of a SM column, added to the model, has been meshed with the same kind of elements as the soil (C3D15). An interaction between soil and column is described by Coulomb friction (Table 4.25).

Obtained from numerical and experimental study total vertical force as a function of displacement is presented in Figure 5.18. A relatively small improvement in terms of bearing capacity can be observed. Measured value of vertical force after 25 mm displacement is about 11.8 kN. Predicted behaviour presents the same trend as the one for foundation without support. Namely, up until 3 mm, calculated and measured forces are coherent, however, after that, it is overestimated. The discrepancy increases and achieves about 2 kN at the end of the test. The cause of the over prediction can be found by analysing force and stress distributions.

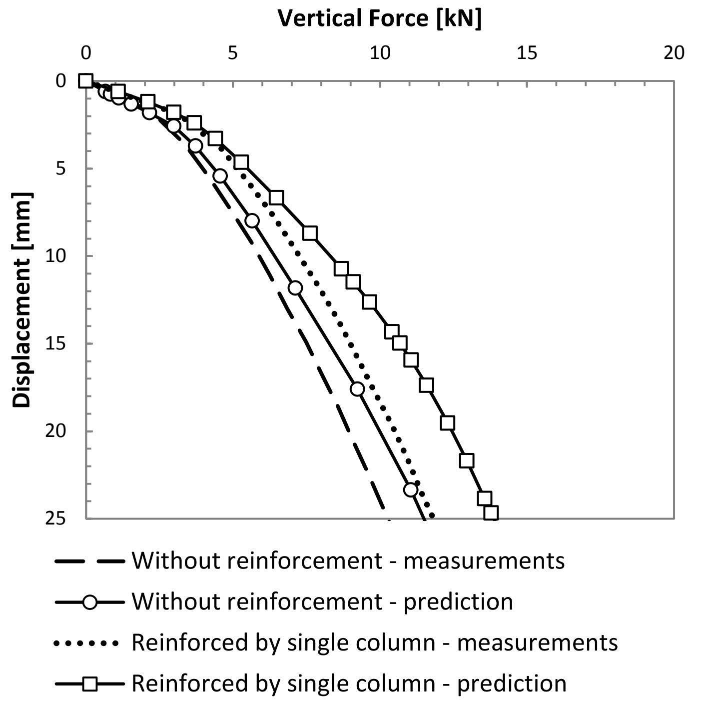

Figure 5.18 Comparison between numerical predictions and measurements for the shallow foundation situated on 'loose' sand

Figure 5.19a depicts distribution of force. The first source of the difference between measured and predicted total force is over prediction of force taken by the column. The discrepancy between curves starts at about 3 mm displacement and rises as a function of displacement.

It has been observed that soil takes significant load during the whole test (Figure 5.19b). The predicted behaviour, overestimates the measured one, also in terms of stress in the soil. It is the second source of the discrepancies between measured and predicted total force. In case of the bigger mixed foundation, proportion between surface of the reinforcement and the foundation being in contact with soil is significant. Column represents just 3% of surface of the footing. That is why even small overestimation of soil's participation in bearing applied load effects with big discrepancies. Unfortunately, in this numerical simulation both over predictions have place.

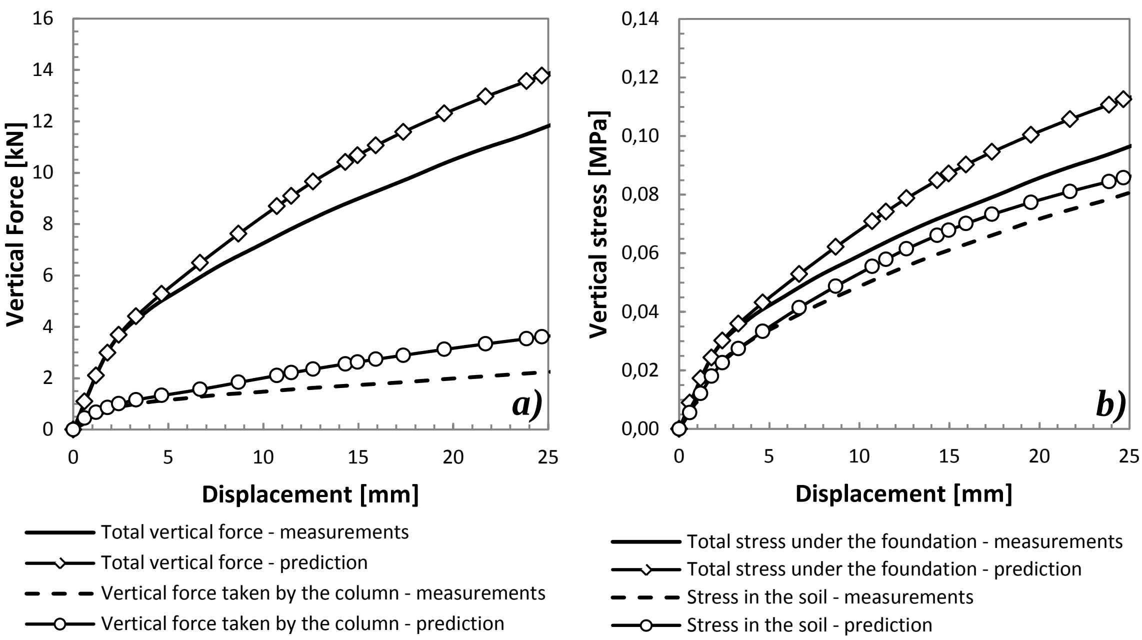

Figure 5.19 The distribution of a) force and b) stress predicted by numerical model

Figure 5.20 helps to analyse contribution of column and soil in sustaining total force. It has been measured that about 80% of the applied load was taken by the soil. Big influence on the soil's contribution has size of the surface in contact – about 97% of the footing. It has been observed that at the beginning of the test, till about 1.5 mm, participation of the soil increases rapidly and achieves about 76% of the total force. Afterwards, contribution very slowly rises till the end of the test, where equals about 80%. The numerically predicted percentage is comparable. Calculated contribution of the soil is a bit underestimated but the difference is constant till about 7.0 mm. Afterwards, predicted contribution stabilized at about 77%, whereas measured one slowly increases.

In case of the column, its contribution is a mirror reflection of the soil's behaviour. At the beginning of the test, till about 1.5 mm, SM element participation considerably decreases till about 24%. Then, decline becomes very slow, and at the end of the test column takes 20% of the load. The predicted contribution of the reinforcement decreases till about 7.0 mm, then stabilised at about 23%.

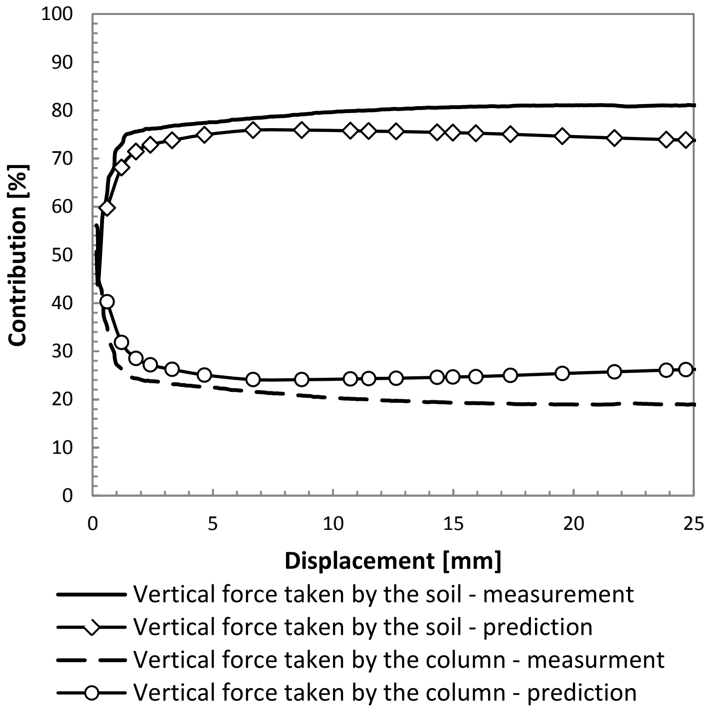

Figure 5.20 Contribution of vertical force taken by soil and column in the total vertical force borne by the shallow foundation reinforced by the 7 days old column

5.3.3.2.3. *Conclusions*

The loading test of the 'big' shallow foundation with and without reinforcement has been presented. Obtained results, not very well but still acceptably reproduce measurements during the whole loading. However, over predictions appear for larger displacements. Results acquired from laboratory and numerical testing are alike at the beginning of the test till about 5 mm. Afterwards, overestimation increases as a function of applied displacement. In case of foundation without support, predicted total force has been 1.3 kN higher than the measured one. Also in case of reinforced footing, overestimation has been reported. Further analyses of the distribution of vertical force and stress have shown that over prediction of total force comes from over prediction of force taken by the column and soil. Nonetheless, comparison of the contribution of each part of the strengthen foundation gives good results. Numerical model well predicted participation and the behaviour of both elements along the test. Discrepancies can be explained, as previously, by the idealized contact between soil and column and perfect adhesion between footing and the soil.

5.3.4. Conclusions

Effect of the reinforcement of a shallow foundation, executed by single SM column has been presented. It has been proven by laboratory and numerical simulations that by introducing only one reinforcing element better performance of the footing can be obtained. Acquired results have shown that increase of mixed foundation's bearing capacity is significant. Properly calibrated constitutive models of all used materials, have permitted correct reproduction of the behaviour of the foundation. Additionally, influence of: soil density, age of reinforcing column and size of the footing, has been presented and discussed.

Differences between forces and stresses borne by mixed foundations on layer of 'loose' and 'dense' sand have been significant. However, it has been found that the percentage of the total force that was taken by the soil is density independent. Age of column have been reported as crucial for the bearing capacity improvement. The older column is used as a reinforcement, the higher performance of the foundation is observed.

It has been noted, that behaviour and bearing capacity of the mixed foundations reinforced by single column is mainly influenced by size of the footing. It is directly related to the force taken by the soil. Whereas the reinforcement takes comparable load regardless the foundation's size.

5.4. Reinforcement by four columns

The reinforcement of a shallow foundation executed by single SM element is very unlikely. The main reason is significant, but still not sufficient improvement of the foundation's bearing capacity. Moreover, in case of using only one column, its location under the foundation is crucial. Keeping in mind the field installation procedure of the SM element, it needs to be remembered that some imperfections such as: location and small differences in column's geometry and verticality can appear. Each of them lead to reduction of the reinforcement efficiency as well as rotation of the foundation. Therefore, more natural solution is to set up more than one supporting element. In this study, mixed foundation consisting of four columns, were chosen as the most representative. The small scale shallow foundation, 0.35 m x 0.35 m (Figure 5.21), was reinforced and loaded in laboratory. Total surface of the foundation and cross sections of reinforcement and soil being in contact with the footing are presented in Table 5.3.

Results of loading tests have been successfully reproduced by a three dimensional finite element modelling. Except bearing capacity and distribution of vertical force, also the influence of the tip's bearing capacity of columns has been studied. In order to investigate its impact, a loading test of a foundation reinforced by group of four columns placed in and heterogeneous soil have been carried out. The heterogeneous soil consists of upper 'loose' and lower 'dense' layers. Results of the calculations and measurements have been compared. In order to discuss improvement brought by the reinforcement executed by the group of four columns, its behaviour have been confronted with behaviours of foundation: without SM elements and mixed foundation supported by a single column.

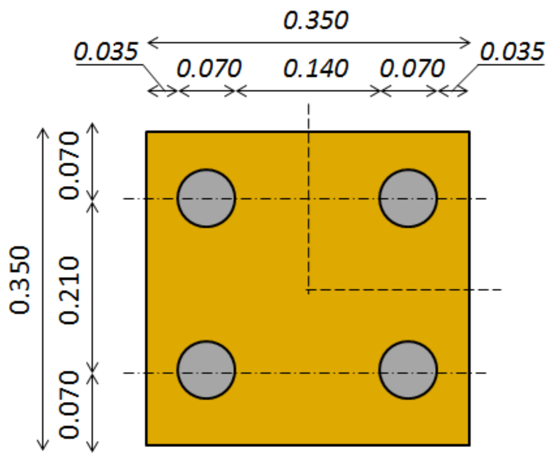

Figure 5.21 Columns' pattern under the shallow foundation (dimensions in meters)

Table 5.3 Surface of the 'big' foundation and proportions between surface of the reinforcement and surface in contact with soil under the foundation

Number of columns	Surface [m^2]	Reinforcement [m^2]	Surface in contact with soil [m^2]	Reinforcement [%]	Surface in contact with soil [%]
One	0.123	0.004	0.119	3.14	96.86
Four		0.015	0.107	12.57	87.43

5.4.1. Experimental setup

The static loading test of the 'big' shallow foundation reinforced by group of four SM columns, was performed by Dhaybi (Dhaybi, 2015). Four columns were installed (according to method depicted by Figure 4.23) in a 1 m^3 chamber of equipped with sensors tank (Figure 5.22). Three LVDT displacement sensors were used in order to control rotation of the foundation during the loading process. Moreover, two big scale force sensors (0.30 m x 0.30 m and 0.35 m x 0.35 m) were used to measure forces on the boards of the chamber during the loading test. This kind of control helps to detect existence of the board effect, which can have an impact on the foundation's behaviour and hence interferes the results. Other type of force sensors were used on the top of columns. Cylindrical, 0.05 m height, sensors were providing value of vertical force taken by the columns. Pattern of the reinforcing elements is presented in Figure 5.21. Distance between columns equals to double diameter, 0.140 m, and they are moved away 0.035 m, from the edge of the foundation.

Two configurations of the soil were tested. The first one, was mixed foundation placed in homogeneous layer of 'loose' sand. The second one, consisted of two soil layers. At the bottom of the tank 0.58 m layer of a 'dense' sand was placed in 0.1 m layers to ensure proper compaction. On its top, in the same way, 0.42 m of the 'loose' sand was situated. Afterwards, four columns were installed one by one in a way that about 0.03 m of the column was embedded inside the denser soil. Due to this heterogeneous support of the column, the influence of the tip's capacity on the total bearing capacity of the column and hence whole mixed foundation was examined.

Results of both tests performed on the foundation reinforced by 7 days old columns are presented in next paragraphs.

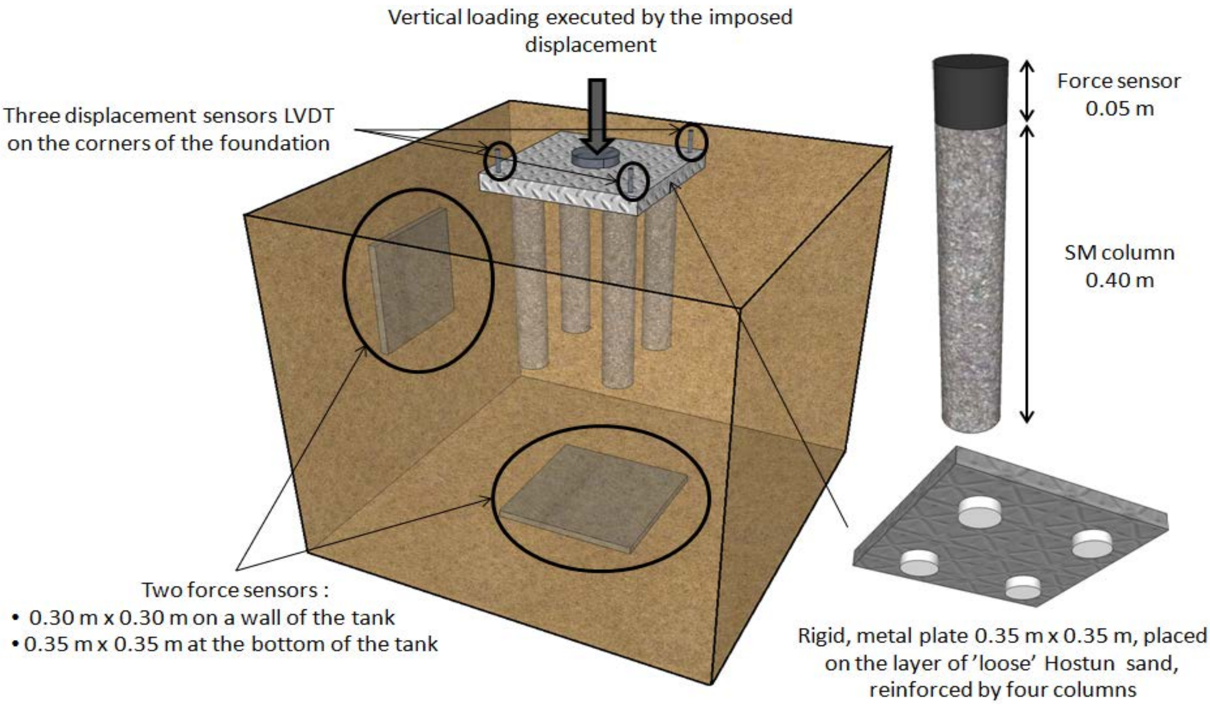

Figure 5.22 Scheme presenting equipped tank for the loading test of the mixed foundation (Dhaybi, 2015)

5.4.2. Numerical modelling

The numerical modelling of the small scale mixed foundation consisting of shallow foundation reinforced by four columns, has been carried out to reproduce the experiments. The loading tests have been analysed by three dimensional model. In order to reduce calculation's time, only quarter of the tank's chamber and mixed foundation have been modelled. Model's dimensions have been assumed in accordance with experimental setup. Numerical calculations have been performed for 7 days old column and for two configurations of sand: homogenous and heterogeneous. Properties of the modelled materials and column-soil interaction are assumed as in previous tests and can be found in Table 4.16 and Table 4.17 for soils and Table 4.23, Table 4.25 for column and contact, respectively. The influence of the density of soil under the columns' tips on the bearing capacity of the column, and hence total bearing capacity of the mixed foundation has been indicated and discussed.

5.4.2.1. Homogeneous layer of soil

In order to reproduce the experimental test, three dimensional model has been used. As mentioned before, to reduce time of the calculations only a quarter of the experiment has been modelled. Due to that, finite element model simplified to one column. Dimensions and mesh used during calculations are presented in Figure 5.23a. 15-node quadratic triangular prism elements (C3D15) have been used to build the mesh of soil and column. The stiff plate representing in laboratory shallow foundation has been replaced by imposed displacement, applied to a surface 0.175 m x 0.175 m, which corresponds to one quarter of the foundation. Boundary conditions are assumed as in case of the bigger foundation reinforced by single column. Thus, vertical displacement are blocked at the bottom. Moreover, symmetric boundaries are applied to walls, which are the planes of symmetry. For the two remaining walls, horizontal displacements are restricted in a way that: the X axis direction for the wall parallel to the YZ plane and the Y axis direction for the one parallel to the XZ plane.

Calculated behaviour has been compared with the unsupported foundation in order to assess efficiency of the reinforcement.

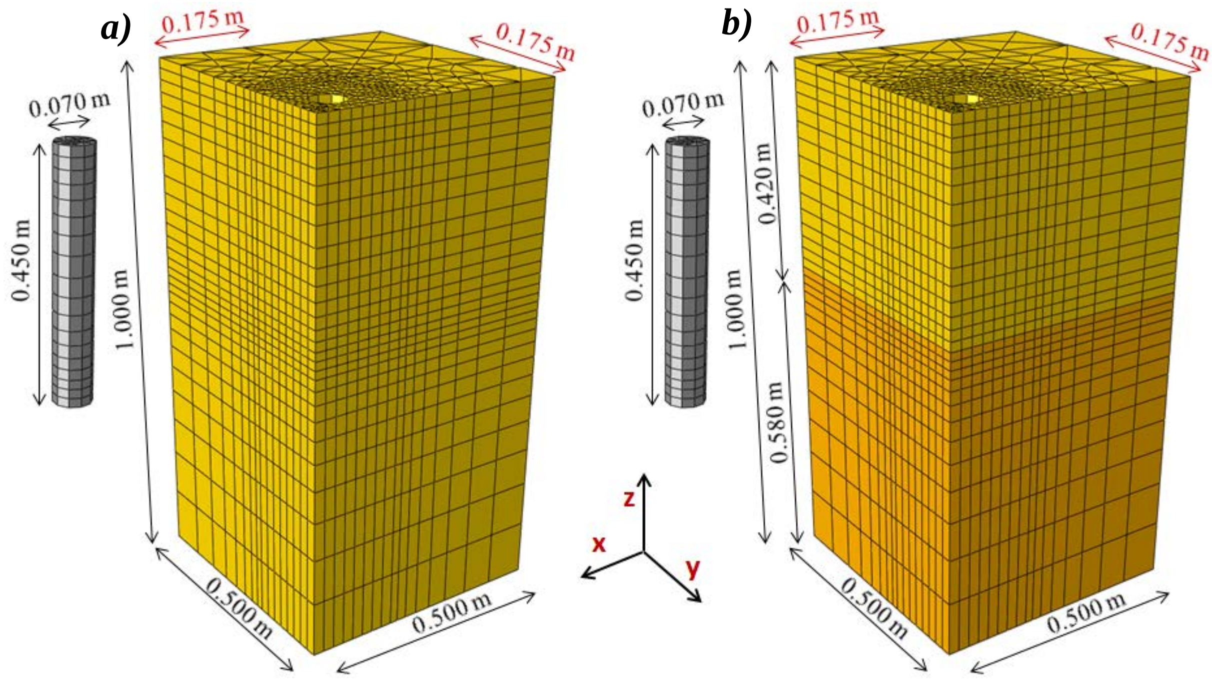

Figure 5.23 Three dimensional mesh and dimensions of the mixed shallow foundation placed on: a) a homogeneous layer of 'loose' sand, b) a heterogeneous layer of sand: upper 'loose' and lower 'dense' layer (dimensions in meters)

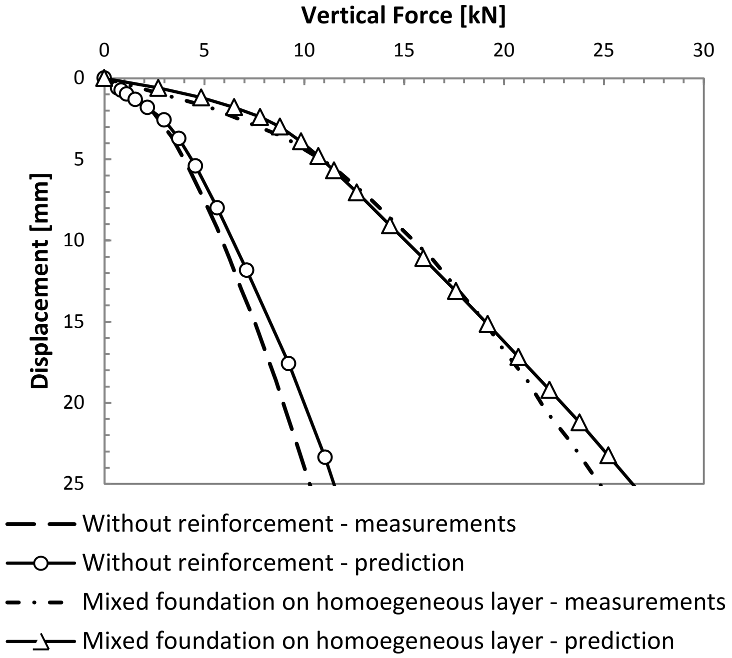

Figure 5.24 Comparison between numerical predictions and measurements for the mixed foundation situated on homogeneous layer

5.4.2.1.1. *Total borne force*

Obtained results for mixed foundation, which consists of shallow foundation and the group of four 7 days old columns, are presented in Figure 5.24. Reinforcement by four columns, provides almost two times and a half bearing capacity of the foundation without reinforcement. Predicted behaviour of the mixed foundation corresponds very well to the observed one. Insignificant overestimation of the force appears at the beginning of the loading, till about 5 mm. Then, minimal underestimation can be observed between 5 and 15 mm. The discrepancy between results increases with the increase of the displacement, between 15 mm and the end of the test – 25 mm. However, the final difference of predicted and measured forces equals 1.2 kN.

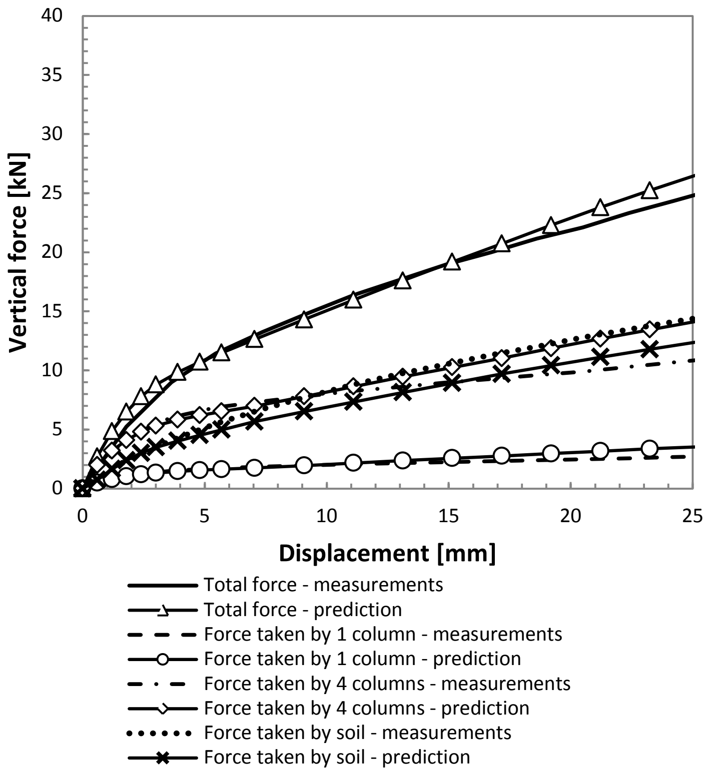

Figure 5.25 The distribution of vertical force predicted by model with homogeneous soil layer

5.4.2.1.2. *Distribution of force*

The distribution of force taken by each part of the mixed foundation has been a subject of detailed analyses. As it has been proven in case of foundation reinforced by a single column, only investigation concerning participation of each element, allows full understanding of the behaviour of the foundation. For mixed foundation consisting of four columns, the total force, the force taken by the one column in a group, four columns and soil is analysed. Since model has been reduced to quarter, the force borne by four columns is calculated as the force sustained by one element and multiplied by number of columns. This approach brings idealization to the modelling because situation where load is evenly distributed between columns is very unlikely in the laboratory and *in situ* conditions.

The distribution of force can be found in Figure 5.25. Results fit well to the measurements, however some differences can be pointed out. The first one appears in case of calculated force taken by one column. Predicted and measured behaviour fits perfectly for smaller displacements. Nonetheless, overestimation starts and increases with increase of the displacement after about 13 mm. The final difference is about 0.75 kN, which is not a very significant discrepancy. However, concerning the assumption that all four columns bear the same force, results with much higher overestimation of the force borne by the group of SM elements. The beginning of both curves, illustrating force borne by columns, fits very well, but about 11 mm overestimation starts and continues up until the end of test. The difference between results, obtained for 25 mm, equals about 3.00 kN. The second discrepancy appears for calculated participation of soil. Similarly to the column case, beginning of curve corresponds very well to the measurements. At about 4 mm, situation changes and force starts to be underestimated. Between 4 and 11 mm, the higher displacement applied to the foundation, the bigger underestimation of force manifests. After 11 mm, difference stabilized and stay constant, about 2.00 kN till the end of the loading test.

5.4.2.1.3. *Conclusions*

The static loading test of the mixed foundation, placed on the homogeneous layer of ‘loose’ Hostun sand, has been presented. Obtained results show good agreement with the experimental findings. Almost two and a half times value of vertical force, than in case of unreinforced foundation have been reported. Installation of four columns under the shallow foundation doubles force borne by the footing reinforced by single SM element.

Despite fact that accuracy of the predictions is satisfactory, some discrepancies appears. They can be explained as in previous cases by the column-soil interaction and idealized contact between foundation, replaced by imposed displacement, and soil. Nevertheless, in this case differences come mainly from the assumption, that approximation of the force taken by four columns is a value calculated for just one element and multiplied by four. This approach is correct for numerical modelling, however this kind of idealized conditions are hardly possible in experiment performed in laboratory and even more unlikely *in situ*. Overestimation of the force taken by one column, which appears for bigger displacements, leads to four times higher overestimation of the force sustained by whole reinforcement. Although, over prediction reaches not considerably high but still not negligible value, the discrepancy is not clearly visible in the total force borne by the mixed foundation. It can be explained by underestimation of the load taken by the soil under the foundation. Summing up, the underestimation of the force borne by soil reduces the overestimation of the participation of four columns, in general giving very well reproduced value of the total force. This test shows how important is analysing not only the total sustain load because its results might be misleading.

5.4.2.2. Two layers of soil

The loading test of the mixed foundation placed in heterogeneous soil have been successfully reproduced by the three dimensional numerical modelling. The dimensions and the mesh used in the calculation can be found in Figure 5.23b. The same kind of mesh and boundary conditions as in case of mixed foundation situated on the homogeneous layer, have been used. For this test SM columns are placed in a way that their tips and last 0.03 m are in the denser layer. Contact between soil and column is modelled by the interface elements with zero initial thickness, obeying the Coulomb failure criterion with the same value of friction coefficient (for the ‘loose’ sand) for the whole length of column.

Due to embedding in the denser soil, bearing capacity of the reinforcing elements is changed. This study helps to understand importance of the support under the tip of the columns and its influence on the bearing capacity of the mixed foundation.

5.4.2.2.1. *Total force*

Results obtained for mixed foundation reinforced by the group of four, 7 days old, columns in heterogeneous soils is presented in Figure 5.26. Measured total force after 25 mm displacement, for case with two layers, equals to almost tripled total force borne by unsupported foundation. Predicted behaviour of the foundation reproduces well the observed one. However, some discrepancies can be pointed out. For the small displacements, value of predicted force is slightly overestimated until 4 mm, where is the same as the measured one. Afterwards, underestimation starts and increases, till about 11 mm where achieves maximum, and then slowly decreases till the about 2.4 kN difference at the end of the test. As in previously examined cases, in order to understand the source of dissimilarities, analysis of the distribution of force under the shallow foundation is necessary.

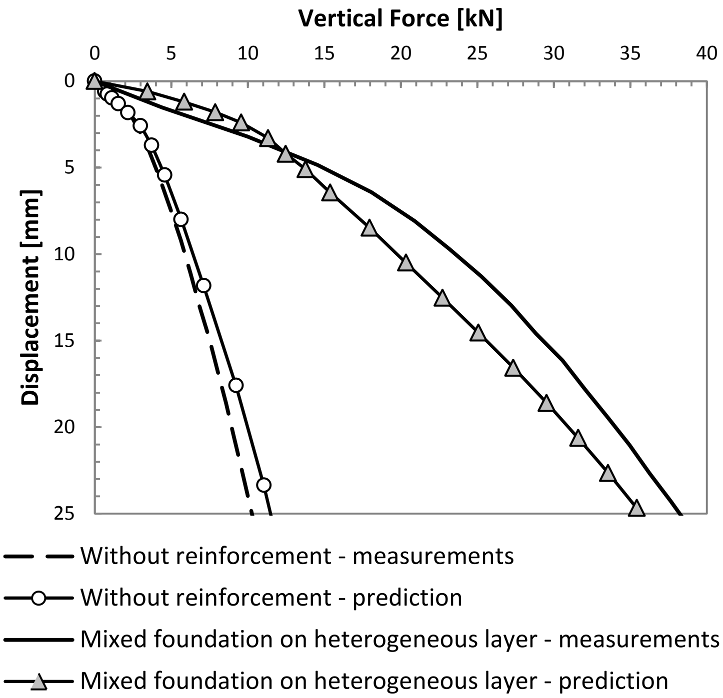

Figure 5.26 Comparison between numerical predictions and measurements for the mixed foundation situated on homogeneous and heterogeneous layer

5.4.2.2.2. *Distribution of force*

The distribution of vertical force under the shallow foundation reinforced by group of four SM columns is presented in Figure 5.27. Results correspond to observed behaviour, however due to small overestimation of force taken by soil and underestimation of the load sustained by one column, discrepancies appear. As it is pointed out in previous case, imprecise prediction of the behaviour of one column in a group results in multiplication of the inaccuracy. In case of analysis of the footing on heterogeneous layer, underestimation has place. At the beginning of the loading test, curves illustrating observed and calculated behaviour are alike. Situation changes at about 3 mm imposed displacement, where increase of the predicted force becomes slower. Underestimation rises till about 10 mm and then starts very slowly decreasing to achieve about 0.8 kN difference for 25 mm. Due to discrepancies, predicted force taken by four columns is underestimated starting from about 3 mm displacement. The same trend of increase and then decrease of the underestimation, as for one column, can be observed. However, in this case underestimation accomplishes, at its maximum, about 4.8 kN.

In contrast to column, behaviour of the soil is overestimated during the whole loading. The highest over prediction can be observed at the beginning of the test. In the test with homogeneous soil, this kind of situation has not had place. Force taken by the soil has been under predicted. What is more, beginnings of curves have been alike. Adding denser layer at the bottom of the tank till depth 0.43 m has significant impact on columns but should not influence behaviour of soil directly under the foundation. Concerning this two observations and results acquired for case consisting of heterogeneous soil layer, it is necessary to compare not only numerical but also experimental results of the loading test. Gathered results can be found in Figure 5.28. As it was expected, numerical results confronted with each other present good agreement. Small difference, maximum 0.7 kN appears at the end of the test. However, experimental results are less coherent. In case of test with heterogeneous soil, the behaviour of soil presents almost linear answer to the imposed displacement. Shape of the curve illustrating soil's behaviour in the second case, is more likely. The discrepancies between measured behaviours might be cause by experiment's imperfections such as incomplete adherence between the shallow foundation and soil at the beginning of the test.

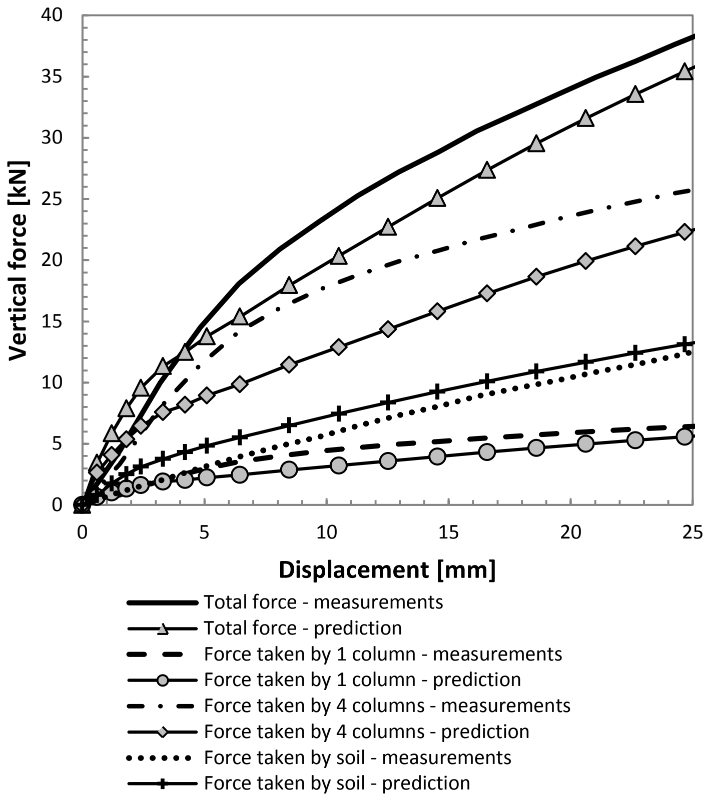

Figure 5.27 The distribution of vertical force predicted by model with heterogeneous soil layer

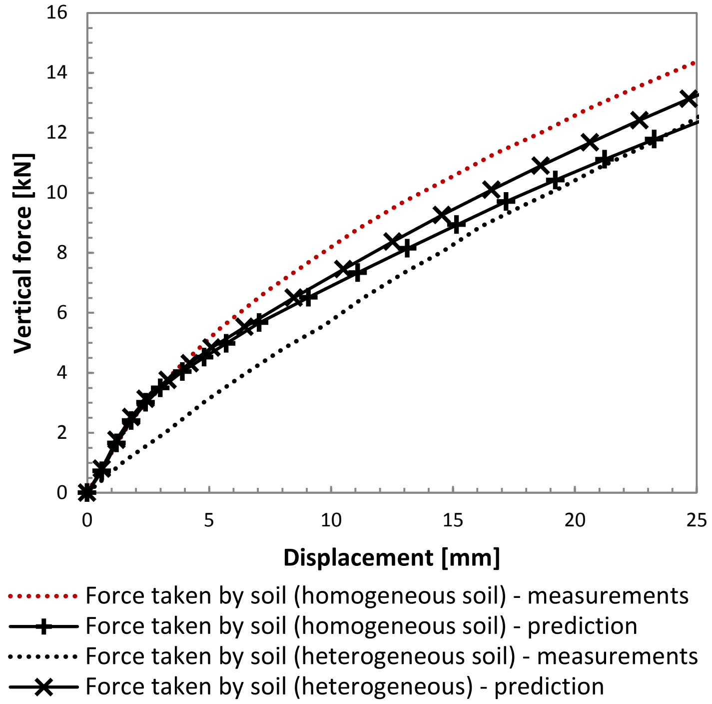

Figure 5.28 The vertical force taken by soil predicted by models with homogeneous and heterogeneous soil layers

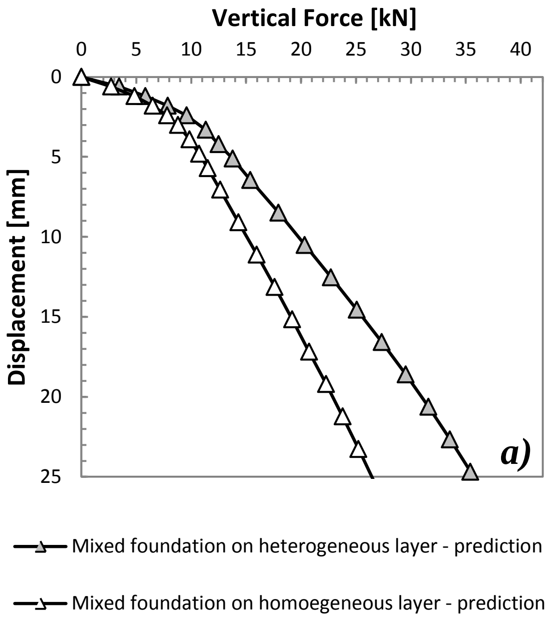

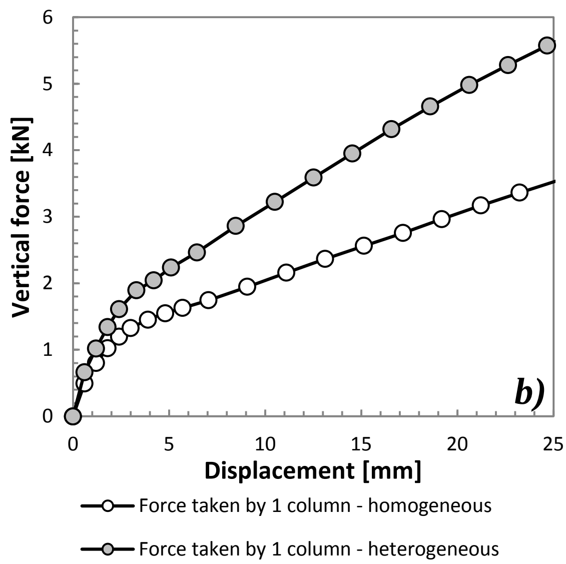

Figure 5.29 Comparison between numerical predictions of mixed foundation situated on homogeneous and heterogeneous layer, a) total force, b) force taken by one column in a group of four

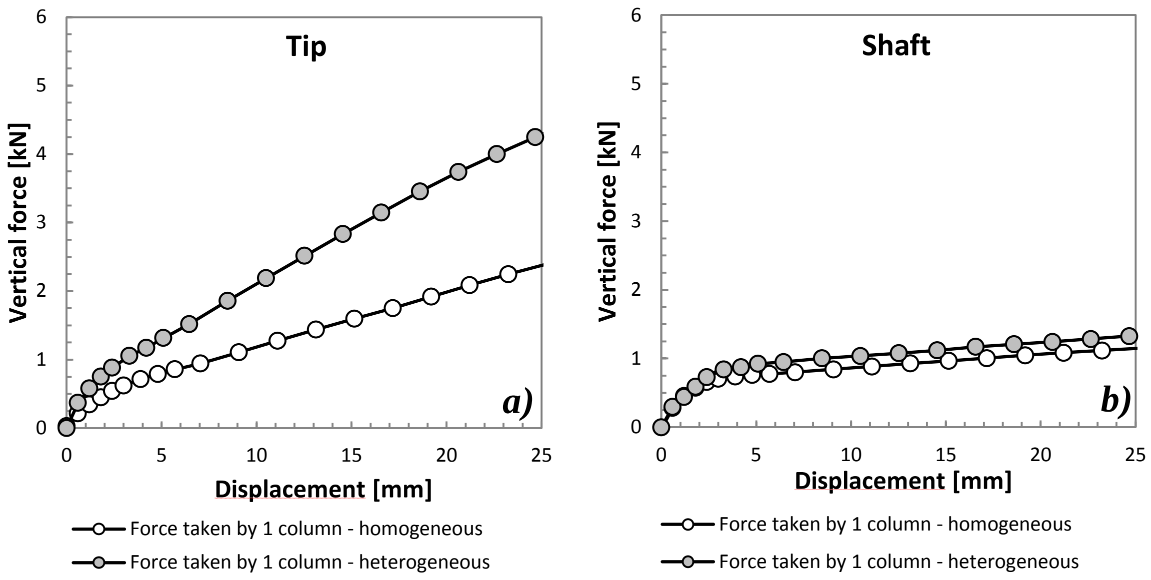

Figure 5.30 Numerical prediction of a)tip and b) shaft capacity of one column in a group of four

5.4.2.2.3. *Mixed foundation on homogeneous and heterogeneous layers*

In order to investigate the influence of the stiffer layer of sand, placed at the bottom of the tank, results of tests performed with two configurations of soil under the mixed foundation have been compared. Predicted behaviours are presented in Figure 5.29a. As it has been expected, higher force has been acquired for foundation with two soil layers beneath. After 25 mm displacement, foundation placed on two layers is capable to sustain 35.7 kN, whereas one placed on homogeneous layer, 26.4 kN. Load taken by the soil under the plate is comparable in both cases (Figure 5.28). Hence, foundation's ability to sustain higher force comes from significantly higher value of force borne by reinforcement. Figure 5.30 presents tip and shaft capacities of one column in the group of four. It can be seen that by embedding last 0.03 m of each column inside denser soil, total bearing capacity has been raised by 2.1 kN after 25 mm displacement (Figure 5.29b). The increase of force is caused by significant increase of the column's tip capacity (Figure 5.30a), whereas shaft capacity (Figure 5.30b) stays almost the same (0.16 kN difference after 25 mm displacement). Due to denser layer at the bottom of the tank, whole reinforcement, is able to bear 8.4 kN more that in case of homogeneous soil. However, difference is not a constant value. The more foundation is displaced, the bigger difference between cases appears.

5.4.2.2.4. *Conclusions*

The static loading test of the mixed foundation placed on the heterogeneous layer of Hostun sand has been presented. In spite of some discrepancies, obtained results show relatively good agreement with the experimental observations. Nearly tripled value of vertical force observed for unsupported foundation, after 25 mm of displacement have been reported.

Discrepancies appearing during the loading test can be explained as previously by the definition of column-soil interaction. Even though, introduced second, lower, layer of sand results in significantly higher foundation's performance by improving bearing capacity of the reinforcing columns, it also brings some uncertainties. In finite element modelling, last 0.03 m of each columns has been assumed as embedded in the denser soil. Nevertheless, concerning the inaccuracies that may arise during columns installation in laboratory conditions, the distance between columns' tips and top of the 'dense' layer might varied from the assumed one.

The idealized contact between foundation and soil reinforced by four columns, could also have influence on results of the modelling. The importance of this adhesion manifests in predicted force taken by the soil. Perfect contact during the whole loading test, in the case of numerical modelling, is provided by an imposed displacement, however in case of experimental study, its execution is much more difficult.

Another source of discrepancies, as in case of homogeneous layer, is the assumption, that force taken by four columns is approximated by value calculated for just one element and multiplied by four. Thus, underestimation of force borne by one column, propagates and multiplies under prediction of the force sustained by whole reinforcement. As explained before, assumption is more likely to be accomplished in numerical calculations.

5.4.3. Summary

Four loading tests of the 'big' shallow foundation has been analysed: without reinforcement, reinforced by a single column and two tests consisting in footing and group of four 7 days old SM columns. In this paragraph all results, presented above, are gathered and compared with each other. The influence of the reinforcement on the behaviour of the footing is presented and investigated. Importance of number of SM columns and homogeneity of soil are pointed out. Analysis is carried out in terms of total force, and force taken by column.

5.4.3.1. Total force

The total force, obtained from all tested configuration of 'big' foundation, as a function of imposed displacement, is presented in Figure 5.31. Reinforcement executed by single column rises foundation's capacity, however, at the end of the test (25 mm), improvement is just about 20%. Installation of four SM columns effects with about 128% higher value of force for the same displacement. Adding stiff layer at the bottom of the tank brings about 208% better results than in case of unsupported foundation. Detailed values of force and percentage of improvements can be found in Table 5.4. As it has been mentioned above, 25 mm displacement is the recommended maximal displacement for the shallow foundation (European Committee for Standardisation, 1995). However, recommendation takes into consideration full scale footings. Therefore, the 25 mm is significantly too high when testing a small scale one. It represents about 7% of 0.35 m x 0.35 m x 0.01 m (length x width x height) foundation edge, so it is relatively big displacement for such a small plate. Hence, analysis of the improvement for lower displacement seems to be more accurate. 5 mm displacement, which correspond to half of the height of the foundation, has been chosen. In this case improvement brought by the reinforcement equals to about 30%, 148% and 210%, for single column, four columns in homogeneous layer and four columns is heterogeneous soil layer. Detailed values are presented in Table 5.5.

Table 5.4 Total force borne by the foundation tested in different configurations of reinforcement after 25 mm displacement

Test	Total force		Force taken by one column		Force taken by four columns	
	[kN]	Improvement [%]	[kN]	Improvement [%]	[kN]	Improvement [%]
Without	11.6	0	-	-	-	-
Single column	13.9	20	3.7	0	3.7	0
Four columns homogeneous layer	26.4	128	3.5	-5	14.0	279
Four columns heterogeneous layer	35.7	208	5.6	51	22.4	506

Table 5.5 Total force borne by the foundation tested in different configurations of reinforcement after 5 mm displacement

Test	Total force		Force taken by one column		Force taken by four columns	
	[kN]	Improvement [%]	[kN]	Improvement [%]	[kN]	Improvement [%]
Without	4.40	0	-	-	-	-
Single column	5.50	25	1.37	0	1.37	0
Four columns homogeneous layer	10.90	148	1.56	14	6.24	355
Four columns heterogeneous layer	13.60	210	2.18	59	8.72	536

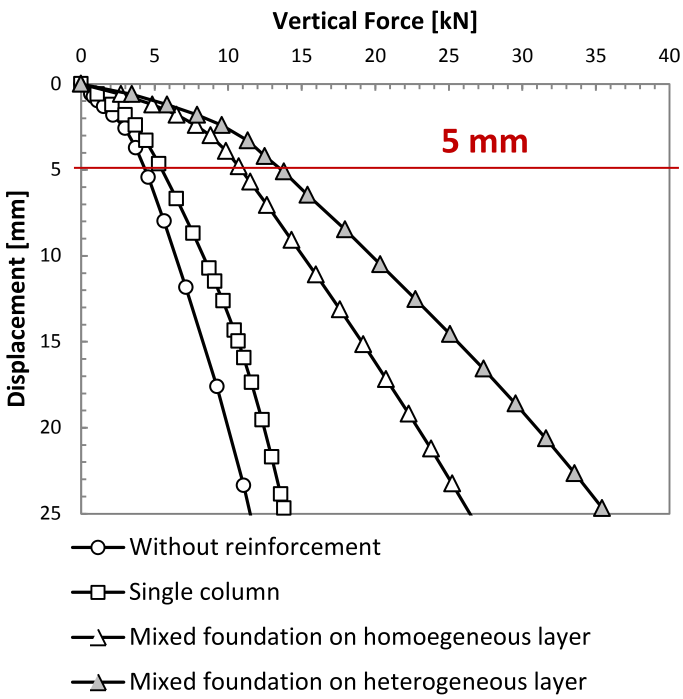

Figure 5.31 Comparison between results of numerical calculations performed for 'big' foundation without reinforcement, reinforced by single column and mixed foundations situated on homogeneous and heterogeneous layers

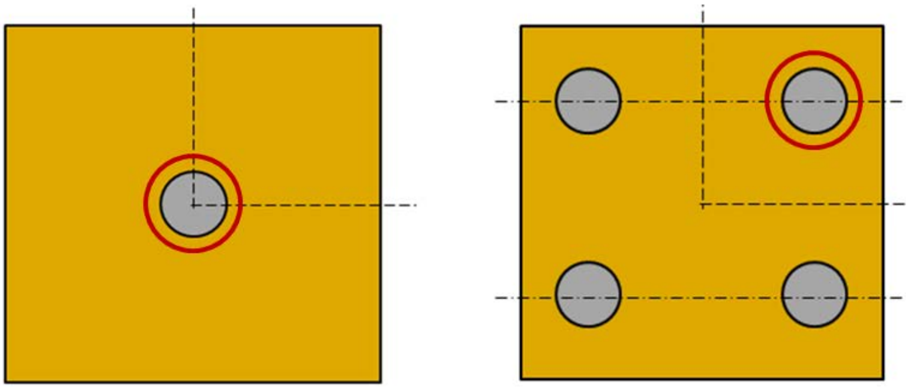

Figure 5.32 Mixed foundation consisting in 'big' footing and a) single column, b) group of four columns

5.4.3.2. Force taken by columns

In terms of force taken by one column (Figure 5.32), three test has been analysed: foundation reinforced by single column and two foundations supported by four SM elements. Vertical force borne by one column as a function of displacement of the foundation is presented in Figure 5.33. The highest load is taken by one column embedded in layer of 'dense' sand. The single column and one column in homogeneous soil behave alike. Insignificant differences appear, however their maximum value does not pass 0.2 kN. Similarly to total force, the load distributed on one SM element can be analysed in details for two different displacements: end of the test – 25 mm and 5 mm (Table 5.4 and Table 5.5). For smaller displacement, force calculated for one layer is 14% higher than the one for single column, whereas improvement in regard of single column in case with two layers equals to about 59%. Comparable improvement has been predicted for heterogeneous soil at the end of the test, about 51%. Unfortunately, in the case of a uniform sand, the enhancement is different than for the 25 mm. Specifically saying, the predicted force is 5% lower than the one, calculated for single column.

The behaviour of the four column acquired from both mixed foundations is compared with the contribution of single column in Figure 5.34. Installation four columns instead of single one, improved force taken by whole reinforcement by 279% and 506% at the end of the test, for model with one and two layers respectively. Enhancement for 5 mm is predicted as about 355% and 536% for homogeneous and heterogeneous soils.

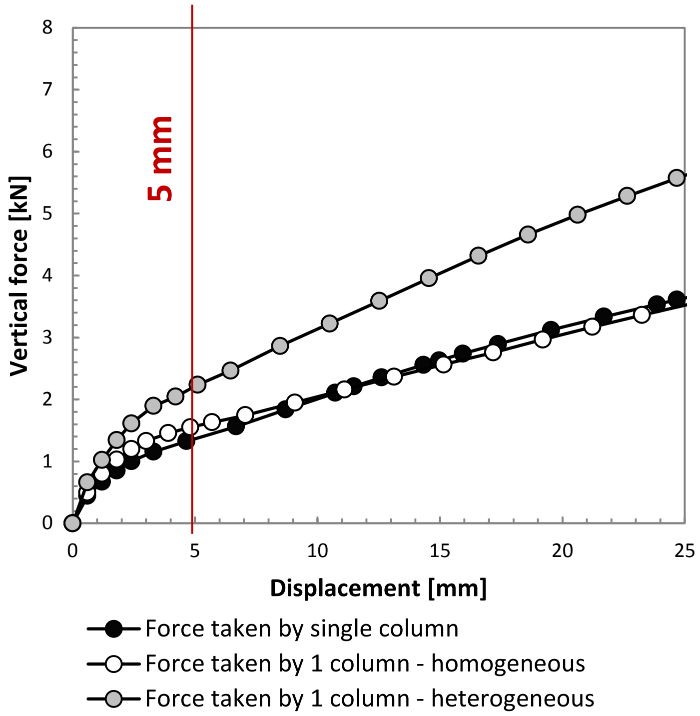

Figure 5.33 The vertical force taken by single column and one column obtained from models with homogeneous and heterogeneous soil layers

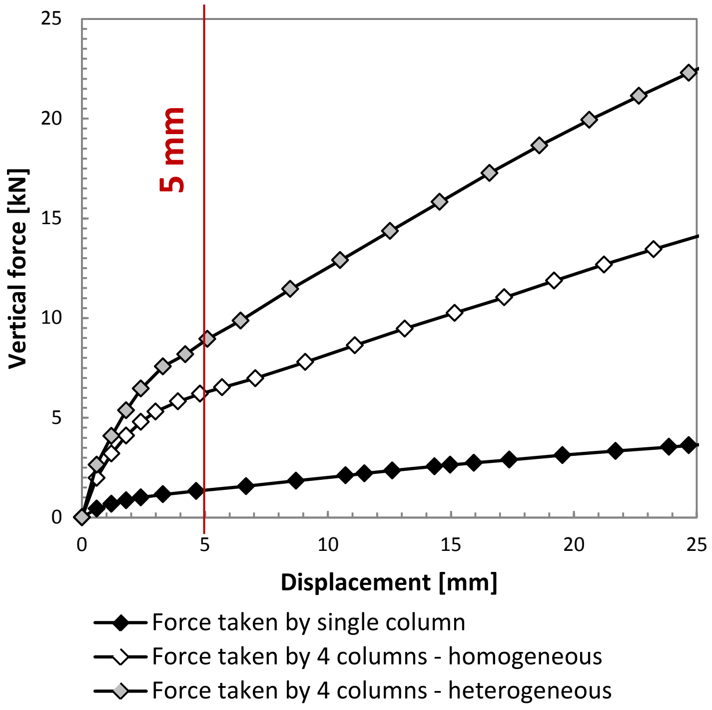

Figure 5.34 The vertical force taken by whole reinforcement: single column and four columns obtained from models with homogeneous and heterogeneous soil layers

5.5. Conclusions

Possibility of using the Soil Mixing method in almost all types of soils with minimum environmental impact makes it highly competitive among all developed techniques of soil reinforcement. Due to that, study presented in this chapter based on the concept of using the Soil Mixing (SM) column as a support of shallow foundations. Findings provided by detailed investigation of the behaviour of the SM column, working as a single element (Chapter 4), brought necessary knowledge to analyse the supported footing. The numerical finite element simulation, carried out with ABAQUS code, allowed one to identify an influence of the SM method on the bearing capacity of the reinforced foundation. Proper calibration of constitutive models of analysed materials (Hostun sand with two densities and 7 and 14 days old SM columns) was confirmed by the successful results of the modelling. Due to the advanced constitutive model of soil, more than elastic properties and constant shear parameters of the material were taken into consideration. Numerical predictions agree well with experimental results in all, ten, studied cases. The positive effect of using the SM method as reinforcement of a shallow foundation was clearly highlighted. The experimentally and numerically investigated cases proved that, the value of the load borne by the foundation increases significantly, while its displacement is substantially reduced.

The finite element axisymmetric analyses were performed in order to study behaviour of the ‘small’, 0.20 m x 0.25 m, shallow foundation. Due to type of calculations, rectangular footing was replaced by a circular one with equivalent diameter. Foundation was tested on ‘loose’ (ρ = 1380 kg/m^3) and ‘dense’ (ρ = 1500 kg/m^3) sands. Improvement brought by installation of a centrally situated column was shown by comparison with behaviour of unreinforced footing. Simulated static loading tests let us investigate the influence of the SM element’s age. Distributions of vertical force and vertical stress were analysed in order to better understand behaviour of each part of the mixed foundation (footing and reinforcement).

As it was observed in case of loading test of single SM column, the age of material affects its bearing capacity. Namely, the older column is, the higher force it can sustain. The same tendency was observed in case of reinforced foundation. The increase of force was more spectacular in case of ‘dense’ sand, however in case of ‘loose’ one, influence was also manifested.

The density of soil is a crucial parameter affecting the bearing capacity of the foundation. Better soil compaction results in higher modulus of deformation and shear parameters. Therefore, higher density leads to noticeably higher bearing capacity of the foundation. It was found that unsupported footing tested on homogeneous layer of ‘dense’ sand was able to sustain comparable force as the one reinforced by 7 days old built on ‘loose’ soil.

Despite significant differences between forces and stresses borne by foundations tested on soil with different densities, almost the same contributions of soil in sustaining total force were found. It can be concluded that for foundation supported by centrally situated SM column, force taken by reinforcing element is about 40% and 45% for younger and older columns respectively. Contribution of soil in total force borne by the mixed foundation is about 60% and 55% of the total force for 7 and 14 days old column.

The behaviour of bigger, 0.35 m x 0.35 m, foundation without support was modelled. Afterwards, two configurations of reinforcement was studied. Firstly, reinforcement executed by a single SM element. Then, configuration with a group of four columns was tested. It was found that force taken by one column is comparable whether it works as a single one or as an element in a group. However, this hypothesis needs further verifications. Additional cases in which the foundation is reinforced by a larger number of columns should be considered. Also other distances between columns should be analysed. As it was expected, efficiency of the improvement provided by single column under the bigger foundation was lower than in case of smaller footing. This can be explained by the cross section of the reinforcement and the surface of the foundation being in direct contact with soil. In case of ‘small’ footing, single column represents about 8% of the surface, however in case of ‘big’ one just 3%. Even though, force taken by the column, in terms of value, was reported as the same in both cases, its contribution in the total force was significantly lower, about 41% and 24% for smaller and bigger footings respectively.

The behaviour of mixed foundation, consisting of ‘big’ footing and group of four, 7 days old, SM columns was investigated. Two loading tests were performed. The first test consisted in loading of mixed foundation installed in homogeneous layer of ‘loose’ sand. In the second one, mixed foundation was installed in heterogeneous layer of soil (‘dense’ sand at the bottom and ‘loose’ and in the upper part of the tank). The aim of these two analyses was to detect the influence of a stiffer layer under tips of the reinforcing elements, on the behaviour of the foundation. In the experimental work, tips and about 0.03 m of the columns were embedded inside stiffer sand, in order to ensure proper contact between columns and ‘dense’ layer. The results for both mixed foundations in terms of: the total vertical force and force taken by reinforcement were compared with footing without support and footing reinforced by single column. Shallow foundations' behaviour was discussed in detail for two displacements: 25 mm, which corresponds to recommended limit of displacement for isolated shallow foundation, and 5 mm. Although the analysed mixed foundation consisted of footing, it should be emphasised that this recommendation applies to full scale foundations. Hence, 25 mm displacement is greatly overstated for the small scale footing. The 5 mm was chose because it represents half of the foundations height.

Denser layer of sand, introduced under the reinforcement’s tip brought expected improvement, due to increased bearing capacity of each column. Effectiveness of the reinforcement was observed almost constant regardless the stage of loading, 210% and 208% after 5 mm and 25 mm respectively. Whereas, footing tested on homogeneous layer resulted in much lower improvement, 148% and 128%. To compare, improvement brought by reinforcement executed by single column equalled to about 20-25%.

Summing up, the Soil Mixing method is a very efficient way of reinforcing shallow foundations. Reinforcement executed by single or four columns effects with significant increase of footing’s bearing capacity and reduction of its displacement. Nevertheless, reinforcement of a shallow foundation carried out by single SM element is very unlikely. A group of columns is more reasonable solution. Moreover, it helps to reduce possible rotation of the foundation, which can be caused by imperfections related to non axial installation of the single column.

Both, numerical and experimental, results represent behaviour of a shallow foundation. Nevertheless, due to scale of the model, it is important to remember, that they should be consider as qualitative, not quantitative. Small scale tests capture mechanisms guiding the behaviour of the reinforced foundation, however their results cannot be directly used in calculations of the full scale footings. In order to use them in design, it is necessary to verify them by full scale tests. Moreover foundation was simulated as perfectly rigid element (replaced by imposed displacement) in order to properly simulate rigid steel plate used in experimental study, however steel plate does not represent well characteristics of a real foundation. Nevertheless, it was necessary to include this assumptions in the numerical model. Future study should investigate behaviour of deformable footing in order to capture its deflection and possible perforation by reinforcing elements.

Concerning numerical simulations, it was presented that constitutive laws used to described all materials were calibrated properly. Parameters of the criterion, that sand with both densities obeys, has been adjusted in agreement with results of laboratory tests and by parametric studies (loading tests of: a single column, a group of columns, a small foundation with and without reinforcement). The author claims that the more advanced models, like the one with the Modified Drucker-Prager with cap criterion, need to be used to correctly describe the behaviour of the soil. The constitutive laws recommended by the author are ones which take into account not only shear failure of the soil, but also compaction/dilation, which is properly described by a cap and its evolution (hardening/softening). Therefore, when it is possible to accomplish laboratory tests on analysed soil, more advanced constitutive models should be used.

Numerical predictions well reproduced observed behaviour of the reinforced footings. Nonetheless, some differences appeared. They might be due to idealized contacts between the foundation and soil. In numerical analyses foundation was modelled by imposed displacement. Also contact between the SM column and soil, with constant value of the interface friction coefficient μ_f, may be a source of discrepancies. In case of axisymmetric calculations, differences can be caused also by different than in experimental test shape of the foundation. Moreover, numerically modelled conditions are perfect in terms of homogeneity of material and repeatability of the geometry. Even though, each experimental test was repeated minimum 3 times and then the average values was considered as representative, this kind of precision is impossible in any, even laboratory conditions. In case of cases calculated with three dimensional type of model, discrepancies can be caused by way of calibration of constitutive laws. As explained above, adjustment was accomplished mainly by axisymmetric parametric studies.

Improvement of the future numerical simulations, might be done by considering other constitutive law for the Soil Mixing columns. The Mohr-Coulomb criterion allows preliminarily estimate behaviour of the column, however in order to model the proper brittle mode of failure and their post failure behaviour, other kind of constitutive model needs to be used. The recommended models are laws used to describe behaviour of concrete, for instance damage plasticity model.

6. Deep foundation reinforced by the Soil Mixing

6.1. Introduction

Two types of foundations can be distinguished: shallow and deep. The shallow foundations (Chapter 5) are used in case of small structures, which carry relatively lower loads, and hence the loads are dissipated into the soil mass not far from the foundation. However when we are considering large structures, which carry significant loads other solutions needs to be applied. In this case, loads are dissipated at greater depths. One guideline of differentiating between the shallow and deep foundations is that in case of the deep foundations the depth of foundation is more than the dimension of the structure (usually the width is considered as the dimension).

In the first part of this chapter, the pile type of foundation and few examples of the use of piles are presented.

In the second part of the chapter methods of theoretical estimation the bearing capacity of the single and group of piles are given.

In the third, main part of the chapter, numerical analysis of concrete pile with and without reinforcement are presented. Reinforcement is executed by group of SM columns. The parametric study illustrates the influence of: configuration of reinforcing columns, vertical distance between the pile's tip and columns' heads, length of columns, columns' diameter and horizontal distance between pile and columns on force borne by the pile.

Eventually in the last part, the efficiency of the reinforcement is discussed.

6.2. Pile foundation

One of the most commonly used type of deep foundations are piles. They are vertical or slightly inclined, relatively slender structures. Piles have many different applications and are chosen as the type of foundation for a variety of reasons, such as (after (Fellenius, 1991)):

- a competent soil layer can only be found at depth;
- the soil layers immediately below the structure, while competent are subject to scour;
- the structure transmits large concentrated loads to the soil that cannot be spread out horizontally by means of a wide, shallow foundation;

- the structure is very sensitive to differential settlement;
- the site has a very high water table and the soil is sensitive to the construction of even shallow excavations required for mat or footing foundations.

In some cases, the piles serve only to improve the bearing capacity, density, or stiffness of the surrounding soil without directly carrying the load of the structure. Some of examples of the use of piles are presented in Figure 6.1.

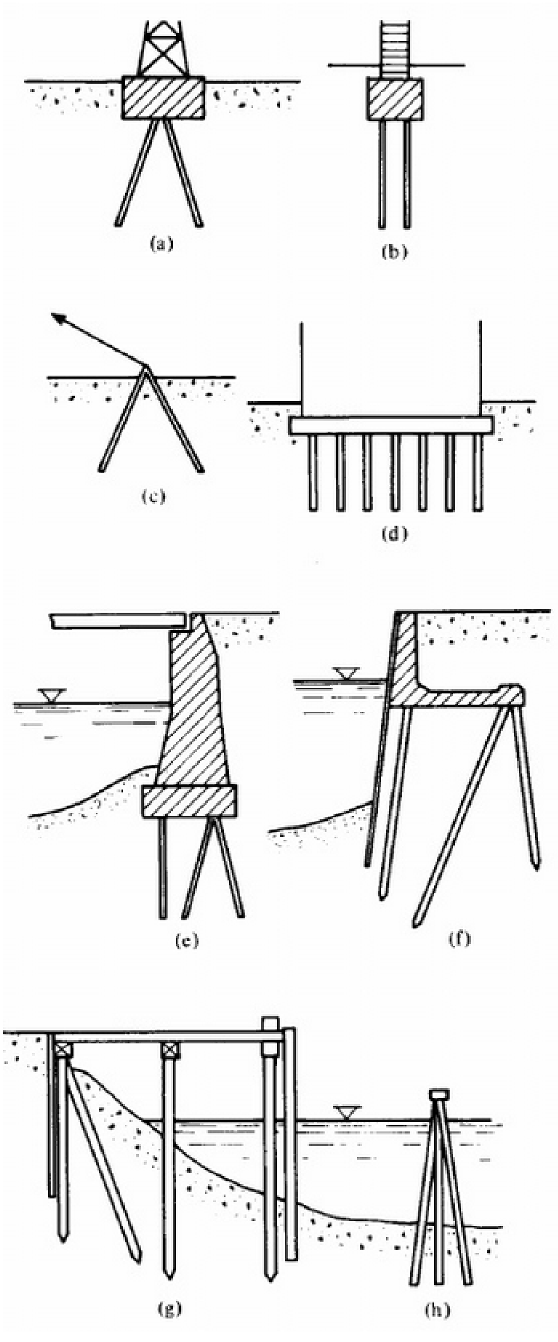

Figure 6.1 Examples of the use of piles (Fellenius, 1991)

Piles can be categorized in many ways, according to different parameters. They can be classified according to the material: wood, concrete, steel or composite pile (any combination thereof). Examples of applications of all kinds of piles are presented in Figure 7.2. Wooden piles are relatively inexpensive construction material and its durability against rotting can be improved using preservatives and advanced techniques. However, the main drawback of this kind of piles is limited structural capacity and their length.

The steel piles offer excessive strength in both compression and tension. In addition, they are highly resistant to structural damages during driving and can suite any desired length. That is why they are good solution in case of heavy structures such as tall buildings situated in soft soils underlain by dense sands or bedrock. The main disadvantages of this kind of piles are: susceptibility to corrosion in marine environment and relatively high cost.

The most commonly used type of piles are concrete ones. They are usually made with steel reinforcement in order to obtain higher tensile strength. Concrete piles are chosen due to their high resistance, flexibility in shape and length and reasonable cost. The two most common types of concrete piles are: precast and cast-in-place. This kind of piles can be selected for foundation construction under the following circumstances (after (Gunaratne, 2006)):

- the need to support heavy loads in maritime's areas;
- existence of stronger soil layer located at relatively shallow depths;
- design of bridge piers and caissons that require large diameter piles;
- design of large pile groups to support heavy extensive structures;
- the need for mini piles to support residential buildings on weak and compressible soils.

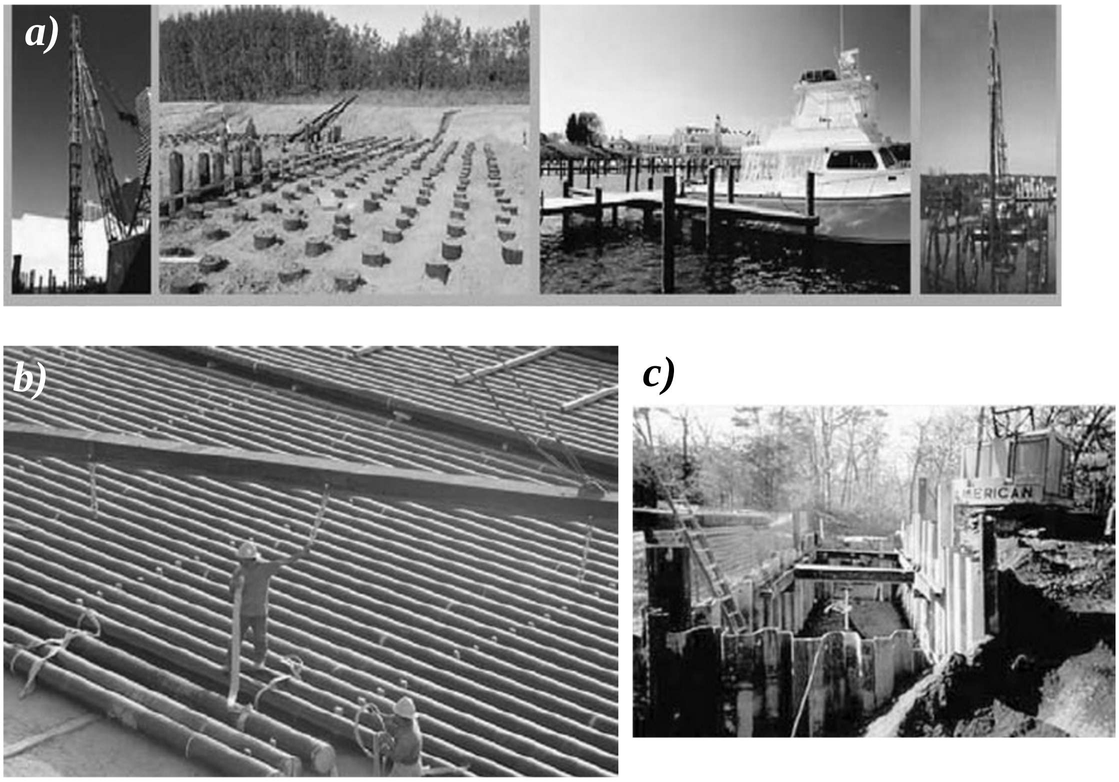

Figure 6.2 a) group of wooden piles in construction, b) production of precast concrete piles, c) steel sheat piles in a cofferdam application (Gunaratne, 2006)

Piles can be classified according to their cross section. They can be circular, octagonal, hexagonal, H-shaped, solid or hollow.

The way of installation is also a method of categorizing. Pile can be installed by means of driving or be bored (made *in situ*) or be installed by combination of driving and *in situ* methods. After Helwany (Helwany, 2007), we can distinguish three types of piles:

- full-displacement piles – driven piles with solid section tend to displace a large amount of soil due to the driving process;
- partial-displacement piles – hollow piles such as open-ended pipe piles tend to displace a minimal amount of soil during driving process;
- no displacement piles – bored piles which do not cause any soil displacement.

Pile driving is achieved by: impact dynamic forces from hydraulic and diesel hammers, vibration or jacking. The method of installation may have a profound effects on its behaviour under load. It may also determine the severity of effect on nearby structures, including undesirable movements, vibrations or even damage of a structure.

6.3. Bearing capacity of a pile

The bearing capacity (called also the ultimate resistance or ultimate load) of a pile consists of a combination of shaft and tip capacities. The pile load caring ability depends on various factors, including:

- pile characteristics such as: pile length, cross section and shape;
- soil configuration and short and long term soil properties;
- pile installation method.

To determining the resistance of a pile, the complex stress–strain history, which includes; the initial in situ condition, pile installation, equilibration and loading should be taken into consideration. All steps, for full-displacement pile are explained in Figure 6.3.

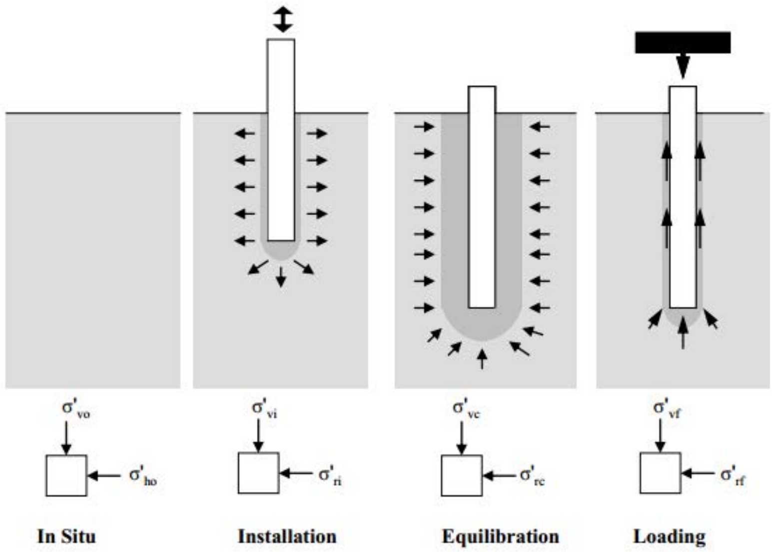

Figure 6.3 Changes in pile stress regime over time in case of full-displacement pile (Doherty & Gavin, 2011)

Piles can be used as single (large diameter piles) elements, but mostly, they are working in groups. The behaviour of a single pile is different from that of an individual pile in group. A pile group can consist of cluster of piles, where the group effect is governing in all directions of load and movement or consist of a row of piles where the pile behaviour is governed by the group effect in one direction, while in the orthogonal direction the piles are independent of the group and behave as a single ones.

In this section two widely used methods for pile design: the α and β methods for single pile and group of piles are presented.

6.3.1. Single pile

6.3.1.1. α-method

The α-method is used to calculate the load capacity of pile in cohesive soils. This method is based on the undrained shear strength of cohesive soils. Thus, it is well suited for short-term pile load capacity calculations. The ultimate loading capacity of a pile is the sum of its shaft and tip capacities.

6.3.1.1.1. *Shaft capacity*

The interface shear stress, f_s, between the pile surface and the surrounding soil determines the value of shaft capacity, Q_s. In this method the interface shear stress is assumed to be proportional to the undrained shear strength, c_u, of the cohesive soil as defined in Equation

6.1. The value of α can be obtained from one of several semi empirical equations availed in literature (Budhu, 1999). The American Petroleum Institute (API, 1984) suggests that α should be expressed as a function of c_u (Equation 6.2).

Therefore, the shaft capacity can be calculated as presented in Equation 6.3. Equation is general and takes into consideration pile with variable diameter that is embedded in a multi-layered soil, where: n is the number of layers, S_i stands for pile's perimeter in i-layer of soil and h_i is the length of pile in i-layer.

$$f_s = \alpha c_u \tag{6.1}$$

$$\alpha = \begin{cases} 1 - \dfrac{c_u - 25}{90} & for\ 25\ kPa < c_u < 70\ kPa \\ 1.0 & for\ c_u \leq 25\ kPa \\ 0.5 & for\ c_u \geq 70\ kPa \end{cases} \tag{6.2}$$

$$Q_f = \sum_{i=1}^{i=n} [\alpha_i (c_u)_i * S_i * h_i] \tag{6.3}$$

6.3.1.1.2. *Tip capacity*

The bearing capacity of the base of the pile is called tip capacity. To determine the value, Terzaghi's bearing capacity equation (Terzaghi, 1943) can be used. Taking into consideration only its part for cohesive soils, the value can be calculated according to Equation 6.4, where $(c_u)_t$ is the undrained shear strength of the cohesive soil under the tip of the pile and N_c is the bearing capacity coefficient. Skempton (Skempton, 1951) suggested that for an undrained cohesive soil (ϕ_u = 0°), the basic Terzaghi equation should be used, but with values of N_c related to the shape and the depth of the foundation (Figure 6.4).

The load tip capacity can be defined by Equation 6.5, where A_t is the cross-section area of the tip of the pile.

$$f_t = (c_u)_t N_c \tag{6.4}$$

$$Q_t = f_t A_t = (c_u)_t N_c A_t \tag{6.5}$$

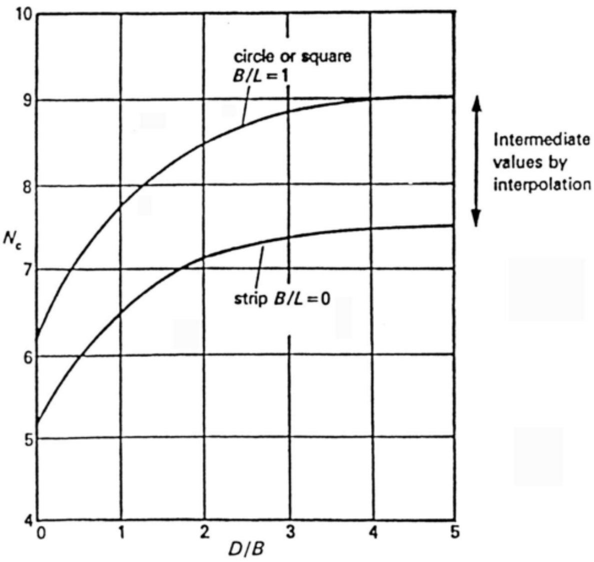

Figure 6.4 Value of bearing capacity coefficient N_c for cohesive soils proposed by Skempton (Skempton, 1951)

6.3.1.1.3. *Ultimate bearing capacity*

The ultimate bearing capacity of pile, Q_{ult}, is the sum of its shaft capacity and tip capacity, like presented in Equation 6.6.

$$Q_{ult} = Q_f + Q_t \tag{6.6}$$

6.3.1.2. β-method

The second method is the β-method, known also as Burland method (Burland, 1973). It can be used for both cohesive and cohesionless soils. The method is based on effective stress analysis and is suited for short- and long-term analyses of pile capacity. Similarly to presented above α-method, the ultimate bearing capacity of a pile is the sum of its shaft and tip capacities.

6.3.1.2.1. *Shaft capacity*

The shaft capacity in β-method is obtained from Equation 6.7, where σ'_v is the vertical effective stress at the pile midpoint and β is a coefficient expressed by Equation 6.8. K_0 is lateral earth pressure coefficient at rest defined previously by Equation 4.4. μ is a friction coefficient between the pile and soil. Value of β coefficient proposed by Burland (Burland, 1973) can be estimated from Equations 6.8 and 4.4 with μ equalled to a tangent of 2/3 of the layer friction angle (Equation 6.9).

$$f_s = \beta\sigma'_v \tag{6.7}$$

$$\beta = \mu K_0 \tag{6.8}$$

$$\mu = tan\frac{2}{3}\phi' \tag{6.9}$$

However, this value is more appropriate for studies of a pile in clays. For sands, McCelland (McClelland, 1974) proposed β = 0.15 – 0.35 for compression and β = 0.10 – 0.25 for tension (uplift piles). Meyerhoff (Meyerhoff, 1976) suggested value of β as a function of friction angle of soil and way of pile's installation. Hence, for bored piles β is 0.10, 0.20, 0.35 for ϕ' = 33°, 35°, 37°, respectively. In case of driven piles β equals to 0.44, 0.75, 1.20 for ϕ' = 28°, 35°, 37°, respectively. Fellenius (Fellenius, 1991) proposed value of β as a function of soil type and friction angle (Table 6.1).

Table 6.1 Ranges of β coefficients (Fellenius, 1991, p. 514)

Soil type	ϕ [°]	β [-]
Clay	25 – 30	0.23 – 0.40
Silt	28 – 34	0.27 – 0.50
Sand	32 – 40	0.30 – 0.80
Gravel	35 – 45	0.35 – 0.80

The shaft friction force, Q_f, between pile surface and soil can be calculated according to Equation 6.10 (general equation for a pile with a variable diameter that is embedded in n layers of soil). As in case of α-method, S_i stands for pile's perimeter in i-layer of soil and h_i is the length of pile in i-layer.

$$Q_f = \sum_{i=1}^{i=n}[\beta_i(\sigma'_v)_i * S_i * h_i] \tag{6.10}$$

6.3.1.2.2. *Tip capacity*

A modified version of Terzaghi bearing capacity equation is used in β-method. Hence, the bearing capacity of the tip of the pile can be calculated according to Equation 6.11, where

$(\sigma'_v)_t$ is the vertical effective stress at the tip of the pile, c'_t is the cohesion of the soil under the tip and N_q and N_c are bearing capacity coefficients. Janbu (Janbu, 1976) proposed equations (Equation 6.12 and 6.13) to estimate bearing capacity coefficients, where η is an angle defining the shape of the shear surface around the tip of a pile as shown in Figure 6.5. The angle varies from 60° (π/3) for soft clays to about 105° (0.58π) for dense sands soils.

$$f_t = (\sigma'_v)_t N_q + c'_t N_c \tag{6.11}$$

$$N_q = (\tan\phi' + \sqrt{1 + \tan^2\phi'})^2 e^{2\eta \tan\phi'} \tag{6.12}$$

$$N_c = (N_q - 1)\cot\phi' \tag{6.13}$$

The corresponding load capacity Q_t can be calculated according to Equation 6.14 where A_t is the cross-section area of the tip of the pile.

$$Q_t = f_t A_t = [(\sigma'_v)_t N_q + c'_t N_c] A_t \tag{6.14}$$

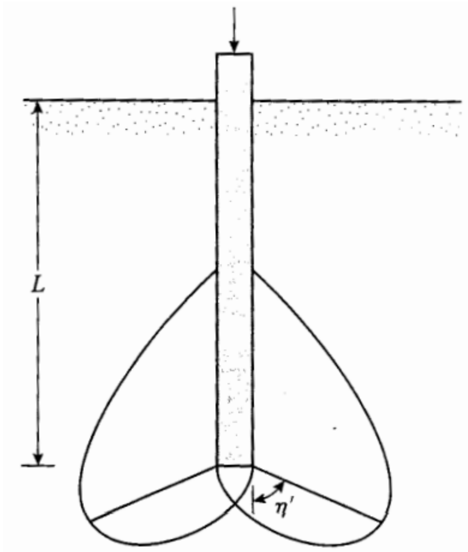

Figure 6.5 Shear surface around the tip of a pile: definition of the angle η (Janbu, 1976)

6.3.1.2.3. *Ultimate bearing capacity*

The ultimate bearing capacity of pile, Q_{ult}, predicted by the β-method, is the same as in case of a previous one, the sum of shaft capacity and tip capacity, like presented in Equation 6.6.

6.3.2. Group of piles

As mention above, structure is very rarely founded on a single pile. The group of piles that transmit the structural load through a pile cap, which is typically a reinforced concrete slab structurally connected to the pile heads to help the group act as a unit (Figure 6.6b). Piles are ordinarily closely spaced beneath structures; consequently, the behaviour of the entire pile group must be considered. The bearing capacity of a pile group is not necessarily the capacity of the individual pile multiplied by the number of piles in the group; the phenomenon by virtue of which this discrepancy occurs is known as group effect and is dependent on spacing between piles.

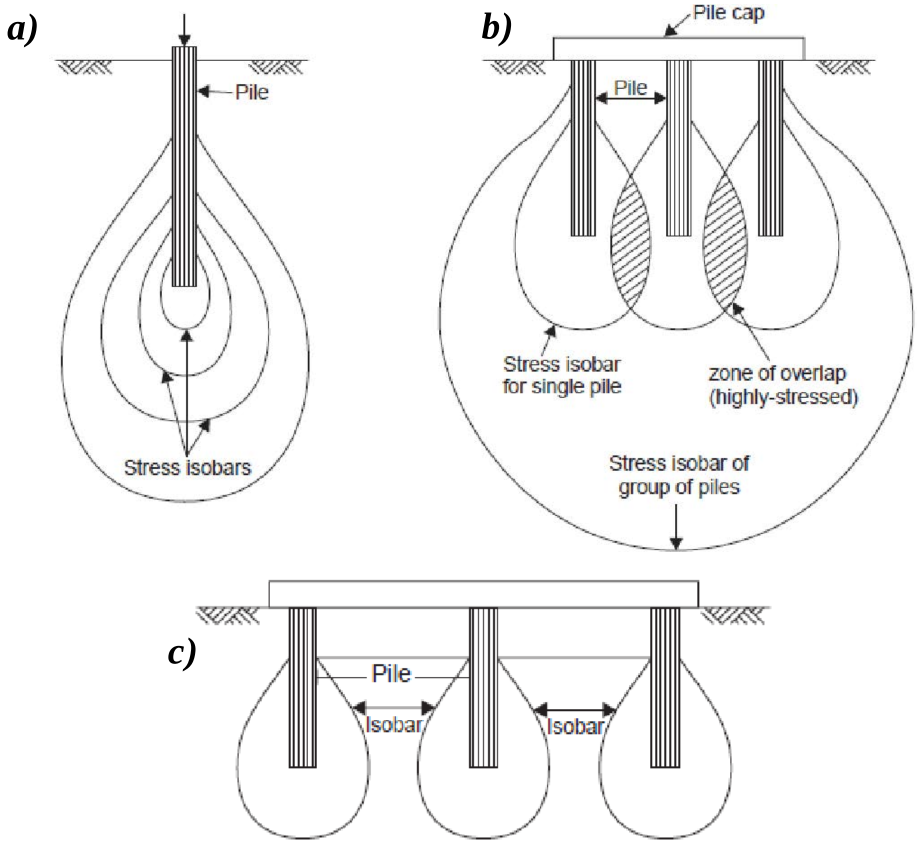

Figure 6.6 Stress isobars for: a) single, b) and c) group of piles (Gunaratne, 2006)

6.3.2.1. Spacing

The number of piles in a group, as well as the pattern and spacing between them is highly dependent on the type of the structure. Representative pile group patterns for wall and column loads are indicated in Figure 6.7. Piles for walls are commonly installed in a irregular, alternating arrangement on both sides of the centreline of the wall. For a column, at least three piles are used in a triangular pattern, even for small loads. When more than three piles are required in order to obtain adequate capacity, the arrangement of piles is symmetrical about the point or area of load application.

The spacing of piles in a group depends on the overlapping of the influence zones and desired efficiency of the pile group.

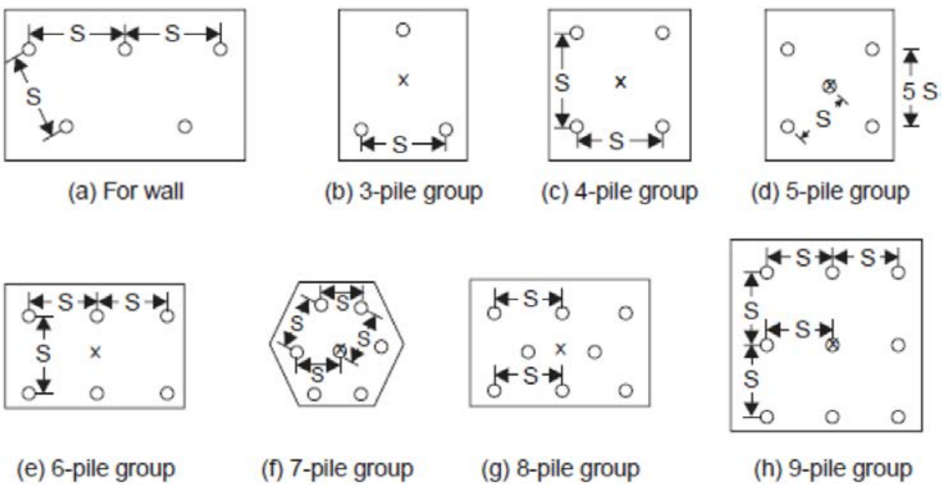

Figure 6.7 Examples of groups of piles patterns (Venkatramaiah, 2006)

The stress distribution caused by a single pile is presented in Figure 6.6a. When piles are working in a group, the influence zones of each can overlap each other there is a possibility of stress isobars of adjacent piles overlapping each other as shown in Figure 6.6b. Since the overlapping might cause failure either in shear or by excessive settlement, this possibility may be avoided by increasing the spacing (Figure 6.6c). Large spacing are not advantageous since a bigger size of pile cap would be needed.

In the case of driven piles the overlap of stresses is greater due to the displacement of soil. If piles are driven in loose sands, compaction takes place and hence, the spacing may be small. However, if piles are driven in saturated silt or clay, compaction does not take place but the piles may experience uplift. To avoid this, greater spacing may be adopted. Smaller spacings may be used for cast *in situ* piles in view of less disturbance.

Point-bearing piles may be more closely spaced than friction piles. The minimum spacing of piles is usually specified in official regulations. The spacing may vary from 2*D* to 6*D* for straight uniform cylindrical piles, where *D* stands for the diameter of the pile. For friction piles, the recommended minimum spacing is 3*D*. For point-bearing ones passing through relatively compressible strata, the minimum spacing is 2.5*D* when the piles install in compact sand or gravel and 3.5*D* when the piles is placed in stiff clay. The minimum spacing may be 2*D* for compaction piles.

6.3.2.2. Mode of failure and bearing capacity

The capacity of a pile group is not necessarily the capacity of the individual pile multiplied by the number of individual piles in the group. Disturbance of soil during the installation of the pile and overlap of stresses between the adjacent piles, may cause the group capacity to be less than the sum of the individual capacities.

The soil between individual piles may become 'locked in' due to densification from driving and the group may tend to behave as a unit or an equivalent single large pile. Densification and improvement of the soil surrounding the group can also occur. These factors tend to provide to the group a capacity greater than the sum of the capacities of individual piles.

The capacity of the equivalent large pile is analysed by determining the skin friction resistance around the embedded perimeter of the group and calculating the end-bearing resistance by assuming a tip area formed by this block, as presented in Figure 6.8.

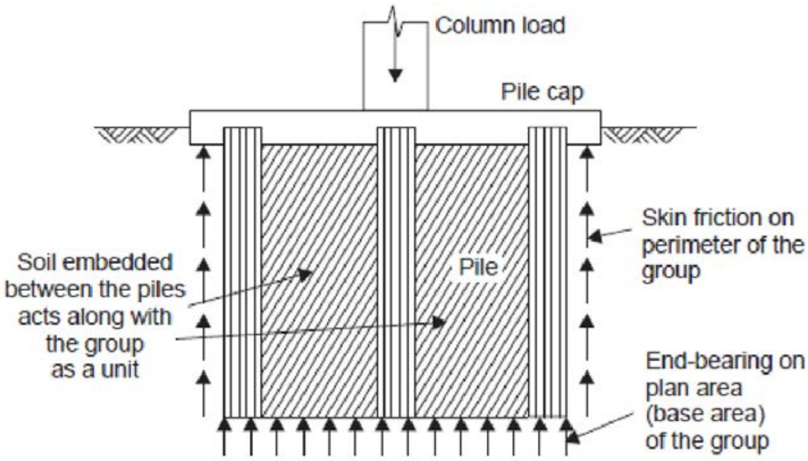

Figure 6.8 The equivalent large pile (Venkatramaiah, 2006)

The skin friction resistance of the single large equivalent pile (block) is obtained by multiplying the surface area of the group by the shear strength of the soil around the group. Its dimensions B_g x L_g x L are defined in Figure 6.9.

The tip bearing resistance is computed by using the general bearing capacity equation of Terzaghi. The bearing capacity factors for deep foundations are used when the length of the pile is at least ten times the width of the group; otherwise, the factors for shallow foundations are used. The capacity of the equivalent large pile is affected by soil type and properties, besides spacing of piles. There is a greater tendency for the group to act as a block or large single unit when the piles are close and the soil is firm or compact.

The ultimate capacity can be calculated using the α-method or the β-method, using Equations 6.15 and 6.16, respectively. Where, S_{ig} is the perimeter of the group of piles, S_{ig} = $2(B_g + L_g)$ and $(A_t)_g$ is the cross-sectional area of the group of piles, $(A_t)_g = B_g L_g$.

$$(Q_{ult})^{\alpha}_{block} = \left\{\sum_{i=1}^{i=n}\left[\alpha_i (c_u)_i * S_{ig} * h_i\right]\right\} + (c_u)_t N_c * (A_t)_g \qquad 6.15$$

$$(Q_{ult})^{\beta}_{block} = \left\{\sum_{i=1}^{i=n}\left[\beta_i (\sigma'_v)_i * S_{ig} * h_i\right]\right\} + \left[(\sigma'_v)_t N_q + c'_t N_c\right](A_t)_g \qquad 6.16$$

In case of the single pile failure mechanism, each single pile in the group fails individually, and the failure of all piles occurs simultaneously. Therefore, the pile group capacity, $(Q_{ult})_{npiles}$, is equal to n times Q_{ult}, where n is the number of piles in the group and Q_{ult} is the load capacity of a single pile. The Q_{ult} for a single pile can be calculated using the α-method or the β-method described above.

Because the mode of failure is not obvious, it is recommended to calculate bearing capacities for both possibilities and take into consideration during design the smaller of the two values.

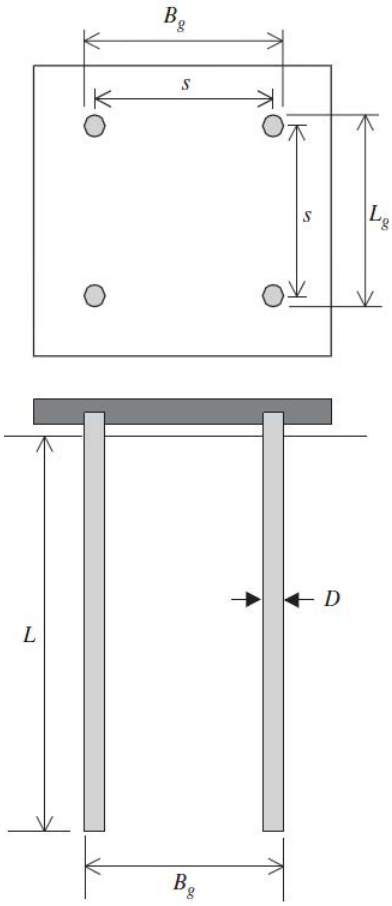

Figure 6.9 Group of piles (Helwany, 2007)

6.4. Numerical modelling

According to author's current knowledge, none experimental studies have been performed to investigate behaviour of deep foundation reinforced by SM technique. Moreover any *in situ* applications have not been reported. Due to lack of experimental data, analysis of reinforced by SM columns, deep foundation has been carried out on theoretical example.

In order to concentrate only on the influence of the reinforcement on the pile's performance, model has been reduced to single pile in homogeneous soil supported by group of SM columns. Properties of soil and column have been assumed as the one reported by Le Kouby, et al. (Le Kouby, et al., 2010). The improvement brought by SM column is analysed in terms of reduction of pile's vertical displacement. The parametric study illustrates the influence of: configuration of reinforcing columns, vertical distance between the pile's tip and columns' heads, length of columns, columns' diameter and horizontal distance between pile and columns on force borne by the pile.

6.4.1. Reinforcement of the deep foundation

Reinforcement of a deep foundation by the SM technique can be carried out in two ways: by installing columns around the foundation (P1) or under it (P2) (Figure 6.10). Columns situated under the foundation can be placed closely to the foundation's tip, in the same soil layer (P2a), or deeper, inside the soil characterized by considerably lower strength (P2b).

Installation of columns directly under the existing pile might lead to unwanted consequences, which can be sudden uncontrollable settlement or even collapse of the supported construction. Hence, installation of columns under the existing deep foundation is not recommended even though this kind of improvement effects with the highest efficiency. Solution proposed as P1 seems to be much safer. Improvement brought by the P1 and mix of P1 and P2a solutions have been a subject of this study and its results are presented and discussed below. The P2b case is analysed according to reference cases defined in RUFEX Project specification (RUFEX, 2010). Two reference projects (Chapter 7) consist in two existing foundations with higher than expected settlements. Due to that foundations have been qualified to be reinforced.

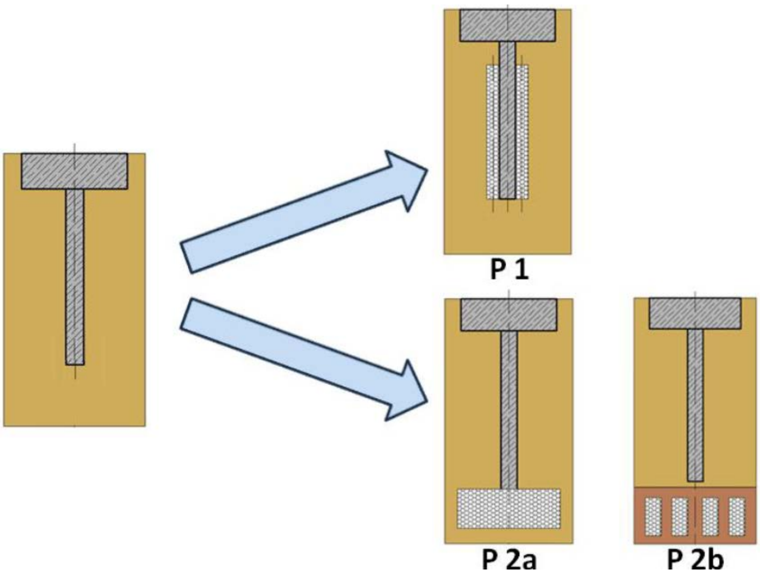

Figure 6.10 Location of columns reinforcing deep foundation

6.4.2. Pile without reinforcement

As mentioned above, lack of experimental results concerning reinforcement of deep foundation by SM technique, obliged author to reduce investigation to theoretical case. Single, concrete pile installed in homogeneous layer of silt have been analysed with a three dimensional finite element model in ABAQUS.

Properties of soil and SM column have been inspired by a paper published by Le Kouby, et al. (Le Kouby, et al., 2010). The paper deals with reinforcement of the railway lines, by the SM method and loading tests of SM elements. It presents results of three full scale loading tests of SM columns. Tested SM columns were installed in silt layer. Its properties can be found in Table 6.2. After installation and curing time, SM elements were tested by static loading test.

Table 6.2 Properties of the natural soil – silt (Le Kouby, et al., 2010)

Parameter	Unit	Silt North of France
Depth	[m]	1 – 4
Density	[kg/m^3]	1990 – 2140
Specific gravity	[-]	2.65
Water content	[%]	16.7 – 25.0
Liquid limit	[-]	27.1 – 39.0
Plasticity Index	[-]	3.0 – 12.5
Proctor limit density	[kg/m^3]	1490
Proctor limit water content	[%]	17.6
Undrained shear strength	[kPa]	296.58 – 325.26
Cohesion	[kPa]	3.00
Internal friction angle	[°]	32 – 35
Young’s modulus	[MPa]	23 – 45

Study, presented in the paper, consists in numerical modelling as well. Properties of the soil and column used in the simulation were calibrated by parametric study in accordance with results of loading test. For the numerical modelling of deep foundation reinforced by SM column, properties of soil are taken as the one presented in the paper. Hence, silt is modelled with elastoplastic law with MC failure criterion, like it was in the reference. Concrete pile is assumed as elastic Parameters used in the simulation are presented in Table 6.3.

Table 6.3 Properties of soil and concrete deep foundation used in numerical modelling of the deep foundation

Parameter	Unit	Silt	Concrete
Constitutive model	[-]	MC criterion	Elastic
Density	[kg/m^3]	2000	2500
Young’s modulus	[MPa]	40	20000
Poisson’s ratio	[-]	0.3	0.2
Friction angle	[°]	32	-
Dilation angle	[°]	2	-
Cohesion	[kPa]	11	-

6.4.2.1. Geometry and mesh

The behaviour of deep foundation is analysed with three dimensional model. Only one quarter of the model is taken into consideration, in order to reduce calculation time. Analysed concrete pile is 10 m long and its diameter equals to 0.5 m. In order to avoid influence of the boundaries on the piles behaviour, 15 m x 15 m x 32 m (length x width x height) model have been used.

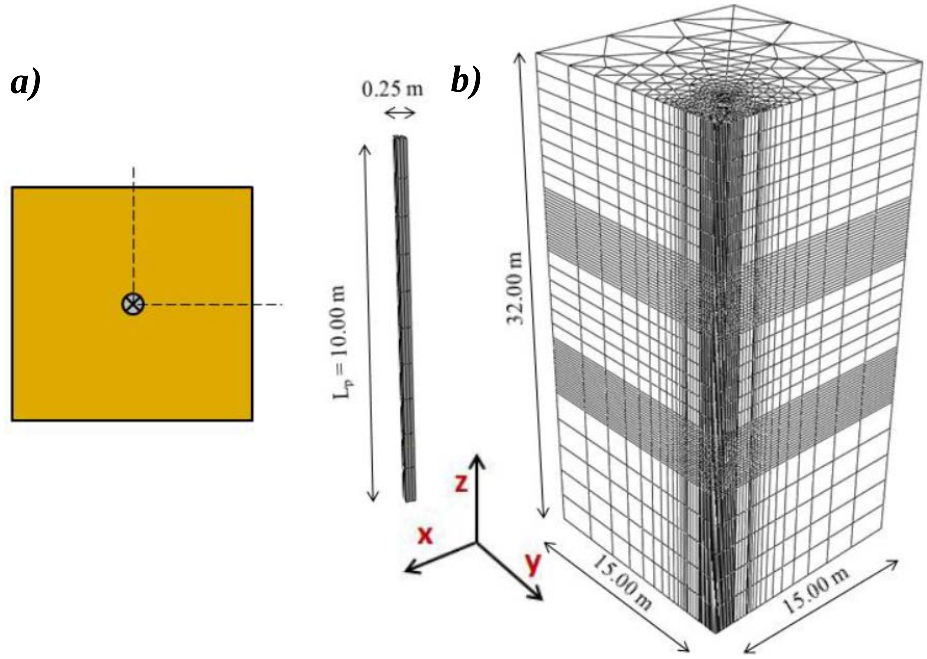

Figure 6.11 a) model of single concrete pile analysed in the study with marked axis of symmetry, b) three dimensional mesh and dimensions (dimensions in meters)

Dimensions and mesh of the calculated case are presented in Figure 6.11. Mesh consists of 15-node quadratic triangular prism elements (C3D15). Model's boundary conditions are assumed as: symmetric boundaries on the planes of symmetry, no horizontal displacement in the X axis direction for the wall parallel to the YZ plane and no horizontal displacement in the Y axis direction for the one parallel to the XZ plane. At the bottom, displacements are restricted in the vertical direction.

Contact between column and soil is defined by model with Coulomb criterion with the friction coefficient equals to μ_f = 0.5. Friction coefficient corresponds to about 0.76 tan ϕ, where ϕ is internal friction angle.

Pile's head is loaded by imposed displacement increasing form 0 mm till 5 cm, which is 10% of the pile's diameter.

6.4.2.2. Results

The theoretical bearing capacity of analysed pile, has been calculated according to β-method. All steps of calculations and final results are presented below:

Lateral earth pressure coefficient: $K_0 := 1 - \sin(\phi) = 0.47$

Pile dimentions: $L_p := 10\text{m} \quad D_p := 0.5\text{m}$

$A_t := 0.25 D_p^{\,2} \cdot \pi = 0.196 \cdot \text{m}^2 \qquad S := D_p \cdot \pi = 1.571\,\text{m}$

$\text{Shaft} := L_p \cdot S = 15.708\,\text{m}^2$

Friction coefficient $\mu := 0.5$

β coefficient: $\beta := \mu \cdot K_0 = 0.235$

Vertical stress at the pile's tip: $\sigma_v := \gamma \cdot L_p = 196.133 \cdot \text{kPa}$

Angle under the pile: $\eta := \pi \cdot 0.45 = 1.414$

Bearing capacity coefficients: $N_q := \left\lfloor \tan(\phi) + \sqrt{1 + (\tan(\phi))^2} \right\rfloor^2 \cdot e^{2 \cdot \eta \cdot \tan(\phi)} = 19.046$

$N_c := \left(N_q - 1\right) \cdot \left(\frac{\sin(\phi)}{\cos(\phi)}\right) = 11.276$

Shaft capacity: $Q_f := \beta \cdot 0.5 \cdot \sigma_v \cdot \text{Shaft} = 362.062 \cdot \text{kN}$

Tip capacity: $Q_t := \left(\sigma_v \cdot N_q + c \cdot N_c\right) \cdot A_t = 757.817 \cdot \text{kN}$

Ultimate capacity: $Q := Q_f + Q_t = 1119.879 \cdot \text{kN}$

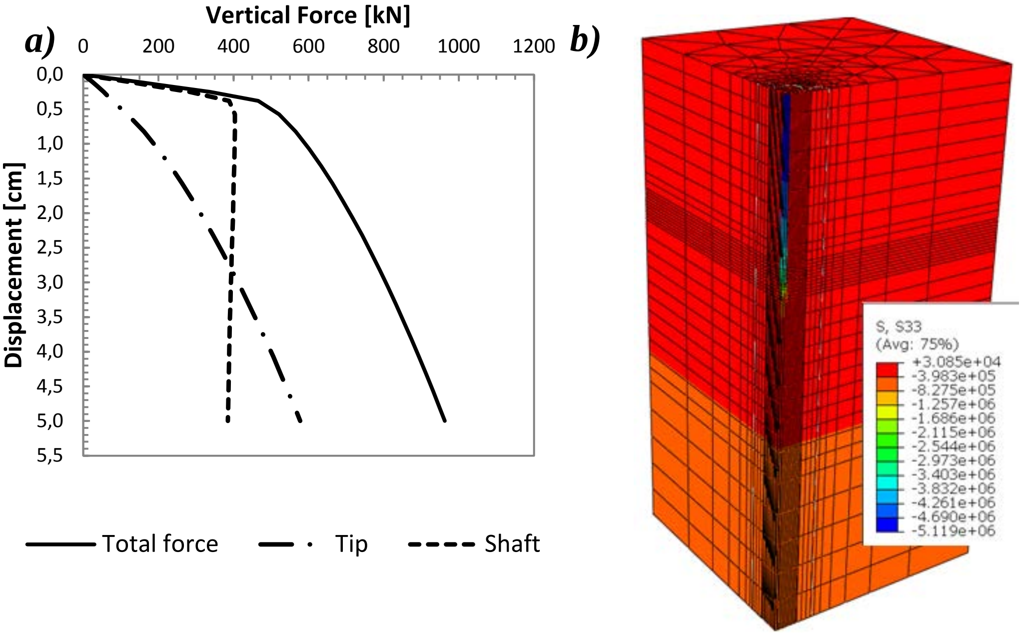

Figure 6.12 a) total, tip and shaft capacity estimated by numerical simulation, b) results obtained for 5 cm displacement.

Results of numerical simulation are presented in Figure 6.12a. It can be observed that, at the beginning of the loading, majority of the load is taken by friction along the pile's shaft, whereas part taken by the tip increases much slower. After about 0.4 cm contribution of the shaft becomes constant, which manifests by plateau. When pile's head displaces 2.7 cm, contributions become equal. Figure 6.12b depicts map of stresses calculated for 5 cm displacement.

6.4.3. Soil Mixing column

Investigation of three SM columns have been presented by Le Kouby, et al. (Le Kouby, et al., 2010). All of them have been examined by static loading test. For this study, 5.3 m long, column, called in the paper P2, installed by KELLER Foundations, has been chosen for analyses.

6.4.3.1. Installation

Column was created as a mixture of silt and cement grout. The water-cement grout was prepared with water/cement ratio of 1. 300 to 400 kg of cement type CEM III/C 32.5 N PM-ES (CEN 2000) per cubic meter of soil was used. The construction procedure had two steps. The used tool has two configurations: it can be folded or opened. In the first phase of the procedure, the tool was driven to an appropriate depth in the folded configuration. Then the tool was opened and jacked down while the soil was sheared and mixed with cement. From the top to the base of the column, both rotation and injection take place; the same happens during the second phase when the tool moves back to the surface. For the instrumentation, a closed steel tube was installed in each test column on the day of construction before the cement set up. The next day, a pile head was built on top of the column with a steel reinforcement to ensure a good connection with the column, so that a vertical load could be applied. The column head (Figure 6.12a) was a 0.60 m square concrete block and was 0.25 m high (Le Kouby, et al., 2010).

After column excavation (Figure 6.13a), it was found that the column's shape was smooth and cylindrical. The measured diameter of the test column was about 0.64 m (instead of the theoretical value of 0.6 m). The section of the column showed, in the centre, a zone with a higher density of cement. Its diameter was about 300 mm, apparently due to applied SM method (Figure 6.13b). A significant heterogeneity appeared between the centre of the column and the outer crown. Samples used to determine columns properties, were taken from the upper part (about 2-3 m from the column's head) of the SM column to perform laboratory tests.

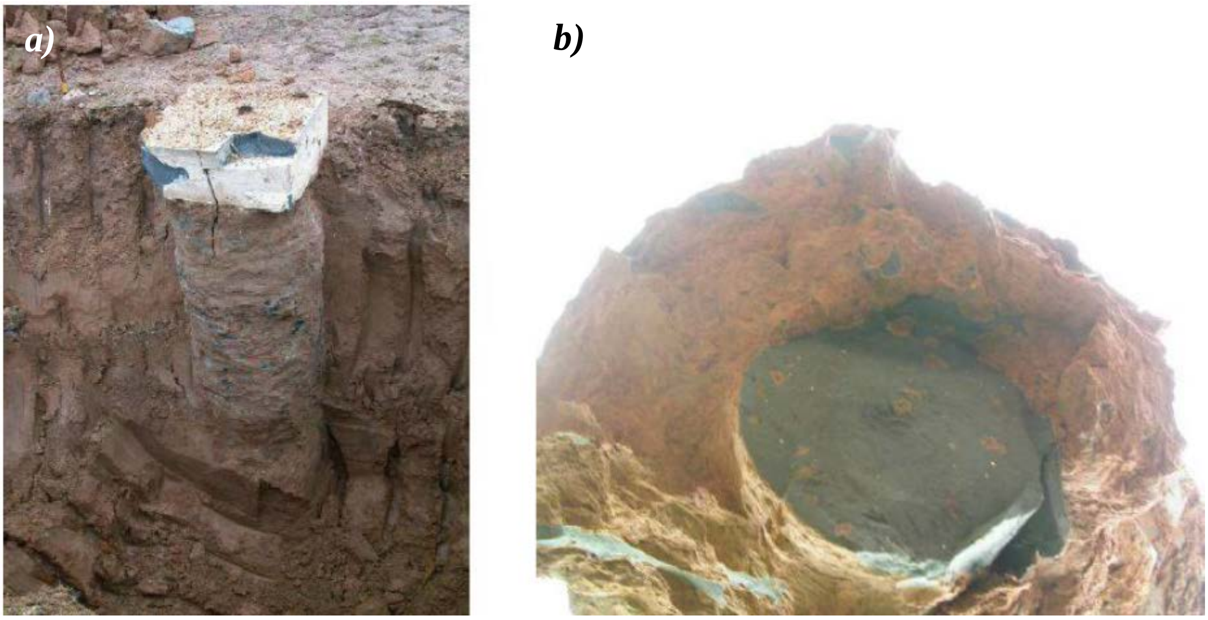

Figure 6.13 a) excavation of column P2 and b) view of the section of a similar (not loaded) column (Le Kouby, et al., 2010)

6.4.3.2. Properties

Elastic properties of column were calibrated by the parametric study performed with numerical model. They are: Young's modulus $E_{col} = 50\ E_{soil} = 2000$ MPa and Poisson's ratio $\nu = 0.2$.

The SM element is modelled with elastoplastic model with MC failure criterion (Table 6.4). Shear parameters are chosen according to properties of full scale column analysed in Chapter 4 and thus friction angle equals to 42°, dilation angle is 5° and cohesion is assumed as 700 kPa, as it was for treated silt.

Table 6.4 Properties of SM column used in numerical modelling of the deep foundation reinforced by SM columns

Parameter	Unit	Soil Mixing
Constitutive model	[-]	MC criterion
Density	[kg/m^3]	2200
Young's modulus	[MPa]	50 E_{soil} = 2000
Poisson's ratio	[-]	0.2
Friction angle	[°]	42
Dilation angle	[°]	5
Cohesion	[kPa]	700

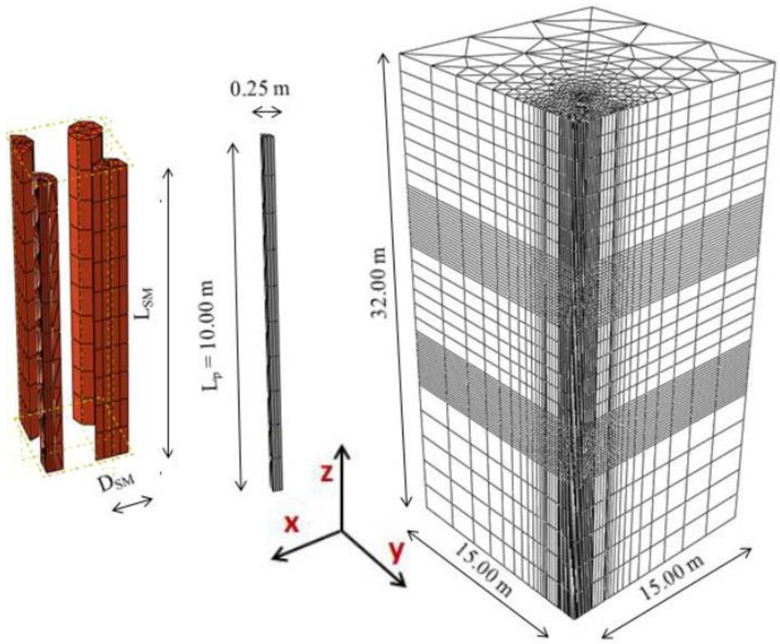

Figure 6.14 Three dimensional mesh and dimensions of the model used to analyse deep foundation reinforced by SM columns (dimensions in meters)

6.4.4. Reinforced pile

In order to analyse different configurations of columns reinforcing single pile, parametric study has been carried out. Influence of columns' pattern, distance between pile's tip and column's heads, length and diameter of columns, and distance between columns' and pile's axes, have been investigated.

Mesh and dimensions of the numerical model are presented in Figure 6.14. Properties of soil, pile (Table 6.3) and contact between pile and soil are assumed the same as in unreinforced case. None contact elements has been used to simulate interaction between columns and soil. Nodes of the finite element mesh of the SM column have been tied to nodes of soils' mesh. Properties of SM column are presented in Table 6.4.

6.4.4.1. Pattern of reinforcing columns

To execute pile's reinforcement by SM columns, four column patterns have been proposed: types A, A0, B and B0. Definition of each of them can be found below (Figure 6.15a):

- *Pattern A* consists in group of four SM columns. Columns are organized in a square shape, where each of them is placed in its vertex. Pile is situated in the centre and distance between its axis and axis of each column is equalled to a_1, whereas columns are moved from each other by a. In numerical approach, model is reduced to one quarter in order to limit calculation time. Due to that, only one column of the group and a quarter of pile are simulated.
- *Pattern A0* consists in group of five columns. Four of them are the same as in A, the last one is added in the centre, axially, under the pile.
- *Pattern B* consists in group of eight columns organized in a circle. Foundation is situated in a way that its axis go through the centre of the circle. In this pattern distances a and a_1 are equalled and represent radius of the circle. In numerical model, only one quarter is analysed. Model reduces to one whole column, two halves and one quarter of the foundation.
- *Pattern B0* consists in group of nine columns. Eight of them are the same as in pattern B and the last one is added in the centre, axially, under the pile.

Patterns A0 and B0 can be applied when reinforcement is installed before the installation of the foundation. However, when the reinforcement is planned for the existing foundations, these patterns are considered as highly dangerous. The danger comes from the presence of the central column. Its installation might cause sudden, uncontrollable settlement.

The influence of the pattern on the behaviour of single concrete pile has been studied by parametric study for all configurations.

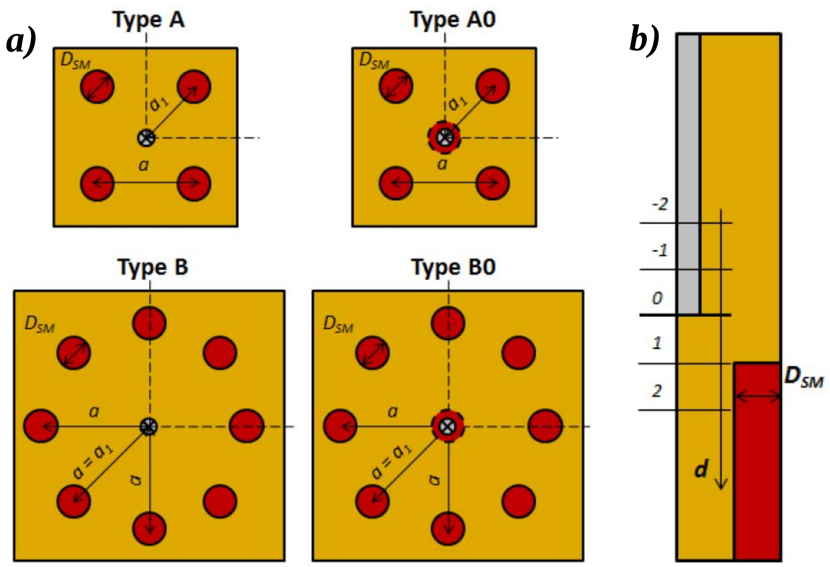

Figure 6.15 a) four patterns of reinforcing columns analysed in the parametric study, b) distance between the pile's tip and a columns' heads

6.4.4.2. Parametric study

6.4.4.2.1. *Distance between the pile's tip and columns' heads*

By d, the vertical distance between the plane defined by the reinforcing columns' heads and plane defined by the pile's tip is understood. It is visualised in Figure 6.15b.

Five values of *d*, -2 m, -1 m, 0 m, 1 m, 2 m, have been tested for all four columns' patterns. All results are calculated with L_{SM} = 10 m long columns. Their diameter is assumed as D_{SM} = 1.0 m. Distance between columns, *a*, equals to 2.0 m.

Results obtained for pattern type A and A0, can be found in Figure 6.16 and Figure 6.17, respectively.

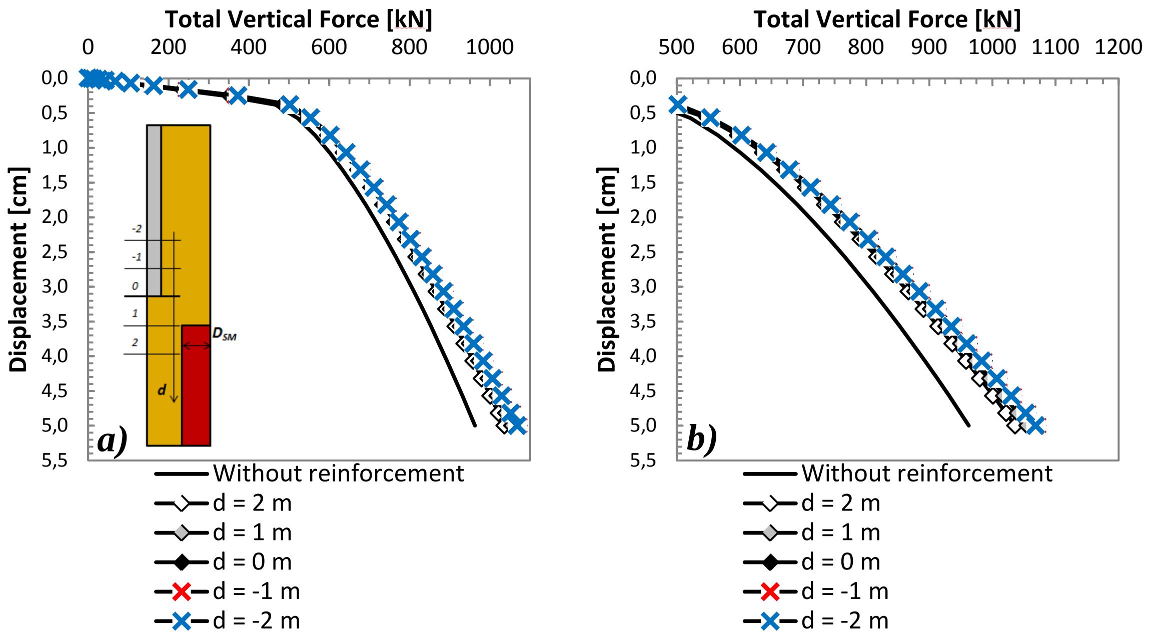

Figure 6.16 Influence of the distance between the pile's tip and columns' heads on behaviour of deep foundation reinforced by SM columns organised according to pattern A. Fixed parameters: L_{SM} = 10 m, D_{SM} = 1.0 m, a = 2 m and a_1 = 1.41 m. a) piles behaviour, b) zoom

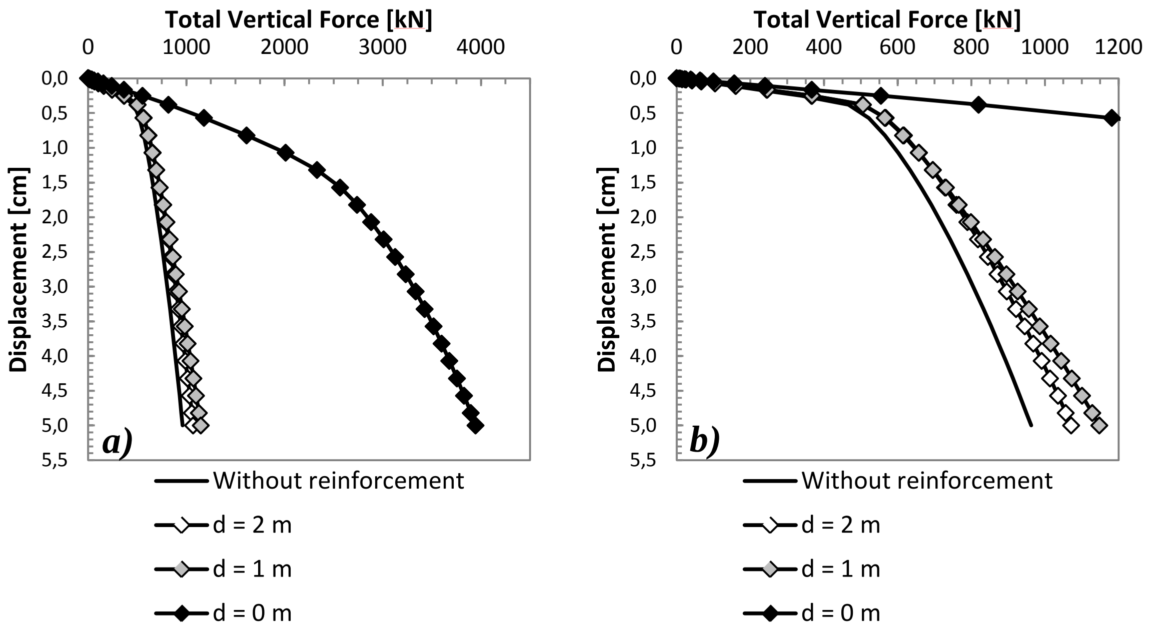

Figure 6.17 Influence of the distance between the pile's tip and columns' heads on behaviour of deep foundation reinforced by SM columns organised according to pattern A0. Fixed parameters: L_{SM} = 10 m, D_{SM} = 1.0 m, a = 2 m and a_1 = 1.41 m. a) piles behaviour, b) zoom

It can be noticed (Figure 6.16) that for columns installed according to pattern A, provided improvement does not change significantly as a function of *d*. However, it can be pointed out that the lowest force is borne when *d* = 2 m (column's head are 2 m under the pile's tip). The best improvement has been acquired from model, where *d* = -1 m. Detailed results and improvement as a function of *d*, for all studied patterns are presented in Figure 6.21 and Table 6.5.

For pattern A0 (Figure 6.15a), only three values of *d*, have been studied. Cases where columns' heads are over the pile's tip (*d* = -2 m and *d* = -1 m) have not been analysed due to the central column in the group, which is situated under the pile. Results are presented in Figure 6.17. Considerable improvement appears for *d* = 0 m. In this case borne force equals about 3950 kN after 5.0 cm displacement. This high value is an effect of significant rise of the bearing capacity of the tip, illustrated in detail in Figure 6.18a. Values of force taken by tip is comparable in case of *d* = 2 m and 1 m. Contribution of pile's shaft is presented in Figure 6.18b. For all reinforced cases, predicted force taken by the friction is higher than the unsupported one. Similarly like for tip's capacity, results for *d* = 2 m and 1 m are comparable. Slopes of illustrating them curves are identical and the same as the one of the unreinforced case. Discrepancy between prediction for *d* = 2 m and 1 m starts to appear at about 0.4 cm, where abrupt increase of displacement not associated with increase of the force appears. However, the behaviour is not identical. In case of smaller distance between pile and columns, very small rise of force as a function of displacement can be noticed. Behaviour of pile being in direct contact with reinforcement is different than the other predictions. Not only tip capacity is significantly higher, also force taken by pile's shaft is about 200 kN higher. Slope of illustrating curve is slightly different than in other reinforced and unreinforced cases. Nevertheless it shows the same tendency, namely, after steep section of the curve, caused by a rapid increase in force, a plateau takes place, accompanied by a gentle increase of force, as it is observed in the case of *d* = 1 m

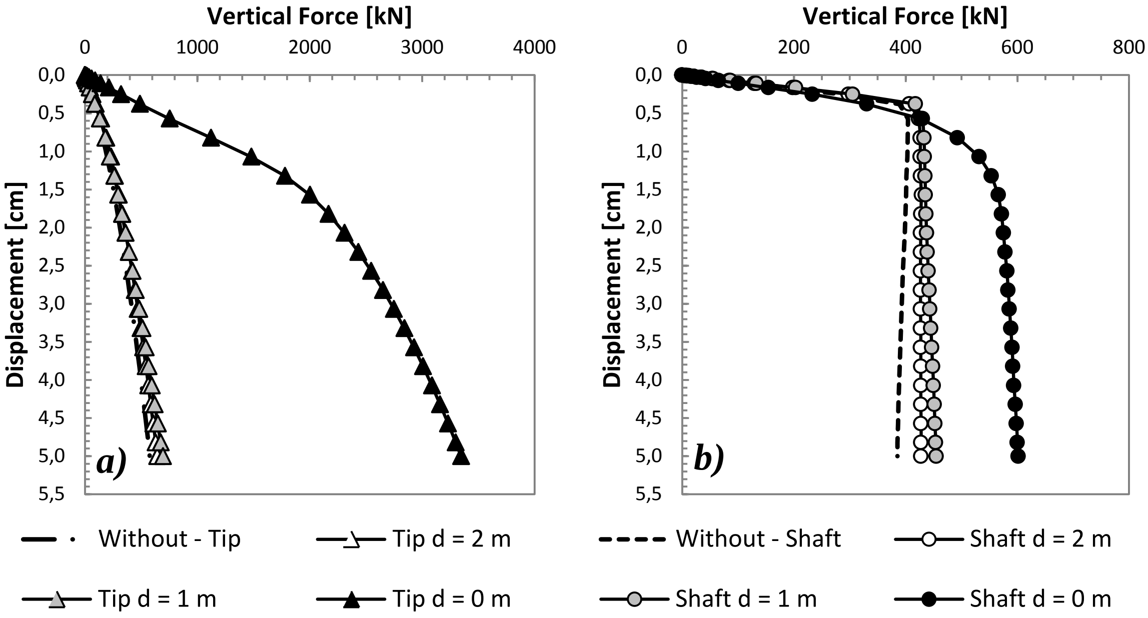

Figure 6.18 Participation of a) tip and b) shaft in total force borne by the pile

Results of modelling of pile reinforced by column organised in patterns B and B0 are presented in Figure 6.19 and Figure 6.20 respectively. Similar behaviour, as for pattern A and A0, can be observed. Improvement of pile's bearing capacity can be noticed, however in case of pattern B, it is almost impossible to distinguish difference between predictions. Value of forces after 5.0 cm displacement, as well as percentage of improvement are presented in Table 6.5.

Due to stiff column supporting pile, its tip's capacity increases significantly in case B0, when *d* = 0 m (Figure 6.20). The influence, considerably smaller, is also present in case of *d* = 1 m.

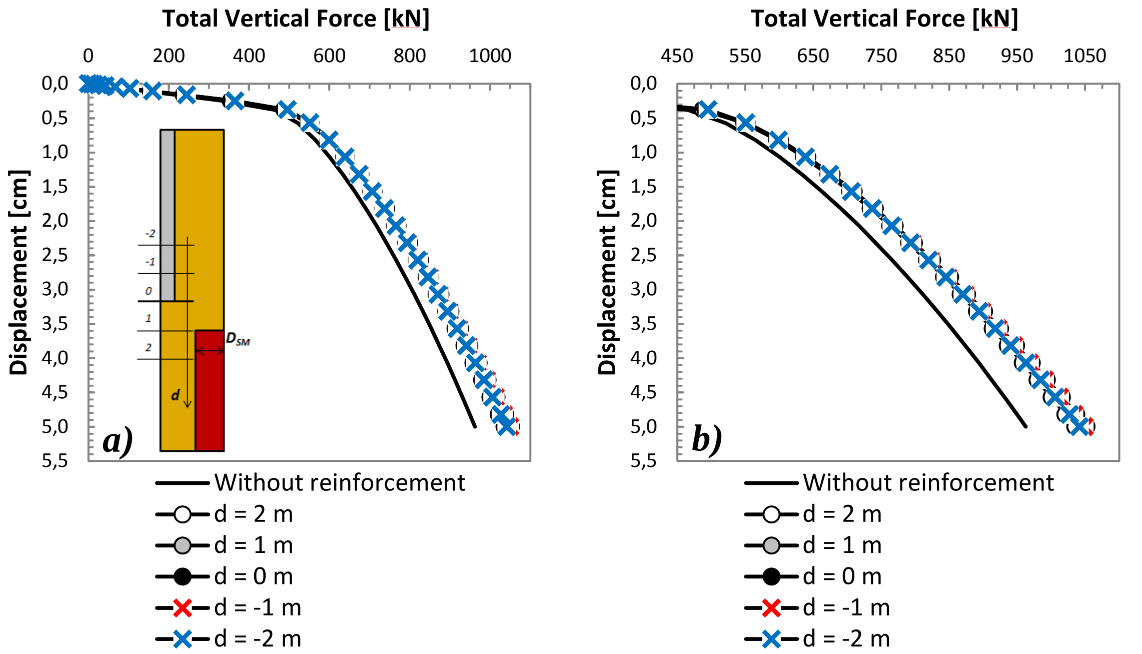

Figure 6.19 Influence of the distance between the pile's tip and columns' heads on behaviour of deep foundation reinforced by SM columns organised according to pattern B. Fixed parameters: L_{SM} = 10 m, D_{SM} = 1.0 m, a = 2 m a) piles behaviour, b) zoom

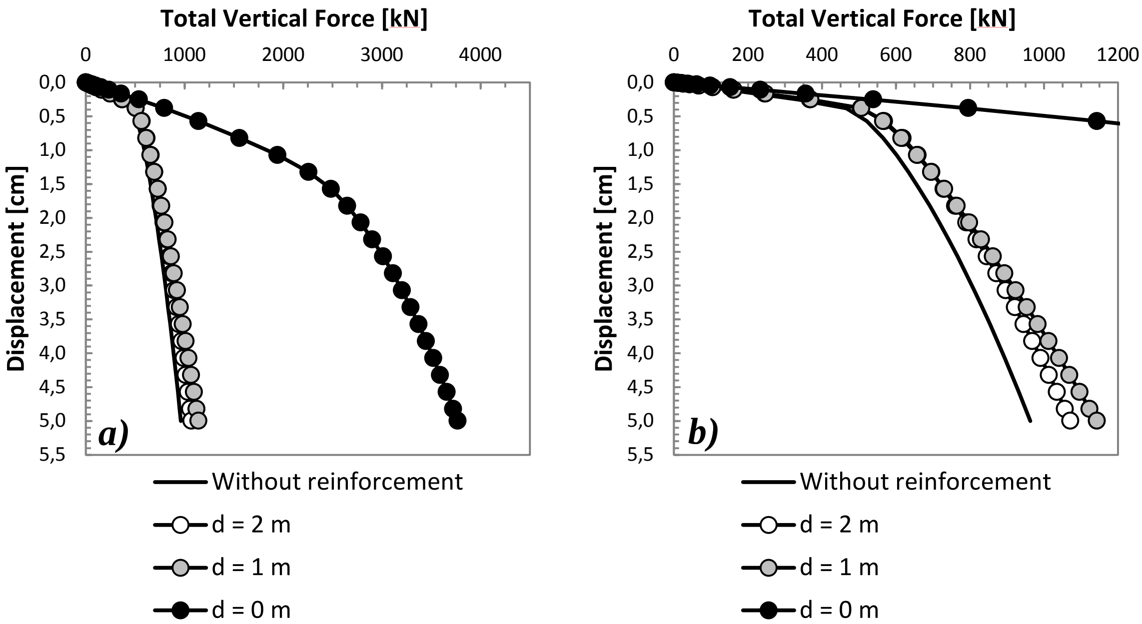

Figure 6.20 Influence of the distance between the pile's tip and columns' heads on behaviour of deep foundation reinforced by SM columns organised according to pattern B0. Fixed parameters: L_{SM} = 10 m, D_{SM} = 1.0 m, a = 2 m a) piles behaviour, b) zoom

Table 6.5 presents values of forces and corresponding to them improvement. The highest forces have been obtained for cases, where central column, situated under the pile is included. The most efficient solution is placing pile directly over the column. Improvement varies between 310.2% - 11.4%, and 291.6% - 11.3% for A0 and B0 respectively. Nevertheless, this case is possible only when the foundation is built after installation of the reinforcement. In case of improving capacity of the existing pile, this kind of solutions should not be taken into account.

Figure 6.21 depicts improvement as a function of distance *d*. Due to considerable differences, logarithmic scale has been used to present results. It was found that reinforcement executed according to pattern A, effects with higher improvement than the reinforcement executed in accordance with pattern B. The maximal value of force, in all four analysed cases, have been calculated for *d* = 0 m, which means that the columns' heads are in the same plane as the pile's tip. Efficiency of the reinforcement depends not only on the distance from the pile's tip by also on the location of the columns (over or under the tip). Results have shown to be not symmetrical towards *d* = 0 m. Moreover, better solution is to place reinforcement over the pile's base. Improvements about 11.3% and 9.0% have been achieved for *d* = -1 m, for A and B patterns respectively. The influence of the reinforcement decrease with the distance and has been observed the smallest in case of *d* = 2 m, only 7.7% and 7.6% for A and B patterns.

Table 6.5 Total borne force after 5.0 cm displacement of the pile's head for patterns A, A0, B and B0 as a function of distance between columns' heads and pile's tip, d

Pattern	*d* [m]					Improvement [%]				
	-2	-1	0	1	2	-2	-1	0	1	2
Without			962.6 kN					-		
A	1068.9 kN	1071.0 kN	1072.2 kN	1055.6 kN	1036.4 kN	11.0	11.3	11.4	9.7	7.7
A0	-	-	3948.2 kN	1148.3 kN	1072.0 kN	-	-	310.2	19.3	11.4
B	1041.9 kN	1049.1 kN	1052.5 kN	1045.7 kN	1035.8 kN	8.2	9.0	9.3	8.6	7.6
B0	-	-	3769.4 kN	1142.9 kN	1071.4 kN	-	-	291.6	18.7	11.3

Fixed parameters: L_{SM} = 10 m, D_{SM} = 1.0 m, a = 2 m

Keeping in mind technique of the columns' *in situ* creation, it is barely possible to be able to keep enough precision to install the SM element in a way, that its upper surface will be in exactly the same plane as the foundation's base. Therefore, it is recommended to place columns slightly higher than the *d* = 0 m plane. It allows keeping higher improvement than in case of column installed below this plane.

Due to danger and technical difficulty, which brings installation of column axial with pile, presented below results of the parametric studies, concentrate only on cases of patterns A and B (cases without central column).

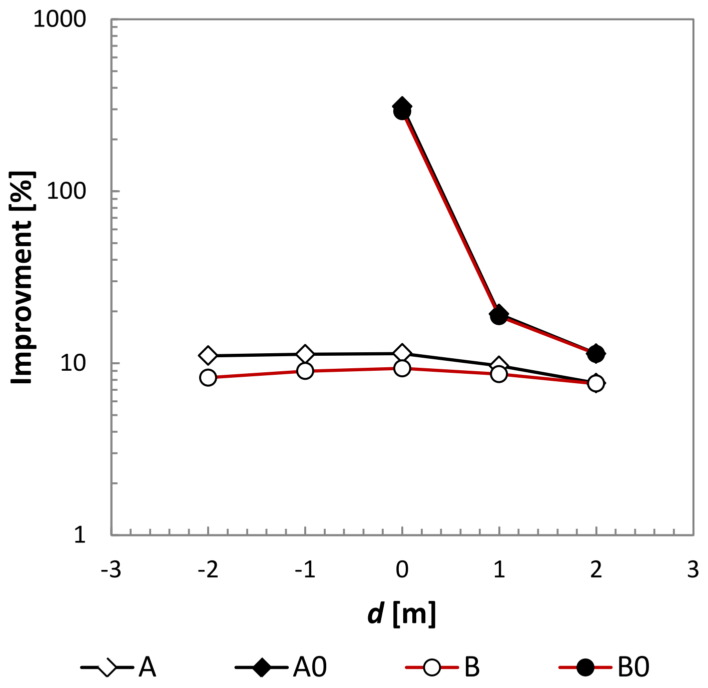

Figure 6.21 Improvement brought by the reinforcement with A, A0, B and B0 patterns, as a function of distance between pile's tip and columns' heads. L_{SM} = 10 m, D_{SM} = 1.0 m, a = 2 m

6.4.4.2.2. *Length of columns*

Designing length of SM columns, it is important to remember limitations, which every technique brings. For instance, in case of the typical Nordic method depth limit is 25 m, whereas in case of Japanese technique maximal depth cannot exceed 48 m (Massarsch & Topolnicki, 2005).

The influence of the length of the reinforcing elements has been investigated by a parametric study. Three lengths of columns have been examined: L_{SM} = 6 m, 10m and 12 m.

Figure 6.22 illustrates influence of the length of columns on the behaviour of the loaded foundation. In all cases improvement of the borne force is visible, however differences between results, obtained for different columns, are almost indistinguishable. Slight difference between calculated forces can be seen in Table 6.6.

Figure 6.23 and Table 6.6 present in details obtained results. It can be seen that columns' length does not have significant impact on the behaviour of pile. In both case, slight difference can be notice only in case of 6 m long columns. For 10 m and 12 m elements, forces at the top of column are alike. Nevertheless, obtained results show that length of reinforcing elements is not an influential parameter.

Table 6.6 Total borne force after 5.0 cm displacement of the pile's head for patterns A and B as a function of columns' length L_{SM}

Pattern	L_{SM} [m]			Improvement [%]		
	6	10	12	6	10	12
Without		962.6 kN			-	
A	1065.7 kN	1071.0 kN	1072.358 kN	10.7	11.3	11.4
B	1043.1 kN	1049.1 kN	1051.197 kN	8.4	9.0	9.2

Fixed parameters: D_{SM} = 1 m, d = -1 m, a = 2 m

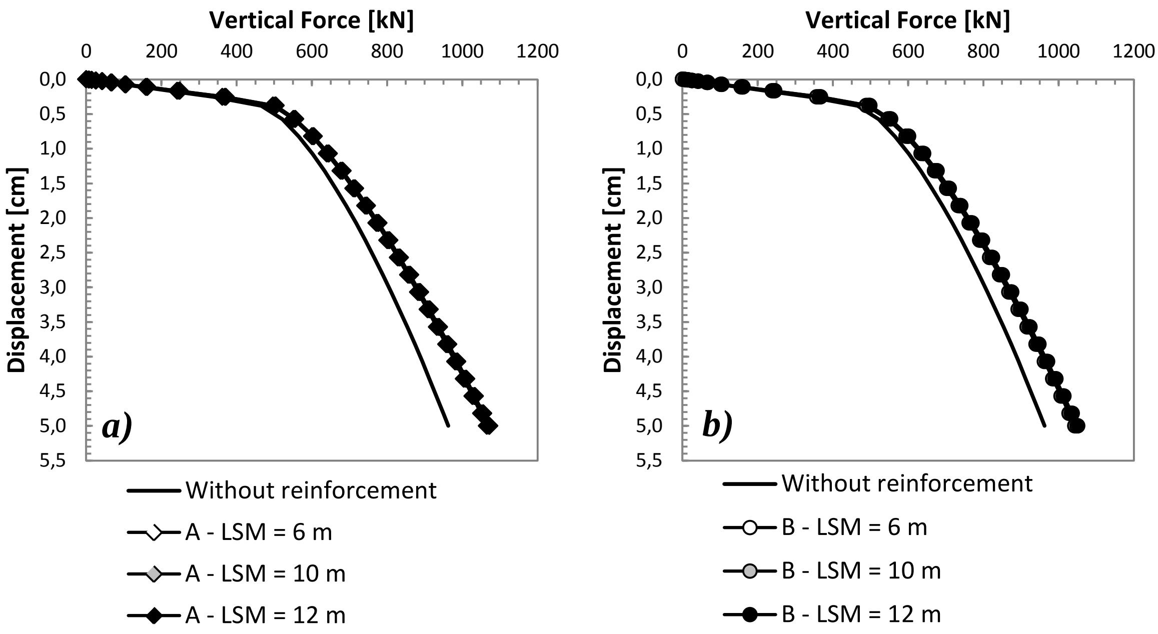

Figure 6.22 Influence of the columns' length L_{SM}, on the behaviour of deep foundation reinforced by SM columns organised according to: a) pattern A, b) pattern B. Fixed parameters: D_{SM} = 1 m, d = -1 m, a = 2 m

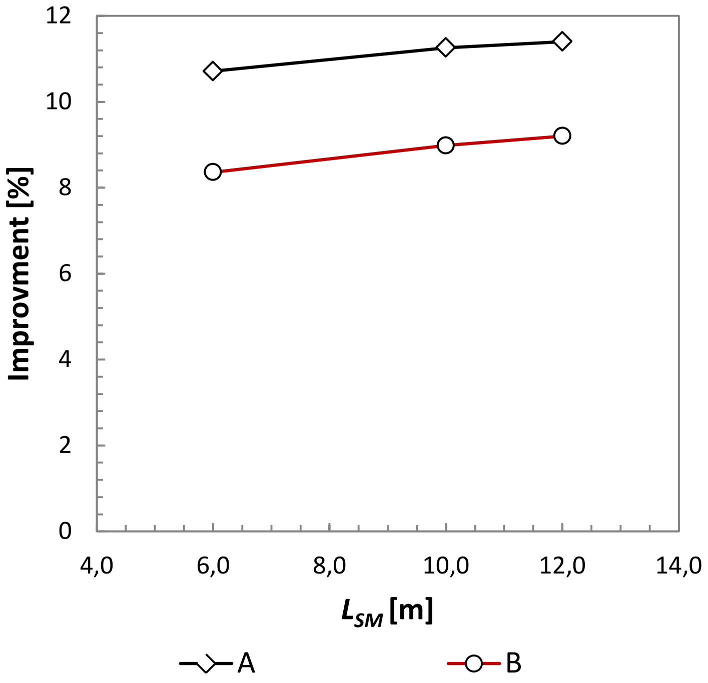

Figure 6.23 Improvement brought by the reinforcement with A and B patterns, as a function of columns' length. Fixed parameters: d = -1 m, D_{SM} = 1.0 m, a = 2 m

6.4.4.2.3. *Diameter of columns*

Diameter of SM column depends on the size of the rotating tool used in installation process. Available on the geotechnical market equipment allows execution of columns with diameters between 0.4 m and 2.80 m. For this theoretical investigation four column's sizes have been chosen according to technical specification of the equipment offered by geotechnical companies. The influence of the diameter of the reinforcing columns has been examined by a parametric study. Diameters taken into consideration are: D_{SM} = 0.4 m, 0.6 m, 1.0 m and 1.5 m.

As explained above, calculations have been performed for two patterns: A and B. Figure 6.24 illustrates behaviour of pile reinforced by SM columns installed: 1 m over the foundation's tip (d = -1 m), with 2 m spacing between columns (a = 2 m). Columns length have been fixed as 10 m.

Results obtained for pattern A are provided in Figure 6.24a. The influence of the columns' diameter is visible. The highest value of force is predicted for the biggest one. Improvement decreases with decrease of the diameter. Slopes of all curves illustrating piles behaviour, are the same for the first 0.3 cm displacement. Afterwards, in case of result obtained for unsupported pile, the increase of force starts to slow down. The longest linear answer to the applied load can be observed for model with the biggest diameter, D_{SM} = 1.5 m. Similar tendency can be observed in case of foundation reinforced by columns organised according to pattern B. Here, also, the best results has been calculated in case of the biggest diameter.

Detailed values of forces and improvements brought by SM elements as a function of columns' diameter can be found in and Figure 6.25.

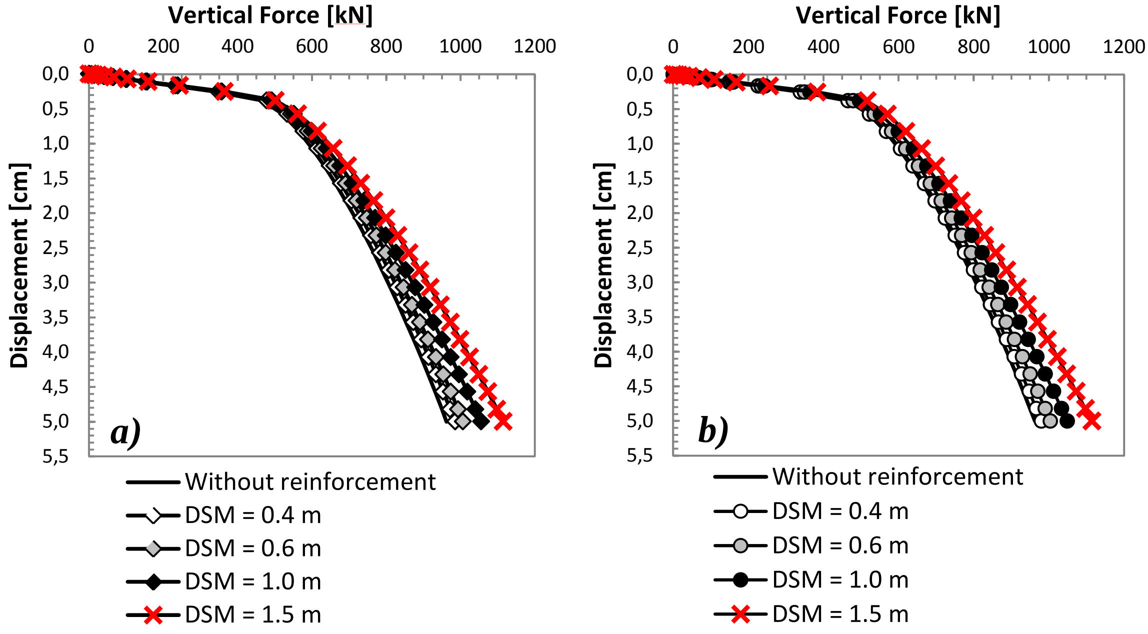

Figure 6.24 Influence of the columns' diameter, D_{SM}, on the behaviour of deep foundation reinforced by SM columns organised according to: a) pattern A, b) pattern B. Fixed parameters: L_{SM} = 10 m, d = -1 m, a = 2 m

Table 6.7 Total borne force after 5.0 cm displacement of the pile's head for patterns A and B as a function of columns' diameter D_{SM}

Pattern	D_{SM} [m]				Improvement [%]			
	0.4	0.6	1.0	1.5	0.4	0.6	1.0	1.5
Without	962.6 kN				-			
A	993.0 kN	1023.3 kN	1071.0 kN	1171.6 kN	3.2	6.3	11.3	21.7
B	979.8 kN	1003.9 kN	1048.8 kN	1114.8 kN	1.8	4.3	9.0	15.8

Fixed parameters: L_{SM} = 10 m, d = -1 m, a = 2 m

Figure 6.25 depicts influence of the columns' diameter on the improvement of the reinforcement. In case of pattern B, relation is represented by almost perfect straight line. Whereas, for pattern A, linearity is a bit disturbed by the result acquired for D_{SM} = 1.0 m, calculated efficiency is a bit lower. It might be explained by difference between mesh used in the calculations. Even though, special attention has been paid in proper calibration of the mesh, its slight influence can appear when difference between results are that small. Finite element mesh sensitivity study has been carried out in order to verify influence of the size of elements on the result of the calculations.

It can be pointed out, that improvement associated with reinforcement executed by columns with D_{SM} = 0.4 m and 0.6 m is significantly small. Keeping in mind number of installed columns, efficiency about 3.2%, 6.3% for A and 1.8%, 4.3% for B, is insufficient.

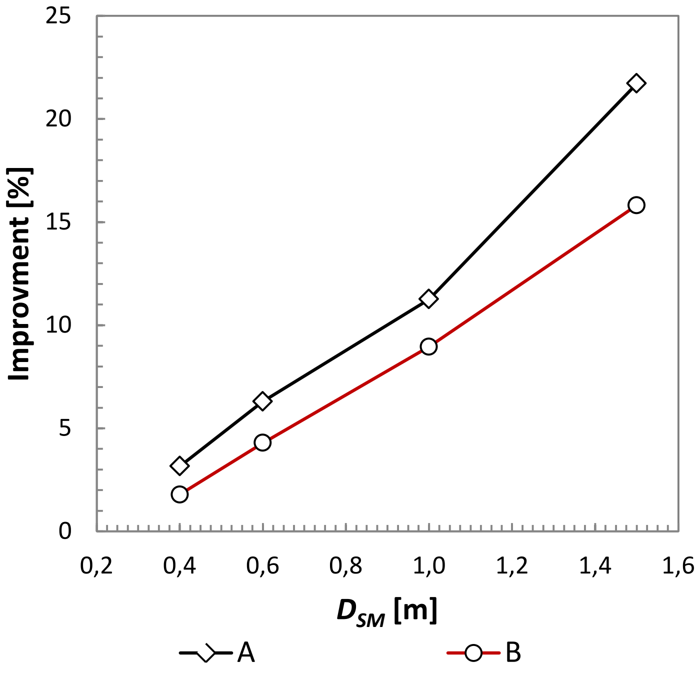

Figure 6.25 Improvement brought by the reinforcement with A and B patterns, as a function of columns' diameter. Fixed parameters: L_{SM} = 10 m, D_{SM} = 1.0 m, a = 2 m

Summing up, diameter of SM column has significant influence on the behaviour of the reinforced pile. Its increase causes rise of the pile's capacity.

6.4.4.2.4. *Distance between columns*

Distance between reinforcing columns has been investigated by parametric study. Three columns' spacing, *a* = 1.5 m, 2.0 m and 3.0 m have been tested and their influence on the piles behaviour pointed out. Other columns' parameters are assumed as: D_{SM} = 1 m, L_{SM} = 10 m, *d* = -1 m. Results, calculated for both patterns are presented in Figure 6.26.

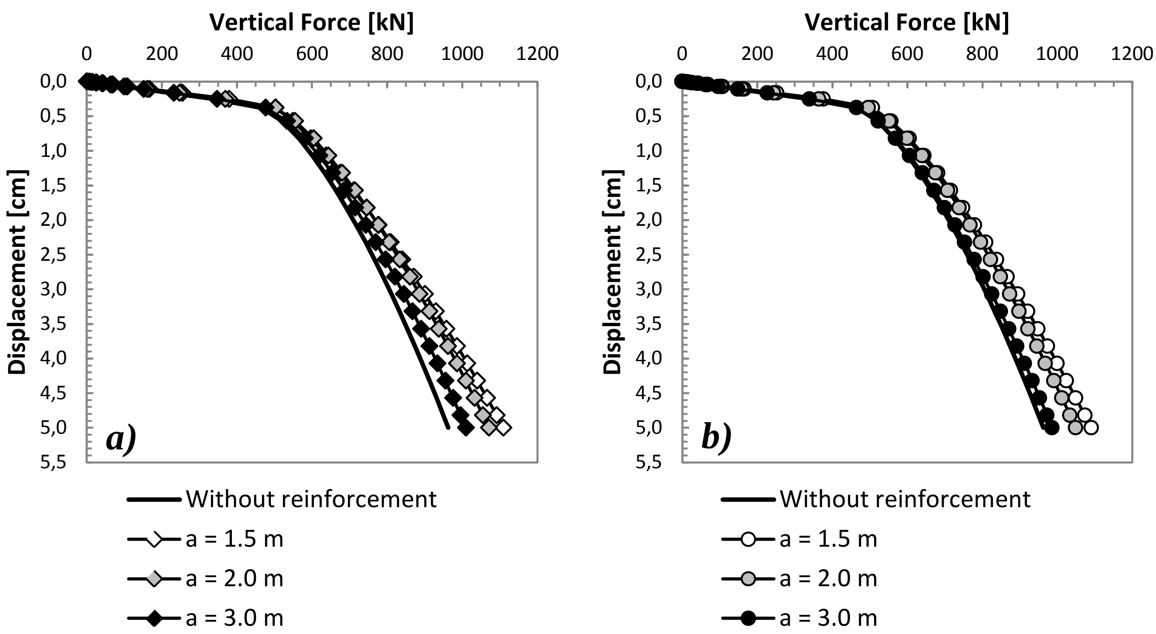

Figure 6.26 Influence of distance between columns a, on the behaviour of deep foundation reinforced by SM columns organised according to: a) pattern A, b) pattern B. Fixed parameters: D_{SM} = 1 m, L_{SM} = 10 m, d = -1 m.

In both cases the same tendency can be observed. Namely, the highest force is reported for a = 1.5 m. Similarly to previous cases of parametric study, beginnings of all curves are alike.

The linear elastic phases ends after about 0.4 cm displacement for all investigated cases, however values of force at this point slightly varies between cases. Even thought the smallest efficiency can be observed for *a* = 3.0 m, in case of pattern A, small improvement can be seen. Difference between results calculated for various spacing starts about 0.4 cm. The increase of force becomes slower for model with the biggest distance between columns, *a* = 3.0 m. Results of simulations with smaller distances between columns stay alike till about 2.6 cm and 1.7 cm for patterns A and B respectively. Afterwards, increase of force as a function of displacement slows down for *a* = 2.0 m. The improvement comes mainly from the increased tip capacity of the foundation. Force taken by pile's tip is presented in Figure 6.27a and Figure 6.28a for patterns A and B respectively. The same behaviour as in case of total force can be observed. The decrease of distance leads to increase of force. Participation of pile's shaft can be found in Figure 6.27b and Figure 6.28b for patterns A and B respectively. Relatively small differences between behaviour of supported and unsupported deep foundation can be found. However, discrepancies between reinforced cases are insignificant in case of pattern A, and very small for pattern B. Forces taken by shaft, acquired from model B with *a* = 3.0 m and unreinforced case are alike. Precise values of total force and improvement, can be found Table 6.8. Improvement as a function of distance between columns is illustrated in Figure 6.29.

Table 6.8 Total borne force after 5.0 cm displacement of the pile's head for patterns A and B as a function of distance between columns, a

Pattern	*a* [m]			Improvement [%]		
	1.5	2.0	3.0	1.5	2.0	3.0
Without		962.6 kN			-	
A	1109.9 kN	1071.0 kN	1009.7 kN	15.3	11.3	4.9
B	1090.9 kN	1049.1 kN	986.3 kN	13.3	9.0	2.5

Fixed parameters: D_{SM} = 1 m, L_{SM} = 10 m, d = -1 m

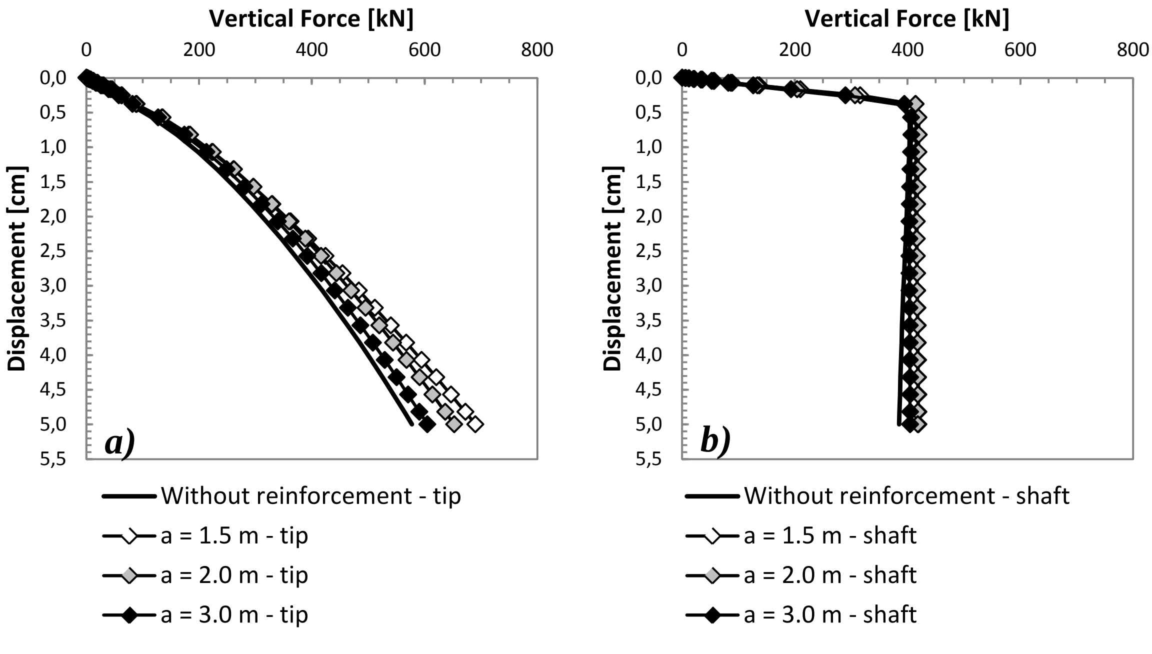

Figure 6.27 Influence of distance between columns a, on: a) tip and b) shaft capacity of pile reinforced by columns organised according to A pattern. Fixed parameters: D_{SM} = 1 m, L_{SM} = 10 m, d = -1 m

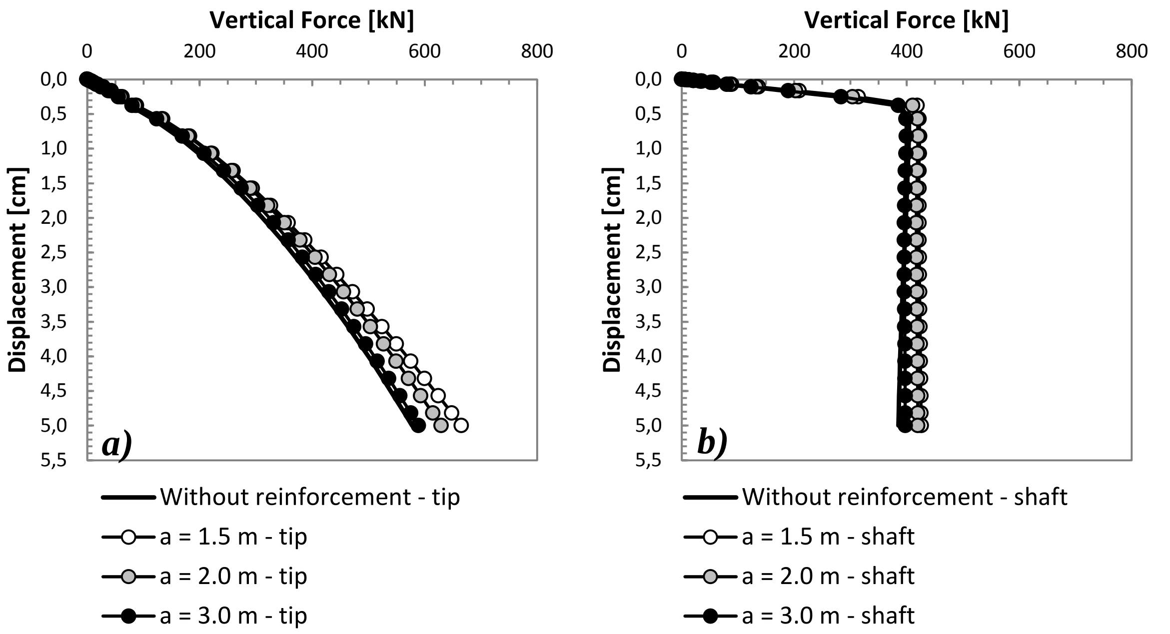

Figure 6.28 Influence of distance between columns a, on: a) tip and b) shaft capacity of pile reinforced by columns organised according to B pattern. Fixed parameters: D_{SM} = 1 m, L_{SM} = 10 m, d = -1 m

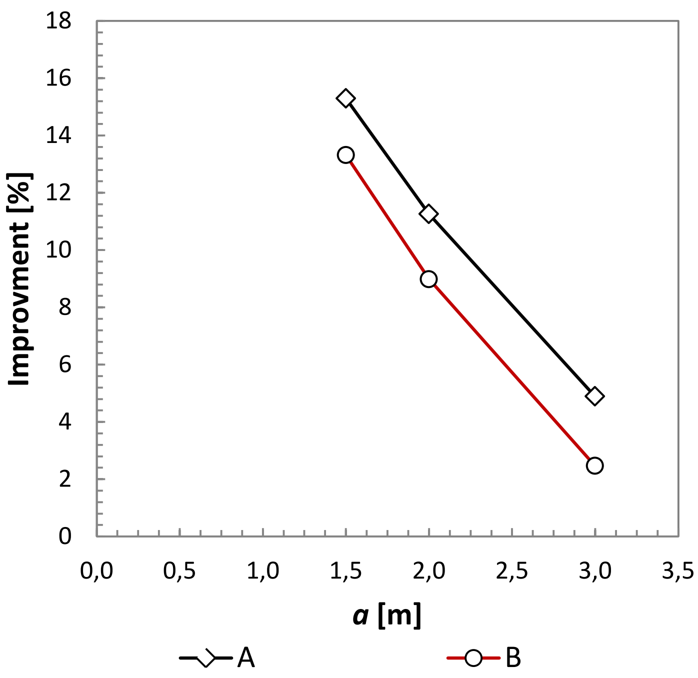

Figure 6.29 Improvement brought by the reinforcement with A and B patterns, as a function of distance between columns. Fixed parameters: L_{SM} = 10 m, D_{SM} = 1.0 m, d = -1 m

The influence of distance between supporting columns has significant impact on the behaviour of the reinforced foundation. The increase of columns' spacing causes decrease of efficiency of the reinforcement (Figure 6.29). The relation between improvement and *a*, is almost linear. It has been observed for both patterns, that for *a* > 2 m, amelioration of pile's capacity is insufficient, about 4.9%, which corresponds to 47.0 kN more that in case of foundation without treatment and about 2.5%, which stands for additional 23.7 kN, for patterns A and B respectively.

6.5. Conclusions

Three ways of reinforcing deep foundations has been presented. In this chapter, two of them have been discussed. The first one, where reinforcing columns are installed under a pile in the same soil layer and the second one where columns are created around the pile. A reinforced single concrete pile has been studied. Parametric study has been carried out in order to investigate the impact of parameters such as: vertical distance between pile's tip and the heads' of supporting columns, diameter and length of the columns, horizontal distance between columns and columns' pattern.

Patterns including central column in a group has been found as the most efficient. Provided improvement achieves about 300%, when pile's tip is supported directly by the column. The radical rise of the performance is caused by significantly higher tip capacity of the foundation. Also, efficiency of reinforcement executed by group of columns organized around the pile in square (pattern A0) and circle (pattern B0), which is placed lower (1 m and 2 m under the pile's tip) is considerably higher than in case of reinforcement without central column (patterns A and B). For SM elements situated 1 m under improvement equals to 19.3% and 18.7% for A0 and B0 respectively. When distance increases to 2 m, improvement of about 11.4% and 11.3% for A0 and B0 can be noticed. Even though efficiency of these kinds of patterns is significantly high (especially when pile's tip is supported directly by the column), they can only be used when SM columns are installed before the foundation. Patterns which include column or columns under the deep foundation cannot be accepted in case of reinforcing existing deep foundation. They are disqualified due to danger of affecting the balance of stresses around pile's tip, which might results in sudden settlement. Moreover, installation of the SM column axial with pile brings some technical difficulties. Therefore, for reinforcement of existing foundations patters without central columns (like the A and B ones) are more recommended.

Reinforcement executed by columns organised in accordance with patterns A and B has been analysed by parametric study. Even though obtained differences in forces have not been found very significant, the maximal improvement is about 28%, some mechanisms have been captured. The biggest influence on the improvement of the foundation's capacity has distance between column and pile in horizontal sense. It has been observed that pile's capacity decreases with the increase of the distance. Although, the same tendency has been found for both patterns, pattern A seems to be more sensitive to changes. Moreover, it has been observed, that presence of the reinforcement influences mainly pile's tip capacity. The friction capacity have been influenced by columns as well, however observed impact has not been significant.

The second important parameter is diameter of the reinforcing columns. Size of columns has been chosen in accordance with specifications of mixing tools, commonly used in geotechnical practice. It has been found that the increase of columns' diameter leads to rise of reinforcement's efficiency. The obtained relation is linear Similarly, to horizontal distance between foundation and supporting elements, higher improvement has been found in case of columns organized according to pattern A.

The third important parameter is distance between columns' heads and tip of the foundation. It was found that the most optimal location is when they are in the same plane. Although, the increase of distance in both directions causes decrease of the reinforcement's efficiency, slightly better performance can be observed for columns placed over pile's tip. Hence, if it is not possible to install SM elements in the same plane, it is recommended to localize columns in a way that their heads are between zero and one meter over the pile's tip.

The length of the column has been found the least influential. Difference between improvement brought by 6 m long pile and the one with 12 m, for both patterns is less than 1%.

Summing up, presented results of the parametric study visualise impact of columns geometry on the performance of the deep foundation. Since study is a theoretical investigation, in order to be able to use its results in engineering practice, results should be confronted with field or/and laboratory tests.

7. Reference cases

7.1. Introduction

In the recent past, several new techniques and applications of the Soil Mixing method have been introduced. Unfortunately, practical experience is still limited to certain soil conditions and specific applications. One of relatively new application field is reinforcement of deep foundations. Deep foundations are commonly used and designed way of founding structures. For some existing constructions the need of verification and improvement of the foundation's capacity might appear. Different reasons can cause the requirement. One of them is higher bearing capacity which may be demanded in case of additional load which is planned to be applied to the supported construction. It is usually the case, when existing objects are going to be adjusted to new functions (warehouse converted into a production halls equipped with devices generating substantial vibrations) or enlarge (additional floors). Reinforcement can be required due to unexpected events during construction process like excessive and/or uneven settlements. In case of some structures this kind of events can disqualified structure's usability.

In this chapter two existing foundations, defined in the General Specification of RUFEX project (RUFEX, 2010) are analysed. In both cases improvement of foundations' capacity is required. In analysis of both reference projects, type P2b (Figure 6.10) of reinforcement of a deep foundation is tested. This way of improvement consists in group of columns installed under the pile's tip in layer of weaker soil.

The first foundation (Project 1) is studied in order to recognize the influence of distance between reinforcing columns on the reduction of foundation's vertical displacement. For the second foundation (Project 4) two methods of analyzing reinforced soft soil are tested and the improvement brought by installed columns is discussed.

7.2. Existing foundation (Project 1)

Subject of a study is existing railway platform founded on the group of piles. Structure is localized in SNCF Atlantic technical centre (Technicentre Atlantique SNCF), Paris, Rive Gauche, France.

The aim of the study is to numerically reproduce behaviour of the existing deep foundation. Afterwards, the influence of the distance between reinforcing columns on foundation's displacement is studied by parametric study.

7.2.1.1. Foundation without reinforcement

The first step of the numerical modelling is to correctly predict measured displacement of the deep foundation. Calculations are made with the three dimensional finite elements model. Five layers of soil have been pointed out in technical report prepared after site investigation by Terrasol (Terrasol, 2009b). Water table level has been found 7 meters under the ground surface. Sketches presenting basic dimensions and stratigraphy of soil are presented in Figure 7.1.

The first layer is fill, which is deposited on layer of old alluvium. Afterwards, coarse limestone has been reported. The fourth layer is clay. The last detected soil has been sand.

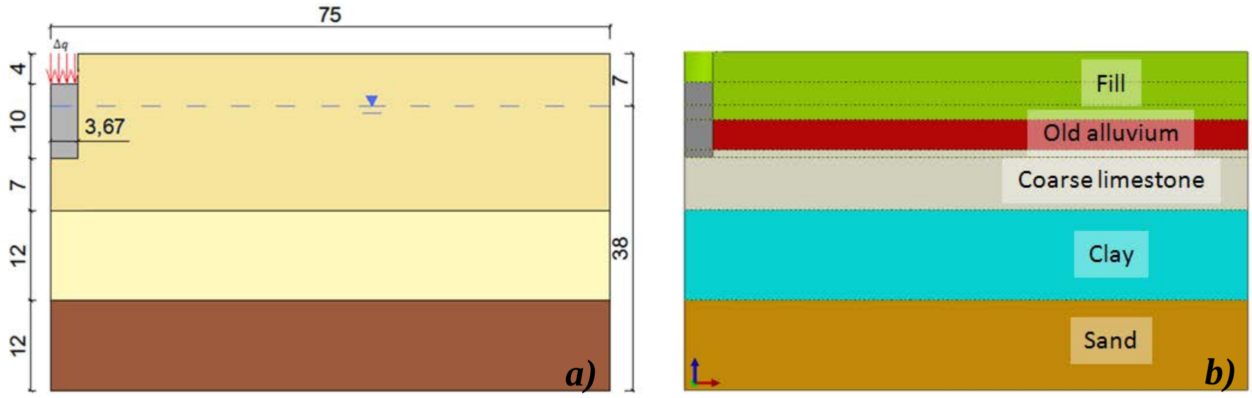

Figure 7.1 a) model dimensions and b) soil stratigraphy

7.2.1.1.1. *Model geometry and mesh*

Existing group of concrete piles, for numerical simulation purposes, has been replaced with equivalent pile with circular section. Diameter and modulus of deformation of the equivalent pile is calculated in accordance with Equation 7.1 and 7.2. Where S_m is section of the group of piles (Figure 7.2), S_{eff} represents effective group section, P_m stands for perimeter and E_b is modulus of deformation of concrete. In these calculations assumed as E_b = 10 GPa. Dimensions of the group of piles and equivalent values can be found in Figure 7.2 and Table 7.1.

$$D_{eq} = \sqrt{\frac{4S_m}{\pi}} \qquad 7.1$$

$$E_{eq} = E_b \frac{S_{eff}}{S_m} \qquad 7.2$$

Table 7.1 Dimensions of the group of piles and equivalent pile representing it in the numerical simulation

Foundation	S_{eff} [m^2]	S_m [m^2]	P_m [m]	D_{eq} [m]	E_{eq} [MPa]
Group of piles	10.17	42.28	26.04	7.34	2400

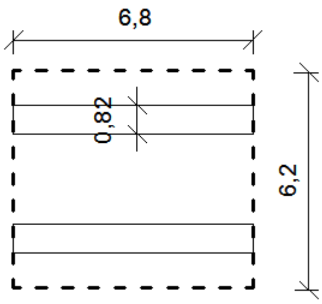

Figure 7.2 Analysed group of piles supporting the railway platform

The 10 meters long pile with diameter 7.34 m has been modelled with fine element code. In order to avoid boundary effect significantly bigger dimensions, regarding the size of the foundation, have been used. To minimize time of very time consuming three dimensional calculations, advantage of planes of symmetry has been used. Thus, only one quarter of the model have been investigated. Mesh and dimensions of the model are presented in Figure 7.3. The finite elements mesh consists of 15-node quadratic triangular prism elements (C3D15). Model's boundary conditions are assumed as: symmetric boundaries on the planes of symmetry, no horizontal displacement in the X axis direction for the wall parallel to the YZ plane and no horizontal displacement in the Y axis direction for the one parallel to the XZ plane. At the bottom, displacements are restricted in the vertical direction.

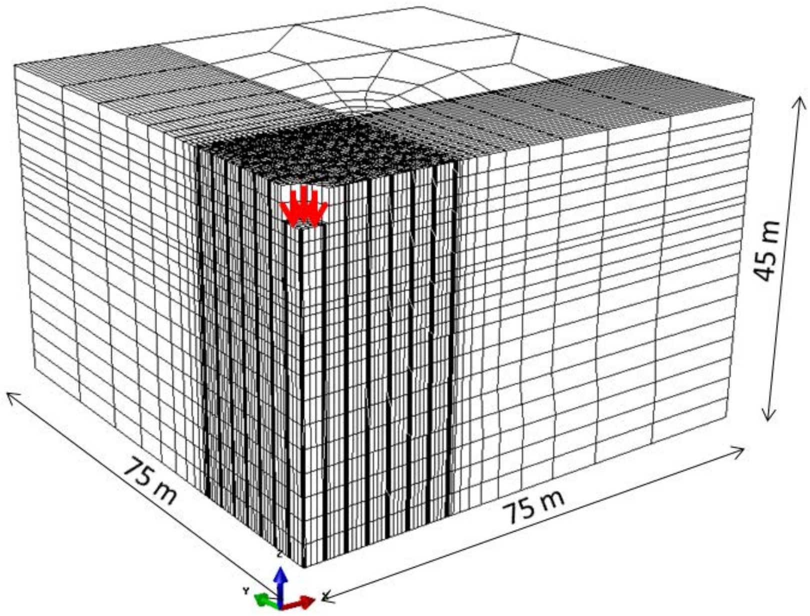

Figure 7.3 Three dimensional mesh and dimensions of the calculated model

Table 7.2 Properties of materials used in numerical calculations

Material	γ [kN/m^3]	ν [-]	E [MPa]	c' [kPa]	ϕ' [°]
Fill	19	0.35	10	-	-
Old alluvium	22	0.35	150	-	-
Coarse limestone	23	0.35	750	200	38
Clay	20	0.35	18	-	-
Sand	20	0.35	160	-	-
Equivalent pile	24	0	2400	-	-

7.2.1.1.2. *Load and constitutive model*

As reported in the report (Terrasol, 2009b), the loading applied to the group of existing concrete piles is F = 55.8 MN. The concentrated force has been replaced with equivalent pressure for the numerical calculations purposes. Its value has been determined in accordance with Equation 7.3. The equivalent pile's head has been loaded with pressure Δp = 1400 kPa.

$$\Delta p = \frac{4F}{\pi {D_{eq}}^2} \qquad 7.3$$

Two types of constitutive models have been used. The concrete equivalent pile has been described by elastic model. Due to lack of more precise data concerning soils, the basic elastic model has been used for four out of five soil layers. Moreover, detected during site investigation water table was not taken into account in numerical simulations. Only coarse limestone, where tip of the pile is embedded, have been defined as material obeying the elastoplastic model with the Mohr-Coulomb failure criterion. Properties of all soils and foundation can be found in Table 7.2. Interface between pile's shaft and soil is modelled by tied contact. Thus, nodes of the shaft and soil being in direct contact are overlapping each other and are bounded.

7.2.1.1.3. *Results*

Results of numerical simulation in terms of vertical displacement and vertical stress are presented in Figure 7.4a and Figure 7.4b respectively. The applied load displaces the pile's head 30.1 mm and its tip 24.8 mm.

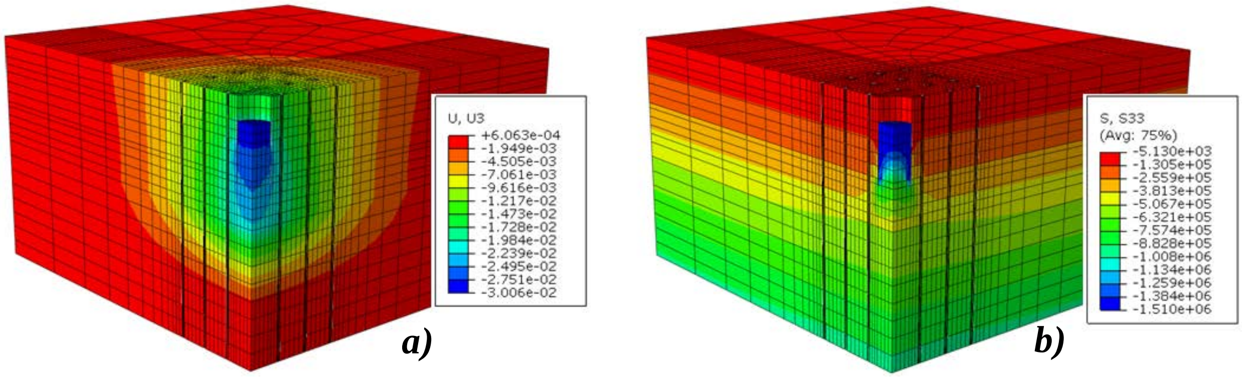

Figure 7.4 Result of the numerical modelling: a) vertical displacement [m], b) vertical stress [Pa]

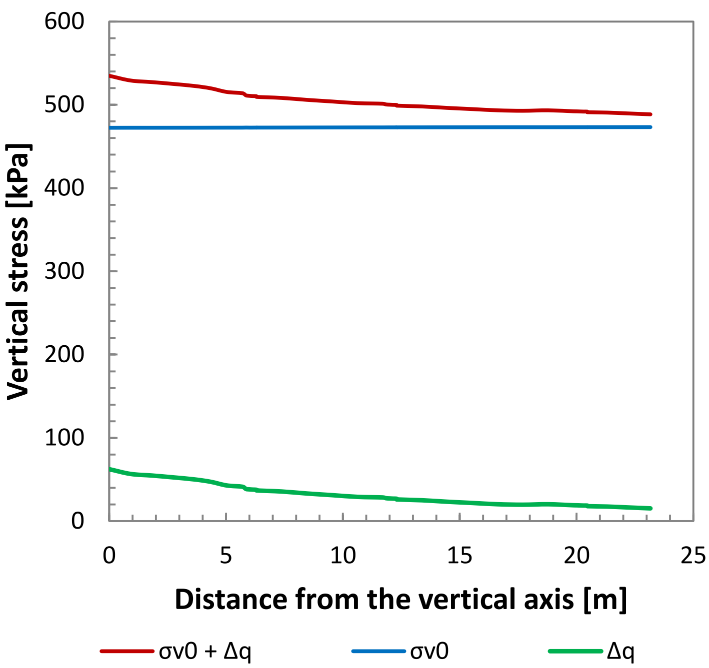

Figure 7.5 Distribution of the vertical stress on the top of the weak layer

7.2.1.2. Reinforced foundation

The next step of the numerical investigation is modelling of the behaviour of deep foundation reinforced by group of SM columns. It has been found that under the layer of stiff coarse limestone, layer of weak clay is situated. As it is mentioned above, for this existing foundation, reinforcement is planned to be installed in a weak layer. Hence, in the numerical simulation columns are assumed in the clay. Due to that length of the column is defined by the height of the strata, L_{SM} = 12 m. Columns diameter has been chosen as D_{SM} = 0.6 m. Columns have been modelled with elastic constitutive model. Its properties compared to the properties of clay can be found in Table 7.3. The modulus of deformation has been assumed as 50 times modulus of the soil. Contact between SM column and surrounding from all sides soil has been assumed the same as the pile – soil one. Hence, nodes of columns mesh, have been bounded with the corresponding nodes in soils.

Decision of the reinforced surface have been taken according to analysis of the vertical stress on the top of the weak layer, presented in Figure 7.5, where σ_{v0} is the stress caused by the geostatic conditions, Δq stands for additional stress propagated to the top of the weak layer caused by load applied to the pile's head, $\sigma_{v0} + \Delta q$ represents sum of the stresses when load applied to the pile is Δp = 1400 kPa.

Table 7.3 Properties of weak soil layer and SM columns used in numerical calculations

Material	γ [kN/m^3]	ν [-]	E [MPa]	c' [kPa]	ϕ' [°]
Weak layer - Clay	20	0.35	18	-	-
Soil Mixing column	22	0.35	900	-	-

Influence of distance between columns, *a*, on the displacement of the pile has been examined. Columns have been organised under the pile in a way presented in Figure 7.6a. Because of significant danger, which any interference with the soil might bring, none of columns has been assumed under the pile. Keeping in mind findings of the study of deep foundation reinforced by SM columns, presented in Chapter 6, this assumption considerably reduces efficiency of the reinforcement.

Area 22 m x 22 m has been reinforced by columns. Results of the calculations in terms of pile's head and tip displacements and improvement are presented in Table 7.4 and Table 7.5 respectively. The influence of the distance between columns on the pile's head and tip displacements is visualised in Figure 7.6b. As it has been expected, increase of spacing leads to decrease of the improvement. The relation is linear for a = 3 m, 4 m and 5 m, afterwards it starts to stabilise.

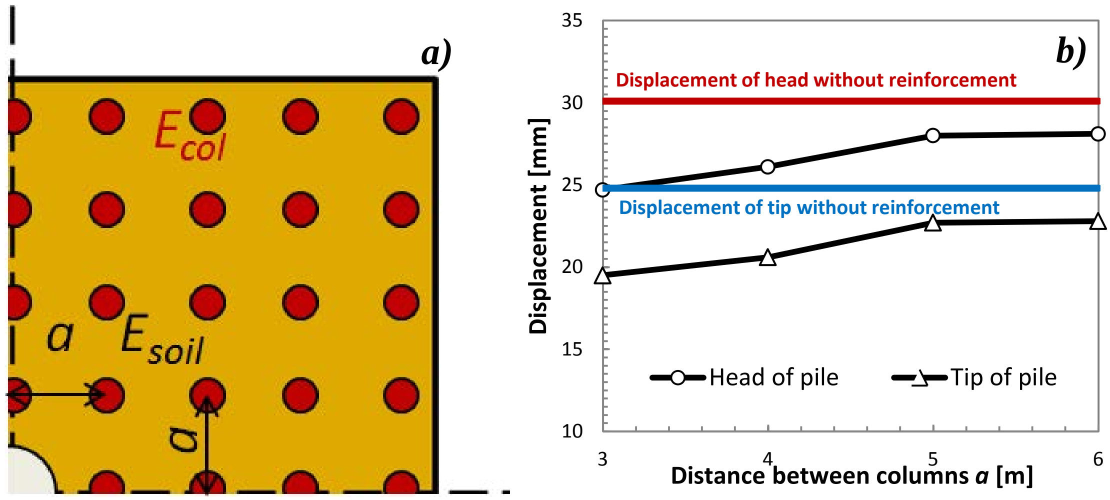

Figure 7.6 a) weak soil under the deep foundation reinforced by group of SM columns, b) reduction of the pile's head and tip displacement as a function of distance between reinforcing columns

Figure 7.7 depicts vertical stress - displacement distribution at the top of the reinforced layer as a function of distance from the pile's axis. Presented example visualised reinforced case, where columns are spaced each 5 m. Distance between SM elements is visible due to peaks appearing each 5 m. Both, displacement and stress are decreasing with the distance from the foundation's axis. The highest displacement is observed under the foundation. It achieves about 19.7 mm displacement. Displacement calculated 22 m from the pile's axis is about 6.0 mm.

Table 7.4 Pile's head and tip displacements with and without reinforcement carried out by group of SM columns under the deep foundation

Displacement	Without	a [m]			
		3	4	5	6
Head [mm]	30.1	24.7	26.1	28.0	28.1
Tip [mm]	24.8	19.5	20.6	22.7	22.8
Difference [mm]	5.3	5.2	5.5	5.3	5.3

Table 7.5 Improvement provided by the reinforcement carried out by group of SM columns under the deep foundation

Displacement	Improvement [%]			
	3	4	5	6
Head [%]	17.9	13.3	7.0	6.6
Tip [%]	21.4	16.9	8.5	8.1

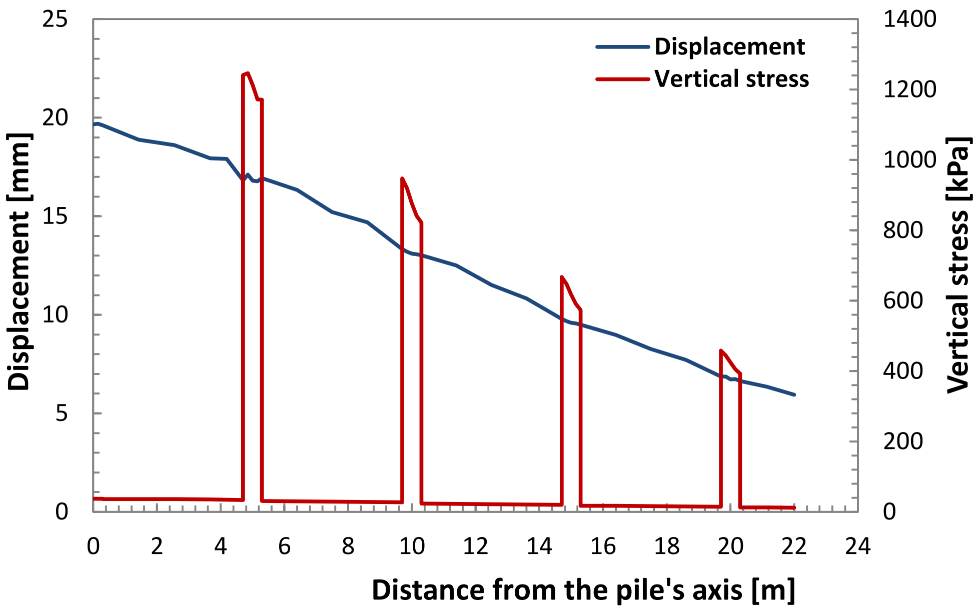

Figure 7.7 The vertical stress and vertical displacements on the top of the weak layer of soil, reinforced by column spaced each 5 m

7.2.1.3. Conclusions

The aim of the study was to investigate the influence of the distance between reinforcing columns on the vertical displacement of existing deep foundation. In order to simplify three dimensional calculations, real foundation has been replaced by an equivalent pile. The symmetry of the model has been used, thus only one quarter of the foundation the has been studied. Another simplification used in the simulation is constitutive model of materials. Due to lack of more precise data, foundation, columns, and all layers are modelled with elastic law. The only exception is layer between foundation and the layer reinforced by columns. It is described by model with MC criterion. Due to risk which brings creation of columns in weak soil directly under the foundation, SM elements have been arranged around the pile. The positive effect of the reinforcement has been presented. A linear relation between displacement of foundation's head and spacing of columns has been found. The same tendency has been observed for the displacement of the pile's tip.

Presented results are theoretical analysis of the behaviour of the reinforced deep foundation and need to be validated by field tests. Column installation process has not been taken into account in the study. Lack of many properties of soils, as well as simplification of the foundation shape do not allow performing more detailed investigation. Nevertheless, it gives general knowledge of the efficiency of the reinforcement.

7.3. Existing foundation (Project 4)

Numerical calculations for the second reference project, called in RUFEX specification Project 4 (RUFEX, 2010), have been performed. An existing monolith deep foundation supporting a gantry crane (ArcelorMittal site, Mardyck, Dunkerque, France) has been modelled. Displacement of the foundation has been considered as unacceptable, that is why it needs to be reinforced. The reinforcement, executed by group of sixteen SM columns, assumed in the three weak layers under the tip of the foundation, has been numerically analysed.

The aim of the study is to investigate the influence of the way of modelling improved weak soil on the displacement of a deep foundation.

7.3.1.1. Foundation without reinforcement

Monolith deep foundation has been simulated with the three dimensional model. Shape of the foundation, its dimensions, and stratigraphy of the ground have been assumed in accordance with technical report, prepared after site investigation (Terrasol, 2009a). The length of the existing foundation is equalled to 10 m. Its cross section is presented in Figure 7.8. Foundation's geometry can be found in Table 7.6, where S_m is the area, P_m stands for perimeter and L is length of the foundation.

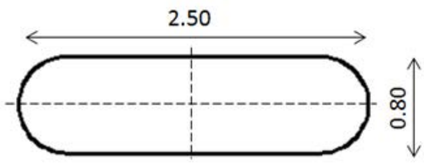

Figure 7.8 Cross section of the monolith deep foundation

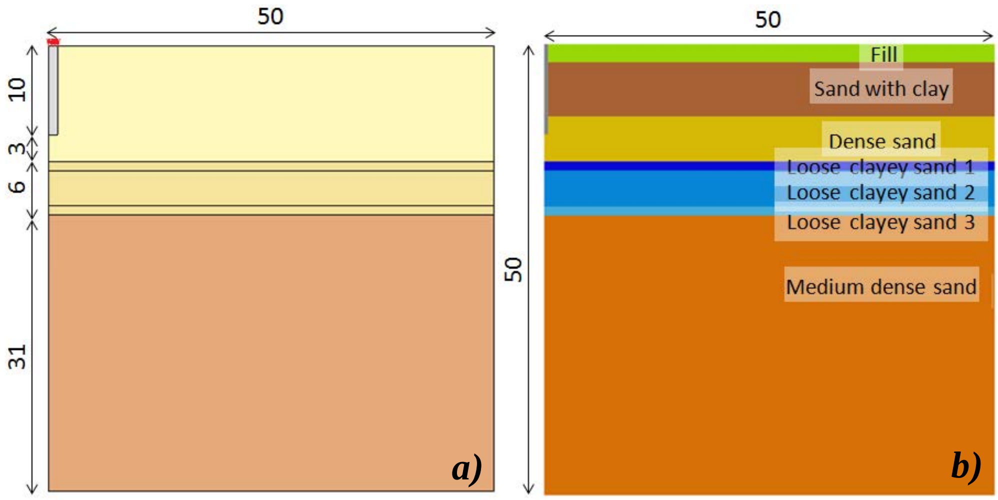

Figure 7.9 a) model dimensions [m] and b) stratigraphy

Table 7.6 Geometry of the foundation

Foundation	S_m [m^2]	P_m [m^2]	L [m]
Monolith foundation	1.86	5.90	10.00

Dimensions of the modelled case are presented in Figure 7.9a. Geotechnical profile of the site is presented in Figure 7.9b. The five layers of soils have been distinguished: fill, sand with clay, dense sand, loose clayey sand and medium dense sand. In the loose clayey sand (weak layer), three sub layers can be pointed out. They are called by numbers, according to the order of their appearance during site investigation.

7.3.1.1.1. *Model geometry and mesh*

A 10 meters long deep foundation has been modelled in its real shape. Model with significantly bigger dimensions, 50 m x 50 m x 50 m (length x width x height) has been chosen in order to avoid interferences caused by the boundary conditions. To reduce duration of the time consuming calculations, again advantage of planes of symmetry has been used, hence one quarter of the foundation has been analysed. Mesh and dimensions of the model are presented in Figure 7.10. Finite elements mesh consists of 15-node quadratic triangular prism elements (C3D15). Boundary conditions are assumed as: symmetric boundaries are applied to the planes of symmetry. Displacements in the X and Y axes direction are restricted on the wall parallel to the YZ and XZ respectively. At the bottom, vertical direction displacements are not allowed.

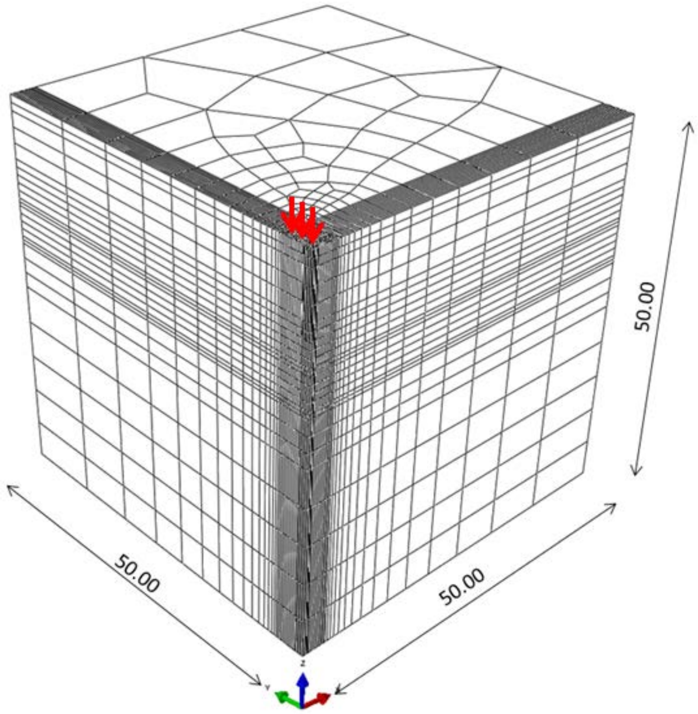

Figure 7.10 Three dimensional mesh and dimensions of the calculated model

Table 7.7 Properties of materials used in numerical calculations

Material	γ [kN/m^3]	ν [-]	E [MPa]	c [kPa]	ϕ [°]	ψ [°]
Fill	20	0.33	0.001	0.1	15	1
Sand with clay	20	0.33	0.001	0.1	15	1
Dense sand	20	0.33	80.000	0.1	35	5
Loose clayey sand 1	20	0.33	4.000	0.1	28	2
Loose clayey sand 2	20	0.33	8.000	0.1	28	2
Loose clayey sand 3	20	0.33	4.000	0.1	28	2
Medium dense sand	20	0.33	30.000	0.1	33	3
Pile	24	0.00	10500.000	-	-	-

7.3.1.1.2. *Load and constitutive model*

According to site report (Terrasol, 2009a), foundation is loaded by concentrated force F = 3150 kN. In numerical model, force has been replaced with equivalent pressure, calculated by Equation 7.3, Δp = 1700 kPa.

Provided shear properties of all analysed soils allow using elastoplastic constitutive model with MC failure criterion. Only concrete foundation is modelled with elastic law. Properties of all materials can be found in Table 7.7. Three weak layers are characterized by significantly low modulus of deformation, 4 MPa for first and third sub layer and 8 MPa for the middle one. Interaction between foundation's shaft and surrounding soil is modelled by interface elements with zero initial thickness, obeying the Coulomb failure criterion. Values of the friction coefficient corresponds to the soil layer (Table 7.8).

Table 7.8 Properties of interface between soil and deep foundation

Parameter	Unit	Fill	Sand with clay	Dense sand
Friction angle of soil	ϕ [°]	15.0	15.0	35.0
Friction coefficient	μ_f [-]	0.20	0.20	0.53
Interface friction angle	ϕ^{int} [°]	11.4	11.4	27.7
Interface friction / Internal friction $\tan \phi^{int} / \tan \phi^{soil}$	[%]	75	75	75

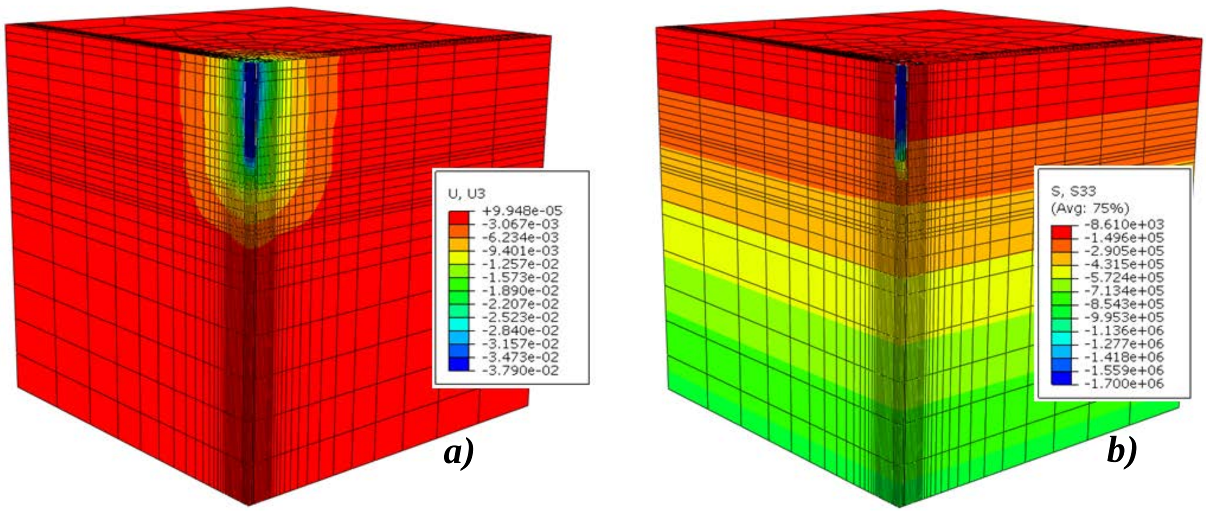

Figure 7.11 Result of the numerical modelling: a) vertical displacement [m], b) vertical stress [Pa]

7.3.1.1.3. *Results*

Obtained results, in terms of vertical displacement and vertical stress are presented in Figure 7.11a and Figure 7.11b respectively.

Figure 7.12a depicts behaviour of unreinforced foundation. Presented curves illustrate displacement of the foundation's head and tip as a function of the applied load. Pressure Δp = 1700 kPa, causes foundation's displacement equalled to 30.79 mm and 29.33 mm for head and tip respectively.

In Figure 7.12b contribution of shaft and tip capacity is presented. The contribution of each part of the foundation varies during the loading. It can be seen that tip of the foundation is more loaded. However, the difference between contributions is very small. Its maximal value, about 4.0% can be observed for 15 mm displacement, where tip takes 52.5% and shaft 47.5% of the total pressure.

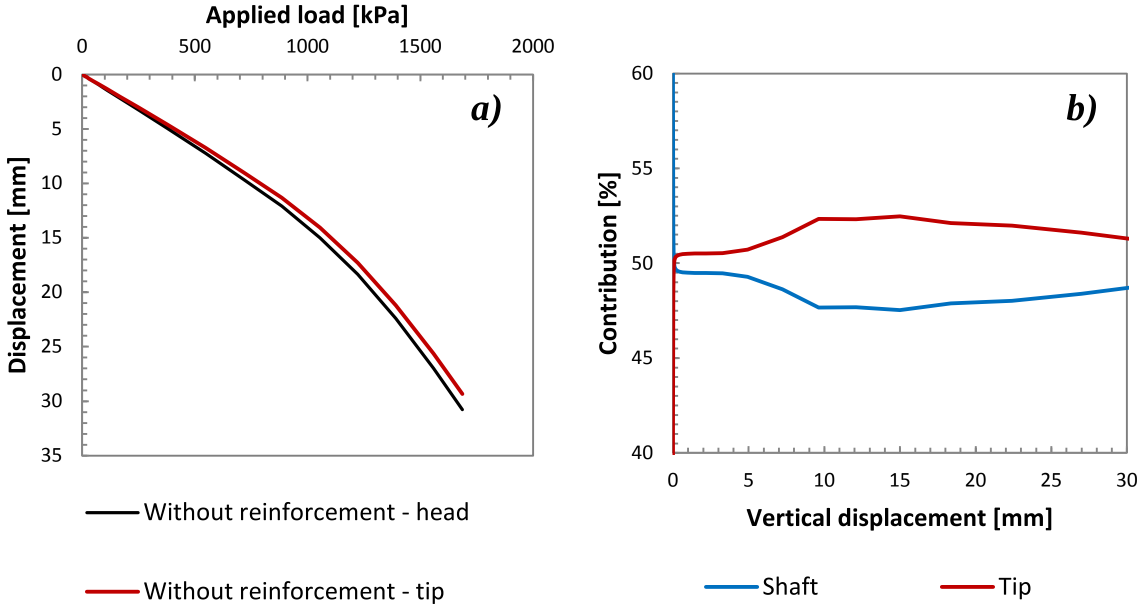

Figure 7.12 Results of numerical modelling of monolith deep foundation without reinforcement: a) behaviour of foundation, b) contribution of foundation's tip and shaft

7.3.1.2. Reinforced foundation

The next step of the numerical modelling is simulation of the foundation reinforced by the group of sixteen columns. Only four of them are modelled due to simplification to one quarter. Similarly to reference Project 1, SM columns are placed in the weak layer under the foundation. Due to shape of the foundation's cross section, reinforced area of soil (3.400 m x 4.250 m) is rectangular. Columns are spaced each 1.700 m in shorter edge of the area and each 2.125 m in the longer one.

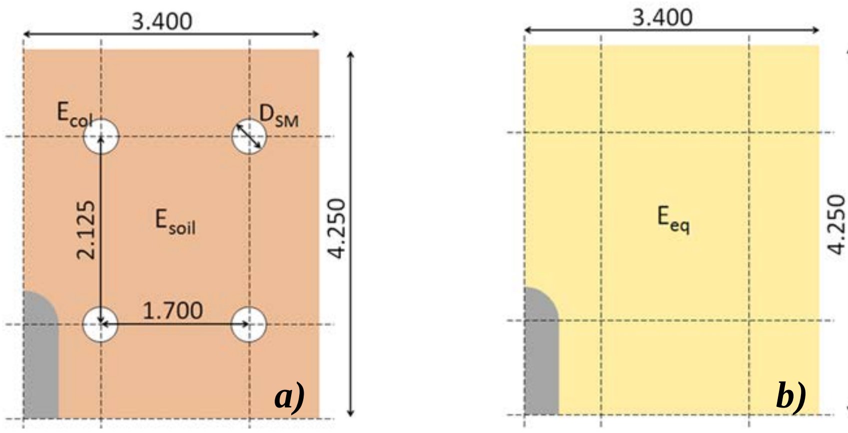

Figure 7.13 Patterns of reinforcing columns placed in the weak layers of soil: a) direct method, b) simplified method

Even though reduction of model size has been accomplished by analysing only one quarter, computation process lasts considerable amount of time. Ou, et al. (Ou, et al., 1996) proposed further simplification for complicated and time consuming calculations. In their study of the embankment built on soil treated by SM columns, they proposed replacing the reinforced ground consisting soil and columns, with homogeneous material characterized by equivalent properties. If this kind of solution was capable of correct preliminary estimation of the behaviour of the reinforced foundation, it would be much more convenient for engineers designing reinforcement. Moreover, in case of axisymmetric foundations, it would permit using axisymmetric type of calculations. In order to verify the simplified method, obtained in this way results have been compared to the one acquired from the direct method. By the direct method, calculations of columns installed in soil are understood.

Two method of calculations are presented in Figure 7.13, direct (Figure 7.13a) and simplified (Figure 7.13b).

7.3.1.2.1. *Direct method*

The height of the weak layer is 6 m, hence reinforcing columns are assumed as 6 m long. Columns diameter has been chosen as D_{SM} = 0.4 m.

Due to more than one sub layer of weak soil, two ways of analysing SM elements have been studied. The first approach (Direct method 1) assumes that column consists of three parts. Thus, the column's modulus of deformation is a function of depth (Figure 7.14a). Modulus of deformation of columns is calculated, as previously, as 50 times modulus of the soil. The second approach (Direct method 2) consists in analysing columns as homogeneous elements (Figure 7.14b). In this case modulus of deformation has been assumed as weighted average of the modulus calculated for the heterogeneous column. Unconfined compressive strength (USC) of each part of column is assumed according to similar cases presented in the literature. Cohesion of column is taken as half of the UCS (Andromalos, et al., 2000) whereas internal friction angle and dilation angle are assumed as 1°.

For both approaches, SM columns are characterized by elastic perfectly plastic model with MC failure criterion. Their properties can be found in Table 7.9. Values of unconfined compressive strength (UCS) of parts of SM column were assumed according to literature results (Taki & Yang, 1991).

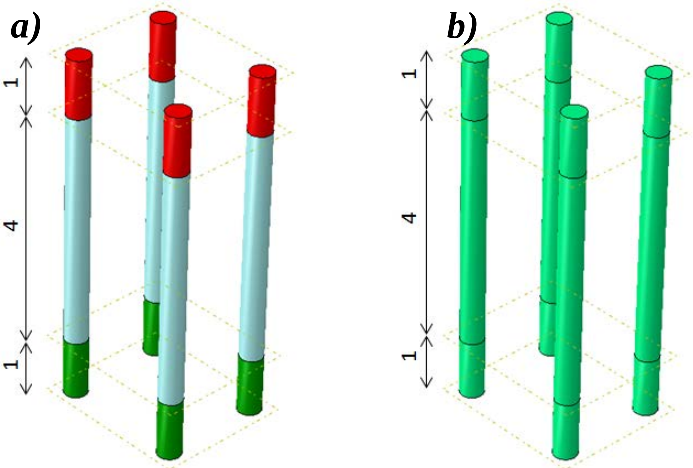

Figure 7.14 Group of SM columns reinforcing intersecting three layers of weak soil, a) heterogeneous SM columns (Direct method 1), b) homogeneous SM columns(Direct method 2)

Table 7.9 Properties of SM columns

Material		γ [kN/m³]	ν [-]	UCS [kPa]	E [MPa]	c [kPa]	ϕ [°]	ψ [°]
Heterogeneous column	Layer 1	22	0	3000	200	1500	1	1
	Layer 2	22	0	4000	400	2000	1	1
	Layer 3	22	0	3000	200	1500	1	1
Homogeneous column		22	0	-	400	1500	1	1

Calculations are performed with the three dimensional model meshed as presented in Figure 7.10. Interaction between columns and soil is assumed as a tied contact, without additional interface elements.

Obtained displacements of head and tip of the deep foundation are presented in Figure 7.15. Figure 7.15a illustrates displacement of the foundation's head as a function of applied pressure, whereas Figure 7.15b represents movement of the foundation's tip as a function of the stress at the tip. Calculations with the direct method 1 (heterogeneous column) effects with

27.90 mm and 26.43 mm displacements of the head and the tip respectively. Thus, displacement has been reduced by about 2.90 mm. Displacements acquired with the direct method 2 (heterogeneous column) are 27.44 mm and 25.98 mm for head and tip respectively. It means that pile's displacement has been reduced by 3.35 mm. Insignificant difference between approaches can be observed (Table 7.10). Discrepancies between acquired results are less than 0.5 mm. It can be assumed that both approaches can be each other's equivalent. Similarities can be explained by insignificant differences between properties of each part of the column.

Improvement of the foundation's performance is presented in Table 7.11. It varies between 9.4% and 9.9% for the head and the tip for heterogeneous columns and 10.9% and 11.4% for homogeneous elements.

Table 7.10 Foundation's head and tip displacements with and without reinforcement carried out by group of SM columns under the deep foundation

Displacement	Approach		
	Without	Heterogeneous column Direct method 1	Homogeneous column Direct method 2
Head [mm]	30.79	27.90	27.44
Tip [mm]	29.33	26.43	25.98
Difference [mm]	1.46	1.46	1.47

Table 7.11 Improvement provided by the reinforcement carried out by group of SM columns under the deep foundation

Displacement	Approach	
	Heterogeneous column Direct method 1	Homogeneous column Direct method 2
Head [%]	9.4	10.9
Tip [%]	9.9	11.4

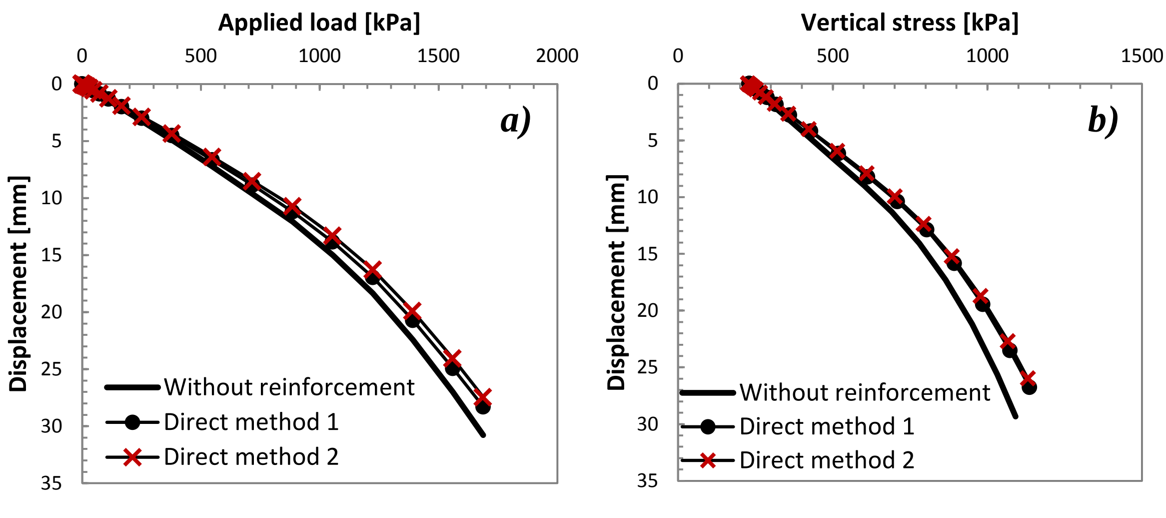

Figure 7.15 Behaviour of: a) the head of monolith deep foundation with and without reinforcement. Simulations performed with heterogeneous (Direct method 1) and homogeneous columns (Direct method 2), b) the tip of monolith deep foundation with and without reinforcement. Simulations performed with heterogeneous and homogeneous columns

Participation of shaft and tip in bearing applied stress as a function of the displacement of the foundation's head is presented in Figure 7.16. As it was found in theoretical study of the pile foundation, presented in Chapter 6, presence of SM columns influence mainly tip capacity. Columns introduced to the weak soil, cause rise of the tip capacity during the whole loading process. The same trend as in case of unsupported foundation can be observed. Contribution of shaft is stable at the beginning, till about 4.0 mm and 3.0 mm displacement, for case without and with reinforcement respectively. Then, it rapidly decreases till about 9.5 mm and 9.0 mm for unreinforced and reinforced foundation. Afterwards, decline stabilizes and shaft contribution achieves its minimal value: 47.5% for case without support after 15 mm. In case of reinforced foundation, results obtained by calculations with both direct methods are comparable. Minimal shaft contribution is accomplished about 20.0 mm and equals to 46.0% and 46.5% for homogeneous and heterogeneous columns. The last part of the loading participation of the shaft increases until 48.7% for foundation without reinforcement. Shaft of the supported foundation takes about 47.0%.

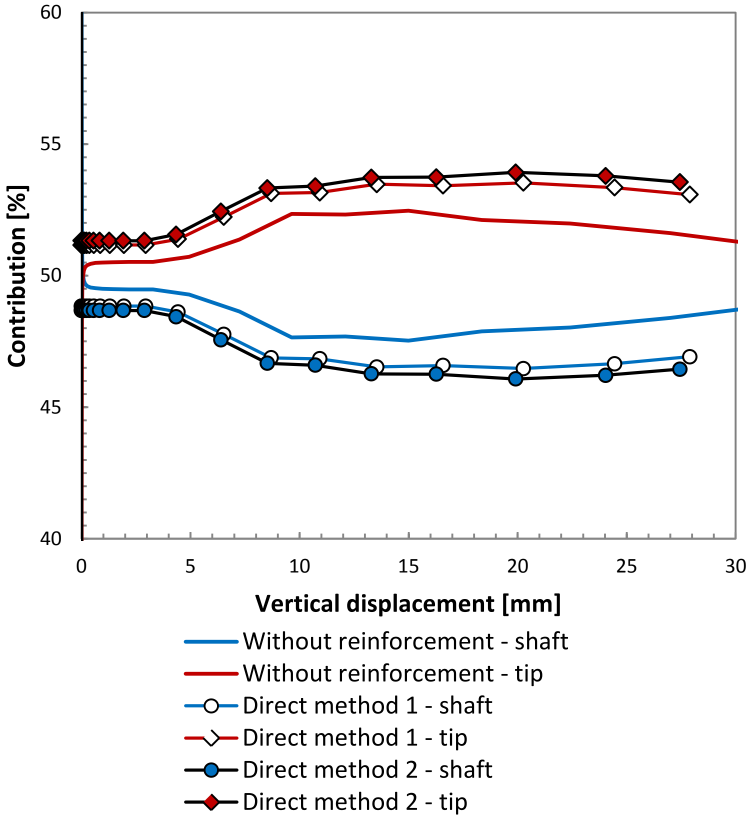

Figure 7.16 Contribution of foundation's shaft and tip as a function of the displacement of the foundation's head

7.3.1.2.2. *Simplified method*

The simplified method, proposed by Ou, et al. (Ou, et al., 1996) and widely used in engineering practice by Terrasol, based on the concept of replacing the reinforced soil, by equivalent material (Figure 7.17). Properties of the equivalent material can be calculated according to characteristics of the soil and SM elements. This approach can be useful for preliminary calculations. It allows using of the axisymmetric type of calculations, where due to its specific columns cannot be simulated in their real shape.

Modulus of deformation of the new material is calculated according to Equation 7.4. Where h is the height of the reinforced layer, U_{yh} is vertical displacement of the head of the SM column, U_{yt} is vertical displacement of the tip of the SM column and Δq stands for the average stress on the top of the weak layer due to load applied to the foundation.

$$E_{eq} = \frac{\Delta q h}{U_{yh} - U_{yt}} \qquad 7.4$$

In order to obtain displacements of the SM column, additional calculations need to be performed. Complementary model is necessary to obtain needed parameters (Equation 7.4).

The concept of the complementary model consisted in modelling quarter of the SM column, reinforced layer and layer directly under it. The model is presented in Figure 7.18b. The dimensions of the model correspond to half distance between reinforcing columns, so 0.850 m and 1.063 m.

The complementary model is loaded in two stages (Figure 7.18a). Firstly, only two layers of soils are analysed. To the top of the complementary model pressure σ_{v0} = 265.01 kPa is applied. The σ_{v0} represents geostatic stress at the level of the top of the weak layer. Its value needs to be obtained from the model of the deep foundation without reinforcement. Secondly, quarter of SM column is added to the complementary model. Moreover additional pressure Δq = 13.48 kPa is applied. The Δq stands for stress at the top of the weak layer caused by load applied to the foundation (Δp = 1700 kPa). Thus, in the second stage of loading, the complementary model is loaded by $\sigma_{v0} + \Delta q$ = 278.49 kPa. Due to unequal distances between reinforcing columns in both planes (1.700 m and 2.125 m) the Δq is taken as average at the top of the reinforced weak layer.

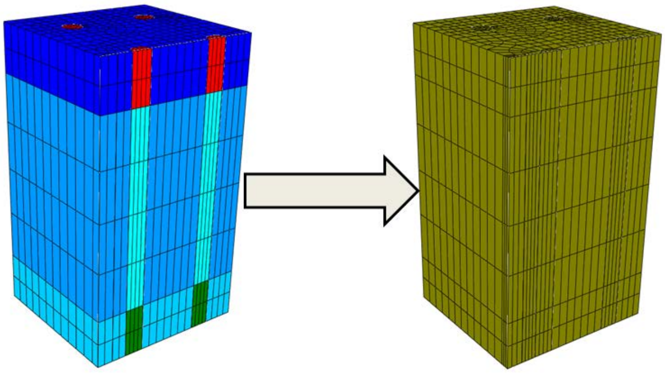

Figure 7.17 Concept of simplified method, reinforced area under the foundation

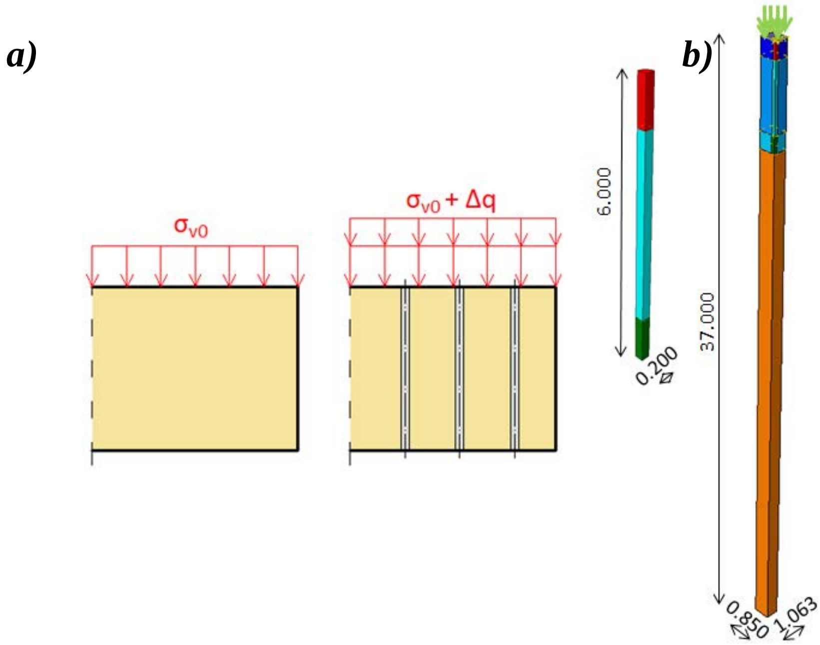

Figure 7.18 Complementary model: a) stages of loading, b) geometry

Table 7.12 Results obtained from complementary model

Displacement of head U_{yh} [mm]	Displacement of tip U_{yt} [mm]	Difference U_{yh} - U_{yt} [mm]	Δq [kPa]	E [MPa]
15.91	10.61	5.30	13.48	15.30

Table 7.13 Properties of equivalent material

Material	γ [kN/m^3]	ν [-]	E [MPa]	c [kPa]	ϕ [°]	ψ [°]
Equivalent soil	20	0.33	15.30	0.001	28	2

Results of the calculations performed with the complementary model are presented in Table 7.12. These displacements allow calculation of the equivalent modulus of deformation according to Equation 7.4.

Properties of equivalent material, used in the further analysis, are presented in Table 7.13. New modulus of deformation is assumed as 15.30 MPa. It is relatively higher value regarding 4.00 MPa and 8.00 MPa which have been reported for weak sub layers. However, is significantly smaller comparing to 200.00 MPa and 400.00 MPa assumed for parts of SM column (direct method 1). The shear properties and unit weight are assumed as for weak soil layer.

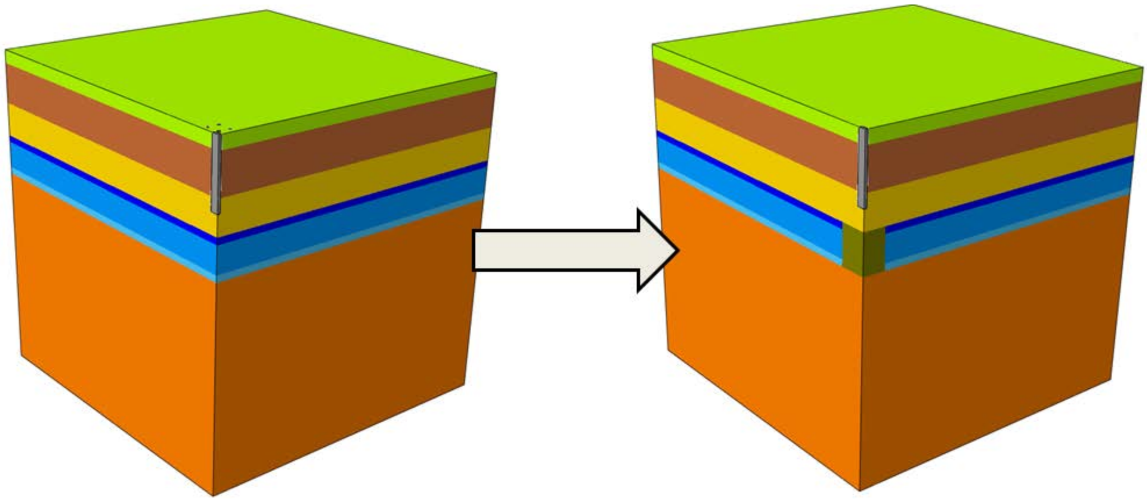

Figure 7.19 Concept of the simplified method

The new, equivalent material has been used in modelling of the behaviour of deep foundation (Figure 7.19). Results of the study in terms of displacement of the head and the tip of the foundation are presented in Figure 7.20 and Table 7.14. Reinforcement reduces the displacement of the foundation's head and tip by 2.49 mm and 2.57 mm respectively.

Analysis of contribution of shaft's and tip's capacity in taking total pressure applied to the foundation, can be found below in Figure 7.22.

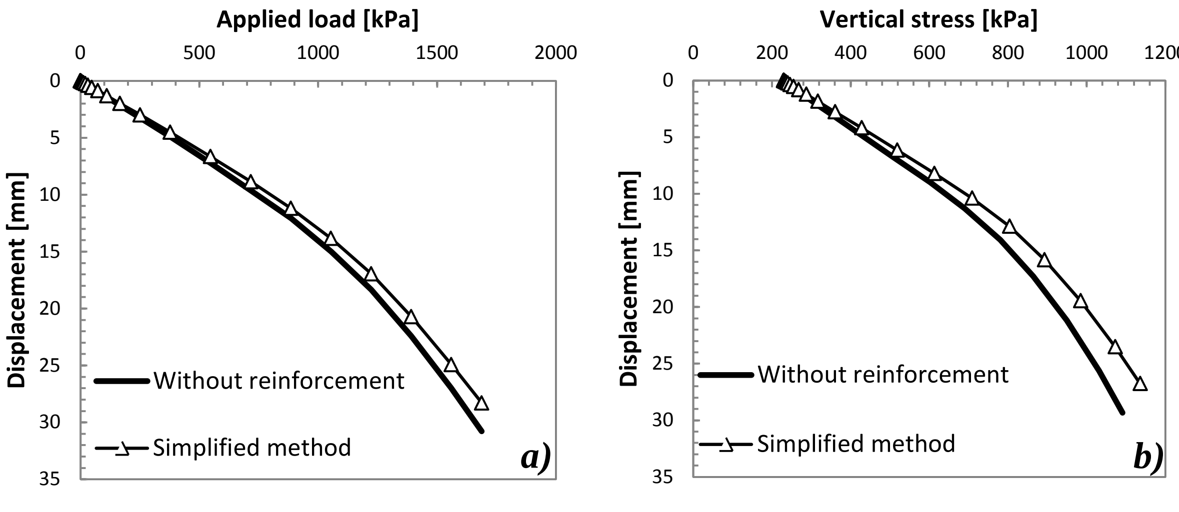

Figure 7.20 Behaviour of: a) the head of monolith deep foundation with and without reinforcement, b) the tip of monolith deep foundation with and without reinforcement. Simulations performed with simplified method of calculations

Table 7.14 Foundation's head and tip displacements with and without reinforcement carried out by group of SM columns under. Calculated with simplified method

Displacement	Without	Simplified method
Head [mm]	30.79	28.30
Tip [mm]	29.33	26.76
Difference [mm]	1.46	1.54

7.3.1.2.3. *Comparison between methods*

Two methods of modelling reinforced layer of soil have been studied. Results of the all three calculations are compared with each other in Figure 7.21a (the head of the foundation) and Figure 7.21b (the tip of the foundation). Values of displacements and improvement brought by the reinforcement can be found in Table 7.15 and Table 7.16 respectively. The differences between displacement of the head and the tip of the foundation are comparable and vary between 1.46 mm and 1.54 mm. Also values of the displacements acquired from all methods are very similar. They vary between 27.44 mm and 28.30 for the head and 26.76 mm and 25.98 for the tip of the foundation. Hence, difference between results obtained from all three methods is about 1 mm. Efficiency of the reinforcement is relatively low and equals to about 10 %.

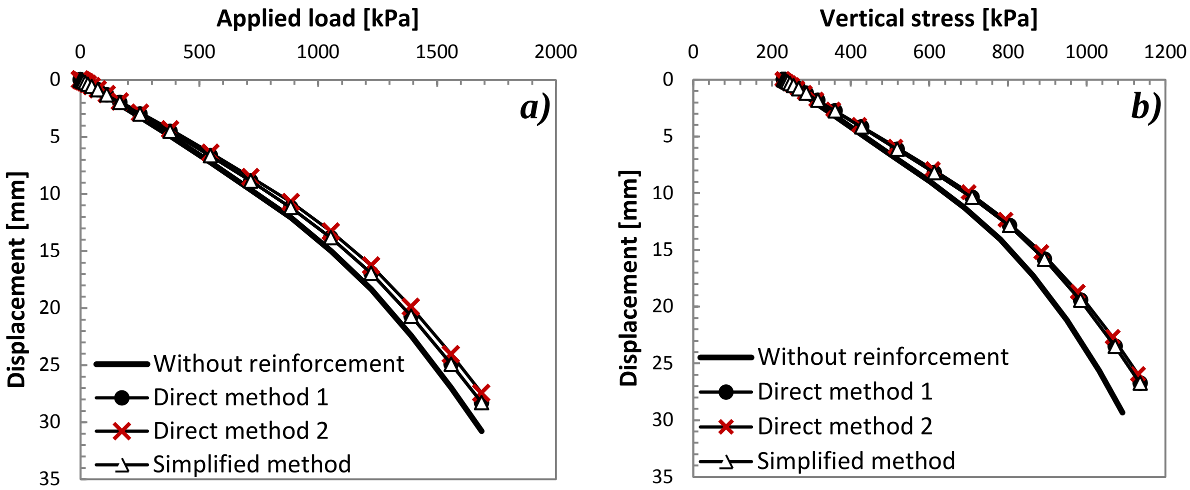

Figure 7.21 Behaviour of: a) the head of monolith deep foundation with and without reinforcement, b) the tip of monolith deep foundation with and without reinforcement. Simulations performed with direct and simplified method of calculations

Table 7.15 Foundation's head and tip displacements with and without reinforcement carried out by group of SM columns under, obtained by direct and simplified methods

Displacement	Without	Approach		
		Direct method 1 Heterogeneous column 	Direct method 2 Homogeneous column 	Simplified method 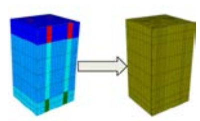
Head [mm]	30.79	27.90	27.44	28.30
Tip [mm]	29.33	26.43	25.98	26.76
Difference [mm]	1.46	1.46	1.47	1.54

Table 7.16 Improvement provided by the reinforcement carried out by group of SM columns under the deep foundation. Calculations carried out by direct and simplified methods

Improvement	Approach		
	Direct method 1 Heterogeneous column 	Direct method 2 Homogeneous column 	Simplified method 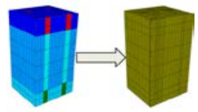
Head [%]	9.4	10.9	8.1
Tip [%]	9.9	11.4	8.8

Figure 7.22 depicts contribution of shaft and tip capacities. Results of all reinforced cases as a function of the displacement of the foundation's head are presented together and compared. Both direct methods effects with very alike distribution of load. In case of reinforcement modelled as equivalent layer, similar tendency can be observed. Contribution of tip is stable at the beginning of the loading till about 3.0 mm. Then it increases till 14.0 mm, where achieves its maximum about 54.5%. After that, a slow decrease of the tip's participation can be noticed. It continues till the end of the loading, Δp = 1700 kPa.

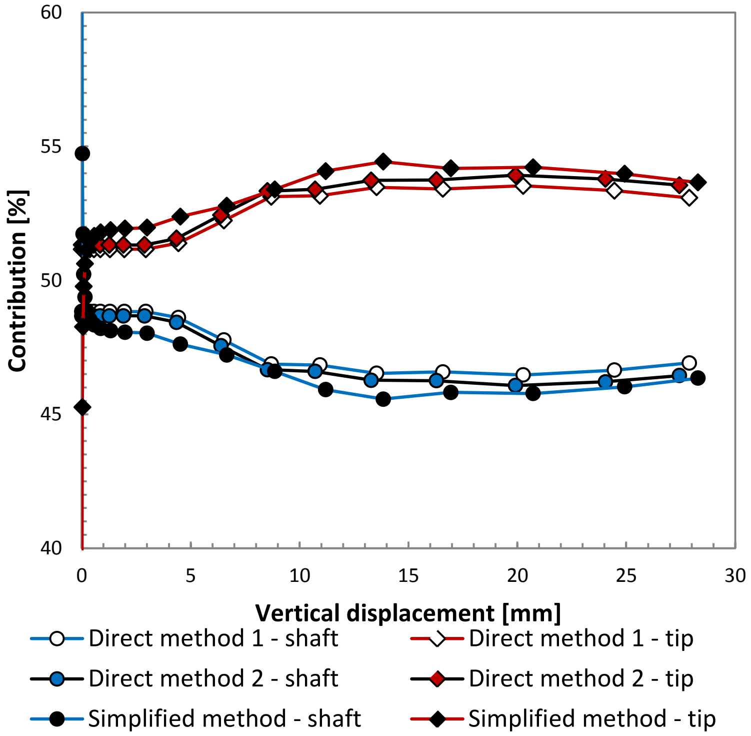

Figure 7.22 Contribution of shaft and tip capacity as a function of displacement of the foundation's head

7.3.1.3. Conclusions

The aim of the study has been to analyse the effect of the reinforcement, on the displacement of the existing monolith deep foundation. The method of the reinforcement and the behaviour of the supported and unsupported foundation have been presented. Two direct methods of analysing SM column created in three layers of weak soil have been presented. The first one consisted of heterogeneous column, where the modulus of deformation changes with depth. The second one, assumed the homogeneous SM element. Results obtained from calculations carried out with both methods, are very alike. Reason of the similarities can be explained by comparable properties of soils, where column was installed. Taking into account findings provided by the full scale loading test of the SM column executed in Vernouillet, France (Paragraph 4.2), the modelling with the heterogeneous column seems to be more appropriate. It has been found that each part of the column installed in multiple layers has different properties.

Two methods of analyzing improved weak soil have been tested. Simplified method based on concept of replacing the reinforced soil with anisotropic material characterized by equivalent properties. Only modulus of deformation of the new material has been calculated. The shear parameters have been assumed the same as the parameters of the reinforced soil. Nevertheless, displacements obtained with the simplified method are coherent with ones calculated with direct methods. It can be concluded that, simplified method can be used to preliminary estimate behaviour of the deep foundation. However further studies need to be performed in order to find a way of estimating shear properties of the equivalent material.

The vertical displacement of the monolith deep foundation decreases due to the reinforcement by sixteen SM columns, nevertheless the improvement (about 10%) is low. However, it is important to remember that the diameter of columns is just 0.40 m. Moreover, the analysed in this study foundation is a support of a gantry crane. In case of this kind of structures, even small reduction of the vertical displacement can be significant and can have influence on their performance. In order to proceed with a design of the reinforcement, it is necessary to perform a field test to ensure at least correct properties of the SM columns.

7.4. Conclusions

Two existing foundations, defined in the General Specification of RUFEX project (RUFEX 2010) have been analysed. The positive influence of the reinforcement of the weak layer of soil situated deeper, under the foundation have been presented.

The aim of the Project 1 was to investigate the influence of the distance between reinforcing columns on the reduction of displacement of a deep foundation. It was found that increase of the distance between reinforcing elements makes improvement less efficient. A linear relation between these two parameters was found.

In analyses of Project 4, the influence of the way (homogeneous and heterogeneous) of modelling column passing three weak layers was investigated. It was found, that in this particular case, the way of modelling columns is not significant due to comparable properties of all three layers. Nevertheless, columns installed in more than one layer should be analysed as heterogeneous.

Two methods of analyzing improved weak soil were presented. The direct method consists in modelling soil and installed SM elements. The simplified method assumes that the whole reinforced area is replaced by new material with equivalent properties. The results of the modelling reveal a coherent reduction of the foundation’s vertical displacement among both methods. Hence, it can be concluded that the simplified method could be used to preliminary estimate the behaviour of the reinforced deep foundation. However, further studies are required to find a way of estimating shear properties of the equivalent material.

Presented investigations are theoretical analyses of the behaviour of the improved deep foundations, while reinforced is placed under the foundation, inside soil with much lower elastic properties. Column installation process has not been taken into account in the studies. Lack of many properties of soils (just elastic ones in case of Project 1) do not allow performing more detailed investigation. Nevertheless, it gives general knowledge of the efficiency of the reinforcement.

8. Conclusions and perspectives

The Soil Mixing method is frequently used as a soil improvement, since 1960s, when it was created. Its biggest advantages is fact that can be applied to almost all ground conditions with minimal environmental impact. In this context, using mixed-in-place columns as reinforcement of the foundations seems to be reasonable. Until now, no specific algorithm for engineers, who want to calculate SM elements has been proposed. Even though, some general guides are given, an investigation by field loading tests and numerical modelling are indispensable.

The aim of this work was to analyse the influence of soil reinforcement executed by the Soil Mixing method on the behaviour of shallow and deep foundations. Numerical investigations were carried out with the use of Finite Element (FE) analyses in ABAQUS. Simulations were attempts to identify the mechanisms guiding the performance of supported foundations.

8.1. Behaviour of a Soil Mixing column

Two investigations of the behaviour of a Soil Mixing column were carried out. Firstly, a full scale loading test was modelled. Analysed column was installed in two soil layers. Study revealed that in such cases column should be modelled as heterogeneous element, where properties are function of its length.

Secondly, a set of simulations reproducing loading tests of single and group of small scale columns was carried out. The single column was modelled according to experimental setup (tested in 1 m^3 tank filled with dry sand). The behaviour of the Soil Mixing columns in a group was analyzed with an assumption that column placed in a non-deformable tube represented the central column in the large group of columns. Diameter of the tube represented distance between columns. Four diameters (0.26 m, 0.35 m, 0.45 m and 0.65 m) were studied.

The influence of a density of soil (ρ = 1500 kg / m^3 and ρ = 1380 kg / m^3), in which columns had been installed, on their bearing capacity and mode of failure was investigated. Moreover, behaviour of 7 and 14 days old columns were studied. Based on the performed analyses and discussion of results, the major findings and conclusions can be drawn in the following:

- It was found that the density of soil had significant influence on the bearing capacity of the column. The rise of soil density results in increase of the bearing capacity.
- The age of the Soil Mixing column was found significant. With age the soil-cement mixture gains resistance, that results in higher modulus of deformation and cohesion of the material.
- Results of numerical simulations helped to detect that during testing columns in tubes, additional, unexpected friction (between soil and tube's walls) had appeared. The friction interfered with the confining pressure. Due to that, test in tubes cannot be considered as a study of columns working in a group. Nevertheless, simulations show influence of different confining pressure on the performance of columns. In order to compared calculated behaviour of columns with the experimental measurements, tube and additional friction were introduced to the numerical model. It was found that the confining pressure influenced column's bearing capacity and mode of failure. For the single column and test in tubes with diameter bigger than 0.26 m, failure occurred in soil, under the column. For tests in tube with diameter 0.26 m, failure was observed in the head of the column.

The results of small and full scale loading tests of the Soil Mixing columns (behaviour and modes of failure) lead to conclusion that they can be analysed as piles made of concrete with low resistance.

8.2. Shallow foundation

Numerical modelling of loading tests of a small scale shallow foundation was performed according to the experimental setup (footing tested in 1 m^3 tank). Two non-deformable footings with different sizes and shapes were simulated. The 'small' one was a steel rectangular plate (0.20 m x 0.25 m x 0.01 m). The 'big' footing was a steel square plate (0.35 m x 0.35 m x 0.01 m). Two kinds of reinforcement were tested. Firstly, mixed foundation, consisting of a footing and a single, centrally situated column, was investigated. Secondly, mixed foundation, consisting of a footing and a group of four Soil Mixing columns, was studied. In order to detect influence of non-homogeneity of soil on the behaviour of the mixed foundation, test with two layers of sand was carried out. The bottom of the analysed tank was filled with denser sand (ρ = 1500 kg / m^3) till the level of 0.58 m. Afterwards, 0.42 m of looser sand (ρ = 1380 kg / m^3) was added. Four columns reinforcing shallow foundation were installed in a way that their last 0.03 m were imbedded in denser layer.

8.2.1. Mixed foundation – single column

The main findings and conclusions are as follows:

- The positive effect of using the Soil Mixing column as reinforcement for a small scale shallow foundation was clearly highlighted. The bearing capacity the foundation increased significantly, whereas its displacement was reduced.
- It was observed that the behaviour of the mixed foundation can be better understood by analysing not only the total force borne by the foundation as a function of its displacement, but also distributions of force and stress.
- The density of soil is crucial to the bearing capacity of the reinforced foundation. However, it was found that the percentage of the total force that was taken by the soil under the foundation changed insignificantly as a function of density.
- The age of the reinforcing column is an important parameter. The older column is used, the higher force borne by the mixed foundation is observed.
- The size of the footing has considerable influence on the bearing capacity of the mixed foundation. The efficiency of the reinforcement executed by single column is significantly lower for bigger footing. It is not surprising, concerning the cross sections of each part of the mixed foundation. Reinforcing column represents 8% and only 3% of the whole footing's surface for smaller and bigger footings respectively.

8.2.2. Mixed foundation – four columns

Reinforcement of the shallow foundation executed by group of columns seems to be more reasonable solution. Firstly, it brings significantly higher efficiency of the reinforcement. Secondly, it helps to reduce possible rotation of the foundation, which might occur due to imperfections of the installation when foundation is supported by single column.

Based on the performed analyses and discussion of results, the major findings and conclusions are:

- The efficiency of the reinforcement was found significant. Reinforcement of homogeneous soil doubled the bearing capacity of unsupported foundation. In case of two layers of sand the bearing capacity was calculated as almost tripled.
- The denser layer at the bottom of the tank causes increase of the bearing capacity of the mixed foundation due to increase of tip capacity of the Soil Mixing columns. However, this layer does not change the force borne by the soil under the footing. So, load taken by the soil is the same for mixed foundation tested on one and two layers of sand.
- It was found that the only way of understanding mechanisms guiding the behaviour of mixed foundation was to analyse performance of each of its elements separately.
- It was observed that columns in a group of four, which were installed three diameters from each others axes, did not affect each other’s capacity. Hence, force taken by one column in the group of four and force carried by single column reinforcing foundation are the same – no group effect.

The results of numerical modelling of all small scale tests agree well with the experimental observations. The obtained improvement of the behaviour of shallow foundation is satisfying. However, it needs to be taken into account that due to considerable lower confinement (1g small scale modelling), materials’ properties and behaviour cannot be directly transferred to the full cases. Hence, acquired results should be considered as qualitative not quantitative

The chosen constitutive model (elastic model with the Modified Drucker-Prager with cap criterion) with the present cap and hardening/softening principle is found to be suitable for modelling the behaviour of the analysed soils, if an appropriate parameters were selected. Proper calibration of the model was confirmed by satisfying results of 18 numerical simulations.

8.3. The deep foundation

The influence of reinforcement executed by group of SM columns on a deep foundation was studied. The Soil Mixing columns can be installed around the foundation or under it. Moreover, reinforcement under the foundation might be placed in the same soil as foundation’s tip or in a deeper layer.

Numerical modelling of the reinforced deep foundations was carried out. Firstly, simulation of a theoretical, concrete pile installed in homogeneous soil was performed. The aim of the investigation was to detect the impact of parameters such as: pattern of reinforcing elements, horizontal distance between SM columns, vertical distance between columns’ heads and tip of the pile, diameter and length of SM elements, on the bearing capacity of the foundation. Secondly, two existing deep foundations, qualified for improvement were analysed. For both foundations, reinforcement was assumed in layer of weak soil under the foundation. By the weak soil, a soil with low elastic parameters was understood. The influence of the spacing of Soil Mixing columns on the performance of the reinforced foundation, was studied. Additionally, two methods of analysing improved weak soil were tested. The direct method consisted in modelling soil and Soil Mixing elements. The simplified method assumed that the whole reinforced area was replaced by new material with equivalent properties. Moreover, two ways of analysing column, created in more than one layer of soil, were studied. The column was investigated as homogenous or heterogeneous element (properties as a function of the column’s length).

8.3.1. Theoretical pile

The main findings and conclusions are as follows:

- The positive effect of the reinforcement on the bearing capacity of deep foundations was found.
- Patterns including central column in a group were found as the most efficient. The radical rise of the performance is caused by significantly higher tip capacity of the foundation. Even though efficiency of these kinds of patterns is significantly (especially when pile's tip is supported directly by the column) they can only be used when SM columns are installed before the foundation. Patterns which include column or columns under the deep foundation cannot be accepted in case of reinforcing existing deep foundation. They are disqualified due to danger of affecting the balance of stresses around pile's tip, which might results in sudden settlement. Moreover, installation of the SM column axial with pile brings some technical difficulties.
- The efficiency of the reinforcement executed by columns organised in accordance with patterns without central column, was not found very significant, however some mechanisms were captured.
- The distance between column and pile in horizontal sense was found the most influential on the improvement of the foundation's capacity. It was observed that pile's capacity decreases with the increase of the distance. Moreover, it was found that presence of the reinforcement influenced mainly pile's tip capacity. The change of the friction capacity was not significant.
- The second important parameter was diameter of the reinforcing columns. It was found that the increase of columns' diameter leads to rise of reinforcement's efficiency. The obtained relation was almost linear.
- The third important parameter was distance between columns' heads and tip of the foundation. It was found that the most optimal location was when they are in the same plane. Although, the increase of distance in both directions caused decrease of the reinforcement's efficiency, slightly better performance can be observed for columns placed over pile's tip. Hence, if it is not possible to install SM elements in the same plane, it is recommended to localize columns in a way that their heads are between zero and one meter over the pile's tip.
- The length of the column was found insignificant.

Presented investigation is theoretical analysis of the behaviour of the reinforced deep foundation. In order to be able to use its results in engineering practice, results should be confronted with results of field tests.

8.3.2. Existing foundations

Two existing deep foundations, qualified for improvement were analysed. Column installation process was not taken into account in the studies.

Lack of many properties of soils (just elastic ones in case of first analysed foundation) and did not allow performing more detailed investigation. Nevertheless, it gives general knowledge of the efficiency of the reinforcement. It was found for the first foundation that increase of the distance between reinforcing elements made improvement less efficient A linear relation between these two parameters was found.

Based on the performed simulation of the second foundation and discussion of results, the major findings are:

- In case of this particular analysed foundation, the influence of the way (homogeneous and heterogeneous) of modelling column passing three weak layers was found insignificant due to similar properties of all three layers.
- Results obtained from the direct method and the simplified method (the whole reinforced area is replaced by new material with equivalent properties) were found coherent. Hence, it can be concluded that the simplified method could be used to preliminary estimate the behaviour of the reinforced deep foundation. However, further studies are required to find a way of estimation shear properties of the equivalent material.

8.4. Perspectives

As a perspective, in order to improve future numerical simulations, other constitutive law for the Soil Mixing elements should be taken into consideration. New model should be capable of modelling brittle mode of failure and post failure behaviour of the material. Recommended models are laws used to describe behaviour of concrete, for instance damage plasticity model.

Furthermore, more *in situ* data are needed to validate theoretical approach presented in this thesis. Moreover, with additional field data Inverse Analysis would be possible.

In the further studies, it is significant to take into account installation process of columns. It is crucial especially for proper and safe design of the reinforcement of existing foundations. Studies of reinforcement by relatively mature Soil Mixing elements, 7 and 14 days old, performed in this thesis, is not sufficient.

Bearing capacity history of an existing foundation reinforced by the Soil Mixing technique, presented in Figure 8.1 helps to understand danger which ill-conceived installation of the reinforcement may lead to. An abrupt settlement and even collapse of the supported structure might occurred if the installation process is not taken into account. It needs to be ensured that the bearing capacity of the existing foundation during and directly after mixing is higher than minimal capacity required by the loaded structure.

Another aspect, touching time related properties of the Soil Mixing elements, is taking into account their time-dependent behaviour, such as creep and ageing processes of the soil-binder mix. Both of them appear after considerable time period and lead to degradation of so-called final bearing capacity (Figure 8.1).

Moreover, cyclic and dynamic behaviour of the Soil Mixing elements should be investigated to comply to construction standards.

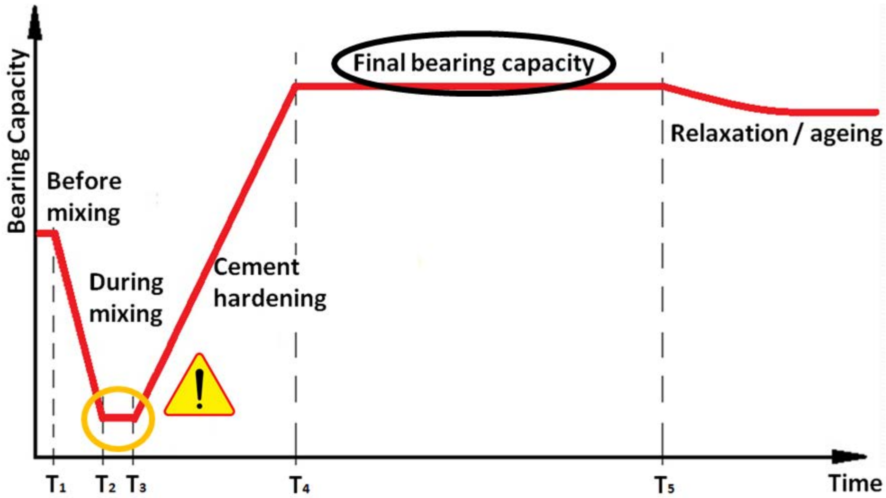

Figure 8.1 Bearing capacity history of an existing foundation reinforced by the Soil Mixing method

Appendix A

The stress tensor

The three-dimensional stress state of material is traditionally defined by the stress tensor, which can be presented relative to a chosen coordinate system by a matrix:

$$\sigma_{ij} = \begin{bmatrix} \sigma_{11} & \sigma_{12} & \sigma_{13} \\ \sigma_{21} & \sigma_{22} & \sigma_{23} \\ \sigma_{31} & \sigma_{32} & \sigma_{33} \end{bmatrix} \qquad \text{A. 1}$$

A common set of stress invariants are the three principal stress invariants. The principal stress coordinate system is the coordinate system in which shear stresses are equalled to 0 – only normal stresses exist. This requirement of zero shear stresses leads to characteristic equation presented in Equation A. 2, where: I_1, I_2, and I_3 are the first, the second and the third invariants of the stress tensor, respectively. They are defined by Equations, A. 3, A. 4 and A. 5. The three roots of the Equation A. 2 are the principal stresses. They are ordered that $\sigma_1 > \sigma_2 > \sigma_3$ and can be presented as a tensor like matrix in Equation A. 6.

$$\sigma^3 - I_1\sigma^2 + I_2\sigma - I_3 = 0 \qquad \text{A. 2}$$

$$I_1 = \sigma_{11} + \sigma_{22} + \sigma_{33} = \sigma_1 + \sigma_2 + \sigma_3 \qquad \text{A. 3}$$

$$I_2 = (\sigma_{11}\sigma_{22} + \sigma_{22}\sigma_{33} + \sigma_{33}\sigma_{11}) - \sigma_{12}^2 - \sigma_{23}^2 - \sigma_{31}^2 = \sigma_1\sigma_2 + \sigma_2\sigma_3 + \sigma_3\sigma_1 \qquad \text{A. 4}$$

$$I_3 = \begin{vmatrix} \sigma_{11} & \sigma_{12} & \sigma_{13} \\ \sigma_{21} & \sigma_{22} & \sigma_{23} \\ \sigma_{31} & \sigma_{32} & \sigma_{33} \end{vmatrix} = \sigma_1\sigma_2\sigma_3 \qquad \text{A. 5}$$

$$\sigma_{ij} = \begin{bmatrix} \sigma_1 & 0 & 0 \\ 0 & \sigma_2 & 0 \\ 0 & 0 & \sigma_3 \end{bmatrix} \qquad \text{A. 6}$$

Stress deviatoric tensor

This stress tensor is often decomposed into two parts: a purely hydrostatic stress, σ_m, defined in Equation A. 7 and the deviatoric stress tensor, s_{ij}, defined by Equation A. 8. Also for this tensor a characteristic equation can be written (Equation A. 9), where: J_1, J_2, and J_3 are the first, the second and the third invariants of the deviatoric tensor, respectively. They are defined by Equations A. 10, A. 11 and A. 12. The first invariant of the deviatoric stress is equalled to 0 due to fact that the stress deviatoric tensor is in a state of pure shear (Wolf, 2008).

$$\sigma_m = \frac{1}{3}(\sigma_{11} + \sigma_{22} + \sigma_{33}) \qquad \text{A. 7}$$

$$s_{ij} = \begin{bmatrix} s_{11} & s_{12} & s_{13} \\ s_{21} & s_{22} & s_{23} \\ s_{31} & s_{32} & s_{33} \end{bmatrix} = \begin{bmatrix} \sigma_{11} - \sigma_m & \sigma_{12} & \sigma_{13} \\ \sigma_{21} & \sigma_{22} - \sigma_m & \sigma_{23} \\ \sigma_{31} & \sigma_{32} & \sigma_{33} - \sigma_m \end{bmatrix} \qquad \text{A. 8}$$

$$s^3 - J_1 s^2 + J_2 s - J_3 = 0 \qquad \text{A. 9}$$

$$J_1 = s_{11} + s_{22} + s_{33} = s_1 + s_2 + s_3 = 0 \qquad \text{A. 10}$$

$$\begin{aligned} J_2 &= \frac{1}{6}[(\sigma_{11} - \sigma_{22})^2 + (\sigma_{22} - \sigma_{33})^2 + (\sigma_{33} - \sigma_{11})^2] + \sigma_{12}^2 + \sigma_{23}^2 + \sigma_{31}^2 \\ &= \frac{1}{6}[(\sigma_1 - \sigma_2)^2 + (\sigma_2 - \sigma_3)^2 + (\sigma_3 - \sigma_1)^2] = \frac{1}{3}I_1^2 - I_2 \end{aligned} \qquad \text{A. 11}$$

$$J_3 = \begin{vmatrix} s_{11} & s_{12} & s_{13} \\ s_{21} & s_{22} & s_{23} \\ s_{31} & s_{32} & s_{33} \end{vmatrix} = s_1 s_2 s_3 = \frac{2}{27} I_1^{23} - \frac{1}{3} I_1 I_2 + I_3 \qquad \text{A. 12}$$

References

ABAQUS, 2010. *Theory Manual.* Version 6.10 ed. : .

Abusharar, S. W., Zheng, J. J. & Chen, B. G., 2009. Finite element modeling of the consolidation behavior of multi-column supported road embankment. *Computers and Geotechnics,* Volume 36, pp. 676-685.

Ahnberg, H., Ljungkrantz, C. & Holmqvist, L., 1995. *Deep stabilization of different types of soft soils.* s.l., Proceedings of the 11th ECSMFE, pp. 7.167-7.172.

Al-Ajmi, A. M. & Zimmerman, R. W., 2005. Relation between the Mogi and the Coulomb failure criteria. *International Journal of Rock Mechanics and Mining Sciences,* Volume 42(3), pp. 431-439.

Ando, Y. et al., 1995. *Recent soil improvement methods for preventing liquefaction.* Rotterdam, s.n., pp. 1011-1016.

Andromalos, K., Hegazy, Y. & Jasperse, B., 2000. *Stabilization of Soft Soils by Soil Mixing.* Noordwijkerhout, Proceedings of Soft Ground Technology Conference, pp. 194-205.

API, 1984. *RP2A: recommended practice for planning, designing and constructing fixed offshore platforms.* 15th edn. Washington: American Petroleum Institute.

Archeewa, E., Puppala, A., Saride, S. & Kalla, S., 2011. *Numerical Model Studies of Deep Soil Mixing (DSM) Column to Mitigate Bridge Approach Settlements.* Dallas, Texas, Proceedings, pp. 3286-3295.

Ardiaca, D. H., 2009. Mohr-Coulomb parameters for modelling of concrete structures. *Plaxis Bulletin,* pp. 12-15.

Asano, J., Ban, K., Azama, K. & Takahashi, K., 1996. *Deep mixing methods of soil stabilization using coal ash.* Tokyo, Grouting and Deep Mixing Conference, pp. 393-398.

Assarson, K., Broms, B., Granhom, S. & Paus, K., 1974. *Deep Stabilization of Soft Cohesive Soils.* Sweden: Linden Alimark.

Axtell, P. J. & Stark, T. D., 2008. Increase in Shear Modulus by Soil Mix and Jet Grout Methods. *DFI Journal*, Volume 2(No. 1), pp. 11-21.

Babasaki, R., Suzuki, K. & Suzuki, Y., 1992. *Centrifuge tests on improved ground for liquefaction.* Rotterdam, Proceedings of the 10th World Conference on Earthquake Engineering, pp. 1461-1464.

Baligh, M. M., 1985. Strain path method. *ASCE J. Geotech. Engng*, Volume 111, pp. 1108-1136.

Barnichon, J. D., 1998. *Finite Element Modeling applied to Petroleum and Structural Geology,* University of Liège: PhD Thesis.

Bell, F. G., 1993. *Engineering treatment of soils.* London: E & FN Spon.

Benz Navarrete, M. A., 2009. *Mesures dynamiques lors du battage du pénétromètre PANDA 2,* Université Blaise Pascal, Clermont-Ferrand: PhD Thesis.

Bergado, D. T., Ruenkrairergsa, T., Taesiri, Y. & Balasubramaniam, A. S., 1999. *Deep soil mixing used to reduce embankment settlement.* s.l., s.n., pp. 145-162.

Bowles, J. E., 1996. *Foundation Analysis and Design, 5th edition.* s.l.:McGraw-Hill.

Branque, D., Gomes Correia, A. & Biarez, J., 1997. *Utilisation d'un modèle élasto-plastique simple dans l'interprétation de l'essai pressiométrique sur sable,* s.l.: Institut Supérieur Technique de Lisbonne, Centre de Géotechnique.

British Cement Association, 2001. *Cement-based Stabilisation and Solidification for the Remediation of Contaminated Land. Findings of a Study Mission to the USA.* , s.l.: s.n.

Broms, B., 1976. *Pile foundations – Pile groups.* Vienna, s.n., pp. 103-132.

Broms, B. B., 1999. *Keynote lecture: Design of lime, lime/cement and cement columns.* Rotterdam, s.n., pp. 125-154.

Broms, B. B., 2000. *Lime and lime/cement columns – summary and visions.* Helsinki, Keynote Lectures NGC – 4th GIGS, pp. 43-93.

Bruce, D. A., 2001. *An Introduction to the Deep Soil Mixing Methods as Used in Geotechnical Applications. Volume III: the Verification and Properties of Treated Ground,* s.l.: FHWA, U.S Department of Transportation.

Brumund, W. F. & Leonards, G. A., 1973. Experimental study of static and dynamic friction between sand and typical constuction materials. *Journal of Testing and Evaluation*, 1(2), pp. 62-66.

Budhu, M., 1999. *Soil mechanics and foundations..* s.l.:John Wiley & Sons.

Burke, K., Furth, A. & Rhodes, D., 1996. *Site remediation of hexavalent chromium in a plaster's sump: heavy metal chemical fixation – A case history.* Orlando, FL, s.n., p. 10.

Burland, J. B., 1973. Shaft friction of piles in clay. *Ground Engineering*, Volume 6(3), pp. 30-42.

Caltrans, 2010. *Deep Soil Mixing (DSM) / Cutter Soil Mixing (CSM),* s.l.: Caltrans.

Carter, J. P., Booker, J. R. & Davis, E. H., 1977. Finite Deformation of an Elasto-Plastic Soil. *International Journal for Numerical and Analytical Methods in Geomechanics,* Volume 1, p. 25–43.

Cement Deep Mixing Association of Japan, 1994. *Publication of CDM Association of Japan,* Tokyo, Japan: s.n.

Chen, W. F. & Mizuno, E., 1990. *Nonlinear Analysis in Soil Mechanics: Theory and Implementation.* New York: Elsevier Science Publishing Company Inc..

Colliat, J., 1986. *Comportement des matériaux granulaires sous fortes contraintes : influence de la nature minéralogique du matériau étudié,* Grenoble: University Joseph Fourier.

Colmenares, L. B. & Zoback, M. D., 2002. A statistical evaluation of intact rock failure criteria constrained by polyaxial test data for five different rocks. *International Journal of Rock Mechanics and Mining Sciences*, Volume 39(6), pp. 695-729.

Combe, A.-L., 1998. *Comportement du sable d'Hostun S38 au traiaxial axisymetrique. Comparaison avec le sable d'Hostun RF,* Grenoble, France: Universite Joseph Fourier, Laboratoire 3-SR.

Coulomb, C. A., 1776. Essai sur une application des regles des maximis et minimis a quelquels problemesde statique relatifs, a la architecture. *Mem. Acad. Roy. Div. Sav*, Volume 7, p. 343–387.

Cudny, M. & Binder, K., 2005. Kryteria wytrzymałości gruntu na ścinanie w zagadnieniach geotechniki. *Inżynieria Morska i Geotechnika*, Volume 6(26), pp. 456-465.

Cuira, F. et al., 2013. *Modélisation numérique du comportement d'une colonne de soil-mixing et confrontation à un essai de chargement en vraie grandeur.* Paris, Proceedings of the 18th International Conference on Soil Mechanics and Geotechnical Engineering, pp. 2461-2464.

Davis, E. H. & Booker, J. R., 1971. *The bearing capacity of strip footings from the standpoint of plasticity theory.* Melbourne, s.n., pp. 276-282.

Desrues, J., 2002. Limitations du choix de l'angle de frottement pour le critère de plasticité de Drucker-Prage. *Revue Française de Génie Civil*, Volume 6, pp. 853-862.

Dhaybi, M., 2015. *Renforcement des fondations superficielles par des colonnes de soil mixing – Analyse phénoménologique par modélisation physique,* INSA Lyon: PhD Thesis.

Dhaybi, M., Grzyb, A., Trunfio, R. & Pellet, F., 2012. *Foundations reinforced by soil-mixing: Physical and numerical approach.* Brussels, s.n., pp. 137-146.

Dhaybi, M. & Pellet, F., 2012. *Physical modelling of a small scale shallow foundation reinforced by Soil-Mixing.* Kuala Lumpur, s.n., p. 599–604.

Doherty, P. & Gavin, K., 2011. The Shaft Capacity of Displacement Piles in Clay: A State of the Art Review. *Geotechnical and Geological Engineering*, Volume 29(4), pp. 389-410.

DorMohammadi, H. & Khoei, A. R., 2008. A three-invariant cap model with isotropic–kinematic hardening rule and associated plasticity for granular materials. *International Journal of Solids and Structures*, Volume 45, p. 631–656.

Dorris, J. F. & Nemat-Nasser, S., 1982. A plasticity model for flow of granular materials under triaxial stress states. *International Journal of Solids and Structures,* Volume 18, pp. 497-531.

Drucker, D. C. & Prager, W., 1952. Soil mechanics and plastic analysis or limit design. *Quarterly of Applied Mathematics*, Volume 10(2), pp. 157-165.

Endo, M., 1976. *Recent development in dredged material stabilization and deep chemical mixing in Japan. Soils and Site Improvement*, s.l.: s.n.

European Committee for Standardisation, 1995. *Eurocode 7: Geotechnical Design—Part 1: General Rules.* Brussels: European Committee for Standardisation.

Fang, Y. S., Chung, Y. T., Yu, F. J. & Chen, T. J., 2001. Properties of soil-cement stabilized with deep mixing method. *Ground Improvement,* Volume 5(2), pp. 69-74.

Fang, Z., 2006. *Physical and numerical modelling of the soft soil ground improved by deep cement mixing method,* The Hong Kong Polytechnic University: PhD Thesis.

Fellenius, B. H., 1991. Pile foundations. In: *Foundation Engineering Handbook.* s.l.:Chapman&Hallm New York, p. 511.

Flavigny, E., Desrues, J. & Palayer, B., 1990. Note Technique le sable d'Hostun <<RF>>. *Revue Française de Géotechnique*, Volume 53, pp. 67-70.

Fukutake, K. & Ohtsuki, A., 1995. *Three dimensional liquefaction analysis of partially improved ground.* Tokyo, Proceedings of Earthquake Geotechnical Engineering, pp. 851-856.

Futaki, M., Nakano, K. & Hagino, Y., 1996. *Design strength of soil cement columns as foundation ground for structures.* Tokyo, Grouting and Deep Mixing Conference, pp. 481-484.

Gay, O., 2000. *Modélisation physique et numérique de l'action d'un glissement lent sur des fondations d'ouvrages d'art,* UJF Grenoble 1: PhD Thesis.

GeoTesting Express, 1996. *Geotechnical Tests on Soil Cement Mix for Central Artery/Tunnel Project*, s.l.: s.n.

Goh, T. L., Tan, T. S., Yong, K. Y. & Lai, Y. W., 1999. *Stiffness of Singapore marine clays improved by cement mixing.* Seoul, Proceedings of the 11th ARC-SMGE, pp. 333-336.

Guimond-Barrett, A., 2011. *Protocole de référence pour la réalisation des mélanges sol-ciment en laboratoire,* Paris: IFSTTAR laboratory.

Guimond-Barrett, A. et al., 2011. *Influence des conditions de mélange et de cure sur les caractéristiques de sols traités au ciment par soil mixing.* Bordeaux, XXIXe Rencontres Universitaires de Génie Civil, pp. 1-10.

Guimond-Barrett, A. et al., 2012. *On the strength and durability of cement-stabilised sands.* Brussels, Proceedings, pp. 345-353.

Gunaratne, M., 2006. *The foundation engineering handbook.* s.l.:Taylor & Francis Group.

Han, J., Oztoprak, S., Parsons, R. L. & Huang, J., 2007. Numerical analysis of foundation columns to support widening of embankments. *Computers and Geotechnics*, Volume 34, p. 435–448.

Han, J., Sheth, A. R., Porbaha, A. & Shen, S. L., 2004. Numerical analysis of embankment stability over deep mixed foundation. *Geotechnical Special Publication ASCE,* Volume 126(2), pp. 1385-1394.

Han, L. H. et al., 2008. A modified Drucker-Prager Cap model for die compaction simulation of pharmaceutical powders. *International Journal of Solids and Structures*, Volume 45, pp. 3088-3106.

Hansen, J., 1970. A Revised and Extended Formula for Bearing Capacity. *Bulletin 28, Danish Geotechnical Society.*

Helwany, S., 2007. *Applied Soil Mechanics with ABAQUS Applications.* Hoboken, New Jersey: J. Wiley & Sons, INC..

Hilt, G. H. & Davidson, B., 1960. Lime fixation in clayey soils. *Highway Reasearch Board Bulletin*, Volume 262, pp. 20-32.

Holtz, R. D. & Kovacs, W. D., 1981. *An Introduction to Geotechnical Engineering.* Eaglewood Cliffs, NJ: Prentice Hall.

Horpibulsuk, S., Chinkulkijniwat, A., Cholphatsorn, A. & Suebsuk, J., 2012. Consolidation behavior of soil–cement column improved ground. *Computers and Geotechnics*, Volume 43, pp. 37-50.

INNOTRACK, 2009. *Subgrade reinforcement with columns Part 1 Vertical columns, Part 2 Inclined columns,* Thematic Priority 6: INNOTRACK Project.

INNOTRACK, 2010. *D2.1.12 GL - Modelling of the track subgrade Part 1: Final report on the modelling of poor quality sites Part 2: Variability accounting in numerical modelling of the track subgrade* , Thematic Priority 6: INNOTRACK Project.

Jaky, J., 1944. The coefficient of earth pressure at rest (A nyugalmi nyomas tenyezoje). *Magyar Mernok es Epitesz-Egylet Kozlonye (Journal of the Society of Hungarian Architects and Engineers),* pp. 355-358.

Janbu, N., 1963. *Soil compressibility as determined by oedometer and triaxial tests.* Wiesbaden, s.n., pp. 19-25.

Janbu, N., 1976. *Static bearing capacity of friction piles.* Moscow, USSR, s.n., pp. 479-488.

Jiang, H. & Xie, J., 2011. A note on the Mohr-Coulomb and Drucker-Prager strength criteria. *Mechanics Research Communications*, Volume 38, pp. 309-314.

Kawasaki, T., Saitoh, S., Suzuki, Y. & Babasaki, R., 1984. *Deep mixing metod using cement slurry as hardening agent.* s.l., Seminar on Soil Improvement and Construction Technology in Soft Ground Improvement, pp. 17-38.

Kawasaki, T., Suzuki, Y. & Suzuki, Y., 1981. *On the Deep Mixing Chemical Mixing Method Using Cement Hardening Agent*, s.l.: Takenaka Technical Research Report 26.

KELLER, 2013. *Deep Soil Mixing (DSM). Improvement of weak soils by the DSM method*, Germany: s.n.

Kikumoto, M. et al., 2008. *A unified method to describe the influences of intermediate principal stress and stress history in constitutive modelling.* Glasgow, Scotland, s.n., pp. 151-157.

Kitazume, M., 2009. *Centrifuge model tests on failure mode of deep mixing columns.* Okinawa, s.n., pp. DI-7.

Kitazume, M., Ikeda, T., Miyajima, S. & Karastanev, D., 1996. Bearing capacity of improved ground with column type DMM. Grouting and Deep Mixing. In: Rotterdam: Balkema, pp. 503-508.

Kohler, R. & Hofstetter, G., 2007. A cap model for partially saturated soils. *International Journal For Numerical And Analytical Methods In Geomechanics*, Volume 32, pp. 981-1004.

Labuz, J. & Zang, A., 2012. Mohr-Coulomb Failure Criterion. *Rock Mechanics and Rock Engineering*, Volume 45, p. 975-979.

Lambrechts, J. R. & Roy, P. A., 1997. Geotechnical special publication 69: Deep soil-cement mixing for tunnel support at Boston's I-93NB/I-90 interchange. In: *In Ground Improvement, Ground Reinforcement, Ground Treatment Developments 1987-1997.* New York: American Society of Civil Engineers, pp. 579-603.

Lancelot, L., Shahrour, I. & Al Mahmoud, M., 1996. Comportement du sable d'Hostun sous fiables contraintes. *Revue francaise de geotechnique*, pp. 63-76.

Lanier, J., 1988. Special stress paths along the limit surface of a sand specimen with the use of a true triaxial apparatus. Dans: *Advanced triaxial testing of soil and rock.* Philadelphia, PA: ASTM, pp. 859-869.

Larsson, S., 2005. State of Practice Report– Execution, monitoring and quality control. In: *Deep Mixing* . s.l.:s.n., pp. 732-786.

Larsson, S., Malm, R., Charbit, B. & Ansell, A., 2012. Finite element modelling of laterally loaded lime–cement columns using a damage plasticity model. *Computers and Geotechnics*, Volume 44, pp. 48-57.

Le Kouby, A., Bourgeois, E. & Rocher-Lacoste, F., 2010. Subgrade Improvement Method for Existing Railway Lines – an Experimental and Numerical Study. *Electronical Journal of Geotechical Engineering*, pp. 461-494.

Lee, C. J., Bolton, M. D. & Al-Tabbaa, A., 2002. Numerical modelling of group effects on the distribution of dragloads in pile foundations. *Géotechnique*, Volume 5(52), pp. 325-335.

LIEBHERR, 2012. *LB series – Soil mixing*, s.l.: Technical report, Austria.

Lorenzo, G. A., 2005. *Fundamentals of Cement-Admixed Clay in Deep Mixing and Its Behaviour as Foundation Support of Reinforced Embankment on Subsiding Soft Clay Ground*, Bangkok, Thailand: Asian Institute of Technology.

Massarsch, K. R. & Topolnicki, M., 2005. *Regional Report: European Practice of Soil Mixing Technology*. Stockholm, s.n.

McClelland, B., 1974. Design of deep penetration piles for ocean structures. *ASCE Journal of Geotechnical Engineering*, pp. 705-747.

Melentijevic, S., Arcos, J. L. & Oteo, C., 2013. *Application of cement deep mixing method for underpinning.* Paris, France, Proceedings, pp. 2549-2552.

Meyerhoff, D. D., 1976. Bearing capacity and settlement of pile foundations. *ASCE Journal of Geotechnical Engineering*, pp. 195-228.

Meyerhof, G., 1963. Some recent research on bearing capacity of foundations. *Canadian Geotechnical Journal*, pp. 16-26.

Miyoshi, A. & Hirayama, K., 1996. *Test of solidifies columns using a combined system od mechanical churning and jetting.* Tokyo, s.n., pp. 743-748.

Mogi, K., 1971. Fracture and flow of rocks under high triaxial compression. *Journal of Geophysical Research*, Volume 76(5), pp. 1255-1269.

Mohr, O., 1900. Welche Umstände bedingen die Elastizitätsgrenze und den Bruch eines Materials?. *Zeit des Ver Deut*, Volume 44, p. 1524–1530.

Mun, B., Kim, T., Moon, T. & Oh, J., 2012. SCM wall in sand: Numerical simulation and design implications. *Engineering Geology*, Volume 151, pp. 15-23.

Nadai, A., 1950. *Theory of flow and fracture of solids.* New York: McGraw Hill.

Nicholson, P. J., Mitchell, J. K., Bahner, E. W. & Moriwaki, Y., 1998. Geotechnical special publication 81: Design of a soil mixed composite gravity wall. In Soil Improvement for Big Digs. In: New York: American Society of Civil Engineers, pp. 27-40.

Noto, S., Kuchida, N. & Terashi, M., 1983. Actual practice and problems on the deep mixing method. *Journal of Japanese Society of Soil Mechanics and Foundation Engineering*, pp. 73-80.

Nozu, M., 2005. *Regional Report: Asia.* Stockholm, s.n.

Okumara, T., 1996. *Deep mixing method Japan.* Tokyo, Japan, pp. 879-887.

Ou, C. Y., Wu, T. S. & Hsieh, H., 1996. Analysis of deep excavation with column type of ground improvement in soft clay. *Journal of the Geotechnical Engineering Division of the ASCE*, Volume 122(9), pp. 709-716.

Pagliacci, F. & Pagotto, G., 1994. *Soil improvement through mechanical deep mixing treatment in Thailand.* Bruges, s.n., pp. 5.11-5.17.

Pestana, J. M., Whittle, A. J. & Salvati, L. A., 2002. Evaluation of a constitutive model for clays and sands: Part I - sand behaviour. *INTERNATIONAL JOURNAL FOR NUMERICAL AND ANALYTICAL METHODS IN GEOMECHANICS*, Volume 26, pp. 1097-1121.

Popa, H. & Batali, L., 2010. Using Finite Element Method in geotechnical design. Soil constitutive laws and calibration of the parameters. Retaining wall case study. *Applied and Theoretical Mechanics*, Volume 5, pp. 177-186.

Porbaha, A., 1998. *State of the art in deep mixing technology: part I. Basic concepts and overview.* s.l., s.n., p. 81 –92.

Porbaha, A., 2000. State of the art in deep mixing technology. Part IV: design considerations. *Ground Improvement*, pp. 3, 111-125.

Porbaha, A., Shibuya, S. & Kishida, T., 2000. State of the art in deep mixing technology. Part III: geomaterial characterization. *Ground Improvement*, Volume 3, pp. 91-110.

Porbaha, A., Tanaka, H. & Kobayashi, M., 1998. State of the art in deep mixing technology: part II. Applications. *Ground Improvement*, pp. 125-139.

Porbaha, A. et al., 2005. *Report: American Practice of Deep Mixing Technology*. Stockholm, s.n.

Prandtl, L., 1921. Uber die eindringungsfestigkeit plastischer baustoffe und die festigkeit von schneiden. *Z. Angew. Math. Mech*, pp. 15-20.

Rathmeyer, H., 1996. *Deep mixing methods for soil subsoil improvement in the Nordic Countries.* Tokyo, s.n., pp. 869-877.

Reavis, G. & Freyaldenhoven, F. C., 1989. GEOJET Foundation System. *Geotechnical News*, Volume 12, pp. 56-60.

Resende, L. & Martin, J., 1985. Formulation of Drucker-Prager Cap Model. *Journal of Engineering Mechanics*, Volume 111(7), pp. 855-881.

RFF, 2013. *Réseau Ferré de France.* [Online] Available at: http://www.rff.fr/ [Accessed 20 01 2014].

RUFEX, 2010. *D01 – Spécifications Générales du Projet*, Paris: RUFEX Project.

Saitoh, S. et al., 1980. *Research on DMM using cementitious agents (part 10)-engineering properties of treated soils.* Tokyo, Proceedings of the 15th National Conference of the JSSMFE, pp. 717-720.

Sandler, I. S., 2005. Review of the development of cap models for geomaterials. *Shock and Vibrations*, Volume 12, pp. 67-71.

Schanz, T., Vermeer, P. A. & Bonnier, P. G., 1999. *The hardening soil model: formulation and verification.* Amsterdam, s.n., pp. 1-16.

Sibelco, 2012. *Properties of Hostun sand.* [Online] Available at: http://www.sibelco.fr/item_img/medias/images/ft13_hn31.pdf

Sivakugan, N. & Pacheco, M., 2011. Designe of shallow foundations. In: *Geotechnical Engineering. Handbook.* s.l.:J. Ross Publishing Inc., pp. 3-2-3-56.

Skempton, A. W., 1951. *The bearing capacity of clays.* s.l., s.n., pp. 180-189.

Sol Solution, 2012. *Projet de Recherche et Développement PANDA 3®(Projet RUFEX). Essais expérimentaux INSA – Contrôle de Compactage,* s.l.: Sol Solution Service Recherche et Développement.

Soletanche Bachy, 2013. *D12 Rapport d'essais de validation,* Paris, France: RUFEX Project.

Spangler, M. G. & Handy, R. L., 1982. *Soil Engineering, 4th edition.* New York: Harper & Row.

Sunyer Amat, A., 2007. *Elastic stiffness moduli of Hostun sand,* s.l.: University of Bristol, Department of Civil Engineering.

Taki, O. & Yang, D., 1991. *Soil cement mixed wall technique.* Denver, USA, s.n., pp. 298-309.

Tang, A. M., Vu, M. N. & Cui, Y. J., 2011. Effects of the maximum grain size and cyclic wetting/drying on the stiffness of a lime-treated clayey soil. *Géotechnique*, Volume 61, p. 421– 429.

Tan, T. S., Goh, T. L. & Yong, K. Y., 2002. Properties of Singapore marine clays improved by cement mixing. *Geotechnical Testing Journal*, Volume 25(4), pp. 422-433.

Tatsuoka, F. & Shibuya, S., 1991. *Deformation characteristics of soils and rocks from field and laboratory tests.* s.l., Proceedings of the 9th ARC on SMFE, pp. 101-177.

Terrasol, 2009a. *Usine de Mardyck – extension du parc a bobines. Avis sur les tassements des barrettes de la File 1,* Paris: s.n.

Terrasol, 2009b. *Projet ATM ILOTS M08 – M09. Estimation des tassements absolus et differentiels,* Paris: s.n.

Terzaghi, K., 1943. *Theoretical soil mechanics.* New York: John Wiley & Sons, Inc..

Topolnicki, M., 2004. In situ Soil Mixing. In: *Ground Improvement.* London and New York: Spon Press, pp. 331-428.

Uddin, K., Balasubramaniam, A. S. & Bergado, D. T., 1997. Engineering behavior of cement-treated Bangkok soft clay. *Geotechnical Engineering,* pp. 89-119.

Venda Oliveira, P. J., Pinheiro, J. L. P. & António, A. S., 2011. Numerical analysis of an embankment built on soft soil reinforced with deepmixing columns: Parametric study. *Computers and Geotechnics*, Volume 38, p. 566–576.

Venkatramaiah, C., 2006. *Geotechnical Engineering.* s.l.:New Age International.

Vesic, A., 1973. Analysis of ultimate loads of shallow foundations. *Journal of the Soil Mechanics and Foundations Division,* p. 45–73.

Voottipruex, P., Suksawat, T., Bergado, D. T. & Jamsawa, P., 2011. Numerical simulations and parametric study of SDCM and DCM piles under full scale axial and lateral. *Computers and Geotechnics*, Volume 38, pp. 318-329.

White, D. J. & Bolton, M. D., 2004. Displacement and strain paths during plane-strain model pile installation in sand. *Géotechnique*, Volume 54, pp. 375-466.

Wikipedia, 2013. *Wikipedia.* [Online] Available at: http://en.wikipedia.org/wiki/File:Section_through_railway_track_and_foundation.png [Accessed 20 01 2014].

Wissa, A. E. Z., Ladd, C. C. & Lamb, T. W., 1965. *Effective stress strength parameters of stabilized soils.* Montreal, Proceedings of the 6th ICSMFE, pp. 412-416.

Wolf, J. A., 2008. *A plasticity model to predict the effects of confinement on concrete,* California Institute of Technology: PhD Thesis.

Yang, D. S., 1997. *Deep mixing. In Situ Ground Improvement, reinforcement and Treatment: A Twenty Year Update and Vision for 21st Century*. Logan, UT, s.n., pp. 130-150.

Yin, J. H. & Lai, C. K., 1998. Strength and stiffness of Hong Kong marine deposits mixed with cement. *Geotechnical Engineering Journal*, Volume 29(1), pp. 29-44.

Zheng, J. J., Abusharar, S. W. & Wang, X. Z., 2008. Three-dimensional nonlinear finite element modeling of composite foundation formed by CFG–lime piles. *Computers and Geotechnics*, Volume 35, p. 637–643.